Enantioselective Catalysis using Heterogeneous and Dissymmetric
Salen Complexes of Mn and Cr

by

Mark D. Angelino

B.S.E., Chemical Engineering (1994)
The Cooper Union

M.S. in Chemical Engineering Practice (1996)
Massachusetts Institute of Technology

Submitted to the Department of Chemical Engineering
in Partial Fulfillment of the Requirements for the Degree of

Doctor of Philosophy in Chemical Engineering

Science

at the

Massachusetts Institute of Technology

September, 1999

Signature of Author..
Mark D. Angelino
Department of Chemical Engineering
July 9, 1999

Certified by..
Paul E. Laibinis
Doherty Assistant Professor of Chemical Engineering
Thesis Supervisor

Accepted by..
Robert E. Cohen
St. Laurent Professor of Chemical Engineering
Chairman, Committee for Graduate Students

1

Enantioselective Catalysis using Heterogeneous and Dissymmetric Salen Complexes
of Mn and Cr

by

Mark D. Angelino

Submitted to the Department of Chemical Engineering
on July 9, 1999 in Partial Fulfillment of the
Requirements for the Degree of Doctor of Philosophy in
Chemical Engineering

ABSTRACT

The first part of this thesis details the development of a covalently linked salen complex onto the surface of a 98 vol% styrene/ 2 vol % divinylbenzene polymeric support. The solid-phase, stagewise method of constructing of the ligand produces a supported catalyst that guarantees accessibility to the active sites and reduces restriction along the approach paths toward the active metal center which govern the enantioselectivity of the catalyst. The enantioselective performance of the supported complex was examined for the epoxidation of olefins using Mn and the ring-opening of epoxides using Cr loaded into the ligand.

The Mn catalyst produced the epoxides of 1,2-dihydronaphthalene, styrene, and cis-β-methylstyrene, and 6-bromo-2,2,3,4- tetramethylchromene with enantiomeric excesses (ee's) of 46, 9, 79, and 77 %, respectively, by reaction with NaOCl(aq). These values are among the highest reported for a heterogeneous version of the Mn-based salen catalyst with that for chromene approximating the value that can be obtained with the homogeneous ligand. Upon recycle, a degradation process was noted under the conditions for epoxidation that resulted in oxidation and decomposition of the ligand. This process also affects the homogeneous catalyst, thereby limiting the recyclability of both the homogeneous and heterogeneous Mn systems for this reaction. This decomposition suggests a process in solution, beyond the commonly cited inactivation process involving a Mn^{IV} dimer, that prevents recycle of the homogeneous catalyst for this reaction.

For the heterogeneous Cr-based, heterogeneous catalyst, epoxyhexane, propylene oxide, and cyclohexene oxide produced trimethylsilyl azido ethers with ee's of 34, 36, and 6 %, respectively, using TMSN$_3$. This reaction employs milder conditions than for epoxidation and allowed reuse of the heterogeneous catalyst without loss of activity or enantioselectivity through three runs with epoxyhexane. During reaction, leaching of Cr from the heterogeneous catalyst was less than 0.1%, suggesting possible reuse of the catalyst over hundreds of cycles before reloading the polymer-supported salen ligand with metal would be necessary.

In the second part of this thesis, the impact on enantioselectivity of the steric architecture of the salen complex was also examined by synthesizing various t-Bu substituted, homogeneous complexes. The epoxidation of chromene, DHN, and styrene by these catalysts using mCPBA as oxidant indicated that a C_2 symmetric catalyst is not required for enantioselective behavior and that the minimum sterics required is a single t-Bu group in the C3 position of the ligand. This addition of a single t-Bu group to the base ligand provided the greatest improvement in ee.

2

Analogous results were also found using these ligands for the Cr-catalyzed ring-opening of epoxides.

These homogeneous complexes also provided some mechanistic insight into the epoxidation and ring-opening reactions. The enantioselective behavior of the homogeneous Mn(salen) catalyst exhibited a departure from Arrhenius behavior with temperature. These strongly suggest a pathway that includes the reversible formation of an intermediate and the irreversible formation of product from this intermediate. This observation is consistent with a metallaoxetane intermediate for the Mn(salen) catalyzed asymmetric epoxidation. Other debated mechanisms for this reaction involving either a concerted or radical pathway cannot explain the observed effects.

A detailed kinetic study of the asymmetric ring opening of epoxides with Cr(salen) catalysts revealed that these catalysts function with similarities to enzymes. Given that the catalysts form enzyme/substrate-like intermediates, the conversion of epoxides into trimethylsilyl-azido ethers could be modeled using an enzyme kinetic model. Notably, the Cr(salen)complex with the full, 4 t-Bu complement exhibited substrate inhibition. The fact that the substrate concentration affects reaction rates using Cr(salen) complexes indicates that current attempts to maximize the efficiency of such catalysts for the asymmetric ring opening of epoxides could be done more effectively.

Thesis Supervisor: Paul E. Laibinis
Title: Doherty Assistant Professor of Chemical Engineering

In dedication to my grandparents and my parents—

Acknowledgments

Many people have enriched my life and/or contributed to my progress as a researcher here at MIT. While it is impossible to thank all of them, the following people deserve special mention:

My thesis advisor, Prof. Paul E. Laibinis, for his support and guidance through these years and for having the patience to let me find my way.

My thesis committee members— Profs. Gleason, Merrill, and Ying— for their advice and encouragement concerning my project.

G. Kane Jennings and Jianfeng Lou, former PEL group members since graduated. They were my predecessors in the group and from whom I learned the most– both in the lab and from our talks about life. Also, my fellow PEL group members in 66-425— for all their friendly discussions and banter during these last few years.

Steven Huang— an undergraduate at MIT— who worked with me on the chromene synthesis and on the chromium reactions. Without his effort, I think this work would be lacking in many ways. He is a bright engineer and good friend.

My friends— Gary, Seth, Raj, Andrey, Chris , Julie, Mark, Cathy— for all the great memories. I thank you, and so does Crappy. My years were more endurable, and some might say even enjoyable, due to the friendships we developed. I wish you all the best of luck, and I look forward to seeing you again— just make it somewhere else.

To Elizabeth— for being a great friend and, more importantly, for teaching me how to enjoy my free time.

Finally, my family— for their eternal support and guidance. I could not have made it even a fraction of the way without you.

Table of Contents

7

List of Figures

10

List of Tables

Chapter 1. Introduction to Asymmetric Synthesis

1.1. Industrial Application of Enantioselective Catalysis

The application of enantioselective catalysts in the formation of chiral, organic compounds has developed into a powerful, industrial tool over the last decade. Its greatest impact has been in the pharmaceutical industry, where chiral drugs have increased from a $32 billion to a $138 billion market from 1992 to 1997.[1,2] As of 1997, approximately two-thirds of the drugs in development are chiral.[3] The increased awareness of the potentially different chemical properties provided between an enantiomeric pair has begun to spread beyond the traditional applications for these chiral compounds and intermediates. For example, chiral liquid crystals, enantiopure polymers, and chiral membrane components are beginning to be utilized in diverse areas such as drug delivery, separation technology, and optoelectronics.[4] Increased access to homochiral materials for these applications requires an improved understanding of the means to synthesize these compounds and of the parameters through which these processes can be optimized.

As the industrial applications of chiral catalysis grow, the challenge becomes to expand the scope of these catalysts from efficient chemical/bench-scale tools to practical, industrial applications.[1,4] While the chemical literature contains a wealth of chiral catalysts with evidence of their selectivities, application of these powerful tools requires a fundamental understanding of the effects of catalyst parameters on reactivities and selectivities. The role of the catalytic ligand and its substituents in altering and potentially optimizing enantiomeric purity is a fundamental topic that needs to be addressed. Pertinent engineering issues arise not only in attempting to understand how to design these catalysts on a molecular level, but also in larger-scale issues involving the separation and recycle of these catalysts.

1.2. Importance of Chirality and Asymmetric Synthesis

While the preceding section impressed upon the economic reality in utilizing chiral catalysis industrially, the basis for their application actually rests in the role of these catalysts. These catalysts operate by directing the formation of one enantiomer over its mirror image, an ability often reserved for biological systems such as enzymes.[1,3] The requirement of enantiomerically

pure compounds is particularly important for the intermediates used to synthesize pharmaceuticals in which a difference in chirality at a particular stereogenic center within a diastereomeric compound may be the difference between a compound being therapeutic or toxic. Aside from this significant hazard, a difference in chirality for a pharmacological compound also introduces other issues. Cell surface receptors provide specific host-guest interactions between microorganisms and chiral compounds. This discriminating ability between the host template and a guest molecule also results in differences in the rates of absorption, activation, and degradation between these enantiomeric, guest compounds.[1] These differences affect the bio-acceptability and necessary dosing of the compounds as well. In accordance with these distinctions, regulatory agencies, such as the Food and Drug Administration (FDA),[5,6] impose strict guidelines for pharmaceuticals that contain asymmetric centers. For these stereoisomeric compounds, each compound must be isolated and individually tested for their pharmacological or toxicological properties.

Traditionally, the production of chiral compounds is performed using biological agents, such as enzymes, where fermentation produces natural products that are enantiomerically pure.[1,3] A classic example is antibiotics, which are produced in this manner. Alternately, traditional chemical procedures often lead to synthesis of the racemate, a 50/50 mixture of enantiomers. In this latter case, the compounds are used in this form with no consideration given to the differing activities of or possible inactivity of one of the pair of compounds.[7] The production of the inactive, and hopefully innocuous, isomer reduces the efficiency of the process yield.

Various processing strategies have been developed for the isolation of single isomers as products. Post-processing steps may include recrystallization or the formation of a diastereomeric pair using resolving agents.[4] In addition, analytical techniques such as high performance liquid chromatography (HPLC) or gas chromatography (GC) have been used.[4] Both sets of techniques function by generating a chemical environment in which one enantiomer preferentially interacts with an agent (whether it be solvent, a resolving agent, or stationary chromatographic film) that makes separation of the two enantiomers feasible. However, the employed resolving agents are frequently expensive, and the relevant chromatographic techniques suffer from high costs and limited throughput. Rather than isolating a single isomer by post-processing steps, synthetic methods can be used to generate enantiomerically pure or enriched products to simplify separational needs. This approach requires the use of pure, chiral

reactants that are synthetically modified to yield the desired product. Nevertheless, the high production costs associated with obtaining and using these chiral reactants often make this strategy impractical. Hence, the costs, whether process-oriented or synthetic, make these strategies prohibitive especially for batches that at the production-scale may measure hundreds of tons.

Homogeneous enantioselective catalysis offers an alternate route to these chiral compounds.[7-9] These catalysts are synthesized using chiral agents that transfer chiral information during the reaction to form the product. The choice of chirality for the agents comprising the catalyst dictates the preferred chirality of the product. Advantages of these synthetic chiral catalysts relative to biocatalysts are the ability to modify the chiral organic ligands to alter the selectivities and increase the scope of reactions for which these catalysts have found applicability.[4,7,10,11] However, limitations do exist. The use of pure, chiral compounds as auxiliaries for these catalysts adds a significant expense to their overall cost. Additionally, the need to separate these metal complexes from the reaction mixture still exists. Heterogenized versions of these catalysts provide a viable solution to this latter, pervasive problem. Such catalysts offer the practical advantages of simplifying the separation and isolation of products (especially on a commercial scale) while permitting easy recovery of the supported catalyst for its potential regeneration and recycle.[1,4]

1.3   History of Enantioselective Catalysis

Since the discovery in the late 19th century by Fischer that enzymes catalyze reactions enantioselectively,[7] the challenge has been to extend this enantioselective ability to synthetic systems. As asymmetric catalysts and resolution techniques have developed, the pool of chiral auxiliaries has grown from naturally occurring, chiral compounds—such as cinchona alkaloids, amino acids, and carbohydrates—to fully synthetic compounds including those containing ferrocene units[12,13] and ligands with asymmetric P or Re atoms.[14,15] Additionally, the ligands for these catalysts have been designed such that their substituents or ligand properties can be modified to a level that does not exist in nature. For example, BINAP ligands (bi-naphthyl diphosphine complexes) used with Ru for the asymmetric hydrogenation of olefins provide axial symmetry which does not exist in nature.[16] As the scope of chiral auxiliaries has increased, the

performance of these artificial asymmetric catalysts has become competitive with natural and selectively evolved biocatalysts.

While the goal in the field of asymmetric catalysis has been to develop catalysts to mimic the ability of enzymes to produce exclusively one enantiomer, several catalysts have been developed that extend beyond the catalytic scope of enzymes.[4] Two such examples are Sharpless' titanium tartrate and Jacobsen's salen-based catalysts. In the case of Sharpless' catalyst, epoxides with enantioselectivities greater than 90 % are routinely produced across a wide range of allylic alcohols.[10,17] The discriminating ability of this catalyst to produce an enantiomeric product approaches that of biocatalysts; additionally, this catalyst has a general level of activity toward allylic alcohols regardless of their degree of substitution that is difficult for enzymatic catalysts to achieve.[10] With Jacobsen's salen-based system, the scope of reactants for the asymmetric epoxidation reaction was extended to unfunctionalized olefins.[11,18-27] The activity toward a variety of substitution patterns for the olefin was maintained while removing the requirement of the allylic alcohol for the Sharpless reaction. In addition, this generality toward substrates was extended to other reactions using the same salen framework including asymmetric aziridinations,[28,29] cyclopropanations,[30] and hydroxylations,[31] and the kinetic resolution of racemic epoxides.[32] Thus, this salen ligand could generate product with high enantioselectivity for a variety of substituted reactants across a variety of reactions. This generality has made the salen complex one of the more viable asymmetric catalysts for industrial application.[32-34]

The ensuing challenge with asymmetric catalysis has been the development of heterogeneous asymmetric catalysts.[9,22,35] The dual ability to preferentially synthesize a particular enantiomer and provide an ease of separation from a reaction would take such catalysts from the realm of a highly efficient chemical tool to that of a practical, industrial application.[1,4] Ligation or incorporation of a homogeneous catalyst onto a support is a commonly used method to achieve an immobilized complex.[35-40] These catalysts—the so-called heterogenized homogeneous catalysts—combine the processing advantages of a heterogeneous catalyst with the potential selectivities of the homogeneous catalysts. In addition, the foundation of knowledge that exists for the homogeneous catalysts can still be utilized as a reference for comparison and optimization. However, limitations to these heterogenized homogeneous catalysts do exist. A variation of the enantioselectivity from the homogeneous case is often observed. In addition, the stability of the ligand is often an issue with either leaching of active metal or fracture of the

ligand occurring. This latter case of ligand fracture is especially problematic in that the ligand, with its chiral component, is necessary for enantioselectivity and is often the bulk of the expense of the process.

Prior work on heterogenizing asymmetric homogeneous catalysts has involved the immobilization of chiral moieties such as the tartrate-titanium isopropoxide system of Sharpless for epoxidation,[41,42] cinchona alkaloid derivatives for dihydroxylation,[35,43-45] and various salen-based ligands for epoxidation.[35,43-45] While the enantioselectivities achieved for the first two cases approached those of the homogeneous catalysts, they suffered upon recycle due to leaching of the metal or a lack of stability. This limitation has restricted their use and further development. In the case of the salen-based catalysts, the Mn-catalyzed epoxidation reaction has had only moderate success in terms of its enantioselective performance.[38,40,46,47] The stability of these heterogenized salen-based catalysts has also not been sufficiently addressed. Therefore, the development of heterogenized homogenous catalysts as applied to asymmetric reactions is a relatively undeveloped area to which the application of engineering principles at a molecular level can potentially provide insight. In addition, as noted from prior attempts at heterogenzing homogeneous catalysts, an understanding of the stability of these catalysts is an issue that also must be addressed for these systems.

1.3 Motivation

While the field of enantioselective catalysis has grown rapidly over the last few decades, the main focus of this research has been an expansion in the variety of asymmetric reactions. As a tool for industrial applications, heterogenized versions of these catalysts would hasten their acceptance and use. However, to achieve this goal, fundamental ligand parameters and their influence on activity and selectivity must be investigated. Ultimately, these principles provide a foundation for the rational design and engineering of these types of catalysts.

This thesis addresses issues of heterogenizing a homogeneous asymmetric catalyst, the salen complex. The earlier portions of this study focus on the synthetic methodology used to construct an immobilized salen complex onto a polymer support and its characterization (Chapter 2), as well as the application of this heterogenized ligand to two classes of reaction (Chapters 3 and 4, respectively). The issue of stability is addressed with each application. The remainder of this thesis explores the roles of symmetry and substitution patterns for the homogeneous ligands

on reactivity and enantioselectivity. This investigation provides insight into the effect of changes imposed structurally upon heterogenizing a homogenous salen complex on the function of the catalyst. These later chapters provide a fundamental understanding of several of the issues encountered in the rational design of such heterogenized salen complexes.

1.4 References

1) Stinson, S. C. *Chemical and Engineering News* **1993**, *71*, 38.

2) Stinson, S. C. *Chemical and Engineering News* **1998**, *76*, 83.

3) Stinson, S. C. *Chemical and Engineering News* **1997**, *75*, 38.

4) Nugent, W.; Rajanbabu, T.; Burk, M. *Science* **1993**, *259*, 479.

5) Administration, U. S. F. A. D. "FDA's Policy Statement for the Development of Neww Stereoisomeric Drugs," Food and Drug Administration, 1992.

6) Shaw, A. "Guideline for Submitting Supporting Documentation in Drug Applications for the Manufacture of Drug Substances," Food and Drug Administration, 1987.

7) Blaser, H. *Chem. Rev.* **1992**, *92*, 935.

8) Ojima, I. *Catalytic Asymmetric Synthesis*; Ojima, I., Ed.; VCH Publishers, Inc.: New York, 1993.

9) Blaser, H. *Tetrahedron* **1991**, *2*, 843.

10) Katsuki, T.; Sharpless, K. B. *J. Am. Chem. Soc.* **1980**, *102*, 5974.

11) Wei, Z.; Loebach, J. L.; Wilson, S. R.; Jacobsen, E. N. *J. Am. Chem. Soc.* **1990**, *112*, 2801.

12) Hayashi, T. *Pure Appl. Chem.* **1988**, *60*, 7.

13) Hayashi, T. ; Hayashi, T., Ed.; Blackwell Scientific Publications: Boston, 1985, p 35.

14) Koenig, K. E. ; Koenig, K. E., Ed.; Academic Press: New York, 1985; Vol. 5, p 71.

15) Zwick, B. D.; Arif, A. M.; Patton, A. T.; Gladysz, J. A. *Angew. Chem., Int. Ed. Engl.* **1987**, *27*, 910.

16) Miyashita, A.; Yasuda, A.; Takaya, H.; Toriumi, K.; Ito, T.; Souchi, T.; Noyoi, R. *J. Am. Chem. Soc.* **1980**, *102*, 7932.

17) Johnson, R. A.; Sharpless, K. B. *Catalytic Asymmetric Synthesis*; Ojima, I., Ed.; VCH Publishers: New York, 1993, p 103.

18) Zhang, W.; Jacobsen, E. N. *J. Org. Chem.* **1991**, *56*, 2296.

19) Larrow, J. F.; Jacobsen, E. N. *J. Org. Chem.* **1994**, *59*, 1939.

20) Hosoya, N.; Hatayama, A.; Irie, R.; Sasaki, H.; Katsuki, T. *Tetrahedron* **1994**, *50*, 4311.

21) Irie, R.; Noda, K.; Ito, Y.; Matsumoto, N.; Katsuki, T. *Tetrahedron Lett.* **1990**, *31*, 7345.

22) Jacobsen, E. N. *Catalytic Asymmetric Synthesis*; Ojima, I., Ed.; VCH Publishers: New York, 1993, p 159.

23) Chang, S.; Lee, N. H.; Jacobsen, E. N. *J. Org. Chem.* **1993**, *58*, 6939.

24) Lee, N. H.; Jacobsen, E. N. *Tetrahedron Lett.* **1991**, *32*, 6533.

25) Sheldon, R.; Kochi, J. *Metal-Catalyzed Oxidations of Organic Compounds*; Academic Press: New York, 1981.

26) O'Connor, K. J.; Wey, S. J.; Burrows, C. J. *Tetrahedron Lett.* **1992**, *33*, 1001.

27) Kureshy, R.; Khan, N.; Abdi, S.; Bhatt, A. *J. Mol. Catal. A: Chem.* **1996**, *110*, 33.

28) Noda, K.; Hosoya, N.; Irie, R.; Ito, Y.; Katsuki, T. *Synlett* **1993**, *7*, 469.

29) Li, Z.; Conser, K. R.; Jacobsen, E. N. *J. Am. Chem. Soc.* **1993**, *115*, 5326.

30) Fukuda, T.; Katsuki, T. *Synlett* **1995**, *8*, 825.

31) Kaufman, M.; Grieco, P.; Bougie, D. *J. Am. Chem. Soc.* **1993**, *115*, 11648.

32) Larrow, J. F.; Schaus, S. E.; Jacobsen, E. N. *J. Am. Chem. Soc.* **1996**, *118*, 7420.

33) Deng, L.; Jacobsen, E. N. *J. Org. Chem.* **1992**, *57*, 4320.

34) Hughes, D. L.; Smith, G. B.; Liu, J.; Dezeny, G. C.; Senanayake, C. H.; Larsen, R. D.; Verhoeven, T. R.; Reider, P. J. *J. Org. Chem.* **1997**, *62*, 2222.

35) Bolm, C.; Gerlach, A. *Eur. J. Org. Chem.* **1998**, 21.

36) Ogunwumi, S. B.; Bein, T. *Chem. Commun.* **1997**, *9*, 901.

37) Vankelecom, I. F. J.; Tas, D.; Parton, R. F.; Van de Vyver, V.; Jacobs, P. A. *Angew. Chem., Int. Ed. Engl.* **1996**, *35*, 1346.

38) Minutolo, F.; Pini, D.; Petri, A.; Salvadori, P. *Tetrahedron: Asymmetry* **1996**, *7*, 2293.

39) Lohray, B. B.; Thomas, A.; Chittari, P.; Ahuja, J. R.; Dhal, P. K. *Tetrahedron Lett.* **1992**, *33*, 5453.

40) De, B. B.; Lohray, B. B.; Sivaram, S.; Dhal, P. K. *Tetrahedron: Asymmetry* **1995**, *6*, 2105.

41) Karjalainen, J.; Hormi, O.; Sherrington, D. *Tetrahedron: Asymmetry* **1998**, *9*, 2019.

42) Karjalainen, J.; Hormi, O.; Sherrington, D. *Tetrahedron: Asymmetry* **1998**, *9*, 1563.

43) Pini, D.; Petri, A.; Salvadori, P. *Tetrahedron: Asymmetry* **1993**, *4*, 2351.

44) Kim, B.; Sharpless, K. *Tetrahedron Lett.* **1990**, *31*, 3003.

45) Song, C.; Yang, J.; Ha, H.; Lee, S. *Tetrahedron: Asymmetry* **1996**, *7*, 645.

46) De, B. B.; Lohray, B. B.; Sivaram, S.; Dhal, P. K. *J. Polym. Sci. A: Polym. Chem.* **1997**, *35*, 1809.

47) Minutolo, F.; Pini, D.; Salvadori, P. *Tetrahedron Lett.* **1996**, *37*, 3375.

Chapter 2. Development of Polymer-Supported Salen Complexes

2.1   Background

2.1.1   The Salen Complex

The salen ligand is a chiral Schiff base (**3**) that is the product of the reaction between 2 equiv. of a salicylaldehyde derivative (**1**) and 1 equiv. of *trans*-1,2-diaminocyclohexane (**3**). The diaminocyclohexane moiety provides chirality to the catalyst. In other related investigations,

1	**2**	**3**
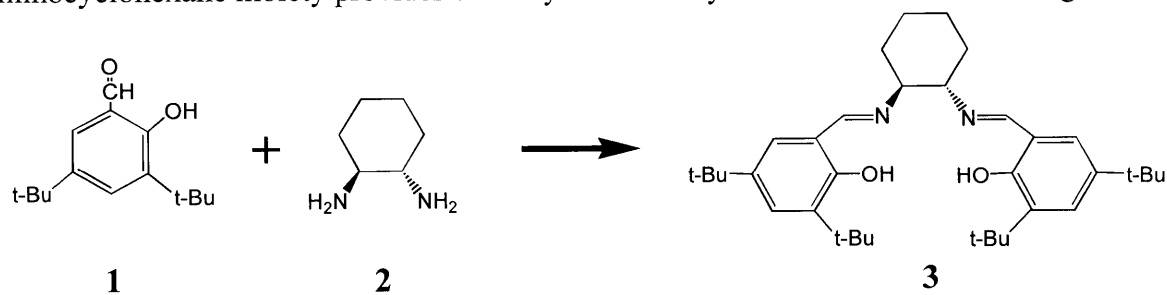
this diamine bridge has also been varied to include chiral 1,2-disubstituted ethylenediamines. In addition, a variety of substituents have been used in place of the tert-butyl groups on the phenyl portions of the ligand structure to alter the steric and electronic properties of the ligand.[1]

Since the epoxidation reaction provided the first demonstration of the enantioselective ability of catalysts employing this salen ligand, the functional aspects of this catalyst will be discussed as they pertain to this reaction. Firstly, the incorporation of Mn^{II} into the ligand results in a Mn^{III} cationic complex that is active for asymmetric epoxidation. The complex formed is thermally stable, and no precautions to exclude air, light, or moisture are necessary for the reaction.[2] The stereoselectivity exhibited by the catalyst results primarily from nonbonded interactions (Figure 2.1). Substrates do not have to contain specific functional groups to achieve the precoordination necessary for enantioselectivity as is required for directed epoxidation methods.[3] For the salen catalyst, the ligand has a nearly planar structure.[4,5] The presence of the bulky t-butyl groups restricts approach to the metal center away from approach paths **a**, **b**, and **c** (Figure 2.1). In approach **d**, facial selectivity is attributed to the larger substituent being directed away from the axial hydrogen on the bridge. In addition, one face of the catalyst has a chlorine atom bonded to the Mn and prevents approach to the metal center from that face. For this catalyst, *trans*-olefins are poor substrates due to steric interference along the approach path.[6]

The enantiomeric selectivity of the catalyst can be modified by manipulation of the steric

20
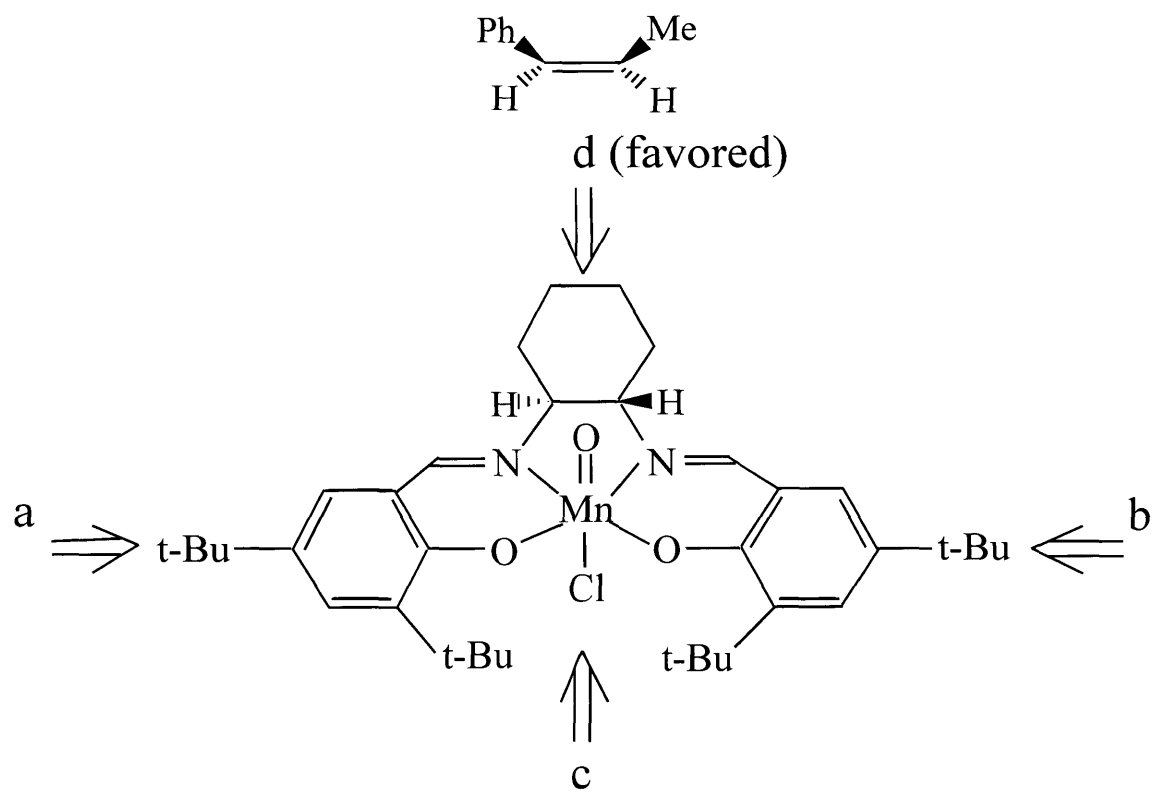
Figure 2.1. Schematic of olefin approach paths toward the active metal center of the oxo-salen complex. Approach paths **a**, **b**, and **c** are sterically hindered by the presence of the bulky *tert*-butyl groups. For reference, the complex is planar in structure with the chlorine and oxo- moieties below and above the plane about the metal center.

size and electronic properties of substituents on the salen ligand. The electronic properties of the substituents in the C5 position (the location of the outer t-butyls in Figure 2.1) provide a means of controlling the degree of enantioselectivity.[6,7] Electron-donating substituents stabilize the oxo intermediate and allow the transfer of oxygen to the alkene to proceed via a more product-like transition state. This intermediate results in more specific nonbonding interactions during the reaction and better enantioselectivity. The sterics of the catalyst are thereby more fully utilized in such a process. With electron-withdrawing groups, the reaction occurs via a more reactant-like transition state, and there is poorer steric differentiation that results in decreased selectivity.[6,8]

2.1.2 Prior Work in Heterogenizing Salen Complexes

Prior work in the area of heterogenizing a salen complex has focused exclusively on the immobilization of the Mn complex for asymmetric epoxidation. The reason for this is other than the high enantioselectivities that this complex has shown for the epoxidation reaction. Homogeneous Mn-salen complexes also undergo a dimerization process in which the catalyst is deactivated during reaction.[9,10] In this process, the cationic Mn^{III} complex (where L = salen ligand) irreversibly binds with an Mn^V-oxo complex and forms a Mn^{IV}-Mn^{IV} dimer. Therefore,

$$[(L)Mn^V = O]^+ \quad \xrightarrow{[(L)Mn^{III}]^+} \quad [(L)Mn^{IV} - O - Mn^{IV}(L)]^{2+}$$
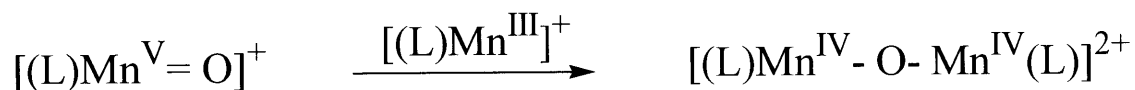
the immobilization of these moieties onto a support would prevent dimerization of the active complex and allow recycle.

A portion of prior heterogenization work with salen complexes has involved their immobilization within zeolites,[11] polymer membranes,[12] and clays.[13] In these cases, the homogeneous catalyst was synthesized within the host material and produced a salen catalyst that was either sterically confined within the rigid support structure (as was the case with zeolites and polymer membranes) or linked via cation exchange with the support structure (as in the case of clays). These attempts at immobilization have successfully demonstrated enantioselectivity toward the epoxidation of olefins (see Chapter 3.1.2 for details and comparative numbers); however, these heterogeneous catalysts exhibited a loss of enantioselectivity upon recycle as was reported in the cases for the zeolite and clay supports.[11,13] This decreasing selectivity upon re-

use of the catalyst could be construed as loss of catalyst and a result of the method of immobilization. Some of these techniques used to immobilize salen ligands involve entrapping the homogeneous ligand into a membrane or zeolite support.[11,12] Leaching and loss of the catalytic ligand may be a possibility for these heterogeneous systems.[14]

Covalent attachment of the salen complex to a support would offer a more robust system for recycle and separations. Polymers, in particular, have demonstrated success as supports in a range of applications including the immobilization of reagents for peptide synthesis[15-17] and metal complexes for the catalytic hydrogenation of olefins.[18-21] The attachment of salen complexes onto a polymeric support could be performed by either of two methods: (i) by polymerization or copolymerization of monomers that contain the preformed complex and polymerizable moieties, or (ii) by chemical modification of accessible functional groups on a preformed polymer.

Prior studies have focused on the first strategy to incorporate homogeneous salen ligands containing pendant vinyl groups covalently into a polymerizing matrix. The homogeneous
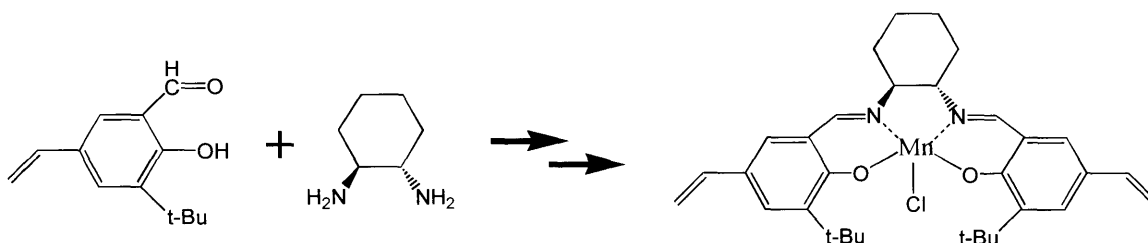
salen units function as a monomer within the mixture. The resulting heterogeneous catalysts have had only moderate success in terms of their enantioselective performance[22-25] (see Chapter 3.1.2). Their lower enantioselectivity is likely due to interference between the macrocyclic structure of the salen complex that governs its chiral discrimination and the proximal structure of the support. The use of multipoint attachment of the salen complex to the polymer causes the approach paths to the metal center as directed by the ligand structure to be altered and the enantioselective ability of the catalyst to be impeded. In addition, this strategy generates catalytic sites within the polymer matrix that may remain inaccessible and thus inactive. The reports using this strategy have suggested unaltered enantioselectivity upon recycle of the heterogeneous catalysts; however, no demonstration of recycle has been published.

2.2   Immobilization Methodology

2.2.1   Synthetic Strategy

With the suggestion of continued performance upon recycle for the covalently linked salen systems, the challenge was to develop an immobilized salen complex that would not be confined rigidly within a support and could provide enantioselectivities like its homogeneous counterpart. At address this issue, a surface modification strategy was used to produce a covalently attached salen complex on a polymer. In particular, polymer supports offer the potential of providing a variety of organic functional groups on their surface for which a broad range of chemistries would be available for attachment.[26]

In this approach (Figure 2.2), the first building block for the salen complex was attached by a covalent bond to pendant chloromethyl groups on the surface of a commercially available polymer resin particle that is regularly used for solid-phase peptide synthesis. The addition of successive organic building blocks to the polymer is repeated in a stepwise manner to produce the desired salen complex on the polymer surface. This solid-phase synthesis of the salen complex allows easy separation of the salen intermediates from the reagents needed for each step. This method is akin to that used in the solid-phase synthesis of peptide and nucleotides as the salen complex is constructed on the surface of a porous polymer in a stepwise manner.[16] However, unlike these other methods of solid-phase synthesis, the completed salen ligand is not cleaved from the surface as the final product is the supported complex.

The principal advantage of this methodology is that it allows the ligand to be synthesized in a sterically unhindered manner. For successful stage-wise construction of the salen complex, the sites for reaction must be readily accessible by the organic building blocks that comprise the ligand. Because of this requirement, these surface sites should also be accessible to the metal being loaded, as well as the olefins and oxidant involved in the epoxidation reactions. This degree of accessibility should maintain differences in the approach paths to the metal center and increase the stereoselectivity observed for the polymer-supported salen complexes. The accessibility should also yield a higher percentage of reactive centers for catalysis than do immobilization strategies based on copolymerization.

This stepwise methodology also allows synthesis of the salen complex in a controlled manner. The structure of the salen complex can be selectively tuned by manipulating the substituents on the building blocks for the salen complex. The approach can also prepare
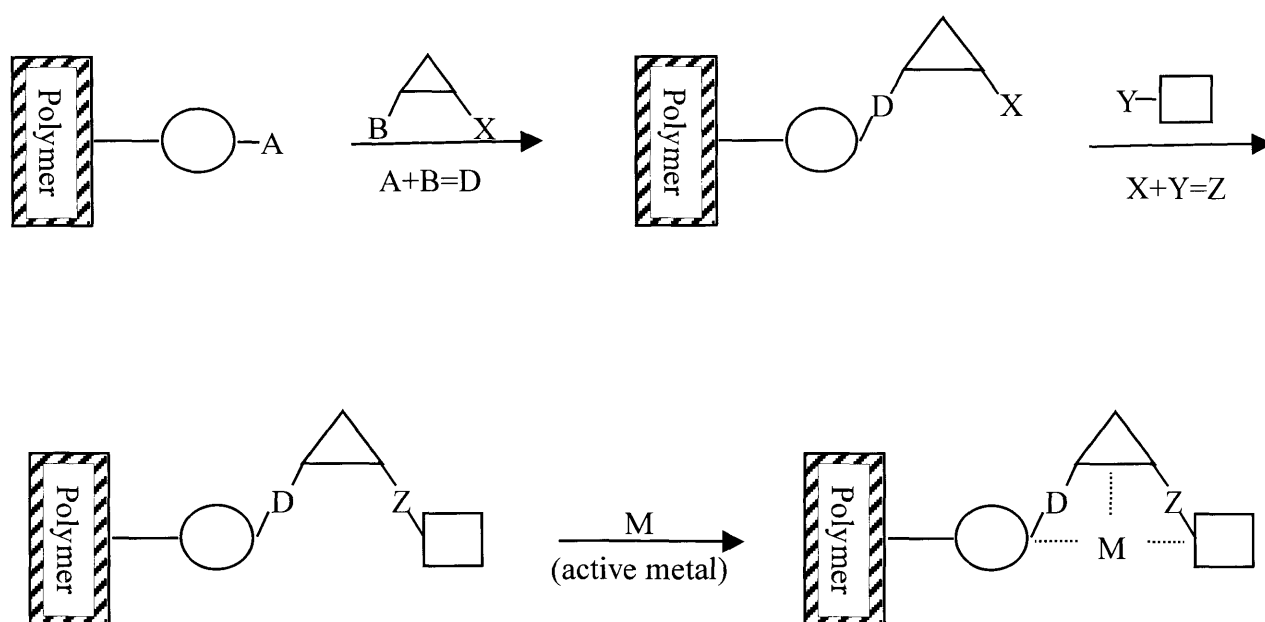
Figure 2.2. Schematic of the general method used for constructing the salen ligand on the polymer support. Sequential addition of ligand moieties allows synthetic flexibility for tuning the substituents on the asymmetric catalyst.

25

unsymmetric salen complexes on the polymer support in a straightforward manner. The preparation of such complexes is synthetically tedious because the traditional synthesis of the salen complex occurs by reaction of the central component of the ligand (a diamine) with two equivalent moieties to produce a symmetric product.[2,4,5,27-29] The reaction of two different moieties with the central component in a homogeneous reaction produces both symmetric and asymmetric ligands that might be separated from each other. Thus, the abilities to control the asymmetry of the catalyst and the placement of substituents on its framework by the solid-phase route (Figure 2.2) allow a greater capacity to modify the electronic and steric properties of the chiral catalyst and allow examination of their effect on the reactivity and selectivity of this catalyst class.[6] Therefore, this systematic approach also provides a versatile method for generating immobilized complexes that are not easily produced by homogeneous methods.

2.2.2 Synthesis of the Supported Salen Ligand

Two different polymer-bound salen ligands were synthesized by a common reaction pathway. These salen complexes (**4** and **5**) differ primarily by two hydroxyl groups in the central region of the salen ligand that chelates the metal center. The hydroxyl groups provide the tetradentate
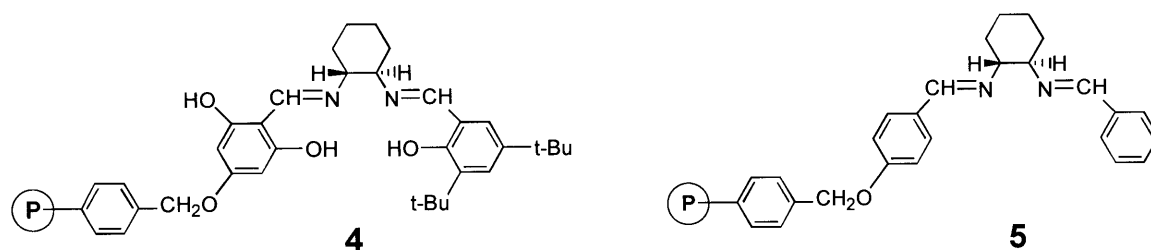
chelation required for the incorporation of metals such as Mn for asymmetric epoxidation[2,4,28] and Cr[30] and Co[31] for the kinetic resolution of epoxides. The other ligand (**5**) provides the bidentate chelating environment required for metals such as Cu that catalyze the aziridination of olefins[32,33] and was used primarily as a model compound in establishing the synthetic methodology.

The supported ligands were constructed in a sequential manner; Figure 2.3 presents the procedure for the heterogeneous synthesis of **5** on the polymer support. The pendant chloromethyl groups on the surface of Merrifield-type peptide resins (98 vol% styrene/ 2 vol% divinylbenzene) provided reactive sites for generating an ether linkage to a hydroxy-

26
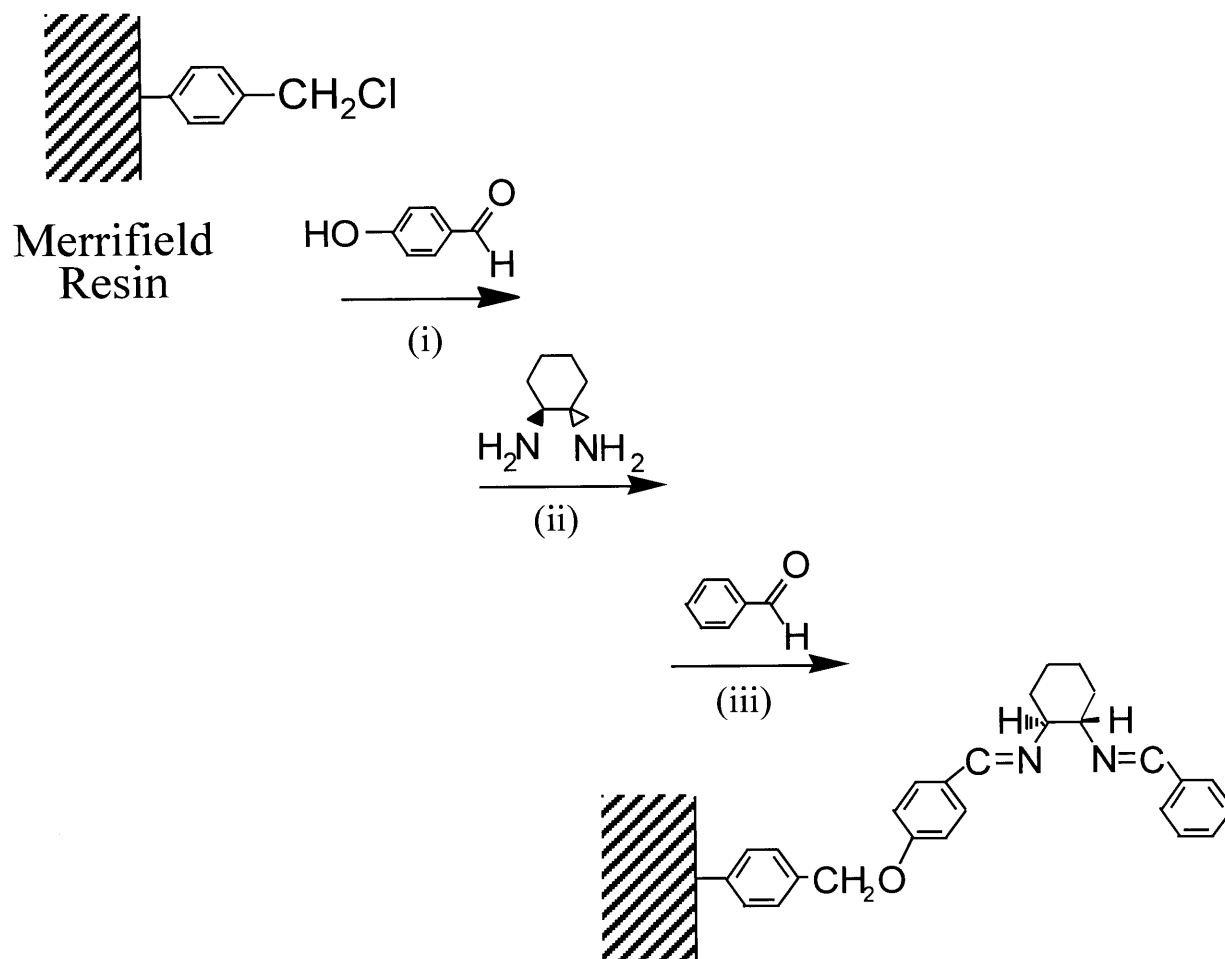
Figure 2.3. Synthetic methodology for the polymer-supported salen complex. Commercially available Merrifield resin was used as the support. Reaction conditions: (i) 4-hydroxy-benzaldehyde, K_2CO_3, and 18-Crown-6 in 1,4-dioxane; refluxed for 24 h at 95 °C. (ii) *trans*-1,2-diamino-cyclohexane in 1,4-dioxane; refluxed for 24 h at 95 °C. (iii) benzaldehyde in 1,4-dioxane; refluxed for 24 h at 95 °C. Following each stage, the resin was dried under vacuum for 24 h at 60 °C.

benzaldehyde. In the synthesis of **4**, the use of 2,4,6-trihydroxybenzaldehyde guaranteed that the attached species would contain a free hydroxyl group adjacent to the aldehyde regardless of which phenol group reacted with the resin; the free hydroxyl group is needed for tetradentate coordination of the metal center. The resulting resin was then reacted with resolved *trans*-1,2-diaminocyclohexane (either the L or D enantiomer depending on the desired chirality of the catalyst) to generate part of the diimine bridge of the salen ligand. For ligand **5**, the second imine bond was formed by reacting benzaldehyde with the free amine. Ligand **4** was constructed by reacting the generated free amine with 3,5-di-*tert*-butyl salicylaldehyde to produce a salen ligand that partially mimicked the local steric environment present in highly enantioselective salen epoxidation catalysts.[1,2,4,28]

For each reaction involved in the synthesis of **5**, 1,4-dioxane was used as solvent. For the case of **4**, N,N-dimethylformamide was substituted for 1,4-dioxane in the initial step involving 2,4,6-trihydroxybenzaldehyde for reasons of better solubility. Ethanol is typically used in the synthesis of the homogeneous complex; however, the styrene/divinylbenzene polymer support is hydrophobic, and the use of ethanol did not result in any significant reaction on the polymer surface. The selection of 1,4-dioxane as solvent was based on its use in reactions between hydroxybenzaldehyde derivatives and benzyl halides[34] and its ability to swell the polymer resin. The swelling by this solvent should increase access by the reagents to reactive sites within the polymer matrix. A drawback in the use of 1,4-dioxane in the heterogeneous synthesis was a need to use resolved 1,2-diaminocyclohexane in a free and uncomplexed state for this reaction. The diamine is resolved by forming a diastereomeric complex with enantiomerically pure tartaric acid (either L or D). For the homogenous synthesis of the catalyst, this diastereomeric complex is soluble in the reaction solvent (ethanol with 15 vol% water) and used directly.[29] As the complex was not soluble in 1,4-dioxane, the tartaric acid portion of the complex was removed from the amine-acid complex with a concentrated KOH solution[35] before reaction. The uncomplexed, resolved 1,2-diaminocyclohexane, which is soluble in 1,4-dioxane, was used in the synthetic procedure.

2.3   Characterization

2.3.1   IR Analysis

The principal evidence for construction of ligands **4** and **5** onto the polymer support is the appearance and loss of IR peaks that correspond to the introduction or transformation of distinct functional groups at each stage in the synthesis of the salen ligand. Table 2.1 provides the key IR peaks for both the heterogeneous ligands and their homogeneous counterparts. Figure 2.4 shows the spectra for the intermediates prepared in the synthesis

Table 2.1. Positions of the primary modes in IR spectra for synthesis of heterogeneous ligands and their homogeneous analogues.

Functional Group	Ligand **4** (cm^{-1})	Homogeneous Analogue (cm^{-1})	Ligand **5** (cm^{-1})	Homogeneous Analogue (cm^{-1})
Aldehydic Carbonyl (C=O)	1678	1678	1694	1690
Imine(C=N) from Reaction of Diamine with Carbonyl	1631	1631	1640	1640
Diimine (C=N) from Completed Ligand	1627	1632	1640	1642
t-Butyl groups (C-H stretch) attached to Completed Ligand	2861, 2962	2872, 2964	2867, 2964	2872, 2964

of ligand **5** along with the spectrum for the Merrifield peptide resin used in our experiments (Figure 2.4a). The peaks in the spectra from 1580-1620 cm^{-1} are assigned to the aromatic stretching modes of the polystyrene-based support and provided an internal standard for comparing spectra. Upon reaction between the resin and 4-hydroxy-benzaldehyde, the spectrum (Figure 2.4b) shows a new peak at 1694 cm^{-1} that corresponds to a carbonyl stretching vibration for the aldehyde. The assignment of this peak is supported by the IR spectrum for the product of the homogeneous model reaction between benzyl chloride and 4-hydroxybenzaldehyde (Figure 2.4c). Further evidence for the reaction on the resin is noted by a decrease in the intensity of the peak at 1265 cm^{-1} (not shown) that corresponds to the H-C-Cl wagging modes of the original chloromethylated resin.

The subsequent reaction of the aldehyde with an amine group of the diaminocyclohexane

29
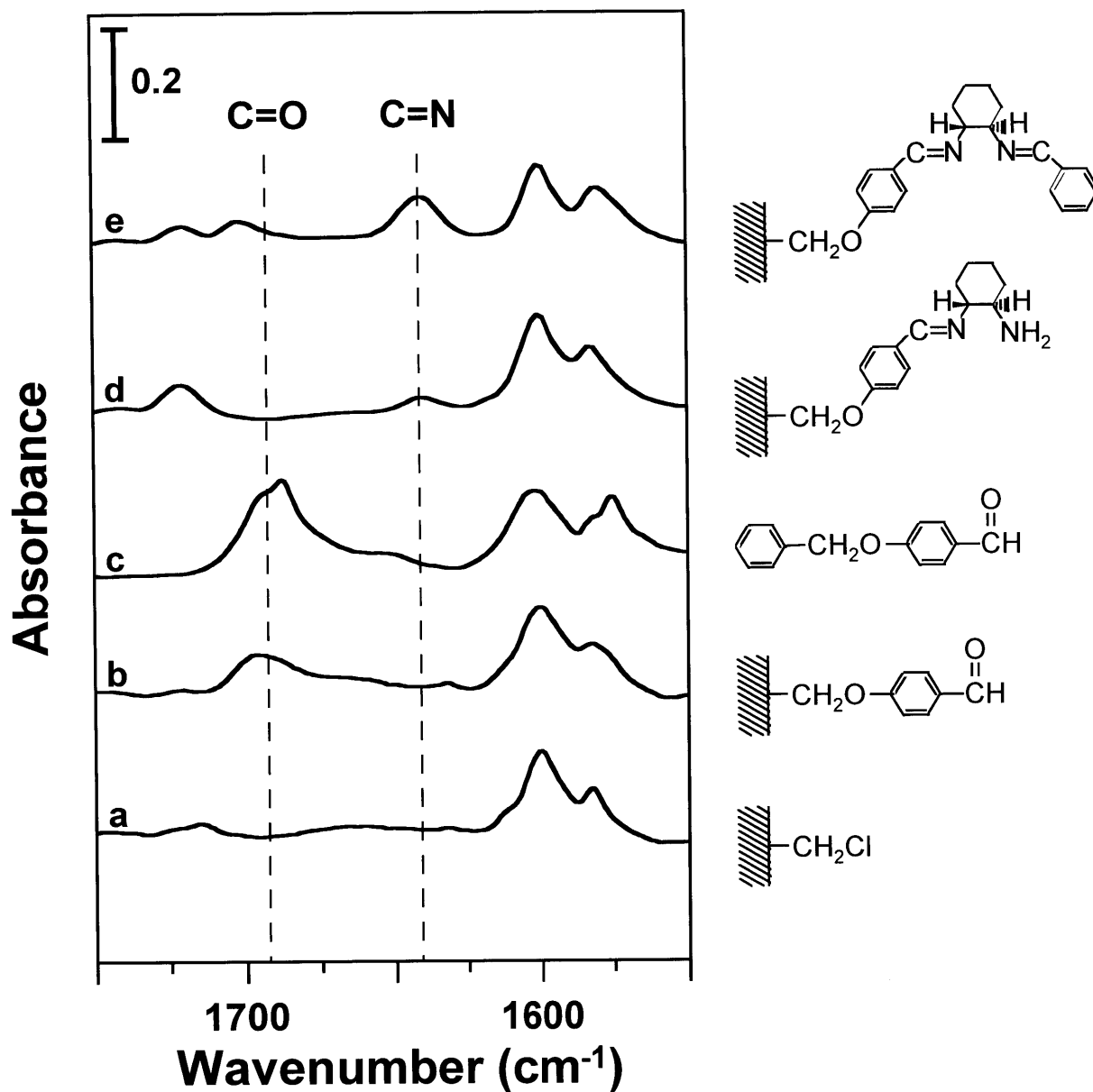
Figure 2.4. Infrared spectra for the stagewise synthesis of the anchored salen complex onto Merrifield resin (chloromethylated polymer of 98 vol% styrene and 2 vol% divinylbenzene). a) Merrifield resin; b) a + 4-hydroxybenzaldehyde; c) benzyl chloride + 4-hydroxybenzaldehyde; d) b + (+/-)-trans-1,2-diaminocyclohexane; e) d + benzaldehyde. The approximate positions of the aldehydic carbonyl and imine stretching vibrations are 1694 and 1640 cm^{-1}, respectively. The additional peak observed at 1720 cm^{-1} is an overtone band characteristic of the phenyl ring. The spectra have been offset vertically for clarity. The peaks between 1580 and 1610 cm^{-1} are aromatic stretching modes due to the polystyrene support.

produces a peak at 1640 cm^{-1} (Figure 2.4d) that corresponds to an imine (C=N) stretching vibration. In Figure 2.4d, the disappearance of the aldehydic carbonyl peak at 1694 cm^{-1} is further evidence of this reaction and its completeness on the resin surface. For comparison, the IR spectrum of a model compound produced by the homogeneous reaction between 4-hydroxy-benzaldehyde and the diamine showed an imine stretching vibration at 1642 cm^{-1}. The reaction of this resin with benzaldehyde to terminate the ligand yields an approximate doubling of the imine peak (Figure 2.4e) indicating the formation of the second imine linkage. Complementary experiments were conducted to terminate the ligand with a substituted benzaldehyde in order to provide independent spectroscopic verification that the second aldehyde was successfully linked to the support. For this purpose, I reacted 3,5-di-*tert*-butyl-2-hydroxybenzaldehyde with the polymer-bound diamine product and used the *tert*-butyl groups as spectroscopic tags for the reaction. Upon subtraction of the spectrum for the precursor resin from that for the product of this reaction, peaks at 2867 and 2964 cm^{-1} were observed in the C-H stretching region that correspond to the symmetric and asymmetric methyl vibrations of the *tert*-butyl groups, respectively. The imine stretching peak for the product formed from this benzaldehyde appeared at 1631 cm^{-1}. In the reaction of the supported diamine with the 3,5-di-*tert*-butyl-2-hydroxy-benzaldehyde, the spectrum also contained a small peak at 1696 cm^{-1}. Due to the presence of a hydroxyl group on the benzaldehyde moiety, reaction may occur between the hydroxyl groups of this compound and unreacted chloromethyl groups on the polymer surface as for the attachment of the hydroxybenzaldehydes in the initial stage of the complex synthesis. The small peak observed at 1696 cm^{-1} is most likely due to aldehyde groups on the polymer from this side reaction. The species generated from this reaction are not expected to complex Mn ions or generate catalytically reactive sites.

The IR spectra for the synthesis of **4** followed the same general stepwise spectral changes as with **5**. Due to the additional substituents on 2,4,6-trihydroxybenzaldehyde, the spectrum after the first step in the reaction sequence was not as clear as that for the product from 4-hydroxy-benzaldehyde in the synthesis of **4**. In particular, a broad doublet of peaks at 1631 and 1678 cm^{-1} was observed for the resin after reaction with 2,4,6-trihydroxybenzaldehyde. Appendix A provides the progression of IR spectra for the synthesis of the 2,4,6-trihydroxybenzaldehyde-based ligand. These same peaks were observed for the product of the homogeneous reaction between benzyl chloride and 2,4,6-trihydroxybenzaldehyde (Table 2.1).

The reaction between the anchored trihydroxybenzaldehyde and free diamine yielded a peak at 1629 cm^{-1} that was assigned to an imine. The complete loss of the aldehydic carbonyl peak at 1678 cm^{-1} provided further evidence of the surface reaction and its completeness. The peak assignment for the imine was confirmed by comparison with the IR spectrum of the product of benzyl chloride and 2,4,6-trihydroxybenzaldehyde reacted with 0.5 equivalents of the diamine (Table 2.1). The ligand-capping reaction on the polymer with 3,5-di-*tert*-butyl-2-hydroxy-benzaldehyde yielded the formation of additional imine groups as evidenced by the C=N stretching mode at 1627 cm^{-1}. As with ligand **5**, the position of the imine absorption peak after reaction with 3,5-di-*tert*-butyl-2-hydroxybenzaldehyde occurred at a lower wavenumber than that for the initial imine linkage. However, unlike ligand **5**, the change in imine intensity was not as conclusive, and the corresponding *tert*-butyl peaks of the ligand-capping moiety provided supplementary evidence as to the reaction of 3,5-di-tert-butyl-2-hydroxybenzaldehyde with the supported diamine. The spectrum for the supported trihydroxybenzaldehyde ligand showed peaks at 2861 and 2962 cm^{-1} for the methyl vibrations of the *tert*-butyl groups. Appendix A also contains the IR spectra indicating the appearance of the *tert*-butyl methyl vibrations from this final stage of synthesis.

The reaction between the 2,4,6-trihydroxybenzaldehyde and the polymer could proceed to form an ether linkage that is either ortho or para to the aldehyde moiety. To examine whether an ether linkage located ortho to the aldehyde might sterically prevent construction of the complete ligand, control experiments using the polymer resin and 2-hydroxybenzaldehyde were performed. The progression of IR spectra for this reaction product was similar to that for **5**. The IR peak for the supported carbonyl was not broadened as was the case with **4** in that hydrogen bonding between the carbonyl and adjacent hydroxyls on the aromatic was not possible (as was the case with the trihydroxybenzaldehyde moiety). This evidence of the supported carbonyl and the subsequent reaction to form the imines for the supported salen ligand demonstrated the possibility of reaction by the ortho substituents on the 2,4,6-trihydroxybenzaldehyde with the polymer resin. Appendix A provides the progression of IR spectra for the synthesis of the 2-hydroxybenzaldehyde-based, heterogeneous ligand. Reaction of the supported salicylaldehyde with 1,2-diaminocyclohexane exhibited complete conversion of the aldehydes to imines by IR. This observation suggests that attachment of 2,4,6-trihydroxybenzaldhyde to the polymer by an ortho hydroxyl group would allow formation of the complete salen ligand structure on the

polymer (as shown for **4**) with the position of complexation being the other ortho-positioned hydroxyl group.

In developing the reaction sequence, control experiments were conducted to ensure that the reactants added at each stage reacted only at the linkage site provided by the previous reaction in the ligand synthesis. This process was accomplished by omitting a step in the ligand synthesis and investigating whether a subsequent step produced any changes in the IR spectra of the resin. For the exposure of the chloromethylated resin to the diamine, no change was observed in the IR spectrum from that of the precursor spectrum. With the terminal benzaldehydes, a small peak at 1696 cm^{-1} was observed when the benzaldehyde contained hydroxyl groups. As indicated earlier, this absorption is likely a result of reaction at the surface between the hydroxyl and chloromethyl groups to form ether attachment.

Ligand **4** was loaded with manganese and chromium ions to examine the utility of the supported salen ligands for enantioselective catalysis (see Chapters 3 and 4, respectively). The addition of the metal ions also allowed assessment of the loading of active ligand on the polymer support (section 2.3.4).

2.3.2. Stability of the Supported Ligands to Solvents

The utility of a heterogeneous catalyst is based partly on the stability of the ligand. As an initial investigation into this issue, the stability of unloaded ligands **4** and **5** were examined using IR spectroscopy. The linkages between the complex and the support were investigated for their resilience to fracture or the entrapment of reactants within the polymer matrix during their synthesis. An examination of the stability of the heterogenized ligands to the specific reaction conditions for epoxidation and for the ring-opening of epoxides to trimethylsilyl-azido ethers will be discussed in more detail in Chapters 3 and 4, respectively.

The primary reason for this initial investigation was that the polymer support contained a low crosslink density (2 %) and could undergo swelling depending on the choice of solvents used for the reactions. This swelling of the polymer system in the presence of certain solvating diluents could result in the entrapping of reactants during the ligand synthesis that could be misconstrued as the immobilization of these species. In addition, the potential loss of ligand due to the low crosslink density of the polymer and its swelling would impact the use of the support as a viable catalytic system for recycle.

In these experiments, the product after each stage of the synthesis was sonicated for 1 h at room temperature in toluene or refluxed for 24 h in 1,4-dioxane or toluene (each is a swelling solvent for the polymer). For each of the polymer systems, the aromatic stretching peaks between 1570 and 1610 cm⁻¹ from the styrene/ divinylbenzene support provided an internal standard and were used for comparing the spectra of the supported ligands. The peak areas for key ligand functionalities (aldehydic carbonyls and imine groups) were normalized to that of the internal standard (aromatic stretching peaks). A comparison of the relative areas of the ligand absorptions before and after exposure to the above conditions was conducted. The results obtained for **5** are shown in Table 2.2.

Table 2.2. Relative peak area loss for functional groups of ligand **5** after solvent exposure (as measured by IR).

Functional Group	Sonication in Toluene (1h)	Reflux in Toluene (24 h)	Reflux in 1,4-Dioxane (24 h)
C=O	2 %	-2 %*	2 %
C=N (imine)	3 %	-5 %*	-5 %*
C=N (diimine from benzaldehyde)	-5 %*	1 %	1 %
C=N (diimine from 35tBu2HB)	-4 %*	NA	3 %

* A negative value implies a gain in relative peak area. After the solvent procedures, the IR peaks of the resulting resins were typically broader.

In general, I observed changes of < 5% (within the error associated with the procedure), suggesting that the supported salen complex (**5**) had relatively good stability under the synthetic conditions and under much greater stresses such as sonication. The same procedures were repeated for ligand **4**; however, since the IR spectra for the synthesis of the 2,4,6-trihydroxy-benzaldehyde-based ligand did not allow isolation of the individual IR peaks, a quantitative analysis was not possible. Qualitatively, there was no clear indication of loss of relative peak area for the key functionalities in Table 2.2 after these procedures were conducted.

2.3.3. Loading of the Supported Ligand

Ligand **4** was loaded with Mn and Cr for further examination of the reactivity and selectivity of the heterogenized ligand. Prior to this investigation, elemental analysis was used to determine the loading level of ligand **4** on the resin and the reaction yields in its synthesis. The Merrifield resin originally contained 2.0 meq Cl/ g resin, and analysis of the chlorine content after reaction to generate the supported carbonyl species suggested that approximately 90 % of the reactive sites were converted in this step. An analysis of the nitrogen composition for the final ligand structure provided an estimated loading of 0.65 meq of ligand/ g of resin. Finally, elemental analysis of the loaded ligand structure indicated that each gram of resin contained 0.13 meq of the active complex with coordinated Mn and 0.375 meq of the active complex with coordinated Cr within the salen ligands.

Of the immobilized ligand sites on a support, 20 and 58 % are loaded with Mn and Cr, respectively. The primary difficulty encountered in the loading procedures is the solubility of the metal salts. The metal salts are highly soluble in water. However, the styrene/ divinylbenzene polymer is not miscible with the aqueous metal-salt solution. Therefore, organic solutions were used for loading the immobilized ligand. In these cases, the solubility of the metal salt was reduced. Hence, an improvement of the loading procedure is likely a function of solvent selection and should be possible. As a first generation of these catalytic ligands, the activity and enantioselectivity of the ligands were examined without further optimization.

For comparison, heterogeneous analogues of Jacobsen's catalyst that were synthesized by incorporating a vinyl-substituted salen complex into the polymerization mixture are reported to contain approximately 0.6 meq of active ligand/ g polymer.[24] An important difference between these two systems is that the former loading level represents accessible ligands on the polymer surface whereas the latter include incorporated ligands within the bulk polymer that may not be active or accessible for reaction.

2.3.4. Specific Surface Area of the Heterogeneous Catalyst

The loading levels produced by this stepwise synthesis may be increased by altering the loading procedure or by increasing the specific surface area of the polymer used for constructing the ligand. In this work, commercially available peptide resins were used based on their ease of accessibility and supply; however, such resins typically have low specific surface areas.[16] As a

support for peptide synthesis, these resin properties are viewed as advantageous in offering high accessibility to immobilized species. However, the specific surface areas and loadings of this polymer support should be amenable to improvements by tailoring the structure and composition of the polymer through its synthesis.

The specific surface areas by the BET method for the peptide resins used in this study were determined to be between 0.06 and 0.2 m^2/g. As these polymers contain a low amount of crosslinker (2 vol% divinylbenzene) relative to the styrene monomer, this combination would be expected to produce a macroporous polymer with a low specific surface area.[36,37] Qualitatively, this result indicates a polymer with primarily external, accessible surface area. As a first generation of a heterogenized salen ligand, this accessibility is a highly desired characteristic.

2.4   Conclusions

The sequential reactions between a chloromethylated polymer (Merrifield resin) and a hydroxy-benzaldehyde, diaminocyclohexane, and a second aldehyde can be used to produce immobilized salen ligands on a polymer support. The construction of the covalently linked salen ligands on the resin particles was monitored through each stage of synthesis by IR analysis. Additionally, investigations of the effects of solvent on the ligand and support were examined by IR spectroscopy. These studies revealed that losses of ligand due to support swelling or potential fracture of ligand bonds was negligible. This solid-phase strategy for constructing a supported salen ligand provides a novel method to immobilize salen frameworks and should allow unhindered access to the approach paths of the catalyst. The reduced accessibility of the approach paths of the salen catalysts has been a problem that has plagued prior attempts at immobilization of this catalyst, and the strategy developed should provide an improvement in observed enantioselectivities.

2.5   Experimental

2.5.1   Materials and Instrumentation

Solvents and chemicals were obtained from Aldrich and used as received unless specified otherwise. (+/-)-*trans*-1,2-diaminocyclohexane was resolved using a procedure similar to that reported by Galsbol.[35]

Infrared spectra were recorded in transmission mode using a Bio Rad FTS 175 spectrometer. ^{1}H NMR spectra were recorded on a Bruker WM-250 (250 MHz) spectrometer and referenced to residual solvent peaks at 7.24 ppm for chloroform and 2.05 for acetone. Deuterated solvents were obtained from Cambridge Isotope Laboratories, Inc. Elemental analyses were performed by Quantitative Technologies, Inc. Specific surface areas were determined using a Quantachrome Autosorb-1 automatic volumetric sorption analyzer.

2.5.2   Synthesis of Supported Ligands 4 and 5

Supported 4-hydroxybenzaldehyde (6). A mixture of Merrifield resin (0.515 g, 2.0 mmol Cl/g), 4-hydroxybenzaldehyde (0.243 g, 2.0 mmol), potassium carbonate (0.136 g, 1.0 mmol), and 18-crown-6 (0.036 g, 0.14 mmol) in anhydrous 1,4-dioxane (20 mL) was heated at reflux under N_2 for 24 h. The product resin was collected by gravity filtration and washed thoroughly with 1,4-dioxane (50 mL) and warm distilled water (20 mL). After drying in air for 12 h, the collected resin was dried under reduced pressure for 24 h at 60 °C. IR(KBr): 1694 (C=O), 1601 (aromatic), 1265 (ω-H-C-Cl) cm^{-1}.

Supported 2,4,6-trihydroxybenzaldehyde (7). A mixture of Merrifield resin (8.11 g, 2.0 mmol Cl/g), 2,4,6-hydroxybenzaldehyde (5.0 g, 32.4 mmol), potassium hydroxide (7.2 g, 128.3 mmol), and 18-crown-6 (0.42 g, 1.59 mmol) in anhydrous DMF (135 mL) was heated at 95 °C under N_2 for 24 h. The product resin was collected by gravity filtration and washed thoroughly with DMF (150 mL) and warm distilled water (150 mL). After drying in air for 12 h, the collected resin was dried under reduced pressure for 24 h at 60 °C. IR(KBr): 1678 (C=O), 1632 (OH), 1601 (aromatic), 1265 (ω-H-C-Cl) cm^{-1}.

Supported *N*-[4-hydroxybenzylidene]-1,2-diaminocyclohexane (8) and supported *N*-[2,4,6-trihydroxybenzylidene]-1,2-diaminocyclohexane (9). (1S,2S)-1,2-Diaminocyclohexane (0.306 mL, 2.55 mmol) and anhydrous pyridine (0.412 mL, 5.1 mmol) were added sequentially

to a mixture of *6* (0.156 g) in 5 mL of anhydrous 1,4-dioxane. The mixture was stirred at reflux for 24 h. The mixture was gravity filtered, and the collected resin was washed with 1,4-dioxane (20 mL) and dried for 12 h in air and for 24 h under reduced pressure at 60 °C. This general procedure was also followed for the reaction of the diaminocyclohexane with *6*. For *8*, IR (KBr): 1640 (C=N), 1601 (aromatic) cm^{-1}. For *9*, IR (KBr): 1654 (OH), 1629 (C=N), 1601 (aromatic) cm^{-1}. Anal. Calcd(100% conversion): C, 74.90; H, 7.17; N, 6.10; Cl, 0.0. Found: C, 59.51; H, 6.29; N, 4.16; Cl, 0.10.

Supported *N*-[4-hydroxybenzylidene], *N*'-[benzylidene]-1,2-diaminocyclohexane *(10)*. A common procedure was used for reaction between the supported *N*-substituted diamines and the terminal benzaldehydes. The benzaldehyde (0.74 mmol) was added to a mixture of 83.7 mg of supported *N*-[4-hydroxybenzylidene]-1,2-diaminocyclohexane (*8* or *9*) and 5 mL of 1,4-dioxane. The mixture was stirred and refluxed for 24 h. Gravity filtration yielded the product which was rinsed with 20 mL of 1,4-dioxane, dried for 12 h in air, and dried for 24 h at 60 °C under reduced pressure. For the reaction between *8* and benzaldehyde, IR (KBr): 1640 (C=N), 1601 (aromatic) cm^{-1}. Anal. Calcd(100% conversion): C, 86.12; H, 6.70; N, 3.84; Cl, 0.0. Found: C, 83.90; H, 7.31; N, 1.82; Cl, 3.30. For the reaction between *8* and 3,5-di-*tert*-butylsalicylaldehyde , IR (KBr): 2966, 2871 (t-butyl), 1696 (C=O), 1647 (OH), 1631 (C=N), 1601 (aromatic) cm^{-1}. For the reaction between *9* and 3,5-di-*tert*-butylsalicylaldehyde, IR (KBr): 2965, 2870 (t-butyl), 1696 (C=O), 1653 (OH), 1627 (C=N), 1601 (aromatic) cm^{-1}.

Loading of polymer-supported ligand (4) with Mn. This procedure is a modification of that reported by Jacobsen et al.[29] Anhydrous DMF (230 mL) and Mn(OAc)$_2$·4H$_2$O (1.48 g, 6.0 mmol) were added to ligand **4** (3.0 g, 0.60 meq ligand/g) in a 2-neck, 250 mL roundbottom flask. The mixture was refluxed and stirred for 8 h while air was sparged through the system. The resin was collected by gravity filtration and dried in air. This resin was combined with 230 mL of 1,4-dioxane (a swelling solvent for the polymer) and tetra-*n*-butyl ammonium chloride (2.52 g, 9.1 mmol). The mixture was stirred and refluxed for 12 h, and the above procedure of filtration and drying was repeated. The collected resin was refluxed in 230 mL of a 90/10 vol% mixture of 1,4-dioxane and water for 8 h. The catalyst was then soxhleted with acetonitrile for 48 h and rinsed with hot toluene. After filtration and air-drying, the resin was dried for 24 h at 60 °C under reduced pressure. This final product was used in subsequent epoxidation reactions. Calcd(100% conversion): C, 76.81; H, 5.97; N, 3.44; Cl, 4.24; Mn, 6.57. Found: C, 80.61; H, 7.32; N, 1.69; Cl, 1.18; Mn, 0.71.

Loading of polymer-supported ligand (4) with Cr. This procedure is a modification of that reported by Martinez et al. for the homogeneous salen ligand.[38] Under an atmosphere of N_2, anhydrous, degassed THF (110 mL) and anhydrous $CrCl_2$ (0.767 g, 6.2 mmol) were added to ligand **4** (2.84 g, 2.0 meq ligand/g) in a 2-neck, 250 mL round bottom flask. The mixture was stirred for 12 h under N_2 and for 12 h in air. The supported catalyst was then stirred with saturated NH_4Cl(aq) (100 mL) for 6 h and saturated NaCl(aq) (100 mL) for an additional 6 h. The resin was collected by gravity filtration and dried in air. The collected resin was soxhleted with acetonitrile for 72 h and rinsed with hot toluene. After filtration and air-drying, the resin was dried for 24 h at 60 °C under reduced pressure. The dried product was used in enantioselective reactions. Calcd(100% conversion): C, 74.99; H, 6.99; N, 2.76; Cl, 3.52; Cr, 5.45. Found: C, 75.31; H, 7.05; N, 1.83; Cl, 3.39; Cr, 1.74.

2.5.3   Synthesis of Homogeneous Salen Analogues

Preparation of Homogeneous Salen Analogues. The following reactions were performed to produce homogeneous analogues of the intermediates generated during the synthesis of the polymer-supported salen complexes. The compounds provided reference data for assigning absorptions in the IR spectra for the polymers.

4-Benzyloxy-2,6-dihydroxybenzaldehyde *(11)*. This procedure is a modification of that reported for the synthesis of 3-benzyloxy-5-hydroxybenzaldehyde.[34] A mixture of benzyl chloride (1.1 g, 1.0 mL, 8.5 mmol), 2,4,6-trihydroxybenzaldehyde (1.44 g, 9.3 mmol), and K_2CO_3 (9.98 g, 72 mmol) in anhydrous DMF (40 mL) was heated at 100 °C for 1 h. The mixture was filtered and heated under reduced pressure. The product was obtained as a viscous, red oil in 85% yield and 85% purity by ^1H NMR. The ratio of para- to ortho-substituted products was greater than 9:1. IR: 1678 (C=O), 1632 (OH), 1600 (aromatic) cm^{-1}. ^1H NMR (CDCl$_3$, 250 MHz) δ 5.05 (s, 2H, *p*-PhC*H$_2$*O), 5.11 (s, 2H, *o*-PhC*H$_2$*O), 6.10 (m, 2H, CH$_2$), 7.29-7.47 (m, 5H, Ar*H*), 8.04 (s, 2H, OH), 10.2 (s, 1H, C*H*O).

General synthesis of related *N,N'*-**bis[benzylidene]-1,2-diamino-cyclohexane compounds.** *N,N'*-**Bis[4-hydroxybenzylidene]-1,2-diamino-cyclohexane** *(12)*. A mixture of 4-hydroxybenzaldehyde (0.221 g, 1.80 mmol) and (1S,2S)-1,2-diaminocyclohexane (0.11 mL, 0.90 mmol) in ethanol (5 mL, 95%, Pharmco) was refluxed for 1 h. The solvent was evaporated under reduced pressure to isolate the title compound in 70 % yield with a purity of 70 % by ^1H

NMR. IR(KBr): 1640 (C=N), 1607 (aromatic) cm⁻¹. ¹H NMR (CDCl₃, 250 MHz) δ 1.6-1.8 (m, 8H cyclohexyl H), 3.5 (m, 2H, cyclohexyl H), 6.8-7.5 (m, 8H, aromatic), 8.1 (s, 2H, HC=N). The syntheses of the following two compounds were identical in procedure except for their respective use of benzaldehyde and 3,5-di-*tert*-butylsalicylaldehyde.

N,N'-Bis[benzylidene]-1,2-diaminocyclohexane *(13)*. The title compound was obtained in 95 % yield with a purity greater than 95 % by ¹H NMR. IR (KBr): 1642 (C=N), 1609 (aromatic) cm⁻¹. ¹H NMR (d₆-acetone, 250 MHz) δ 1.51-1.80 (m, 8H, cyclohexyl H), 3.35 (s, 2H, cyclohexyl H), 7.32- 7.64 (m, Ar*H*), 8.21 (s, 2H, *H*C=N).

N,N'-Bis[3,5-di-*tert*-butylsalicylidene]-1,2-diaminocyclohexane *(3)*. The title compound was obtained in 70 % yield with a purity greater than 70 % by ¹H NMR. IR (KBr): 2964, 2872 (t-butyl), 1632 (C=N), 1598 (aromatic) cm⁻¹. ¹H NMR (CDCl₃, 250 MHz) δ 1.21-2.0 (m, 44H, cyclohexyl H/ t-butyl H), 3.3 (bs, 2H, cyclohexyl H), 6.95-7.27 (m, 4H, Ar*H*), 8.28 (s, 2H, *H*C=N).

2.5.4   Investigation of the Stability of Heterogeneous Ligands to Solvents

For the heterogenized ligands at each stage of their synthesis, a baseline correction to their IR spectrum was performed. The spectrum was then shifted so that the IR baseline had a minimum absorbance of zero. The peak areas were determined using the integrate function in the Bio Rad software. The relative ratio of the area of a functional group peak (carbonyl or imine) was determined with respect to the aromatic stretching vibrations of the polymer support at ~1600 cm⁻¹. These ratios were compared before and after exposure to the various solvating or sonicating conditions.

2.6　References

1)　Jacobsen, E. N. *Asymmetric Catalytic Epoxidation of Unfunctionalized Olefins*; Ojima, I., Ed.; VCH Publishers: New York, 1993, p 159.

2)　Zhang, W.; Jacobsen, E. N. *J. Org. Chem.* **1991**, *56*, 2296.

3)　Katsuki, T.; Sharpless, K. B. *J. Am. Chem. Soc.* **1980**, *102*, 5974.

4)　Zhang, W.; Loebach, J. L.; Wilson, S. R.; Jacobsen, E. N. *J. Am. Chem. Soc.* **1990**, *112*, 2801.

5)　Pospisil, P. J.; Carsten, D. H.; Jacobsen, E. N. *Eur. J. Chem.* **1996**, *2*, 974.

6)　Jacobsen, E. N.; Zhang, W.; Guler, M. L. *J. Am. Chem. Soc.* **1991**, *113*, 6703.

7)　Dumont, W.; Poulin, J.; Dang, T.; Kagan, H. B. *J. Am. Chem. Soc.* **1973**, *95*, 8295.

8)　Palucki, M. *Studies in Enantioselective Oxygen Atom Transfer Catalyzed by (Salen)Mn(III) Complexes*; PhD Thesis, Harvard University: Cambridge, 1995, p 192.

9)　Collman, J. P.; Lee, V. J.; Kellenyuen, C. J.; Zhang, X. M.; Ibers, J. A.; Braumna, J. I. *J. Am. Chem. Soc.* **1995**, *117*, 692.

10)　Razenberg, J. A. S. J.; Nolte, R. J. M.; Drenth, W. *Tetrahedron Lett.* **1984**, *25*, 789.

11)　Ogunwumi, S. B.; Bein, T. *Chem. Commun.* **1997**, *9*, 901.

12)　Vankelecom, I. F. J.; Tas, D.; Parton, R. F.; Van de Vyver, V.; Jacobs, P. A. *Angew. Chem., Int. Ed. Engl.* **1996**, *35*, 1346.

13)　Fraile, J. M.; Garcia, J. I.; Massam, J.; Mayoral, J. A. *J. Mol. Catal. A :Chem.* **1998**, *136*, 47.

14)　As was later noted (see Chapter 3.2.4), the failure of these systems upon recycle can also be attributed to issues regarding the stability of the salen complex to the oxidative conditions for epoxidation.

15)　Stewart, J. M. *Polymer-Supported Synthesis and Degradation of Peptides*; Stewart, J. M., Ed.; Wiley & Sons: New York, 1980, p 380.

16)　Merrifield, R. B. *J. Chem. Soc.* **1963**, *85*, 2149.

17)　Akelah, A.; Sherrington, D. C. *Polymer* **1983**, *24*, 1369.

18)　Jacobsen, S.; Clements, W.; Hiramoto, H.; Pittman, C. U., Jr. *J. Mol. Catal.* **1975**, *1*, 73.

19)　Pittman, C. U., Jr. *Catalysis by Polymer-Supported Transition Metal Complexes*; Pittman, C. U., Jr., Ed.; Wiley & Sons: New York, 1980, p 249.

20)　Grubbs, R. H.; Kroll, L. C. *J. Am. Chem. Soc.* **1971**, *93*, 3062.

21) Guyot, A.; Graillat, C. H.; Bartholin, M. *J. Mol. Catal.* **1977**, *3*, 39.

22) De, B. B.; Lohray, B. B.; Sivaram, S.; Dhal, P. K. *Tetrahedron: Asymmetry* **1995**, *6*, 2105.

23) De, B. B.; Lohray, B. B.; Sivaram, S.; Dhal, P. K. *J. Polym. Sci. A: Polym. Chem.* **1997**, *35*, 1809.

24) Minutolo, F.; Pini, D.; Salvadori, P. *Tetrahedron Lett.* **1996**, *37*, 3375.

25) Minutolo, F.; Pini, D.; Petri, A.; Salvadori, P. *Tetrahedron: Asymmetry* **1996**, *7*, 2293.

26) Ayres, J. T.; Mann, C. K. *Polymer Letters* **1965**, *3*, 505.

27) Hosoya, N.; Hatayama, A.; Irie, R.; Sasaki, H.; Katsuki, T. *Tetrahedron* **1994**, *50*, 4311.

28) Irie, R.; Noda, K.; Ito, Y.; Matsumoto, N.; Katsuki, T. *Tetrahedron Lett.* **1990**, *31*, 7345.

29) Larrow, J. F.; Jacobsen, E. N. *J. Org. Chem.* **1994**, *59*, 1939.

30) Larrow, J. F.; Schaus, S. E.; Jacobsen, E. N. *J. Am. Chem. Soc.* **1996**, *118*, 7420.

31) Tokunaga, M.; Larrow, J. F.; Kakiuchi, F.; Jacobsen, E. N. *Science* **1997**, *277*, 936.

32) Li, Z.; Conser, K. R.; Jacobsen, E. N. *J. Am. Chem. Soc.* **1993**, *115*, 5326.

33) Noda, K.; Hosoya, N.; Irie, R.; Ito, Y.; Katsuki, T. *Synlett* **1993**, *7*, 469.

34) Wooley, K. L.; Hawker, C. J.; Frechet, J. M. J. *J. Chem. Soc., Perkin Trans. 1* **1991**, 1059.

35) Galsbol, F.; Steenbol, P.; Sorenson, B. S. *Acta. Chem. Scand.* **1972**, *26*, 3605.

36) Wang, Q. C.; Svec, F.; Frechet, J. M. J. *J. Polym. Sci. Pt A: Polym. Chem.* **1994**, *32*, 2577.

37) Moore, J. C. *J. Polym. Sci.* **1964**, *A2*, 835.

38) Martinez, L. E.; Leighton, J. L.; Carsten, D. H.; Jacobsen, E. N. *J. Am. Chem. Soc.* **1995**, *117*, 5897.

Chapter 3. Heterogeneous Asymmetric Epoxidation of Unfunctionalized Olefins

3.1   Background

3.1.1   Enantioselectivity of Homogeneous Mn(salen) Complexes

As a proposed asymmetric catalyst, the standard by which a heterogeneous system is ultimately measured is its ability to produce one enantiomer over the other as compared to the homogeneous catalyst. This measure for enantioselectivity is termed the enantiomeric excess (ee) and is defined as

$$ee\ (\%)= \frac{C_{major} - C_{minor}}{C_{major} + C_{minor}} \times 100\ \%$$

where C_{major} and C_{minor} are the concentrations of major and minor product enantiomers in a reaction solution. This section discusses the activity and selectivity of homogeneous Mn(salen) complexes toward various olefins. In order to establish a baseline of comparison between the homogeneous and heterogeneous catalytic systems, the focus is on those olefins used to test the polymer-supported salen catalyst.

For the Mn-catalyzed asymmetric epoxidation reactions, a range of oxidants and substituted olefins were examined to test the efficacy of the homogeneous catalysts.[1] The selected olefins for investigating the catalytic ability of the heterogeneous salen complex are styrene (**14**), *cis*-β-methylstyrene (**15**), 1,2-dihydronaphthalene (DHN; **16**), and 6-bromo-2,2,3,4-tetramethyl chromene (chromene; **17**). The values for conversion, yield, and ee demonstrate the activity and enantioselectivity of the homogeneous catalyst for these olefins and are provided in Table 3.1. The literature on epoxidation reactions with these catalysts tends to utilize many different solvent systems, oxidants, reaction temperatures, and even catalyst substitution patterns. The values listed in Table 3.1 are for reaction conditions that closely mimic those used with the heterogeneous catalyst to allow a level form of comparison of the catalytic behaviors. Specifically, the reaction conditions for the homogeneous epoxidation results use CH_2Cl_2 as solvent, aqueous sodium hypochlorite as oxidant (NaOCl), and the *N,N'*-bis[3,5-di-*tert*-butylsalicylidene]-1,2-diaminocyclohexane (**3**) as the catalytic ligand. The motivation

Table 3.1. Reported Values for the Asymmetric Epoxidation of Various Olefins using Homogeneous Mn(salen) Complexes.
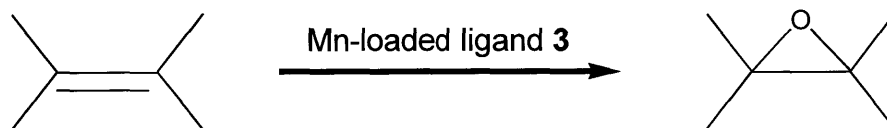
Olefin		Method[a]	Conversion (%)	Yield (%)[b]	Ee (%)[b]
Ph⟋═	**(14)**	**A**[c]	99	31	45
Ph⟋═Me	**(15)**	**B**[d]	99	84[f]	92
(naphthalene/dihydronaphthalene structure)	**(16)**	**C**[d]	99	67	86
Br-(chromene structure)-O	**(17)**	**C**[e]	99	84	85

[a] Method A: NaOCl (pH 11.35), CH_2Cl_2 as solvent, 25 °C. Method B: Same as A but at 0 °C. Method C: Same as B but with 0.2 equiv 4-phenylpyridine N-oxide employed as additive.

[b] Yields and ee's were determined using chiral capillary GC. Yields were evaluated by integration of product peaks against an internal quantitative standard.

[c] Reaction performed in our laboratory using commercially available N,N'-bis(3,5-di-tert-butylsalicylidene)-1,2-cyclohexane-diaminomanganese (III) chloride catalyst. Reported literature values involved other substituted Mn(salen) catalysts.

[d] Jacobsen, E.N. In *Catalytic Asymmetric Synthesis*, Chapter 4.2; *Asymmetric Catalytic Epoxidation of Unfunctionalized Olefins*; Ojimia, I. (Ed.); VCH Publishers: New York; pp 159-202.

[e] Brandes, B.D. and Jacobsen, E.N. *Tet. Lett.,* **1995**, 36:29, 5123.

[f] Yield is reported as a mixture of cis- and trans- products in a ratio of 11.5: 1.

for selecting these reaction parameters is explained in greater detail in Section 3.2.1.

The selected olefins span a range of substitution patterns, from mono- to tetrasubstituted. DHN, cis-β-methylstyrene, and chromene provide cases that typically produce high enantio-selectivities in the homogeneous case and serve as practical tests to the effectiveness of the Mn-loaded polymer catalyst **4**. In the homogeneous case, enantioselectivities can range from 70-98 % for these olefins depending on the substitution pattern on the catalyst structure.[2-7] Additionally, cis-β-methylstyrene provides a good test as to whether the heterogeneous catalyst is cis-selective in the formation of the resulting epoxide as is the homogeneous catalyst.[8] The homogeneous Mn(salen) complex preferentially forms the cis-epoxide with a cis/trans selectivity ranging from 3 to 29:1 for cis-β-methylstyrene depending on the oxidant used and the substitution pattern on the salen ligand.[9] For the case of ligand **3** (Table 3.1), the cis/trans ratio is 11.5.

Finally, styrene provides the test case of a terminal olefin, as mono-substituted olefins typically provide lower enantioselectivities than more highly substituted olefins. This result is due to an enantiomeric 'leakage pathway' in which isomerization occurs during production of the epoxide such that increased amounts of the minor enantiomer are generated.[10] The isomerization process also occurs for the more highly substituted olefins, but in those cases, the presence of a substituent group (R ≠ H) on the carbon-carbon double bond results in the *trans*-epoxide rather than the competing enantiomer (as is the case with R = H). As a result of isomerization, terminal olefins (where R = H) have reduced enantioselectivities as noted with ee's ranging from 30- 70% for cases such as styrene and 3,3-dimethyl-1-butene depending on the reaction conditions.[8,11,12]

3.1.2 Heterogenized Mn-Complexes: Selectivity of Prior Systems

One of the aims of heterogenizing a homogeneous catalyst is to allow recycle of the catalytic system. In particular, for Mn(salen) complexes, immobilization of the ligand would prevent dimerization of the homogeneous complex which is considered to be the principal pathway for deactivation (Chapter 2.1.2). Toward the achievement of this goal, various systems have been examined, with such attempts falling into two categories: 1) modification of the catalytic ligand to allow its covalent attachment to a surface or 2) immobilization of the homogeneous ligand by steric occlusion or cation exchange with the support. Prior results from both efforts are discussed
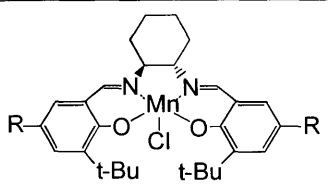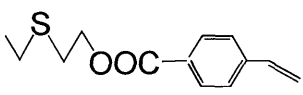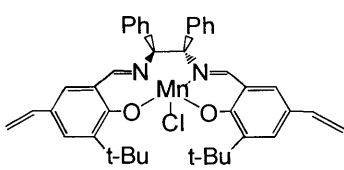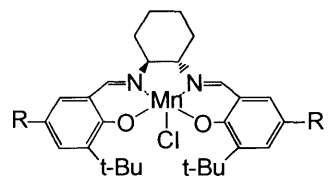
below to provide some insight into the prior research in this area and provide a reference for comparison of the polymer-supported Mn-catalyst **4** with these other heterogeneous systems. This survey provides some measure of the catalytic ability (activity and selectivity) and recyclability (if reported) for these systems.

For those systems where a salen ligand is modified for covalent attachment, pendant vinyl groups are often incorporated into the salen complexes by synthetic procedures. The complex is then copolymerized with other monomers to form a polymer matrix (which have been 10 mol % ligand monomer and either 75/15 mol % styrene/divinylbenzene or 90 % ethylene glycol dimethacrylate).[13,14] Results for these systems in the asymmetric epoxidation of various olefins are summarized in Table 3.2. The conditions for these heterogeneous epoxidation reactions differed from those for the homogeneous systems discussed earlier in their choice of oxidant (m-chloroperoxybenzoic acid (m-CPBA) or iodosylbenzene (PhIO)) and solvents (CH_2Cl_2, CH_3CN, or heptane).

The immobilized catalysts in Table 3.2 produce epoxides with lower enantioselectivities than the corresponding homogeneous catalyst. Catalysts **18** and **20** in Table 3.2 generate epoxides with ee's of 2-14 % for styrene, 41 % for *cis*-β-methylstyrene, and 10-28 % for DHN, while the corresponding homogeneous catalyst generates epoxides with ee's of 45, 92, and 86 %, respectively, for these olefins. The lower ee's for reactions using these heterogeneous catalysts may be due to the multipoint attachment of the ligand within the polymer matrix. By embedding the salen ligand and constraining its structure within a matrix, the approach paths to the metal center as directed by the ligand structure may be altered and impede the enantioselective ability of the catalyst. Support for this hypothesis is the case of **19** (Table 3.2) where the addition of a linker between the ligand and the support produced increased ee's for the epoxidation reaction (+2 % for styrene, +21 % for *cis*-β-methylstyrene, and +11 % for DHN); however, the enantioselectivities were still below those for the homogeneous catalyst. While the enantioselective ability of these immobilized catalysts are lower than their homogeneous counterpart, a claimed advantage for these systems is the recyclability of these catalysts without any change in their of activity or selectivity upon reuse.[13,15] Notably, these reported claims of recycle are not substantiated with experimental evidence.

In the alternate case where the homogeneous catalyst is immobilized by steric occlusion within a zeolite or a polymeric membrane or by cation exchange within a clay support, the ee's produced by these catalysts in the epoxidation of olefins are higher than those for the covalently

Table 3.2. Reported Values for the Asymmetric Epoxidation of Olefins using Heterogeneous Mn(salen) Complexes

Catalyst System	Catalyst	Olefin	Conversion[a] (%)	Yield[a] (%)	Ee (%)[a]
18 R= CH=CH$_2$ **19** R= (structure, OOC-styryl) (10 mol% monomer, 75 mol% styrene, 15 mol% divinylbenzene)	18[b]	styrene	96	99	14
	18[b]	cis-β-methylstyrene	78	96	41
	18[b]	DHN	95	48	10
	19[b]	styrene	98	94	16
	19[b]	cis-β-methylstyrene	92	97	62
	19[b]	DHN	99	40	21
20 (10 mol% monomer, 90 mol% ethyelene glycol dimethacrylate)	20[c]	styrene	NA	72	< 2
	20[c]	DHN	NA	70	28
21 R= Me, zeolite EMT **22** R= t-Bu, polydimethyl-siloxane membrane **23** R= t-Bu, laponite (clay)	21[d]	styrene	15	NA	34
	21[d]	cis-β-methylstyrene	15	NA	80
	22[e]	styrene	84	94	52
	22[e]	trans-β-methylstyrene	13	97	18
	23[f]	DHN	66	45	32
	23[f]	DHN	77	56	34

[a] Conversions, yields, and Ee's were determined using chiral capillary GC. Conversions and yields were evaluated by integration of peaks against an internal quantitative standard.

[b] Minutolo, F., Pini, D., Petri, A., and Salvadori, P. *Tetrahedron: Asymmetry*, **1996**, 7:8, 2293. Reaction conditions are CH$_3$CN as solvent, mCPBA/NMO as oxidant, and 0 °C.

[c] De, B.D., et al. *Tetrahedron: Asymmetry*, **1995**, 6:9, 2105. Reaction conditions are CH$_3$CN as solvent, PhIO as oxidant, and 25 °C.

[d] Ogunwumi, S.B. and Bein, T. Chem. Commun., **1997**. 9, 901. Reaction conditions are CH$_2$Cl$_2$ as solvent, NaOCl(aq) as oxidant, and 25 °C.

[e] Vankelecom, I.F.O. et al. *Angew. Chem. Int. Ed. Engl.*, **1996**, 35, 1346. Reaction conditions are heptane as solvent, NaOCl(aq) as oxidant, and 25 °C.

[f] Fraile, J.M., Garcia, J.I., Massam, J., and Mayoral, J.A. *J. Mol. Catal.*, **1998**, 136, 47. Reaction conditions are CH$_3$CN as solvent, PhIO as oxidant, and 25 °C.

linked catalytic systems (Table 3.2). For the olefins examined, the ee's approach those of the homogeneous catalyst with ee's of 52 and 80 % achieved for styrene and *cis*-β-methylstyrene, respectively (vs. 45 and 92 % for the homogeneous cases). These results are not surprising considering that fundamentally the homogeneous catalyst is being used. However, while claims of recycle have also been made for these systems, data for the clay- and zeolite- supported catalysts (**21** and **23**, respectively) suggest that reuse of the catalyst with unaltered activity and selectivity is not achieved. In both systems, subsequent reuse of the catalyst showed reduced enantioselectivity.[16,17] In addition, the catalyst leached from the membrane system due to swelling of the membrane upon exposure to solvent.[18]

As a consequence of this prior work on immobilizing a salen catalyst, a surface modification strategy (Chapter 2.2) was developed for these complexes. As was shown by the higher ee for olefin epoxidation using an increased tether length between ligand and support, less restriction of the ligand structure and approach paths upon immobilization may further increase the enantioselectivities possible with a heterogeneous system. In addition, prior work in this area indicates that immobilization of the complex by covalent attachment allows recycle without loss of activity and selectivity.

3.2   Results and Discussion

3.2.1 Selection of Reaction Parameters for Epoxidation

As mentioned in Section 3.1.1, the reaction parameters for the homogeneous and polymer-supported catalytic reactions were maintained in this work as similar as possible to establish a means of comparison. Particularly, the oxidant, NaOCl(aq), and solvent, CH_2Cl_2, were the same. The selection of NaOCl(aq) as oxidant was an issue of practicality. NaOCl(aq) is available commercially as household bleach and does not have the decomposition problems associated PhIO,[19] which disproportionates to $PhIO_2$, or the handling hazards of purified m-CPBA[20] or peroxides—all of which are other oxidants that have been used for the epoxidation reactions.[6,10,21] In addition, the ee's for the homogeneous reactions do not differ appreciably with the stoichiometric oxidant used indicating a common oxo intermediate for the active catalytic complex and allowing their interchange without affecting selectivities.[3]

The selection of CH_2Cl_2 as solvent was primarily driven by the choice of oxidant. The oxidant, in this particular case, is active for the production of racemic epoxide without the

presence of a catalyst. It was determined that by decreasing the miscibility of the reaction system with the aqueous oxidant, the competing reaction toward racemate could be reduced. This hypothesis was confirmed experimentally using the commercially available homogeneous (S,S)-catalyst (Mn-loaded **3**) for the epoxidation of DHN. The ee for this reaction with DHN varied from 37 to 82 % as the solvent was switched from CH_3CN to CH_2Cl_2. The principal explanation for this difference is that CH_3CN is readily miscible with the aqueous oxidant (NaOCl), and the oxidant activity toward production of racemate lowers the ee of the reaction system. In contrast, CH_2Cl_2 is immiscible with the aqueous oxidant solution, and the rate of racemate formation from the oxidant alone is less than the rate of oxo-transfer aided by the enantioselective catalyst. A similar decrease in ee between these two solvents was also observed for the polymer-supported catalyst (Section 3.2.2). The choice of solvent became particularly important for the polymer-supported complex as longer reaction times were necessary than for the homogeneous case (Section 3.2.2).

Additionally, 4-phenylpyridine- N-oxide, which enhances ee's slightly for the homogeneous case,[4] was used in the heterogeneous reactions. These *N*-oxide donor ligands have been suggested to enhance the mass-transfer of the hypochlorite ion from the aqueous phase to the organic phase and to stabilize the homogeneous catalytic structure during reaction.[22-24]

3.2.2   Polymer-Supported Mn-Complex: Activity and Selectivity

With the assertion of recycle without alteration of activity or selectivity for the covalently linked salen systems, the challenge becomes to develop an immobilized salen complex that combines a robust covalent link to a support with an attachment methodology that minimizes interference with the approach paths to the metal center. This latter factor may explain the decreased ee's for the reported covalently linked systems (see Section 3.1.2). The surface modification methodology developed in Chapter 2.2 is a strategy that should provide less constraint along the approach paths toward the metal center and result in an improvement in enantioselectivity.

To this effect, supported ligand **4** was loaded with Mn[II] and evaluated as an asymmetric catalyst for the epoxidation of 1,2-dihydronaphthalene (DHN), *cis*-β-methylstyrene, styrene, and 6-bromo-2,2,3,4-tetramethyl chromene using an aqueous solution of sodium hypochlorite (NaOCl) as oxidant. The conditions for these reactions were analogous to those used by others for related homogeneous catalysts (see Section 3.1.1).[3,25]
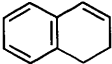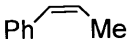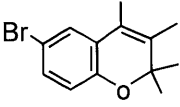
An investigation of the activity for the heterogeneous catalyst was conducted using a ligand with the (S, S)-configuration corresponding to a resolved D-*trans*-1,2-diamino-cyclohexane as the chiral moiety. The epoxidation results for DHN indicated differences in ee that depended on the solvent (Table 3.3). The ee varied from 7 to 46 % as the solvent was switched from CH_3CN to CH_2Cl_2. This trend was verified using the homogeneous catalyst where changes in ee from 37 to 82 % were observed with a change in solvent. As was noted in section 3.2.1, this result is likely due to the miscibility of the aqueous oxidant with the solvent and the reactivity of this oxidant to form racemate (ee = 0 %). In particular, with the longer required reaction times for the heterogeneous catalyst under the two-phase reaction conditions (NaOCl(aq) and CH_2Cl_2), the need to minimize the competing reaction toward racemate was paramount to achieve any significant ee. In a one-phase system, the competing reaction toward racemate dominates and does not allow the observation of enantioselectivity as produced by the catalyst.

With regard to these longer reaction times for the two-phase system of oxidant and solvent, the case of DHN provides a typical example as reaction times for complete conversion of olefin vary from 2 h for the homogeneous catalyzed reaction and 20 h for the heterogeneous counterpart. The reduced activity for the heterogeneous catalyst (by roughly a factor of 10) was not strictly limited to DHN as olefin, nor limited to this polymeric catalyst. The reactivities for the reported heterogeneous systems (Section 3.1.2) are also lower than those for the corresponding homogenous systems.[13,17] The polymeric and zeolite systems have diffusional limitations that account for their longer required reaction times. In the present catalytic system, the ligands were constructed by functionalization of accessible sites on the support surface. The specific surface areas for the resins used in this study (determined as between 0.06 and 0.2 m^2/g) as well as the low cross-link density (2 mol% divinylbenzene) both indicate a macroporous polymer structure with a primarily externally accessible surface.[26,27] As such, diffusional limitations should not be a factor.

The reactivity is most likely affected by change to the micro-environment around the ligand. For the salen complex, the epoxidation reaction is ligand accelerated. Ligand acceleration implies that the reaction rate to form epoxides is increased when Mn is incorporated into the ligand rather than simply present as a free metal salt. Using NaOCl(aq) as oxidant, the reactivity of Mn toward DHN was determined to be 60 times faster when Mn was incorporated in homogeneous salen ligand as opposed to simply using the free metal salt. Since the reaction

Table 3.3. Heterogeneous Epoxidation of Olefins with NaOCl(aq) Using Polymeric Mn-Catalyst **4**.

polymeric Mn-catalyst **4**

NaOCl(aq), solvent, 23 °C
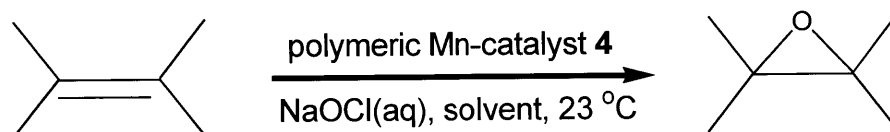
Olefin		Solvent	Time	Conversion (%)	Yield (%)[a]	Ee (%)[b]
	(16)	CH₃CN	2 h	99	56	7
"	"	CH₂Cl₂	20 h	99	42	46
Ph—	**(14)**	CH₂Cl₂	20 h	23	7	9
PhMe	**(15)**	CH₂Cl₂	20 h	93	2/27[c]	79/12[d]
	(17)	CH₂Cl₂	6 h	97	31	77

[a] Yields were determined using capillary GC by integration of product peaks against an internal quantitative standard (chlorobenzene).

[b] Ee's determined by chiral GC. Product assignments performed by comparison of elution order with authentic samples prepared using the (*S,S*)-form of Jacobsen's catalyst.

[c] Reported yields are for *cis/trans* epoxides, respectively.

[d] Ee's refer to *cis/trans* enantiomers, where the trans enantiomers were resolved using ¹H NMR in the presence of Eu(hfc)₃.

rate is accelerated by the ligand, changes to the ligand either direct or caused by its micro-environment should have an impact on its reactivity. The heterogeneous and homogeneous ligands differ in two particular ways. The heterogeneous ligand is dissymmetric (whereas the homogeneous case is C_2 symmetric) and has a non-polar microenvironment due to localization within the styrene/divinylbenzene support. In Chapter 5, the effects of dissymmetry within the ligand are detailed using homogeneous salen complexes constructed from two different aldehydic units. The reactivities of these dissymmetric homogeneous analogues were generally the same as Mn-loaded ligand **3**. This result suggests that the reduction in activity of the heterogeneous catalyst for epoxidation is likely due to its proximity to the polymer support and local changes in the catalyst's microenvironment rather than the dissymmetry of the ligand.

With regard to the selectivities of the polymer-supported catalyst, Table 3.3 shows ee's obtained with the heterogeneous complex (**4**). While the ee's for DHN and *cis*-β-methylstyrene (46 % and 79 %, respectively) are lower than those produced by the homogeneous complex (86 and 92 %, respectively, under similar conditions)[2,3,5], these values are significantly higher than those reported for heterogeneous systems that use two-point attachment of the ligand to a polymeric support (28 and 62 %, respectively).[13,15] With chromene **17**, the ee by the heterogeneous catalyst (77 %) approaches that for the homogeneous case (85 %). For this latter olefin, results from other heterogeneous systems do not exist for comparison.

The effects of the dissymmetry of the ligand and the polymer microenvironment on the enantioselectivity of the heterogeneous system need to be established. From the results in Chapter 5 investigating the ee's of these same olefins using a series of dissymmetric, homogeneous Mn(salen) ligands, there is a baseline of enantioselectivity established by the salen complex without any t-Bu substituents, and the addition of t-Bu groups serves to increase and refine the selectivity. With DHN and *s*tyrene, their baseline of enantioselectivity is much lower (25 and 5 %, respectively) than for chromene (70%). Hence, with DHN and styrene, the full steric complement of t-Bu groups is necessary to achieve a high degree of enantioselectivity; with chromene, high ee's can be achieved with less steric bulk required on the catalyst. Even without the full steric complement of t-Bu groups, the baseline of enantioselectivity for chromene is high.

When these results for the dissymmetric, homogeneous Mn(salen) ligands are compared to the heterogeneous results (Table3.3), the effect of the reduced sterics of the heterogeneous ligand are noted. With chromene, since the amount of sterics necessary to achieve high

enantioselectivity is small, the heterogeneous system does provide enantioselectivity comparable to the homogeneous system. With DHN and styrene, the reduced sterics of the heterogeneous ligand from the full complement of 4 t-Bu groups results in lower enantioselectivities than the homogeneous case. For these compounds, it was noted (Chapter 5) that high enantioselectivities required increased sterics. However, the enantioselectivities observed for DHN and styrene are even below the base case of a homogeneous Mn(salen) ligand without any t-Bu groups. It is here that the effect of the microenvironment may play a role. The impact of the microenvironment within this scheme may be in altering this baseline of enantioselectivity.

As for the enantioselectivity of products generated by the polymeric catalyst with styrene, the ee of 9 % in Table 3.3 is within the range reported for other polymer-supported salen ligands (2 to 16 %).[15,28] The lower value for styrene is consistent with the behavior of the homogeneous catalyst that also displays lower ee's with terminal olefins (50-60 %); such terminal olefins are suggested to proceed through an enantiomeric "leakage" pathway.[2,29] As discussed in section 3.1.1, this "leakage" pathway results in the production of the minor enantiomer with terminal olefins rather than the trans-products of epoxidation. The result is a reduction in the observed enantioselectivity.

The epoxidation results with cis-β-methylstyrene also may explain the low enantioselectivity of the polymer-supported catalyst for styrene. In contrast to the homogeneous case where the catalyst is cis-selective,[8] the dominant product of the reaction with the heterogeneous catalyst is the trans-epoxide (a ratio of 13:1 over the cis-epoxide). This result indicates a rotation of the carbon-carbon bond before the formation of the second carbon-oxygen bond of the epoxide. While the enantioselectivity of the trans-epoxide was only 12 % (Table 3.3), its much lower value is not surprising as the homogeneous salen-catalyst is less enantioselective for the trans-epoxide than the cis-epoxide.[2,6] The analogous rotation and collapse for styrene would produce the competing enantiomer and reduce the observed ee. The reported 12 % ee value for the case of styrene (Table 3.3) is higher than some values (< 2 %[28]) and less than others (16 %[14]) that have been reported for immobilized polymeric salen complexes using pendant vinyl groups. However, a comparative trans-selectivity for a di-substituted olefin such as cis-β-methylstyrene has not been reported in these cases as to offer a possible reason for the reduced ee values.

The enantioselectivity results for the polymer-supported salen complex are the highest reported values using a covalently linked ligand. The advantage of the present strategy is that it

covalently attaches the ligand to a support in a manner such that the ligand and approach paths to the metal center are less constrained. This reduction in the constraint of the approach paths ultimately improves the enantioselectivities that are achieved. Additionally, the methodology used for ligand construction offers the possibility for further straightforward optimization of the ligand structure because of its stepwise synthetic approach. The next section addresses the recyclability of this covalently attached salen ligand.

3.2.3 Recycle of the Polymer-Supported Mn-Complex

As a proposed asymmetric, heterogeneous catalyst, the polymeric salen complex must demonstrate potential as an enantioselective agent within a reaction mixture and also exhibit ease of separation and recyclability for the catalyst. The previous section addressed the potential utility of the supported complex as an enantioselective reagent. While the recyclability of salen-based heterogeneous catalysts for asymmetric epoxidation has been suggested in the literature, little evidence has been offered to support these claims.[13,14,17,30] This section addresses the issue of recyclability for the polymer-supported salen complex (4) for Mn-catalyzed epoxidation.

The ability to separate and recycle the polymer-supported catalyst was examined employing a simple filtration process. When resin which had been contacted with olefin and oxidant under typical reaction conditions for 40 h and was subsequently filtered on filter paper, rinsed, and dried under vacuum for reuse, the catalyst activity and enantioselectivity for epoxidation was monitored when added to a fresh reaction mixture. With the supported Mn-ligand (4), the ee's for the epoxidation reaction decreased with each use of the catalyst (as shown in Figure 3.1a for 1,2-dihydronaphthalene). For this olefin, the enantioselectivity of the catalyst decreased from 46 to 4 % ee over three uses. In addition, the catalyst was less active (Figure 3.1b) indicating a loss of catalytic sites. These results were also noted in reactions with the other olefins.

Attempts to reload the supported ligand with Mn^{II} after these recycles did not regain the initial enantioselectivity or activity for the supported complex and suggested that their loss in function was not due simply to leaching of Mn from the salen site. These results contrast the suggestions of sustained performance for other heterogeneous Mn-salen complexes upon recycle;[13-15,28,31,32] however, no data have been reported to confirm these claims or their levels of stability.
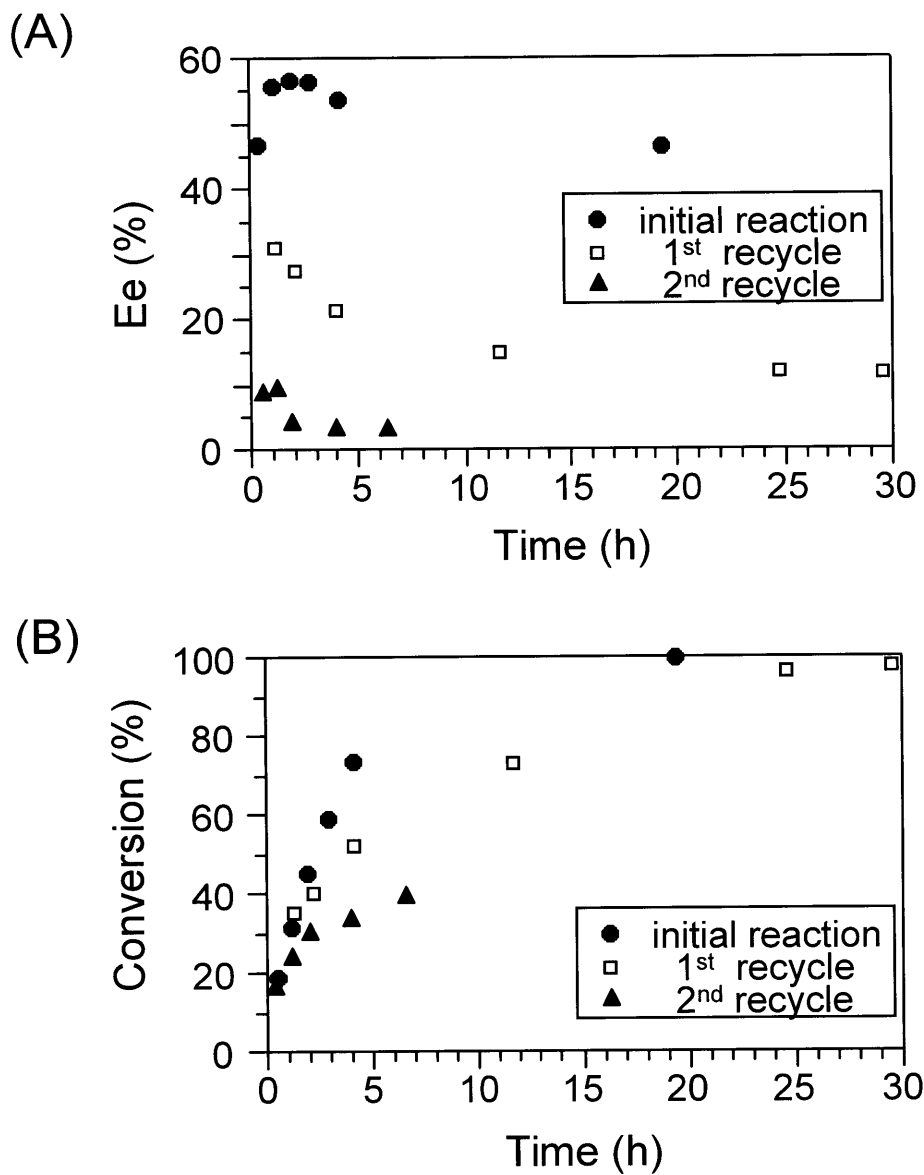
Figure 3.1. Kinetic data for freshly prepared and recycled heterogeneous Mn-ligand (**4**) for catalyzing the epoxidation of 1,2-dihydronaphthalene with NaOCl(aq) as oxidant at 22 °C. a) enantioselectivity and b) conversion of the reaction as a function of time for each run.

The observed loss of catalytic sites coupled with the suggestion of recycle with other covalently linked ligand systems indicates that either the method of ligand attachment is failing or that the ligand itself must be altered during reaction. Upon initial inspection, the prolonged exposure (up to 40 h) to oxidant may be adversely affecting the salen complex or the tether to the support resulting in a reduction in activity. This possible loss of catalytically active sites on the support would increase the impact on the ee of the competing reaction by oxidant to form racemate. The following section assesses the stability of the ether link and the salen structure to the oxidative conditions for epoxidation. This investigation is viewed as a necessary prerequisite to exploring its enantioselective potential as a recyclable catalyst in heterogeneous reactions.

3.2.4. Stability of the Supported Complex to Reaction Conditions

While the literature in the area of heterogeneous, asymmetric epoxidation using salen ligands has suggested recycle with unaltered efficiency, the results using polymer-supported salen complex (4) in section 3.2.1 indicated otherwise. This section addresses the cause of this failure to offer recyclability with unaltered activity and selectivity. Since the principal difference between catalyst (4) and the other covalently linked systems is the link to the surface, initial examination of the stability of the catalyst focused on the ether tether to the polymer surface.

For the results in Figure 3.1, the prolonged exposure (~40 h for each run) of the heterogeneous catalyst (4) to NaOCl(aq) was determined to be responsible for the degraded behavior. While reduced reaction times offered improved recyclability, the polymer continued to exhibit a decrease in activity due to loss of catalytic sites. Infrared spectra of the resin after exposure to oxidant exhibited a new peak at 1701 cm^{-1}, indicating the formation of a new carbonyl species. This peak could have resulted from either oxidation of the benzylic ether linkage or fracture of the salen imine to regenerate the supported 2,4,6-trihydroxybenzaldehyde. To investigate these possibilities, I examined the progression of IR spectra after attachment of 4-hydroxybenzaldehyde (4HB) and 2,4,6-trihydroxybenzaldehyde (246HB) to the chloro-methylated polymer support (98 vol% styrene, 2 vol% divinylbenzene; Merrifield's resin), through the synthesis of the ligand, and after their exposure to NaOCl (Figure 3.2 and Table 3.4); the 4HB ligand provided a structural analogue for comparison with the 246HB system. The aldehydic carbonyls for the 4HB and 246HB supported ligands appear at 1694 and 1678 cm^{-1}, respectively. As the ligand structures are completed by sequential additions of diamino-

P—⎡ ⎤—CH₂Cl

HO—⬡—C(=O)H (p-Hydroxybenzaldehyde structure)

OH O, HO, OH, H (2,4,6-trihydroxybenzaldehyde structure)

Attached p-Hydroxybenzaldehyde:

Absorbance

1800 1700 1600 1500

1800 1700 1600 1500

(i)
(ii)

(i)
(ii)

Constructed Salen Ligand:

Absorbance

1800 1700 1600 1500

1800 1700 1600 1500

(iv)

(iii)
(iv)

After Exposure to NaOCl:

Absorbance

1800 1700 1600 1500

1800 1700 1600 1500

Wavenumber (cm⁻¹)

Conditions

(i) H_2N NH_2 (cyclohexane diamine)

(ii) t-Bu, O, t-Bu, OH, H (di-tert-butyl salicylaldehyde)

(iii) $Mn(OAc)_2$ in DMF/NaCl(aq)

(iv) CH_2Cl_2/ NaOCl(aq)

For comparison:

P—⬡—CH(=O)

I 0.05

1800 1700 1600 1500

Wavenumber (cm⁻¹)

Figure 3.2. Progression of IR spectra for two salen-based heterogeneous ligands through construction and after exposure to NaOCl(aq). The 4-hydroxybenzaldehyde-based ligand is provided for comparison to the 2,4,6-trihydroxybenzaldehyde-based ligand. The IR spectrum of a formylated resin is also shown for comparison to that of the ligands after their exposure to the oxidant. The dashed and solid lines mark the positions for the aldehydic and diimine peaks, respectively, for the corresponding ligands, with the lower three panels displaying aldehydic peaks at a common position (~1700 cm⁻¹).

-cyclohexane and 3,5-di-*tert*-butyl-2-hydroxybenzaldehyde, the aldehydic peaks are replaced in the spectra by peaks for the diimine at 1640 and 1627 cm^{-1}, respectively. Upon exposure

Table 3.4. Infrared Peak Assignments (cm^{-1}) for Heterogeneous Ligands Before and After Exposure to NaOCl(aq).

	Infrared Peaks (cm^{-1})		
Functional Group	**4HB Ligand**	**246HB Ligand**	**Formylated Resin**
Aldehydic carbonyl	1694	1678	1700
Imine[a]	1640	1629	1640
Diimine[b]	1640	1627	NA
Aldehydic carbonyl (after exposure to NaOCl)	1699	1701	NA
Imine (produced with carbonyl formed from exposure)	1642	1642	NA

[a] Functional group formed from the reaction of 1,2-diaminocyclohexane with supported carbonyl moieties.

[b] Second imine bond formed during reaction of benzaldehydic unit with supported diamino-cyclohexane moieties.

of the two ligand structures (with the 246HB ligand loaded with Mn^{II} prior to this step) to NaOCl(aq), the resulting spectra suggest formation of a common derivative as both samples exhibit a peak at ~1701 cm^{-1}. This peak position is the same as for a formylated resin (1700 cm^{-1}) and is greatly shifted from the positions of the aldehydes that would result from cleavage of the imines (i.e., 1694 and 1678 cm^{-1} for the 4HB and 246HB ligands, respectively). As a control, the chloromethylated resin was similarly exposed to NaOCl and did not exhibit an IR absorption peak at 1700 cm^{-1}. Further suggestion of their common structure was obtained by the reaction of these resins with diaminocyclohexane after their exposure to NaOCl. In both cases, the resulting imines showed a common peak at 1642 cm^{-1} and had the same peak position as the imine produced by reaction of the formylated resin with diaminocyclohexane.

Fracture of the ether tether was also examined under the reaction conditions for epoxidation using benzyl phenyl ether as a homogeneous model for the heterogeneous link. A solution of this compound was exposed to NaOCl(aq) under the conditions for the heterogeneous reactions, and aliquots of the solution were characterized by gas chromatography to quantify any loss of this compound against an internal standard (chlorobenzene). Degradation of the ether and

formation of benzaldehyde, indicating the ability of this linkage to fragment under the reaction conditions, was consistently observed.

Since IR and GC studies both indicated that fracture of the ether was a likely mechanism that resulted in cleavage of the catalytic ligand from the surface, other chemistries for attachment were evaluated to provide a covalent link to the surface that would be able to withstand the oxidative conditions for epoxidation. Sulfur links to the surface were examined. Initial studies were conducted in the homogeneous phase using benzyl sulfide and benzyl sulfone as the model compounds for considered links. As before, the peak areas associated with these compounds were monitored by GC relative to an internal standard (chlorobenzene). Figure 3.3 shows the variation in sulfide and sulfone concentration with time under the reaction conditions. While the sulfide link (thioether) fractured completely in NaOCl(aq) within 2 h, the sulfone link remained intact for at least 24 h of exposure to the oxidative conditions for epoxidation. Partial oxidation of the sulfide to a sulfone appears to stabilize the link against to the oxidative conditions required for epoxidation. For benzyl sulfide, the sulfone was not a product of the oxidative conditions for epoxidation.

While the sulfur link to the surface seemed to provide a viable option to the cleavage problems associated with the ether link, various other observations with the heterogeneous system (4) during the epoxidation reaction indicated that the ether functionality was not the only obstacle to producing a stable heterogeneous system. As part of the stability study of the heterogeneous ligand, GC and ^{1}H NMR were used to characterize the decomposition products present in solution. The principal species observed was 3,5-di-*tert*-butyl-2-hydroxy-benzaldehyde— the compound used to form the second imine of the supported complex — suggesting that imine cleavage within the salen complex is an additional pathway for loss of catalytic behavior beyond the cleavage of the ethereal tether. In addition, the reaction solution contained *N*-[3,5-di-*tert*-butyl-2-hydroxybenzylidene]-1,2-diaminocyclohexane–the compound formed from cleavage of only the first imine of the supported complex–and no evidence of the complex that would form by cleavage of the ether alone. The ^{1}H NMR of the partial degradation product, *N*-[3,5-di-*tert*-butyl-2-hydroxybenzylidene]-1,2-diaminocyclohexane, was confirmed using a standard synthesized independently. These latter results indicate that the stability of the imine groups that comprise the salen ligand also poses a challenge to creating a recyclable heterogeneous complex for epoxidation.

The stability of the imine functionality to the epoxidation conditions was further
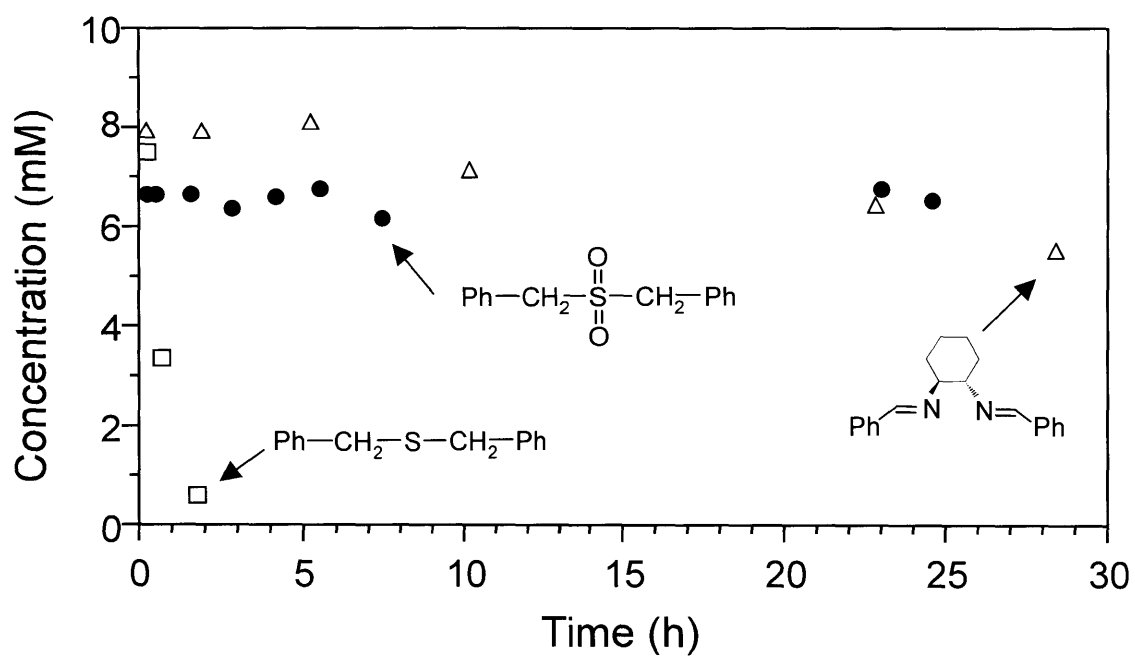
Figure 3.3. Stability experiments of two sulfur-based model compounds and a diimine analogue through exposure to the epoxidation conditions. The conditions of exposure mimicked that for the epoxidation reaction with the exception of catalyst. The loss in compound peak was monitored against chlorobenzene (internal standard) using GC.

investigated using a homogeneous diimine-containing model compound (12) that was synthesized from diaminocyclohexane and two equivalents of benzaldehyde (Figure 3.3). The hydroxyl groups in the interior of the salen ligand that are necessary for tetradentate ligation of the metal were purposely omitted from this ligand to minimize its partitioning into the basic NaOCl(aq) solution. Exposure of this diimine to the reaction conditions for 30 h resulted in ~25% fracture of the imine and generated benzaldehyde (as identified by GC). The reactivity of the imine bond to these conditions suggests that the salen ligand is not a suitable candidate for use as a recyclable heterogeneous catalyst for epoxidation. Figure 3.3 also shows the decomposition of N,N'-bis[benzylidene]-1,2-diaminocyclohexane with exposure time to NaOCl(aq).

The degradation of the Mn-loaded salen ligand during exposure to the epoxidation conditions has also been noted in some recent papers.[16,24] In addition, various reports indicate the use of donor ligands (such as substituted pyridine-N-oxides) to slightly enhance the stability of the Mn-salen catalyst in the epoxidation reaction.[22,24,33,34] No mechanistic details of this degradation have been reported. The presented observations regarding the lack of stability associated with the homogeneous ligand, as well as the heterogeneous version, during its exposure to NaOCl for the epoxidation reaction provide additional information to the deactivating processes occurring to the catalyst in solution (beyond the commonly cited dimerization process[35]) that prevent significant recovery and reuse of the homogeneous catalyst. These limitations directly impact the development and consideration of the homogeneous Mn-based catalysts as recyclable heterogeneous systems.

We examined alternatives to NaOCl(aq) for the heterogeneous epoxidation reactions using catalyst (2). m-Chloroperoxybenzoic acid (m-CPBA) is a commonly used oxidant with the homogeneous salen catalysts;[36] however, we observed similar reductions in activity and enantioselectivity during reuse of the heterogeneous catalyst with this oxidant. Iodosylbenzene is another commonly used oxidant for the homogeneous reaction; however, Fraile et al. and Ogunwumi et al. have reported decreased activity and enantioselectivity with clay- and zeolite-supported salen complexes upon their recycle using iodosylbenzene and NaOCl as oxidant.[16,17] The degradation of the catalyst during the epoxidation reaction appears to apply beyond NaOCl as oxidant and across polymers, zeolites, and clay as supports.[16,17] The lack of long-term stability by the framework of the homogeneous ligand to the epoxidation conditions is reflected in the poor recyclability of the homogeneous catalyst for this reaction. This observation

questions the suitability of the salen complex as a heterogenized catalyst for epoxidation, and more importantly, the extent to which reported heterogeneous, salen catalysts for epoxidation will maintain their activity and enantioselectivity upon recycle. Chapter 4 addresses the case for use of this polymer-supported salen complex as a recyclable catalyst in less severe reaction conditions.

3.3   Conclusions

Salen complexes of Mn for the catalytic asymmetric synthesis of epoxides from olefins have been immobilized onto a polymeric support. For this catalyst, 1,2-dihydronapthalene, styrene, *cis*-β-methylstyrene, and chromene form epoxides with ee's of 46, 9, 79, and 77 %, respectively, by reaction with NaOCl(aq). These values are below those for analogous homogeneous catalysts but are among the highest reported for heterogeneous versions of the Mn-based salen catalyst. The heterogeneous salen catalyst oxidatively decomposes upon exposure to the oxidant, NaOCl(aq), and a similar process appears to affect the homogeneous catalyst as well. This degradation process occurs also with oxidants such as iodosylbenzene and mCPBA that have also been used for these epoxidation reactions. This decomposition severely limits the potential utility of heterogenized salen complexes for use in epoxidation reactions and limits the extent to which either the heterogeneous or homogeneous catalyst can be recycled for such reactions. Additionally, this decomposition suggests a process in solution,[16,24] beyond the commonly cited inactivation process involving a Mn^{IV} dimer,[35] that prevents recycle of the homogeneous catalyst for this reaction.

3.4 Experimental

3.4.1 Materials

Solvents and chemicals were obtained from Aldrich and used as received unless specified otherwise. Deuterated solvents were obtained from Cambridge Isotope Laboratories, Inc. Styrene, styrene oxide, 1,2-dihydronaphthalene, and 1-phenyl propylene oxide (epoxide of *cis*-β-methylstyrene) were obtained from Aldrich and used as received as reactants and GC calibration standards. The oxidant, NaOCl(aq), was prepared as a 0.55 M solution from Clorox household bleach (buffered with 0.05 M Na_2HPO_4 and at pH = 11.35).

3.4.2 Instrumentation and Analyses

Infrared spectra were recorded in transmission mode using a Bio Rad FTS 175 spectrometer. ^{1}H NMR spectra were recorded on a Bruker DPX-400 (400 MHz) spectrometer and referenced to residual solvent peaks at 7.24 ppm for chloroform and 2.05 for acetone. Conversions, yields, and enantiomeric excesses for asymmetric reactions were determined by gas chromatography using a Hewlett-Packard HP6890 series gas chromatograph (fid detector) with a β-Dex 120 chiral phase capillary column (Supelco, Inc.; 30 m × 0.25 mm i.d., 0.25 μm film). Chlorobenzene was used as a quantitative internal standard. For the *trans*-epoxide of *cis*-β-methylstyrene, Eu(hfc)$_3$ was used to obtain the enantiomeric excess by ^{1}H NMR.[37]

3.4.3 Synthesis of Olefins and Epoxides for Use as Reactants and Calibration Standards

cis-β-**methylstyrene (14).** This compound was prepared by the procedure of Schaub et al.[38] Purification was performed by flash chromatography (SiO$_2$, 10 vol% EtOAc/ 90 vol% hexanes). The product was obtained in 30 % yield and 96 % purity by ^{1}H NMR. The ratio of *cis*- to *trans*-olefin was 89:11. ^{1}H NMR (CDCl$_3$, 400 MHz) δ 7.28 (m, 5H, Ar*H*), 6.45 (m, 1H, *cis-H* and *trans-H*), 6.25 (m, 0.11H, *trans-H*), 5.81 (m, 0.89H, *cis-H*), 1.90 (m, 3H, -C*H*$_3$).

     (1S, 2R)- 1,2-epoxy-1,2,3,4-tetraydronaphthalene. A solution of 1,2-dihydronaphthalene (3 mL, 230 mmol) and CH$_2$Cl$_2$ (184 mL) was stirred at room temperature. 4-Phenylpyridine-N-oxide (0.59 g, 3.4 mmol) and commercially available Mn-loaded (S,S)-ligand **3** (876 mg, 1.4 mmol) were added to the mixture followed by an aqueous solution of 0.55 M

NaOCl (104.4 mL). The solution was stirred for 20 h after which the phases were separated. The organic phase was dried over Na_2SO_4, filtered, and concentrated in vacuo to afford crude product. Purification by flash chromatography (SiO_2, 40 vol% EtOAc/60 vol% hexanes) resulted in product (14 % yield) with 92.7 % purity. ^{1}H NMR ($CDCl_3$, 400 MHz) δ 7.44 (dd, 1H, Ar-H), 7.25-7.21 (m, 2H, Ar-H), 7.11 (d, 1H, Ar-H), 3.88 (d, 1H, epoxide-H), 3.75 (m, 1H, epoxide-H), 2.81 (m, 1H, aliphatic-H), 2.55 (m, 1H, aliphatic-H), 2.42 (m, 1H, aliphatic-H), 1.78 (m, 1H, aliphatic-H).

6-Bromo-2,2,3,4-tetramethyl chromene (17). This compound was prepared by the procedure of Brandes.[39,40] From the four reaction steps and after purification by flash chromatography (SiO_2, 100 vol% pentane), the product was obtained in 10.7 % yield and 95 % purity by ^{1}H NMR. ^{1}H NMR ($CDCl_3$, 400 MHz) δ 7.24 (d, 1H, Ar-H), 7.17(dd, 1H, Ar-H), 6.68 (d, 1H, Ar-H), 1.96 (s, 3H, -CH_3), 1.82 (s, 3H, -CH_3), 1.39 (s, 3H, -CH_3).

6-Bromo-3,4-epoxy-2,2,3,4-tetramethyl chromene. A solution of 6-bromo-2,2,3,4-tetramethyl chromene (2.20 g at 95% purity, 7.82 mmol) and CH_2Cl_2 (9.8 mL) was stirred at room temperature. 4-Phenylpyridine-N-oxide (0.27 g, 1.53 mmol) and Mn-loaded racemic ligand 3 (243 mg, 0.38 mmol) were added to the mixture followed by an aqueous solution of 0.55 M NaOCl (32 mL). The solution was stirred for 54 h after which the phases were separated. The organic phase was dried over Na_2SO_4, filtered, and concentrated in vacuo to afford crude product. Purification by flash chromatography (SiO_2, 4 vol% EtOAc/96 vol% pentane) resulted in product (53.9 % yield) with 91 % purity. ^{1}H NMR ($CDCl_3$, 400 MHz) δ 7.49 (d, 1H, Ar-H), 7.29 (dd, 2H, Ar-H), 6.70 (d, 1H, Ar-H), 1.70 (s, 3H, -CH_3), 1.52 (s, 3H, -CH_3), 1.46 (s, 3H, -CH_3), 1.20 (s, 3H, -CH_3).

3.4.4 Representative Reaction for Mn-Catalyzed Epoxidation

Heterogeneous ligand (4) catalyzed epoxidation of 1,2-dihydronaphthalene. A solution of 1,2-dihydronaphthalene (157 µL, 1.2 mmol), CH_2Cl_2 (9.65 mL), and chlorobenzene as internal standard (24.1 µL, 237 µmol) was stirred at room temperature. 4-Phenylpyridine-N-oxide (53 mg, 3.0 mmol) and supported ligand 4 (600 mg, 0.129 meq Mn/g) were added to the mixture followed by an aqueous solution of 0.55 M NaOCl (10.9 mL). Aliquots (0.05 mL) of the reaction mixture were periodically removed and characterized by GC using a chiral phase capillary column. The samples were filtered through a pad of alumina before characterization.

Typical GC conditions were: 1.3 mL/min at constant flow, 250 °C inlet temperature, and a temperature program of a 120 °C isotherm for 40 min.

Characterization of catalyzed epoxidation of styrene by GC. Typical GC conditions were: 1.5 mL/min at constant flow, 250 °C inlet temperature, and a temperature program of a 90 °C isotherm for 30 min.

Characterization of catalyzed epoxidation of *cis*-β-methylstyrene by GC. Typical GC conditions were: 1.3 mL/min at constant flow, 250 °C inlet temperature, and a temperature program of a 110 °C isotherm for 20 min.

Characterization of catalyzed epoxidation of 6-bromo-2,2,3,4-tetramethyl chromene by GC. Typical GC conditions were: 2.1 mL/min at constant flow, 250 °C inlet temperature, and a temperature program of a 110 °C isotherm for 10 min, 5 °C /min ramp to 150 °C, 150 °C isotherm for 82 min.

3.4.5 Synthesis of Analogues for Stability Studies

Poly(p-formylstyrene) resin. This polymer was prepared by the procedure of Ayres et al.[41] IR(KBr): 1700 (C=O), 1602 (aromatic) cm^{-1}.

Supported *N*-[benzylidene]-1,2-diaminocyclohexane. (1S,2S)-1,2-Diaminocyclohexane (212 μL, 1.77 mmol) and sodium sulfite (440 mg, 3.5 mmol) were added sequentially to a mixture of poly(p-formylstyrene) resin (93.9 mg) in 10 mL of anhydrous 1,4-dioxane. The mixture was stirred at room temperature for 24 h. The mixture was vacuum filtered, and the collected resin was washed with 1,4-dioxane (20 mL) and dried for 12 h in air and 24 h under reduced pressure at 60 °C. IR (KBr): 1640 (C=N), 1601 (aromatic) cm^{-1}.

N-(benzylidene)-1,2-diaminocyclohexane. A mixture of 3,5-di-*tert*-butyl-2-hydroxybenzaldehyde (0.39 g, 1.66 mmol) and racemic *trans*-1,2-diaminocyclohexane (2.0 mL, 16.6 mmol) in ethanol (10 mL, 95%, Pharmco) was refluxed for 1 h. The solvent was evaporated under reduced pressure to isolate the title compound with excess 1,2-diaminocyclohexane. ^{1}H NMR (CDCl$_3$, 400 MHz) δ 13.72 (s, 1H, Ar-O*H*), 8.44 (s, 1H, -*H*C=N), 7.40 (s, 1H, Ar-*H*), 7.11 (s, 1H, Ar-*H*), 2.8-2.9 (m, 2H, -N*H$_2$*), 1.5-1.9 (m, 8H, cyclohexyl-*H*).

3.4.6 Stability of Homogeneous Analogues to Epoxidation Conditions by GC

Procedure for *N,N'*-bis[benzylidene]-1,2-diaminocyclohexane stability study. A solution of *N,N'*-bis[benzylidene]-1,2-diaminocyclohexane (23 mg, 79 μmol) and chlorobenzene (25 μL, 246 μmol) in CH_2Cl_2 (10 mL) was stirred at room temperature. An initial sample was characterized by GC. NaOCl(aq) (11.3 mL, 0.55 M) was added to the solution, and aliquots (1 μL) of the organic phase of the continuously stirred mixture were periodically removed and characterized by GC. Typical GC conditions were: 1.3 mL/min at constant flow, 250 °C inlet temperature, and a temperature program for a 120 °C isotherm of 10 min, 20 °C/min ramp to 200 °C, and an 200 °C isotherm for 60 min.

Procedure for benzyl sulfide and benzyl sulfone stability study. A solution of benzyl sulfide (15.7 mg, 73.3 μmol) and chlorobenzene (24.4 μL, 240 μmol) in CH_2Cl_2 (9.8 mL) was stirred at room temperature. An initial sample was characterized by GC. NaOCl(aq) (11.1 mL, 0.55 M) was added to the solution, and aliquots (1 μL) of the organic phase of the continuously stirred mixture were periodically removed and characterized by GC. Typical GC conditions were: 1.3 mL/min at constant flow, 250 °C inlet temperature, and a temperature program for a 90 °C isotherm of 10 min, 10 °C/min ramp to 200 °C, a 200 °C isotherm for 20 min, 40 °C/min ramp to 220 °C, and a 220 °C isotherm for 34 min. The same procedure and temperature program were used for the sulfide and sulfone studies.

3.5   References

1)   Jacobsen, E. N. *Asymmetric Catalytic Epoxidation of Unfunctionalized Olefins*; Ojima, I., Ed.; VCH Publishers: New York, 1993, p 159.

2)   Zhang, W.; Loebach, J. L.; Wilson, S. R.; Jacobsen, E. N. *J. Am. Chem. Soc.* **1990**, *112*, 2801.

3)   Zhang, W.; Jacobsen, E. N. *J. Org. Chem.* **1991**, *56*, 2296.

4)   Jacobsen, E. N.; Deng, L.; Furukawa, Y.; Martinez, L. E. *Tetrahedron* **1994**, *50*, 4323.

5)   Larrow, J. F.; Jacobsen, E. N. *J. Org. Chem.* **1994**, *59*, 1939.

6)   Irie, R.; Noda, K.; Ito, Y.; Matsumoto, N.; Katsuki, T. *Tetrahedron Lett.* **1990**, *31*, 7345.

7)   Hosoya, N.; Hatayama, A.; Irie, R.; Sasaki, H.; Katsuki, T. *Tetrahedron* **1994**, *50*, 4311.

8)   Palucki, M.; McCormick, G. J.; Jacobsen, E. N. *Tetrahedron Lett.* **1995**, *36*, 5457.

9)   Palucki, M. *Studies in Enantioselective Oxygen Atom Transfer Catalyzed by (Salen)Mn(III) Complexes*; Phd Thesis, Harvard University: Cambridge, 1995, p 192.

10) Palucki, M.; Pospisil, P. J.; Zhang, W.; Jacobsen, E. N. *J. Am. Chem. Soc.* **1994**, *116*, 9333.

11) O'Connor, K. J.; Wey, S. J.; Burrows, C. J. *Tetrahedron Lett.* **1992**, *33*, 1001.

12) Mikame, D.; Hamada, T.; Irie, R.; Katsuki, T. *Synlett* **1995**, *8*, 827.

13) De, B. B.; Lohray, B. B.; Sivaram, S.; Dhal, P. K. *Tetrahedron: Asymmetry* **1995**, *6*, 2105.

14) Minutolo, F.; Pini, D.; Salvadori, P. *Tetrahedron Lett.* **1996**, *37*, 3375.

15) Minutolo, F.; Pini, D.; Petri, A.; Salvadori, P. *Tetrahedron: Asymmetry* **1996**, *7*, 2293.

16) Fraile, J. M.; Garcia, J. I.; Massam, J.; Mayoral, J. A. *J. Mol. Catal. A :Chem.* **1998**, *136*, 47.

17) Ogunwumi, S. B.; Bein, T. *Chem. Commun.* **1997**, *9*, 901.

18) Janssen, K. B. M.; Laquiere, I.; Dehaen, W.; Parton, R. F.; Vankelecom, I. F. J.; Jacobs, P. A. *Tetrahedron: Asymmetry* **1997**, *8*, 3481.

19) Merkusheu, E. B. *Russ. Chem. Rev.* **1987**, *56*, 826.

20) Bortolini, O.; Campestrini, S.; DiFuria, F.; Modena, G. *J. Org. Chem.* **1987**, *52*, 5093.

21) Pietikainen, P. *Tetrahedon Letters* **1994**, *35*, 941.

22) Senanayake, C. H.; Smith, G. B.; Ryan, K. M.; Fredenburgh, L. E.; Liu, J.; Roberts, F. E.; Hughes, D. L.; Larsen, R. D.; Verhoeven, T. R.; Reider, P. J. *Tetrahedron Lett.* **1996**, *37*, 3271.

23) Skarzewski, J.; Gupta, A.; Vogt, A. *J. Mol. Catal. A: Chem.* **1995**, *103*, L63.

24) Hughes, D. L.; Smith, G. B.; Liu, J.; Dezeny, G. C.; Senanayake, C. H.; Larsen, R. D.; Verhoeven, T. R.; Reider, P. J. *J. Org. Chem.* **1997**, *62*, 2222.

25) Sasaki, H.; Irie, R.; Hamada, T.; Suzuki, K.; Katsuki, T. *Tetrahedron* **1994**, *50*, 11827.

26) Moore, J. C. *J. Polym. Sci.* **1964**, *A2*, 835.

27) Wang, Q. C.; Svec, F.; Frechet, J. M. J. *J. Polym. Sci. Pt A: Polym. Chem.* **1994**, *32*, 2577.

28) De, B. B.; Lohray, B. B.; Sivaram, S.; Dhal, P. K. *J. Polym. Sci. A: Polym. Chem.* **1997**, *35*, 1809.

29) Brandes, B. D.; Jacobsen, E. N. *J. Org. Chem.* **1994**, *59*, 4378.

30) Vankelecom, I. F. J.; Tas, D.; Parton, R. F.; Van de Vyver, V.; Jacobs, P. A. *Angew. Chem., Int. Ed. Engl.* **1996**, *35*, 1346.

31) Kureshy, R. I.; Khan, N. H.; Abdi, S. H. R.; Iyer, P. *React. Funct. Polym.* **1997**, *34*, 153.

32) De, B. B.; Lohray, B. B.; Sivaram, S.; Dhal, P. K. *Macromolecules* **1994**, *27*, 1291.

33) Chang, S. *Highly Enantioselective Catalytic Routes to Trans Epoxides by Manganese Complexes*; PhD Thesis, Harvard University: Cambridge, 1996, p 190.

34) The use of donor ligands for the heterogeneous complex was also attempted without enhancement of recyclability.

35) Collman, J. P.; Lee, V. J.; Kellenyuen, C. J.; Zhang, X. M.; Ibers, J. A.; Braumna, J. I. *J. Am. Chem. Soc.* **1995**, *117*, 692.

36) We examined the heterogeneous catalyst (**4**) using m-CPBA with 4-methylmorpholine-N-oxide (NMO). The latter compound forms a salt with the oxidant and prevents the competing reaction between the oxidant and olefin to produce a racemic product. We observed that the heterogeneous catalyst using m-CPBA/NMO as oxidant also exhibited decreased activity and enantioselectivity upon recycle.

37) Tu, Y.; Wang, Z. X.; Shi, Y. *J. Am. Chem. Soc.* **1996**, *118*, 9806.

38) Schaub, B.; Jeganathan, S.; Schlosser, M. *Chimia* **1986**, *7-8*, 71.

39) Brandes, B. D. Personal Communication, February 1998.

40) Brandes, B. D.; Jacobsen, E. N. *Tetrahedron Lett.* **1995**, *36*, 5123.

41) Ayres, J. T.; Mann, C. K. *Polymer Letters* **1965**, *3*, 505.

Chapter 4. Heterogeneous Enantioselective Ring-Opening of Epoxides

4.1 Background: Homogeneous Cr(salen) Complexes

In much the same manner that chiral epoxides are valued synthetic organic building blocks, chiral 1,2-amino alcohols are an important class of intermediates relevant to the formation of biologically-active compounds such as antibacterial agents, anti-hypertensives, and inhibitors against SIV infection.[1-3] While the need for these chiral amino alcohols has increased, the methods to produce these compounds, particularly the 1-amino-2-ols, remain limited. Traditional synthetic routes involve the reduction of α-amino acids to form racemic 2-amino-1-ols or the ring-opening of enantiomerically pure epoxides to generate chiral 1,2-amino alcohols.[4-6] Methods to synthesize chiral 1,2-amino alcohols from non-chiral reactants would have tremendous industrial application.

   With the proven efficacy of chiral salen complexes for asymmetric epoxidation, these complexes have also been used for the generation of chiral 1,2-amino alcohols. The same structural elements that govern enantioselectivity in the formation of chiral epoxides using Mn(salen) complexes are effective in the enantioselective synthesis of 1,2-amino alcohols from epoxides using Cr(salen) complexes (1).[2,7] Stereochemical communication by the ligand is

1
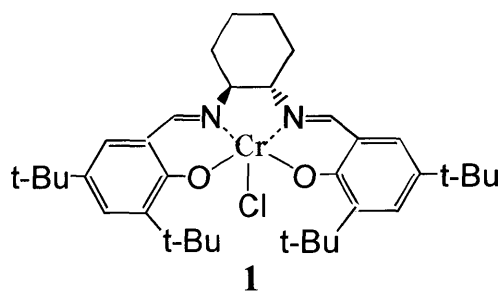
conducted in a similar manner for both classes of reaction. For the Cr-catalyzed reaction, 1,2-azido trimethylsiloxy ethers are generated from epoxides using trimethyl silyl azide (TMSN$_3$); these azido trimethylsiloxy ethers can then be easily hydrolyzed to generate the desired 1,2-amino alcohols. This asymmetric reaction works for both meso epoxides as well as racemic mixtures of epoxides.

   In the reaction with a racemic mixture of epoxides, one enantiomer is selectively ring-

opened to form a chiral azido product. The enantioselectivity of the product is determined by the enantiomeric composition of the reactant and is conversion dependent. As the "favored" enantiomeric epoxide is selectively reacted, the reactant pool becomes concentrated with the "disfavored" enantiomeric epoxide. Then, as conversion increases, the catalyst reacts to a greater extent with this "disfavored" enantiomeric epoxide and generates increasing amounts of the competing chiral, azido product. The ee of the product approaches 0 % as the conversion approaches 100 %. This process of enriching the composition of the reactant in one enantiomer is termed a kinetic resolution. Hypothetically, for a catalyst operating with 100 % selectivity, termination of the reaction at 50 % conversion would permit isolation of enantiopure azido product and enantiopure epoxide. With meso epoxides, these compounds are C_2 symmetric in that they are superimposable on their mirror images. As these compounds contain a single, achiral form, enantioselective generation of product using the Cr(salen) complex does not proceed with a kinetic resolution of the reactant. The Cr(salen) complex in the case of meso epoxides functions in the same manner as the Mn complex for epoxidation. The approach of the molecule to the metal center of the ligand and the preferred fracture of the epoxide on one face determines enantioselectivity. Also, as in the epoxidation reaction, a constant level of enantioselectivity is observed during the ring-opening of meso epoxides.

Table 4.1 presents the reported selectivities for several epoxides with Cr(salen)-1. For both meso and racemic epoxides, the enantioselectivities of the products are typically > 80 % ee and often much higher.[2,7] Cyclohexene oxide (2) provides the case of a meso epoxide as reactant. Epoxyhexane (3) and propylene oxide (4) are examples of racemic epoxides, and they undergo a kinetic resolution under the catalytic conditions. The maximum ee's reported for these reactants are 88, 97, and 97 % for cyclohexene oxide, epoxyhexane, and propylene oxide, respectively. While also exhibiting the high enantioselectivity typically observed for the Mn-catalyzed asymmetric epoxidation reaction, the Cr-catalyzed ring-opening reactions are kinetically much slower. To achieve 50 % conversion, the ring-opening reactions require from 18 to 27 h (at 0 °C) depending on epoxide while the epoxidation of olefins using mCPBA requires only several minutes for complete conversion (see Chapter 5).

As with the Mn(salen) complexes used for asymmetric epoxidation, separation of the Cr(salen) catalyst from the reaction mixture and reuse of the catalyst still remains a practical goal. With the heterogeneous Mn-catalyst for epoxidation, its poor recyclability was due to reactions with the oxidant (section 3.2.4). As the conditions associated with the asymmetric

Table 4.1. Reported Values for the Asymmetric Ring-Opening of Epoxides using Homogeneous Cr(salen) Complexes.

Cr-loaded ligand (**1**)

2 mol% catalyst, TMSN$_3$, 0 °C
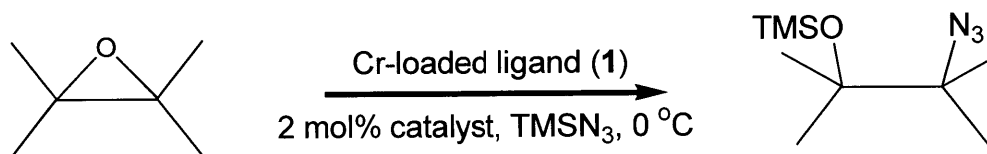
Epoxide		Time (h)	Conversion (%)	Yield (%)[c]	Ee (%)[d]
	(**2**)[f]	18	99[a]	80[a]	88
	(**3**)[g]	27	99[b]	89[b,e]	97
	(**4**)[g]	18	99[b]	98[b,e]	97

[a] Reaction had 3.0 M epoxide in diethyl ether and 1.1 equiv. TMSN$_3$ relative to epoxide.

[b] Reaction performed without solvent and 0.5 equiv. TMSN$_3$ relative to epoxide.

[c] Isolated yields.

[d] Ee's determined using chiral capillary GC.

[e] Yields based on TMSN$_3$.

[f] Martinez, L.E. et al. *J. Am. Chem. Soc.*, **1995**, 117, 5897.

[g] Larrow, J.F. et al. *J. Am. Chem. Soc.*, **1996**, 118, 7420.

ring-opening reaction are milder, a heterogeneous Cr-catalyst might offer the possibility of recyclability, and with this reasoning, the Cr-catalyzed reaction was selected as a candidate for examining the heterogenization of a homogeneous, enantioselective catalyst. The immobilization of a salen complex for the Cr-catalyzed ring-opening of epoxides had not been previously reported.

4.2   Results and Discussion

4.2.1   Selectivity and Activity of Heterogeneous Cr(salen) Complex
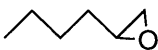
As a potentially robust system for examining the effects of heterogenizing homogeneous salen catalysts, an immobilized Cr^{III}(salen) complex (**5**) was synthesized and its ability to catalyze the enantioselective formation of azido-trimethylsiloxy ethers from epoxides was investigated. This

5
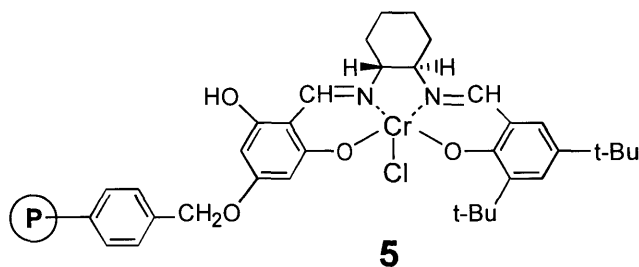
reaction was selected based on the ability of the homogeneous salen complex to perform this reaction with high enantioselectivity across many different epoxides[2,7] and operate under relatively mild conditions. The results of the Mn-catalyzed epoxidation in section 3.2.4 demonstrated the susceptibility of the salen ligand to decomposition in the presence of various oxidants. As the conditions for the asymmetric ring-opening reaction include only the epoxide and $TMSN_3$, they should not present as harsh an environment for the immobilized complex as the oxidants required for epoxidation.

These Cr-catalyzed reactions were conducted at 0 °C using 1 mol % of catalyst (0.375 mequiv/g loading) relative to the epoxide, 0.5 equiv of $TMSN_3$, and no solvent. The heterogeneous reaction using ligand **5** proceeded with moderate enantioselectivities of 34, 36, and 6 % for epoxyhexane, propylene oxide, and cyclohexene oxide, respectively (Table 4.2). The reproducibility of the enantioselectivities measured between uses of fresh catalyst was ± 2 %

Table 4.2. Heterogeneous Ring-Opening of Epoxides with TMSN$_3$ by Polymeric Catalyst **5**.[a]

Epoxide		Time	Yield (%)[b]	Ee (%)[c]
(structure)	**(2)**	44 h	40	6
(structure)	**(3)**	60 h	44	34
(structure)	**(4)**	17 h	47	36

[a] Reactions performed at 0 °C using 0.5 equiv of TMSN$_3$ relative to epoxide, no solvent, and 1 mol % of catalyst.

[b] Determined using capillary GC by normalizing product peak areas against an internal standard (chlorobenzene).

[c] Determined by chiral GC.

for each of the epoxides (as determined from at least five different runs using fresh catalyst). Over the course of the reaction, the enantioselectivity for the product of cyclohexene oxide was constant. This behavior is consistent with that for the enantioselective ring-opening of meso epoxides using a Cr(salen) complex. As a note, control experiments were conducted with Cr salt in place of Cr(salen) ligand. These reactions proceed more slowly than the reaction involving Cr-ligand, and the rates were, in fact, negligible over the time scale of the experiments conducted. Hence, the competing reaction, if any, of free Cr in solution should not impact on the ee results presented.

With epoxyhexane and propylene oxide, a slight decrease in ee (< 5 %) for the products was observed as the reaction progressed that were consistent with the kinetic resolution process. For epoxyhexane and propylene oxide, reactions for which excess $TMSN_3$ (as opposed to 0.5 equiv relative to epoxide) were provided showed a further decrease in enantioselectivity of the product as conversion increased; this behavior is further reflective of kinetic resolution occurring during reaction.

For comparison, the ee's using **5** are lower than those for the homogeneous reaction with the Cr^{III} complex (**1**) (97, 97, and 88 %, respectively)[2,7] and may be due to the dissymmetric structure and reduced sterics of the immobilized ligand, or its proximity to the support. The effects of catalyst dissymmetry and steric factors are addressed in Chapter 6 where efforts were made to elucidate their role on enantioselectivity using a series of structurally-varied homogeneous Cr(salen) catalysts. In addition, two variants of the heterogeneous ligand (**5**) were synthesized that contain only a single *t*-butyl in the lower "pocket" position (**6**) and without any *t*-butyls (**7**). The procedure for their synthesis is provided in section 4.2.2; however, discussion of the enantioselectivity of these ligands is deferred to section 6.2.5 so that comparisons can be drawn to that of the homogeneous ligand variants.

To compare the relative rates for the homogeneous and heterogeneous catalysts (**1** and **5**, respectively), their different conditions for their reactions have to be taken into account. For the heterogeneous catalyst, reactions were conducted without solvent, with 0.5 equiv $TMSN_3$, and with 1 mol % of catalyst relative to epoxide. In these cases, the reaction times to achieve 50 % conversion were 60, 17, and 44 h, respectively, for cyclohexene oxide, propylene oxide, and epoxyhexane. For the homogeneous cases,[2,7] reaction times to achieve 50 % conversion for propylene oxide and epoxyhexane were 18 and 27 h while the reaction time for 100 % conversion of cyclohexene oxide was 18 h. These reported homogeneous results were obtained

using a higher catalyst concentration (2 mol %), and the reaction with cyclohexene oxide used diethyl ether as solvent. Thus, in contrast to the epoxidation reactions where differences in reaction times of an order of magnitude were observed between the heterogeneous and homogeneous reactions (Section 3.2.2), the kinetics for the ring-opening reactions using the heterogeneous catalysts approximate those for the homogeneous reaction.

4.2.2   Recycle and Stability of Heterogeneous Cr(salen) Complex

With the immobilized Mn(salen) ligand, the heterogeneous Cr(salen) complex has indicated its utility as an asymmetric catalyst in its demonstration of enantioselective behavior. However, as a heterogeneous catalyst, the true test of this catalyst is its recyclability and, more importantly, its enantioselectivity and activity upon reuse.

To this effect, the activity and enantioselectivity of Cr-catalyst (**5**) was examined using epoxyhexane through three consecutive uses (Figure 4.1). Since the epoxyhexane is a racemic mixture, kinetic resolution of the epoxide also occurs during the reaction.[2] Figure 4.1a shows the ee as a function of time for generation of the azido products as well as the ee for residual epoxyhexane due to the kinetic resolution process. In general, the enantioselectivity of the product, as well as the kinetic resolution of the reactant, show no decline in performance between the runs.

The activity of the heterogeneous catalyst (**5**) was examined by monitoring the yield of azido trimethylsiloxy ether product as a function of time (Figure 4.1b). Analogous to the enantioselectivity, the activity of the catalyst showed no decline in performance through three uses of the catalyst. Some variation in the reaction kinetics was noted for each run. However, similar variations were also noted with the fresh catalyst. The kinetic behavior using the heterogenized Cr(salen) complex was also similar between the three epoxides tested. The linear correlation for yield as a function of time was also observed for cyclohexene oxide and propylene oxide.

Several points need to be mentioned regarding the reproducibility of the reaction kinetics for the Cr-catalyzed ring-opening reactions. The literature reports difficulties in reproducing the reaction kinetics for the homogeneous reaction and suggests a possible dependence on the degree of hydration of the catalyst.[8] From experiments using homogeneous Cr(salen) complexes (Chapter 6), the reaction kinetics were found to also depend on the order of addition of reactants
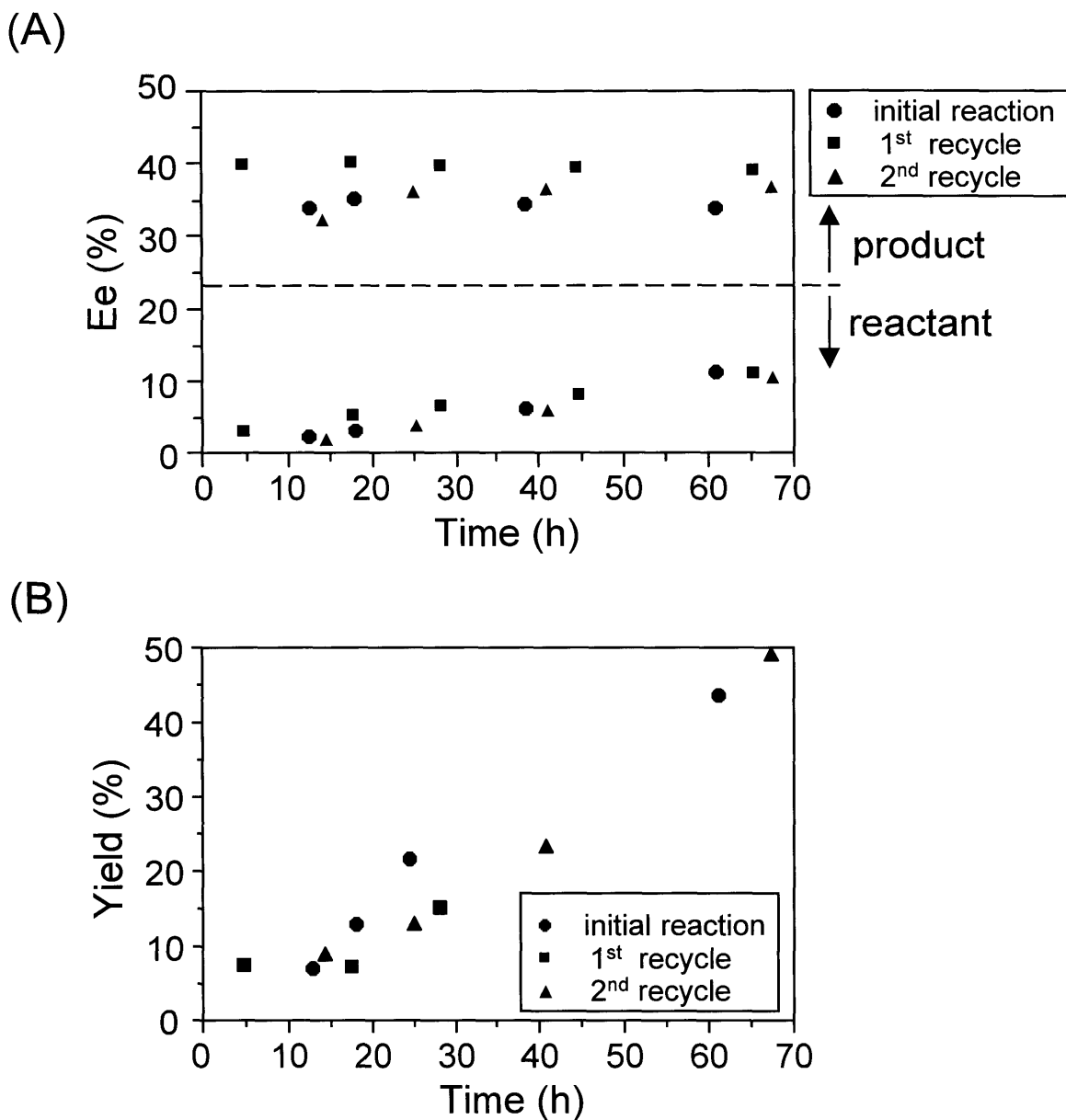
Figure 4.1. Kinetic data for freshly prepared and recycled heterogeneous Cr-ligand (5) for catalyzing the asymmetric ring-opening of epoxyhexane with $TMSN_3$ at 0 °C.
a) enantioselectivity and b) yield of the reaction as a function of time for each run.
The enantioselectivities are for the product azido-trimethylsiloxy ethers and residual reactant (epoxide) that undergoes kinetic resolution.

and the equilibration time before addition of TMSN$_3$. Reproducible kinetics were regularly achieved for the homogeneous system when the epoxide and catalyst were sequentially added and stirred for a minimum of 0.5 h before the addition of TMSN$_3$. These conditions were used for the heterogeneous runs, and their explanation is detailed in Chapter 6 through a discussion of the mechanism for the Cr-catalyzed ring-opening reaction.

Further evidence of the stability of the supported catalyst for this reaction is provided by measurement of the free Cr concentration in a solution after a reaction cycle using plasma emission spectrometry (ICP). The solution from a reaction mixture was filtered, concentrated, and dissolved in 0.9 mL of deionized water. ICP analysis indicated that the contacting solution after reaction contained 2 ppm of Cr. Based on the initial loading of the supported catalyst (0.375 mequiv/g), it was estimated that the loss corresponds to potentially hundreds of recycles of the heterogeneous catalyst. As the principal cost of these supported asymmetric catalysts is the chiral components of the ligand framework and not the metal center, the stability of the ligand framework through the reaction conditions allows reloading of the metal center into the salen ligand and regeneration of the catalytic activity for further reactions and recycle.

The stability of the heterogeneous Cr-catalyst (**5**) under the conditions for ring-opening of epoxides sharply contrasts that of the Mn-catalyst under the conditions for epoxidation of olefins. The observed stability and moderate enantioselective ability of the Cr-catalyst — the former being an often overlooked attribute in this research area — provide a starting point for further manipulation of the polymer and/or ligand structure as a means to optimize the enantioselective performance of the catalyst.

4.3   Conclusions

For the heterogenized Cr-catalyzed ring-opening of epoxides, epoxyhexane, propylene oxide, and cyclohexene oxide were converted to azido trimethylsiloxy ethers with ee's of 34, 36, and 6 %, respectively, by reaction with $TMSN_3$ at 0 °C. These values are less than those reported for the homogeneous case; however, they represent the first results for heterogenized versions of this catalyst. In contrast to the results for epoxidation, the catalyst was stable to the conditions for the ring-opening reactions as the heterogeneous catalyst could be recycled three times without loss of activity or enantioselectivity. In addition, elemental analysis indicated that the catalyst could likely be recycled hundreds of times before reloading of the Cr would be necessary. The stabilities of the salen ligand and the bound metal center for the supported Cr complexes appear sufficient for generating effective and recyclable heterogeneous catalysts.

4.4   Experimental

4.4.1   Materials and Instrumentation

Solvents and chemicals were obtained from Aldrich and used as received unless specified otherwise. Atomic absorption standards for Cr were obtained from Sigma. Procedures for the synthesis of polymer supported ligand (**5**) and the loading of supported ligands (**5**), (**6**), and (**7**) with Cr were provided in Section 2.5.

Conversions, yields, and enantiomeric excesses for asymmetric reactions were determined by gas chromatography using a Hewlett-Packard HP6890 series gas chromatograph (fid detector) with a β-Dex 120 chiral phase capillary column (Supelco, Inc.; 30 m × 0.25 mm i.d., 0.25 μm film). Chlorobenzene was used as a quantitative internal standard. ICP was performed using a Perkin Elmer Plasma 40 Emission Spectrometer.

4.4.2   Synthesis of Aldehydic Precursors and Supported Ligands (6) and (7)

3-*tert*-butyl-2-hydroxybenzaldehyde. This compound was prepared by the procedure of Palucki.[9] Purification by flash chromatography (SiO_2, 10 vol% EtOAc/90 vol% hexanes) resulted in product (39 % yield) with 88 % purity. The principal impurity is 2-*tert*-butyl phenol which is unreactive in the ligand formation step with *trans*-1,2-diaminocyclohexane. ^{1}H NMR ($CDCl_3$, 400 MHz) δ 11.77 (s, 1H, -O*H*), 9.86 (s, 1H, -C*H*O), 7.50 (d, 1H, Ar-*H*), 7.39 (d, 1H, Ar-*H*), 6.93 (t, 1H, Ar-H), 1.40 (s, 9H, - C(C*H*₃)₃).

Supported *N*-[2,4,6-trihydroxybenzylidene], *N'*-[3-*tert*-butyl-2-hydroxybenzylidene]-1,2-diaminocyclohexane *(6)*. A common procedure was used for reaction between the supported *N*-substituted diamines and the terminal benzaldehydes. 3-*tert*-butyl-2-hydroxybenzaldehyde (0.74 mmol) was added to a mixture of 83.7 mg of supported *N*-[2,4,6-trihydroxybenzylidene]-1,2-diaminocyclohexane (**9** in section 2.5.2) and 5 mL of 1,4-dioxane. The mixture was stirred and refluxed for 24 h. Gravity filtration yielded the product which was rinsed with 20 mL of 1,4-dioxane, dried for 12 h in air, and dried for 24 h at 60 °C under reduced pressure. For the reaction with 3-*tert*-butyl-2-hydroxybenzaldehyde to form (**6**), IR (KBr): 2965, 2869 (t-butyl), 1629 (C=N), 1602 (aromatic) cm⁻¹. For the reaction with benzaldehyde to form (**7**), IR (KBr): 1632 (C=N), 1601 (aromatic) cm⁻¹.

4.4.3 Synthesis of Azido-Trimethylsiloxy Products for GC Calibration Standards

1-Azido-2-trimethylsiloxypropane. This compound was prepared by the procedure of Larrow et al.[2] Racemic, Cr-loaded ligand **1** was used to synthesize the products. Purification by flash chromatography (SiO_2, 1 vol% EtOAc/99 vol% hexanes) resulted in product (18 % yield) with 88 % purity. ^{1}H NMR ($CDCl_3$, 400 MHz) δ 3.91-3.98 (m, 1H, -CHOSi), 3.16 (dd, 1H, -CH_2N$_3$), 3.02 (dd, 1H, -CH_2N$_3$), 1.15 (d, 3H, -SiCH$_2$CH_3), 0.14 (s, 9H, -OSi(CH_3)$_3$).

1-Azido-2-(trimethylsiloxy)cyclohexane. This compound was prepared by the procedure of Martinez et al.[7] Racemic, Cr-loaded ligand **1** was used to synthesize the products. Purification by flash chromatography (SiO_2, 7 vol% EtOAc/93 vol% hexanes) resulted in product (30 % yield) with 81 % purity. ^{1}H NMR ($CDCl_3$, 400 MHz) δ 3.38-3.44 (m, 1H, -CHOSi), 3.15-3.20 (m, 1H, -CHN$_3$), 1.88 (m, 3H, cyclohexyl-H), 1.65 (m, 3H, cyclohexyl-H), 1.33 (m, 2H, cyclohexyl-H), 0.13 (s, 9H, -OSi(CH_3)$_3$).

1-Azido-2-trimethylsiloxyhexane. This compound was prepared by the procedure of Larrow et al.[2] Racemic, Cr-loaded ligand **1** was used to synthesize the products. Purification by flash chromatography (SiO_2, 3 vol% EtOAc/97 vol% hexanes) resulted in product (29 % yield) with 93 % purity. ^{1}H NMR ($CDCl_3$, 400 MHz) δ 3.73-3.77 (m, 1H, -CHOSi), 3.15 (m, 2H, -CH_2N$_3$), 1.45 (m, 2H, -CH_2CHOSi), 1.19-1.29 (m, 4H, -CH_2CH_2-), 0.88 (t, 3H, - CH_3), 0.13 (s, 9H, -OSi(CH_3)$_3$).

4.4.4 Representative Reaction for Cr-Catalyzed Ring-Opening of Epoxides

Heterogeneous ligand (5) catalyzed ring-opening of epoxyhexane. Cr-loaded supported ligand **5** (0.05 g, 0.375 meq Cr/g) and azidotrimethylsilane (333 µL, 2.5 mmol) were added to a solution of epoxyhexane (603 µL, 5.0 mmol) and chlorobenzene, as internal standard (1.5 µL, 15 µmol), at 0° C. The reaction was continuously stirred. Aliquots (0.05 mL) of the reaction mixture were periodically removed and characterized by GC using a chiral phase capillary column. The samples were filtered through a pad of alumina before characterization. Typical GC conditions were: 1.3 mL/min at constant flow, 250 °C inlet temperature, and a temperature program for a 50 °C isotherm of 20 min, 15 °C/min ramp to 80 °C, and an 80 °C isotherm for 50 min.

Characterization of catalyzed ring-opening of propylene oxide by GC. Typical GC conditions were: 1.3 mL/min at constant flow, 250 °C inlet temperature, and a temperature program of a 55 °C isotherm for 45 min.

Characterization of catalyzed ring-opening of cyclohexene oxide by GC. Typical GC conditions were: 1.3 mL/min at constant flow, 250 °C inlet temperature, and a temperature program of a 95 °C isotherm for 50 min.

4.4.5 Representative Catalyst Recycle Procedure

Recycled use of heterogeneous ligand (5) for catalyzed ring-opening of epoxyhexane. After initial use of heterogeneous ligand (5), the reaction solution was gravity filtered to isolate the catalyst. After rinsing the resin three times with acetonitrile (10 mL), the resin was air dried for 4 h and dried for 2 h at 60 °C under reduced pressure. The resulting material was then used in a subsequent catalyzed ring-opening reaction.

Procedure for quantitation of Cr in solution. Prior to analysis, a calibration curve for Cr was generated using various atomic absorption standards at a wavelength of 205.552 nm on the emission spectrometer. After a reaction, samples were prepared by gravity filtering the reaction solution to remove the catalyst resin, the filtrate concentrated under reduced pressure to remove solvent and other volatile organics, and the filtrate residue solubilized in 0.1 mL of tetrahydrofuran. The resulting solution was mixed with 0.9 mL of DI water, and the emission spectrum for Cr (at 205.552 nm) was measured in duplicate. A standard of 10 vol% tetrahydrofuran and 90 vol% de-ionized water was also examined as a baseline value.

4.5   References

1)   Schaus, S. E.; Jacobsen, E. N. *Tet. Lett.* **1996**, *37*, 7937.

2)   Larrow, J. F.; Schaus, S. E.; Jacobsen, E. N. *J. Am. Chem. Soc.* **1996**, *118*, 7420.

3)   Shioiri, Y.; Hamada, Y. *Heterocycles* **1988**, *27*, 1035.

4)   Blaser, H. *Chem. Rev.* **1992**, *92*, 935.

5)   Hanson, R. M. *Chem. Rev.* **1991**, *91*, 437.

6)   Klunder, J. M.; Ko, S. Y.; Sharpless, K. B. *J. Org. Chem.* **1986**, *51*, 3710.

7)   Martinez, L. E.; Leighton, J. L.; Carsten, D. H.; Jacobsen, E. N. *J. Am. Chem. Soc.* **1995**, *117*, 5897.

8)   Hansen, K. B.; Leighton, J. L.; Jacobsen, E. N. *J. Am. Chem. Soc.* **1996**, *118*, 10924.

9)   Palucki, M. *Studies in Enantioselective Oxygen Atom Transfer Catalyzed by (Salen)Mn(III) Complexes*; PhD Thesis, Harvard University: Cambridge, 1995, p 192.

Chapter 5. Homogeneous Mn(Salen) Ligands: Subsituent Effects and Mechanistic Observations

5.1   Background

The focus of the previous chapters has been the development of heterogenized analogues of homogenous salen complexes for asymmetric epoxidation and ring-opening of epoxides. However, as the research progressed in these areas, several questions developed regarding the particular characteristics of the ligand that govern enantioselective behavior and the mechanisms of these salen-catalyzed reactions. To address these issues, an investigation of substitutional effects on the performance of homogeneous salen complexes was undertaken.

As an efficient catalyst for the asymmetric epoxidation of unfunctionalized olefins, much attention has been devoted in the chemical literature to the demonstration of enantioselectivity in the conversion of various olefins to epoxides using the salen complex.[1] Fewer studies have examined the relevant mechanistic issues for these processes. To date, there have been some elucidations of the roles that additives have on reactivity and selectivity and that electronic effects by substituents have in altering enantioselectivity.[2-4] Much remains unknown about the operation of these catalysts.

Typically, the salen complexes examined in these studies are C_2-symmetric and contain t-butyl groups on the ligand structure that guide the olefins along specific approach paths to the metal center and thereby provide enantioselectivity. The effects of altering the steric architecture of the salen ligand or removing its C_2 symmetry on enantioselectivity have not been addressed. In addition, the mechanism by which oxo-transfer occurs during epoxidation is still debated in the literature.[5-7] The present investigation into the mechanism for Mn(salen) catalyzed epoxidation may potentially offer further insight into the generation of superior enantioselective performance for these salen catalysts. These issues are discussed in this chapter.

5.1.1   Dissymmetry and Ligand Substitution Effects on Enantioselectivity for Homogeneous Mn(salen) Complexes

Since the enantioselectivity resulting from the use of the salen complexes is determined by nonbonding interactions between the olefin and catalyst (see section 2.1.1), one method of modifying the stereochemical communication between these two species is to change the

substituents on the salen complex. For example, variations in the substituents on the aromatic moieties of the catalyst framework can alter the electronic character of and the approach paths to the oxo-metal complex.[2,3,8] The selection of ligands with substituents of differing electron donating capabilities has been previously demonstrated to impact enantioselectivity.[2,3] The electronic nature of the substituents at the C5 positions (R_1 and R_4) has been suggested to alter the position along the reaction coordinate of the transition state involving the olefin-catalyst intermediate. With electron-donating substituents, the metal-oxo bond for the intermediate has
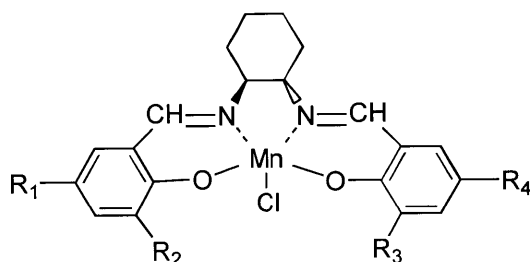
been determined from electrochemical studies to have increased stability.[3] According to the Hammond postulate, the increased stability of the oxo-intermediate should lead to oxygen transfer via a more product-like transition state where the oxygen atom is more closely held to the metal center. This stabilized intermediate requires a greater level of interaction between the catalyst and olefin and allows the possibility of increased stereochemical communication and higher enantioselectivity.[2] Electron-withdrawing substituents at the C5 position produce the opposite effect. A less stable metal-oxo bond is generated and produces a more reactant-like transition state, a less closely held oxygen atom. The result of the interaction of olefin with this oxo-intermediate is reduced stereochemical communication and lower enantioselectivity.

The reported work on the impact of the steric architecture of the salen complex on enantioselectivity has focused on the need for steric bulk at the C3 position (R_2 and R_3) to achieve catalysts with high enantioselectivities.[8] A variety of substituents have been used to provide steric impediments at these positions to block any approach toward the metal center that would not involve a transfer of chiral information, i.e. along a path not involving the chiral, diimine bridge.[1] For the salen ligands examined, a consistent trend emerges in that these ligands have demonstrated the steric importance of the C3 positions by typically using bulky substituents of the size of a t-butyl group or larger.[1] In addition, these salen complexes were produced with two identical benzaldehydic moieties about the central diamine giving C_2 symmetry to the

catalyst. Hence, these demonstrations have involved significant increases in steric size from two, single hydrogen atoms to two t-butyl groups or larger. While the case of a salen complex with methyl groups in the two C3 positions has been reported,[9] the effects of ligand dissymmetry and the investigation of the minimum steric bulk required are still areas of little research and ones of importance in establishing rational design principles for this class of catalysts.

Enantioselective catalysis by unsymmetric salen complexes has been reported in a few recent papers.[10-14] These complexes have included those containing a single salicylidene unit[11,12,14] or mono-substituted ethylenediamine bridges where these differences introduce various electronic factors that make direct comparison with salen-based systems difficult.[13] The syntheses of unsymmetric bis-salicylidene salen complexes have been reported recently;[10] however, the examination of the enantioselective behavior of these complexes in the epoxidation of olefins has not been reported. Rather, the only study that has examined enantioselectivity involved the use of a heterogeneous salen ligand for epoxidation (Chapter 3).[15] In that work (Chapter 3), the enantioselectivity of the heterogeneous catalyst was lower than its homogeneous, C_2-symmetric counterparts. This difference in enantioselective behavior could be a result of either the presence of the polymer support or the dissymmetry of the ligand and its lack of the full steric complement of the traditional homogeneous systems. These issues motivated the present investigation.

5.1.2 Mechanism of Oxo-Transfer using Mn(Salen) Ligands for Epoxidation

While the principal focus of research on these highly enantioselective catalysts for epoxidation has been the effects of substitutional changes for the ligand, a by-product of these works has been the development of proposed reaction mechanisms for epoxidation using these salen complexes.[5,7,16,17] A commonly postulated intermediate in these mechanisms has been a Mn^V-oxo complex.[18] The existence of this intermediate was postulated by analogy to a Cr^V-oxo salen intermediate that had been previously isolated and characterized.[19] Recently, the existence of the Mn^V-oxo intermediate was confirmed.[20]

As the salen ligand became more prominent as an enantioselective agent for the epoxidation reaction, various mechanisms that involved a Mn^V-oxo intermediate were proposed for this one oxygen atom transfer process. Currently, there is no universal mechanism for

epoxidation by metal catalysts. Even with the salen complex, the pathway seems to depend on the metal or ligand used.[21] Figure 5.1 illustrates the three principal mechanisms that have been postulated for the epoxidation reaction using the salen catalyst. Pathway **A** involves a concerted mechanism and has been proposed for metalloporphyrins that were developed to mimic the enzyme cytochrome-P-450.[22] This route is the weakest of the postulated mechanisms for the salen complex as it does not account for the observed isomerization of *cis*-olefins (such as *cis*-β-methylstyrene) to form *cis*- and *trans*- products during the epoxidation reaction.[8,23]

Pathways **B** and **C** both allow the possibility of isomerization. In pathway **B**, a radical intermediate is generated during the epoxidation reaction whereby rotation about the C-C bond before closure of the epoxide ring can produce a *trans*-product. In contrast, pathway **C** postulates the reversible formation of a metallaoxetane intermediate that can then form either the epoxide directly (as in the concerted mechanism **A**) or a radical intermediate that can access an isomerization pathway (as in the strictly radical mechanism **B**).

The arguments in support of pathways **B** and **C** are due to a similar set of experiments; however, they have yielded opposing conclusions.[5,21] In these experiments (Figure 5.2), the rate of rearrangement of a phenyl-cyclopropyl ring (a radical probe) adjacent to an olefin was monitored during the epoxidation reaction by the Mn(salen) complex in order to test for a radical intermediate. As the rate of rearrangement of this probe in the presence of a radical ($\sim 10^{11}$ s^{-1}) [21] is faster than the rate of oxygen donation from the Mn(salen) oxo-intermediate to the olefin (2 x 10^{10} s^{-1}), the presence of a radical is detected by the formation of rearranged product epoxide, whereas the epoxide product would contain an intact probe if no radical is present.

In one set of experiments (Figure 5.2a), an intact radical probe was found for the epoxidation of *trans*-2-phenyl-1-vinylcyclopropane. The authors of this work suggested that since a radical was not detected by the probe during the epoxidation reaction, an alkyl substituted olefin (where the probe was considered the alkyl substituent) must undergo epoxidation by a concerted mechanism (**A**). As isomerization has been reported to occur for aryl-substituted *cis*-alkenes during their salen-catalyzed epoxidation, the authors suggested that aryl-substituted olefins behave differently and undergo epoxidation through a nonconcerted mechanism involving a radical intermediate (**B**). The authors provided no evidence for this latter hypothesis and did not discuss the possibility of pathway **C** and a metallaoxetane intermediate. [21]

Rather than have two distinct mechanisms (**A** and **B**) for the epoxidation of alkyl- and aryl-substituted olefins, the results from a second set of experiments also involving a radical
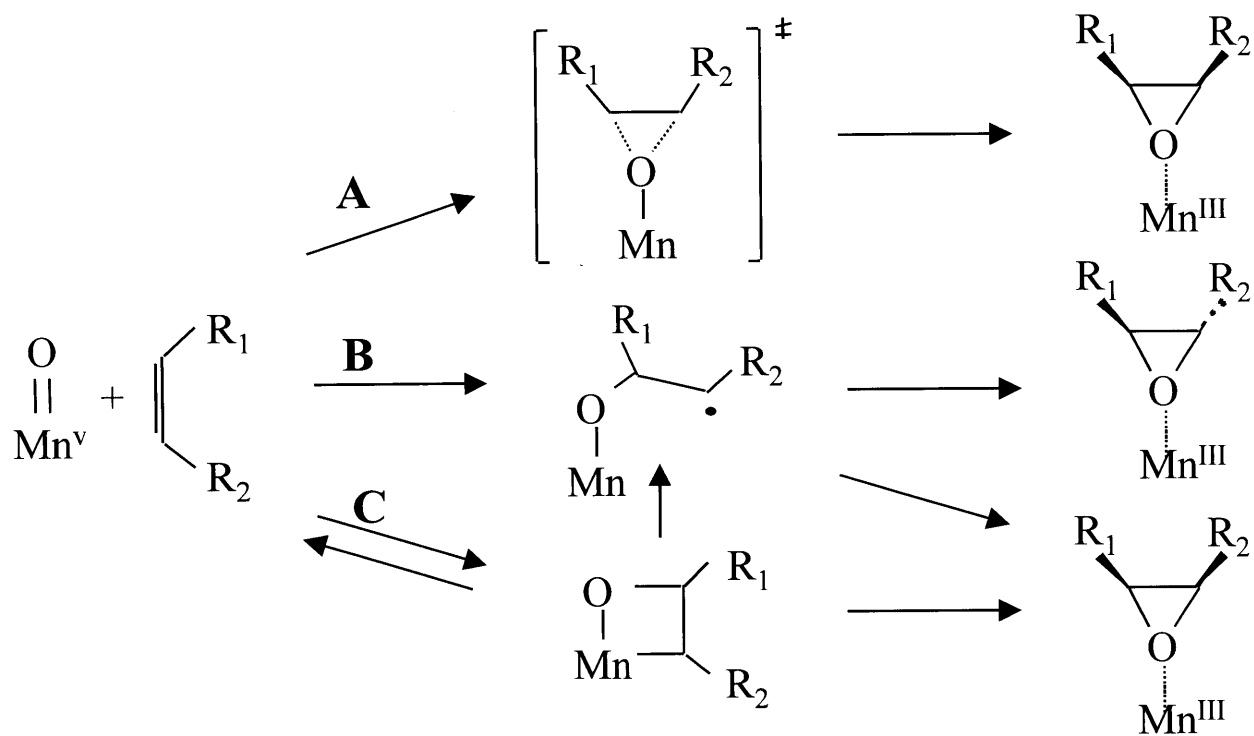
Figure 5.1. Schematic illustration of the potential pathways and intermediates involved in the epoxidation of unfunctionalized olefins using Mn(salen) complexes. Pathway **A** is a concerted mechanism. Pathway **B** involves the irreversible formation of a radical oxo-intermediate. Pathway **C** includes the reversible formation of a metallaoxetane.

A
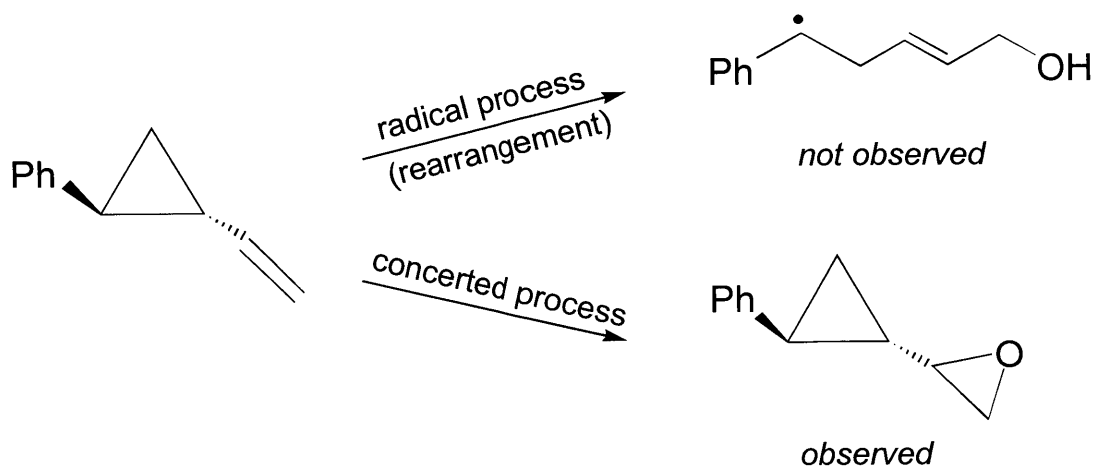
B
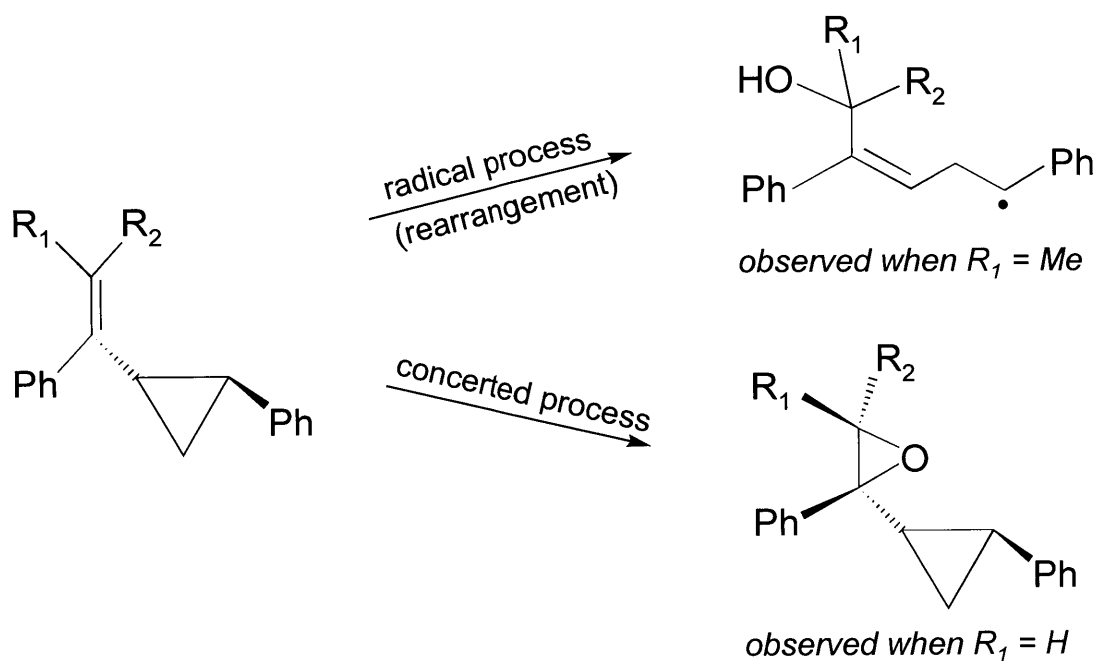
Figure 5.2. Summary of reported experiments using a phenylcyclopropyl probe as a free radical detector in the Mn(salen)-catalyzed epoxidation reactions. Reaction **A** using *trans*-2-phenyl-1-vinylcyclopropane resulted in an intact radical probe suggestive of a concerted process for epoxidation.[21] Reaction **B** with an aryl-substituted olefin resulted in an intact radical probe after epoxidation when the reactant was not highly substituted.[5] This latter case was used to support the existence of a metallaoxetane intermediate in the epoxidation mechanism.

probe have been reported to support pathway **C**.[5] In these experiments (Figure 5.2b), the same radical probe (a phenylcyclopropyl group) was located adjacent to the alkene bond of the reacting olefins and was found to remain intact during the epoxidation of several aryl-substituted olefins.[5] With bulkier substituents on the olefins (in addition to the bulk provide by the probe), the product contained an increased amount of the rearranged radical probe. To explain these results, a metallaoxetane intermediate was argued. The authors concluded that steric crowding around the metal center due to bulkier substituents caused homolysis of the metal-carbon bond of the metallaoxetane and availed access to a radical pathway for olefins with bulky substituents. Figure 5.1 illustrates this possible radical pathway for mechanism **C**. As the steric bulk of a substituent (R_2) on the olefin increases, the highly constrained intermediate (the metallaoxetane) has an increased possibility of fracture and access to the radical pathway.

In addition to the radical probe experiments, tests of the postulated mechanisms **B** and **C** has involved examinations of the relationship between asymmetric induction and temperature. For this analysis, the ratio of rate constants to produce each enantiomer during the epoxidation reaction is related to an Arrhenius expression. A non-linearity in a plot of this Arrhenius expression (log k_{major}/k_{minor}) versus inverse temperature (an Eyring plot) has been suggested to indicate the presence of a reversibly formed intermediate along a reaction coordinate,[24] and such a non-linearity would lend credence to the reversibly formed metallaoxetane (**C**). At present, conflicting results have been obtained, where the differences in reaction conditions between data sets and the presence of competing reactions (particularly isomerization and kinetic resolution) for the selected olefins complicate interpretation.[6,7] Thus, systemic collection of observations regarding the mechanism of oxygen transfer with this series of catalysts may clarify an ongoing debate in this area.

5.2   Results and Discussion

5.2.1   Synthesis of Dissymmetric Salen Structures

In general, tests of the enantioselective ability of different salen structures have used symmetric ligands formed from a single, chiral diamine and two equivalents of a salicylaldehyde moiety.[1] This simple, one-pot condensation procedure produces structures with C_2-symmetry where the substituents on the salicylaldehyde moieties contribute equally to the electronic and steric properties of the ligand. Some salen ligands lacking C_2-symmetry have been reported, but their

structures have departed substantially from the bis-salicylidene framework. Examples include the pairing of a single salicylidene unit with a pyrone (**1**)[11], a picolinamide (**2**)[14], or an acetylacetone (**3**) unit.[11,14,25] The only reported cases of bis-salicylidene salen ligands that
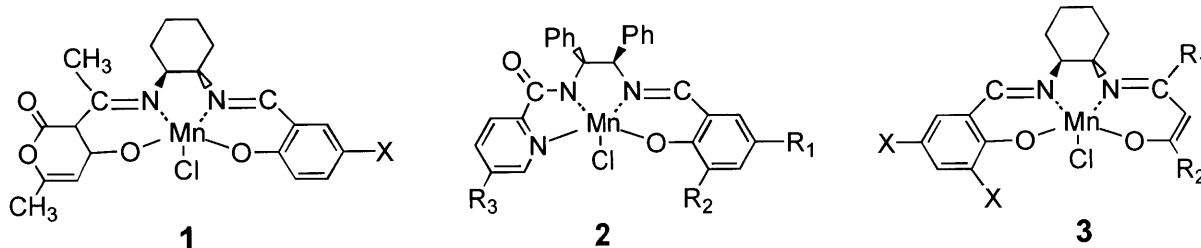
lack C_2 symmetry due to substitutional patterns and their examination in epoxidation reactions have involved those presented in Chapter 3 on heterogeneous supports.[12,15] Recently, the syntheses of several unsymmetric bis-salicylidene salen ligands were reported based on a stepwise protocol;[10] however, an examination of their activity hasn't yet been reported. Thus, no homogeneous analogues have been examined to date that can serve to elucidate the role, if any, of symmetry on enantioselective performance.

This chapter focuses on the enantioselective behavior of a series of homogeneous Mn(salen) complexes that include ligands which lack C_2-symmetry but maintain the bis-salicylidene structure. These ligands were synthesized by including equimolar amounts of two different, substituted salicylaldehydes in the one-pot condensation typically used to generate the homogeneous, symmetric ligands. The resulting mixture of product ligands contained a statistical distribution of possible products (namely, two symmetric and one dissymmetric ligands) that were separated from each other by column chromatography to produce the designed ligands.

The series of salen catalysts examined here incorporated (1S, 2S)-(-)-diamino-cyclohexane as the chiral source and differed in the number and position of the *tert*-butyl groups on the salicylidene units. In addition, a structure with a single methyl group in the C3 position was synthesized to examine the effect of reducing the steric bulk in the C3 position from that of a traditional *tert*-butyl group.[26]

90
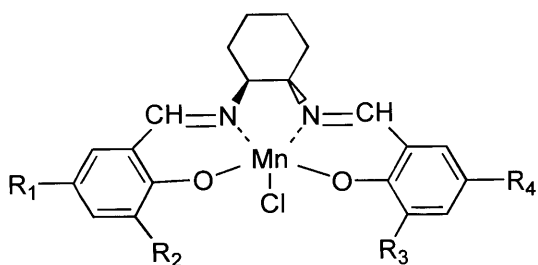
4::	R$_1$= t-Bu ;	R$_2$= t-Bu ;	R$_3$= t-Bu ;	R$_4$= t-Bu
5:	R$_1$= t-Bu ;	R$_2$= t-Bu ;	R$_3$= H ;	R$_4$= H
6:	R$_1$= H ;	R$_2$= t-Bu ;	R$_3$= t-Bu ;	R$_4$= H
7:	R$_1$= H ;	R$_2$= H ;	R$_3$= t-Bu ;	R$_4$= H
8:	R$_1$= H ;	R$_2$= H ;	R$_3$= Me ;	R$_4$= H
9:	R$_1$= H ;	R$_2$= H ;	R$_3$= H ;	R$_4$= H

The principal analytical technique used to characterize salen ligands **4- 9** was ^{1}H NMR.[27]
The symmetric ligands (**4, 6,** and **9**) were the only products generated in the condensation
reaction for their synthesis. For the dissymmetric ligands, their synthesis allows the possibility
that the corresponding symmetric ligands may be an impurity in these isolated ligand structures.
However, no evidence of these alternate ligands was observed in the ^{1}H NMR spectra of the
dissymmetric structures. The main points of distinction between the possible ligand structures
by ^{1}H NMR are the peak positions for the hydroxyl and imine protons in the salen structures.
The proton peaks from these functional groups were shifted slightly (0.01 – 0.13 ppm) for the
symmetric and dissymmetric structures and could readily be distinguished from each other.
Notably, the proton peaks change from a singlet to a doublet for the imine (*H*C=N) and from a
singlet to a pair of singlets for the hydroxyl groups between the symmetric and dissymmetric
ligands. The proton peaks in the aromatic region of the ^{1}H NMR spectra also differ between the
symmetric and dissymmetric systems. For example, the symmetric ligands have proton peaks
for a single type of salicylaldehyde environment. For the dissymmetric ligands, two sets of
aromatic peaks are present in the ^{1}H NMR spectrum in an equivalent ratio from the two differing
salicylidene components. In addition, thin layer chromatography of the purified dissymmetric
ligands showed no evidence of the symmetric ligands in these materials.

5.2.2   Effects of Variation in Steric Architecture on Enantioselectivity

The impetus for this investigation into the catalytic behavior of dissymmetric salen ligands and
the minimum steric requirements for these catalysts to be functional for asymmetric epoxidation
was the work involving the heterogenized Mn(salen) complex in Chapter 3. In that work, lower
enantioselectivity values for epoxidation were obtained with the heterogeneous catalyst than with
the homogeneous, bis-di-*tert*-butyl catalyst used for comparison. The cause of these lower
enantioselectivities is difficult to distinguish as it could result from either the dissymmetry of the
heterogeneous ligand structure, the influence of the support, or both. As noted earlier, little work

has been reported on the performance of dissymmetric Mn(salen) ligands produced from two different salicylaldehyde moieties in asymmetric epoxidation reactions.

As discussed in section 5.2.1, a series of structurally related salen ligands was synthesized and loaded with Mn for testing in the epoxidation reaction. The olefins examined with these ligands include those used with the heterogeneous salen complexes, namely styrene, 1,2-dihydronapthalene (DHN), and 6-bromo-2,2,3,4-tetramethyl chromene. The reaction conditions for epoxidation with these ligands used CH_2Cl_2 as solvent and 6 mol% catalyst relative to olefin. The oxidant in this study was m-chloroperbenzoic acid (mCPBA) with 4-methylmorpholine-N-oxide (NMO). As discussed in section 3.2.2, NMO forms a salt with mCPBA that requires the presence of the metal found in the ligand in order to be active for epoxidation. This attribute prevents the occurrence of the competing uncatalyzed reaction between the oxidant and olefin that would produce racemic epoxides.
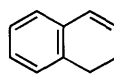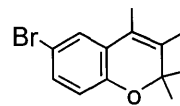
The oxo intermediate for these epoxidation reactions is postulated to be the same regardless of the oxygen donor,[28] and the selection of mCPBA as oxidant was based on issues of practicality. In the following section, mechanistic information is presented based on measured variations in selectivity for this series of catalysts with temperature. In Chapter 3, the oxidant used was 0.55 M NaOCl in water, and its use for the present mechanistic study placed a lower limit on the temperature range for which selectivity data could be obtained due to the freezing point of the solution (~0 °C). Additionally, an upper temperature limit is set by the convention of performing these epoxidations at room temperature or lower to minimize side-product formation. The epoxidation results in Tables 5.1 and 5.2 are from room temperature (23 °C) reactions—the same temperature as used in the heterogeneous case (Chapter 3). A full temperature profile from 23 to -78 °C was also performed with the results accompanying discussion of temperature effects in section (5.2.4).

For the results from these various catalytic ligands, a reference point for comparison was the results for the salen ligand synthesized from 2 equivalents of salicylaldehyde to form a ligand lacking any *tert*-butyl substituents (9). The enantioselectivities by 9 in the epoxidations of styrene, DHN, and chromene were 4.0, 27.8, and 71.2 %, respectively (Table 5.1). These enantioselectivity values are considered reference points as they indicate the base selectivity of the salen structure for a particular olefin. The selectivity for this ligand is derived primarily from the non-bonding π-π interactions between the electron clouds from the salicylaldehydic moieties of the ligand and the aromatic portion of the approaching olefin. The repulsion between the

Table 5.1. Enantioselective Epoxidation of Olefins with mCPBA/NMO Using Various Substituted Mn(salen) Complexes.

$$\text{Mn(salen) ligand} \atop \text{mCPBA/NMO, CH}_2\text{Cl}_2, 23\ ^\circ\text{C}$$
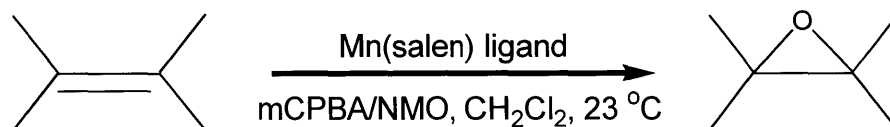
Enantioselectivity (% ee)[a]

Catalyst[b]	Ph⟍═	(naphthalene)	Br-(chromene)
9	4.0	27.8	71.2
8	4.6	20.8	67.5
7	44.5	66.8	91.4
6	47.6	79.3	83.8
5	40.0	67.3	70.8
4	42.3	75.8	58.0

[a] Ee's determined by chiral GC. Product assignments performed by comparison of elution order with authentic samples prepared using the (S,S)-form of Jacobsen's catalyst.

[b] Reactions conducted using 6 mol% salen ligand relative to epoxide.

electron clouds of the ligand and the substituted olefin directs the aromatic portion of the olefin toward the chiral diamine bridge or the exposed portion of the ligand near the unsubstituted C3 positions. The approach pathway associated with the diamine bridge provides a transfer of chiral information during the epoxidation, whereas approach to the Mn center between the C3 positions of the salicylaldehydic moieties involves no transfer of chirality (giving only a racemic product). The enantioselectivities using 9 provide insight into the relative enantioselective performances of the salen ligands with respect to each olefin and establish a baseline from which the effects of structural modifications to the ligand can be examined.

As a potential pathway for generating racemic product, the approach to the metal center along the path between the C3 ligand positions is considered a major leakage pathway (ee = 0 %) for ligand 9. In order to block this pathway and potentially achieve higher enantioselectivity in the epoxidation of olefins, the effect of additional steric bulk at the C3 positions of the ligand was examined. In specific, ligands were synthesized to have a single methyl group (8), a single *tert*-butyl group (7), and two *tert*-butyl groups (6) at the C3 positions of the base ligand (9). For these ligands, the addition of a single methyl group (Me) did not appreciably alter the enantioselectivities observed with the base ligand (Table 5.1). With DHN and chromene, the introduced methyl group caused the ee's by 9 of 27.8 and 71.2 % to decrease to 20.8 and 67.5 %, respectively. An analogous result was also reported for a symmetric salen ligand with two Me groups in the C3 positions where the reaction of the ligand with two methyl groups and of the olefins indene and 6-cyano-2, 2-dimethylchromene exhibited lowered enantioselectivities than 9. [9] The indication is that the presence of a single Me, or even two methyl groups, at the C3 positions does not provide the steric hindrance necessary to block the approach path between the C3 positions to the metal center that allows generation of a racemic product. In addition, the complexed salen ligand is generally reported to have a planar structure.[8,9] With the incorporation of substituents in the C3 position of the ligand, the planar structure of the ligand may become buckled. For a single Me substituent, this buckling effect would potentially increase exposure of the Mn center for reaction and increase the possibility of an approaching olefin to contact the active metal center with reduced chiral discrimination as provided by the ligand. In effect, these structural differences might decrease the ee's from those observed for the base ligand (9). For substituents at the C3 positions with greater steric bulk, the possible impact of a buckled ligand framework in reducing enantioselective performance may be offset by a

much greater impact of reducing the approach path between the C3 positions to the metal. This latter effect reduces the production of racemate and increases ee.

When the steric bulk at a C3 position is increased from a single Me group (**8**) to a single *t*-butyl group (**7**), the largest change in ee for a single substitution on the ligand is observed for each of the three olefins examined (Table 5.1). The ee's increased from 4.0, 27.8, and 71.2 % for styrene, DHN, and chromene using the base ligand (**9**) to 44.5, 66.8, and 91.4 %, respectively, with **7**. The implication is that a single t-Bu group is large enough to sterically block the approach path to the metal center and reduce a major leakage pathway (between the C3 positions) that leads to formation of racemic product. The further addition of a second *t*-butyl group to the other C3 position (**6**) offers an incremental increase in the ee's for styrene and DHN (~ 3- 13 %), but this incremental change in ee is much smaller than that from the first addition of a *t*-Bu to the base ligand structure (Table 5.1). Hence, in these cases, a slight increase in ee is attained with the addition of *t*-Bu groups beyond the first one, but the largest impact is by a single *t*-Bu group in the C3 position. Additionally, the advantage of a C_2-symmetric catalyst structure is to provide additional steric hindrance to block the racemic reaction pathway and increase ee; however, this symmetry parameter for the ligand is not a requirement for the catalyst to produce epoxides enantioselectively. The basis for the use of C_2-symmetric ligand structures appears more an issue of synthetic ease than a necessity for enantioselective operation.

With chromene, the ee for the epoxide product decreases with increased steric bulk on the ligand. As for the single Me ligand (**8**), a buckling of the ligand structure may similarly occur with the single *t*-Bu ligand (**7**). This buckling of the ligand may be beneficial for the case of catalyst **7** and the tetra-substituted olefin (chromene). The high level of steric interaction between the ligand and olefin may hinder approach to the metal center in cases of more highly substituted ligand structures. With the single *t*-Bu substituted ligand, there is sufficient steric bulk to block the racemic leakage pathway between the C3 positions, but its steric bulk has not been increased to the extent that the greater interference between the ligand and olefin would be problematic. This non-C_2-symmetric ligand structure (**7**) provides one of the highest reported ee values to date for this olefin, and a value that is higher than those reported for many symmetric, diaminocyclohexane-based salen catalysts.[29]

With the substituted ligands (**5**) and (**4**), the principal difference between these and the other ligands is the presence of an additional *t*-Bu group (or groups) at the C5 positions of the salicylaldehyde moieties. For styrene and DHN, a comparison between ligands (**5**) and (**4**) and

their respective C3-only functionalized analogues, (7) and (6), shows that the ee's change by < 5 % with the addition of a *t*-Bu group at C5. The incremental effect of the additional steric bulk at the C5 position does not seem to provide any significant improvement to the selectivities attainable at room temperature (23 °C). With chromene, as was suggested earlier, the addition of *t*-Bu groups beyond a single group at the C3 position of the salen ligand appears to interfere with approach of this tetra-substituted olefin to the metal center and produce lower enantioselectivities for the product epoxide. In fact, the highly substituted ligand (4) provided the lowest ee value of all the ligands investigated. A further examination of these effects at lower temperatures will be discussed in the section 5.2.4.

From this investigation of the enantioselective performance of the sterically modified ligands, one observation is that ligand **9** does provide a baseline for the enantioselective performance of the catalysts. Also, modification of the steric bulk on the base ligand does not provide an unlimited increase and refinement of selectivity. Rather, changes in the ligand structure can provide only moderate increases in enantioselectivity above the baseline established by the ee using **9**. The implication is that if the olefin is a poor match to the salen framework (as demonstrated by low enantioselectivity for the products using **9**) slight structural modifications of the catalyst cannot alter the basic relationship between olefin and salen framework.

Additionally, an understanding of the relationships and energetics of the different enantioselective behaviors of the catalysts with performed systematic structural changes to the ligand may allow for the rational design of such salen catalysts. For this analysis, an appropriate thermodynamic measure for these systems is the free energy change in the transition state responsible for observed differences in enantioselectivity ($\Delta\Delta G^{\ddagger}$). The basis of linking enantioselectivity and $\Delta\Delta G^{\ddagger}$ is discussed in section 5.2.4. The underlying premise is that the selectivity of the reaction is established by the difference in energetics between the two available enantiomeric pathways as measured by $\Delta\Delta G^{\ddagger}$ (see Figure 5.3). Therefore, if the transition state is a local minimum in the potential energy diagram for the reacting system, the difference in heights for the energy barriers to form one enantiomer over an other is related to $\Delta\Delta G^{\ddagger}$. As this free energy change increases, the difference between the energy barriers to form one enantiomer over the other is increased, and ee is increased. At room temperature, the largest change in selectivity was observed with the addition of a single t-Bu group (7); this result also corresponds to the largest change in $\Delta\Delta G^{\ddagger}$ for a single substitution (see Figures 5.4- 5.6 in section 5.2.4).

Initial Reaction
Mixture

ΔG

$\Delta G^{\neq}_{minor}$

$\Delta G^{\neq}_{major}$

$\Delta\Delta G^{\neq}$

minor
product

major
product

Reaction Coordinate

$$\Delta\Delta G^{\neq} = \Delta G^{\neq}_{major} - \Delta G^{\neq}_{minor}$$

Figure 5.3. Reaction coordinate diagram illustrating the link between enantioselectivity and differences in energy barriers for Mn(salen) catalyzed asymmetric epoxidation. In this diagram, enantioselectivity is strictly governed by the difference in the heights of the energy barriers to form either the major or minor product epoxide.

Therefore, the impact on enantioselective performance of modifying the steric bulk of the ligand can be correlated to a thermodynamic parameter ($\Delta\Delta G^{\ddagger}$). This premise is explored further in the examination of temperature effects on enantioselectivity (section 5.2.4) and in the mechanistic interpretation of these temperature effects (section 5.2.5).

5.2.3 Effects of the Variation of Steric Architecture on Activity

In addition to effects on enantioselectivity, the activity of the various homogeneous catalysts toward epoxidation was also examined. The corresponding conversion and yield data for these epoxidation catalysts are presented in Table 5.2. Prior to an analysis of these results, a brief explanation of the sampling procedure is required. Epoxidations involving mCPBA/NMO are fast reactions; in most cases, the reactions are complete within a few minutes. To a solution of olefin, NMO is added prior to the catalyst, allowed to stir with the catalyst, and then the oxidant is added. The addition of NMO prior to oxidant inactivates mCPBA toward the competing uncatalyzed reaction to form racemic epoxide. The complex formed between NMO and mCPBA is inactive toward reaction until a metal is present, and the formation of this complex is faster than the reaction to form epoxide.[30] However, the mCPBA/NMO complex becomes inactive even in the presence of catalyst after several minutes in solution.[30]

Experiments were also conducted with reaction sample injected into the GC for analysis at varying time intervals after oxidant was added. The conversions and yields obtained were identical for samples taken > 5 min after addition of oxidant. Sampling of the reactions at times greater than 5 min indicated no change of conversion and yield from those values at 5 min. The data presented throughout this chapter were obtained using the protocol of 15 minutes of stir time after addition of the oxidant.

For styrene and DHN, the reactants are completely consumed after 15 min for all the catalysts regardless of the amount of steric bulk about the metal center. With the tetra-substituted olefin (chromene), the steric bulk of the catalyst has a distinct impact on the rate of consumption of olefin. Complete consumption of the olefin within the 15 min reaction period only occurred for the less substituted catalysts (**7**, **8**, and **9**). With increased substitution on the ligand, conversion further declines during the 15 min reaction period (66 to 42 % for catalysts **6** and **4**). The steric bulk of the ligand appears to hinder the approach of the tetra-substituted olefin to the metal center and reduce the rate of reaction. Kinetically, the increased steric substitution

98

Table 5.2. Conversion and Yield Data for Olefin Epoxidation with mCPBA/NMO Using Mn(salen) Complexes.
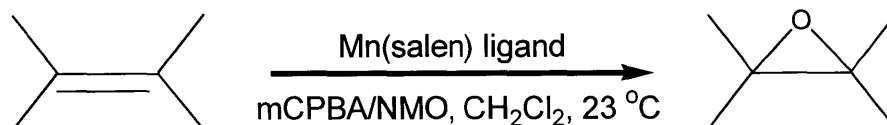
$$\text{Conversion/Yield}^a \ (\%/\%)$$

Catalyst[b]	Ph⟍⟍ [c]	[naphthalene-dihydro] [d]	Br-[chromene]
9	99/60	99/39	99/98
8	99/61	99/38	99/99
7	97/83	99/41	97/79
6	98/86	99/43	66/48
5	98/92	99/33	60/42
4	97/86	99/39	42/32

[a] Yields and ee's determined by chiral capillary GC. Yields measured by integration of product peaks against an internal quantitative standard.

[b] Reactions conducted using 6 mol% salen ligand relative to epoxide.

[c] Major side-product is phenylacetaldehyde.

[d] Major side-products are naphthalene and tetralone.

on the catalyst appears to reduce the approach paths of chromene to the metal center. The decreased collision frequency between the catalyst and olefin causes a reduced level of conversion.

For each olefin, the ratio of yield to conversion remained relatively uniform during epoxidations conducted with each of the structurally varied salen catalysts (particularly with the t-butyl substituted catalysts). There is some discrepancy for the less substituted catalysts (8 and 9) as they show lower yields for styrene, similar yields for DHN, and higher yields for chromene relative to the other catalysts. The difference in yields for the less substituted catalysts (8 and 9) may be due to the less restrictive coordination environment possible with these catalysts. A difficulty in interpreting the yield data stems from the fact that side-product can form during the epoxidation, and the epoxides may also undergo cleavage to generate by-products after formation.

As to any link between enantioselectivity with activity for these reactions, no such correlation is observed. For the chromene reactions using catalysts 4, 5, and 6, the conversions were lower with these catalysts than with the less substituted catalysts. Reactions repeated with greater amounts of the mCPBA/NMO mixture relative to the olefin (8:1 as changed from the original 4:1 ratio) produced increased conversions and yields, and unchanged enantio-selectivities. Similarly, reactions performed at lower temperatures that did not go to completion in the 15 min reaction period showed higher conversions when repeated using a higher ratio of mCPBA/NMO to olefin, but proceeded with the same ee. The enantioselectivity of the reactions appeared to be independent of conversion and yield.

A related set of reactions were performed at room temperature using NaOCl(aq) as oxidant. For these diffusionally limited reactions (due to the immiscibility of the solvent and aqueous oxidant solution), the ee's showed no change with conversion and were close to those obtained using mCPBA/NMO (Table 5.1): this latter result provides further support for a common oxo-intermediate regardless of oxidant. The enantioselectivities of the product epoxide by using NaOCl(aq) as oxidant were slightly lower (< 5%) than those by mCPBA due to the competing reaction of oxidant with olefin to form racemate in the former case. This competing reaction was suppressed for mCPBA by use of a complex with NMO that is inactive to olefin epoxidation without catalyst.

The activity of the different salen ligands for epoxidation is linked to the steric interaction between the catalyst and olefin. With more highly constrained systems, the rate of reaction is

reduced. However, this interplay between the steric bulk of the catalyst and its activity during epoxidation does not affect the enantioselectivity of the products generated. The enantioselectivities for the Mn(salen) complexes are independent of the rate of conversion. Rather, the steric bulk of the catalyst play a role in enantioselectivity as a thermodynamic parameter (as indicated in section 5.2.2) than as a kinetic one.

5.2.4   Temperature Effects on Enantioselectivity

The effect on selectivity of varying ligand substituents was examined for structurally different catalysts at 23 °C (section 5.2.2). In general, when temperatures were varied from 23 to −78 °C, the addition of a single t-Bu group in the C3 position of the ligand structure had the largest impact on selectivity. The enantioselectivity of a reaction can also vary with temperature for a particular catalyst structure. In many situations, temperature is used as a parameter to optimize the enantioselectivity of a reaction. Such a relationship between enantioselectivity and temperature was investigated for structurally varied homogeneous Mn(salen) complexes.

The temperature dependence of enantioselectivity for these homogeneous Mn(salen) catalysts are presented in Figures 5.4– 5.6 as plots of $Rln(k_{major}/k_{minor})$ against $1/T$, where k_{major} and k_{minor} are the rate constants for forming the major and minor enantiomeric products. The figures show Eyring plots and allow correlation of the enantioselectivity data with thermo-dynamic parameters. $Rln(k_{major}/k_{minor})$ can be expressed as a function of $\Delta\Delta G^{\ddagger}$ (the difference in Gibbs free energy between two transition states) and further related to the activation parameters $\Delta\Delta H^{\ddagger}$ and $\Delta\Delta S^{\ddagger}$ via the equation

$$\ln \frac{(k_{major})}{(k_{minor})} = \frac{-\Delta\Delta G^{\ddagger}}{RT} = \frac{-\Delta\Delta H^{\ddagger}}{RT} + \frac{\Delta\Delta S^{\ddagger}}{R} \tag{1}$$

These various thermodynamic parameters provide insight into the enantioselectivity process.

The Eyring plots for styrene, DHN, and chromene (Figures 5.4 - 5.6, respectively) using the homogeneous Mn(salen) catalysts all show a departure from the relationship between enantioselectivity and temperature as given by eq 1. For salen catalyzed reactions, Eyring plots have been reported with both linear and non-linear behavior.[6,7] Arguments presented against the non-linear data sets cite the possibility of isomerization of the olefin during epoxidation and
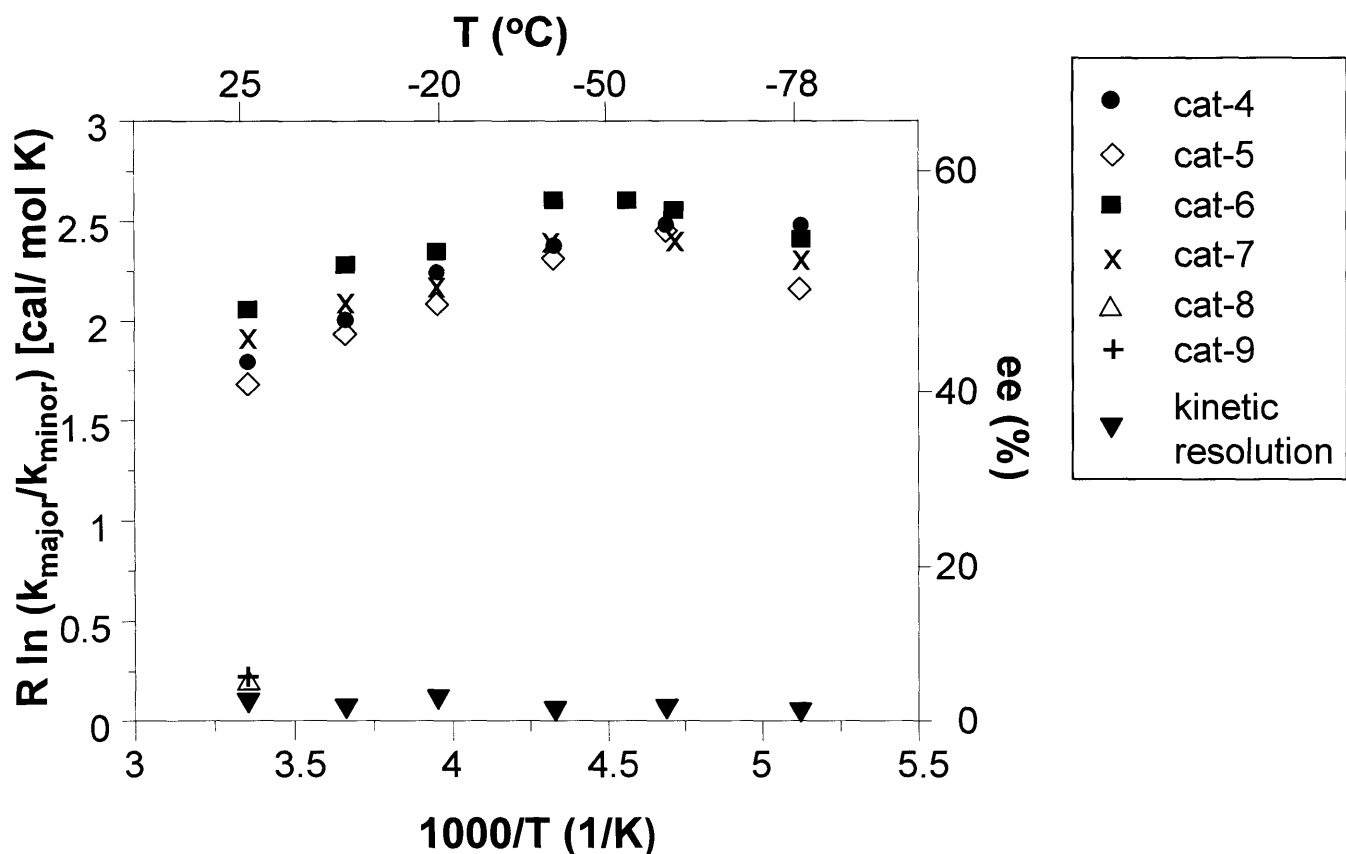
Figure 5.4. Eyring plot for the epoxidation of styrene using various homogeneous Mn(salen) complexes. The reaction was performed at the indicated temperature with 0.125 M olefin and 7.5 mM catalyst in CH_2Cl_2. Prior to the addition of oxidant (mCPBA), NMO was stirred in the reaction solution for 10 min. After 15 min of reaction, the epoxidation reaction was quenched with a 1.35 M solution of methyl sulfide in CH_2Cl_2 and analyzed by GC using a chiral column. Kinetic resolution of racemic styrene oxide was conducted using **4** under the identical conditions for epoxidation indicated above.
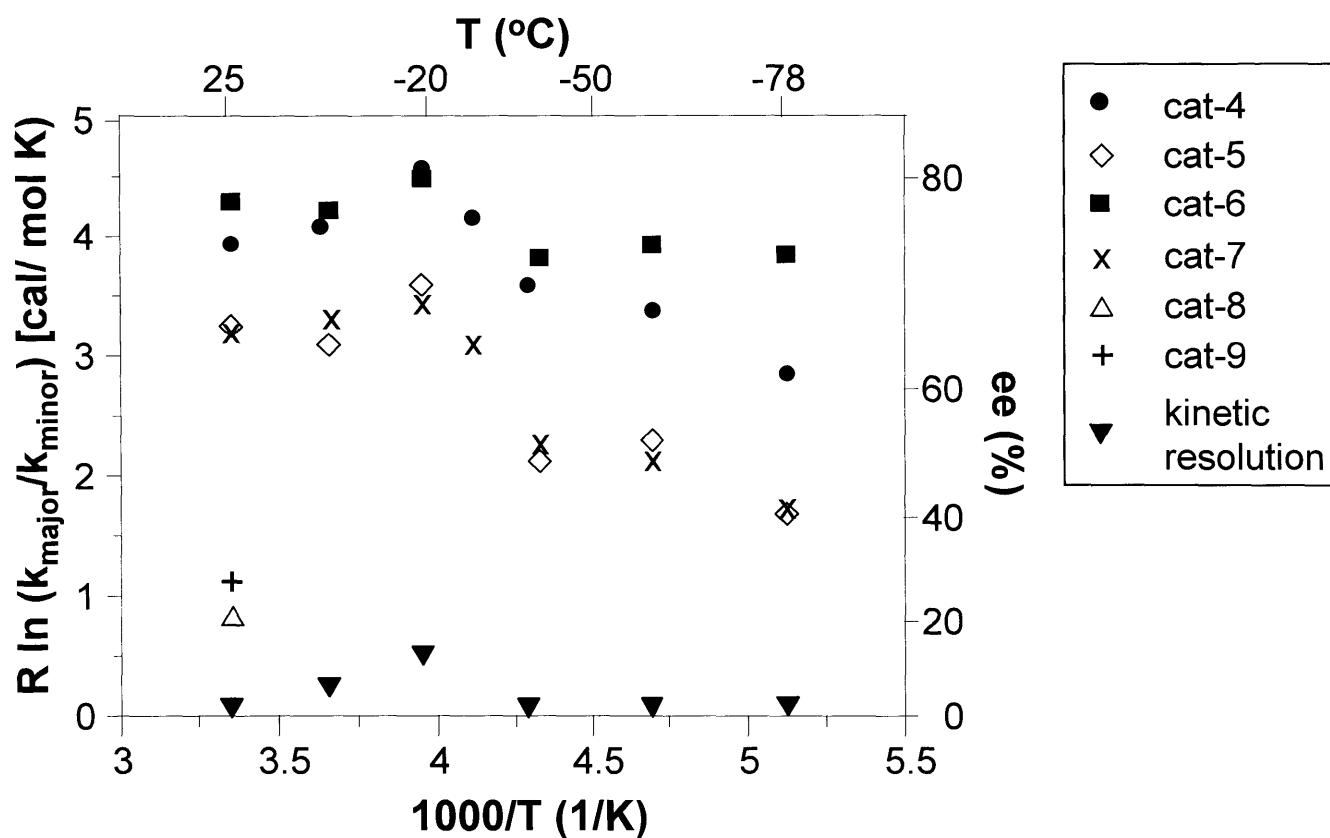
Figure 5.5. Eyring plot for the epoxidation of 1,2-dihydronaphthalene using various
homogeneous Mn(salen) complexes. The reaction was performed at the indicated temperature
with 0.125 M olefin and 7.5 mM catalyst in CH_2Cl_2. Prior to the addition of oxidant (mCPBA),
NMO was stirred in the reaction solution for 10 min. After 15 min of reaction, the epoxidation
reaction was quenched with a 1.35 M solution of methyl sulfide in CH_2Cl_2 and analyzed by GC
using a chiral column. Kinetic resolution of racemic epoxide of 1,2-dihydronaphthalene was
conducted using **4** under the identical conditions for epoxidation indicated above.
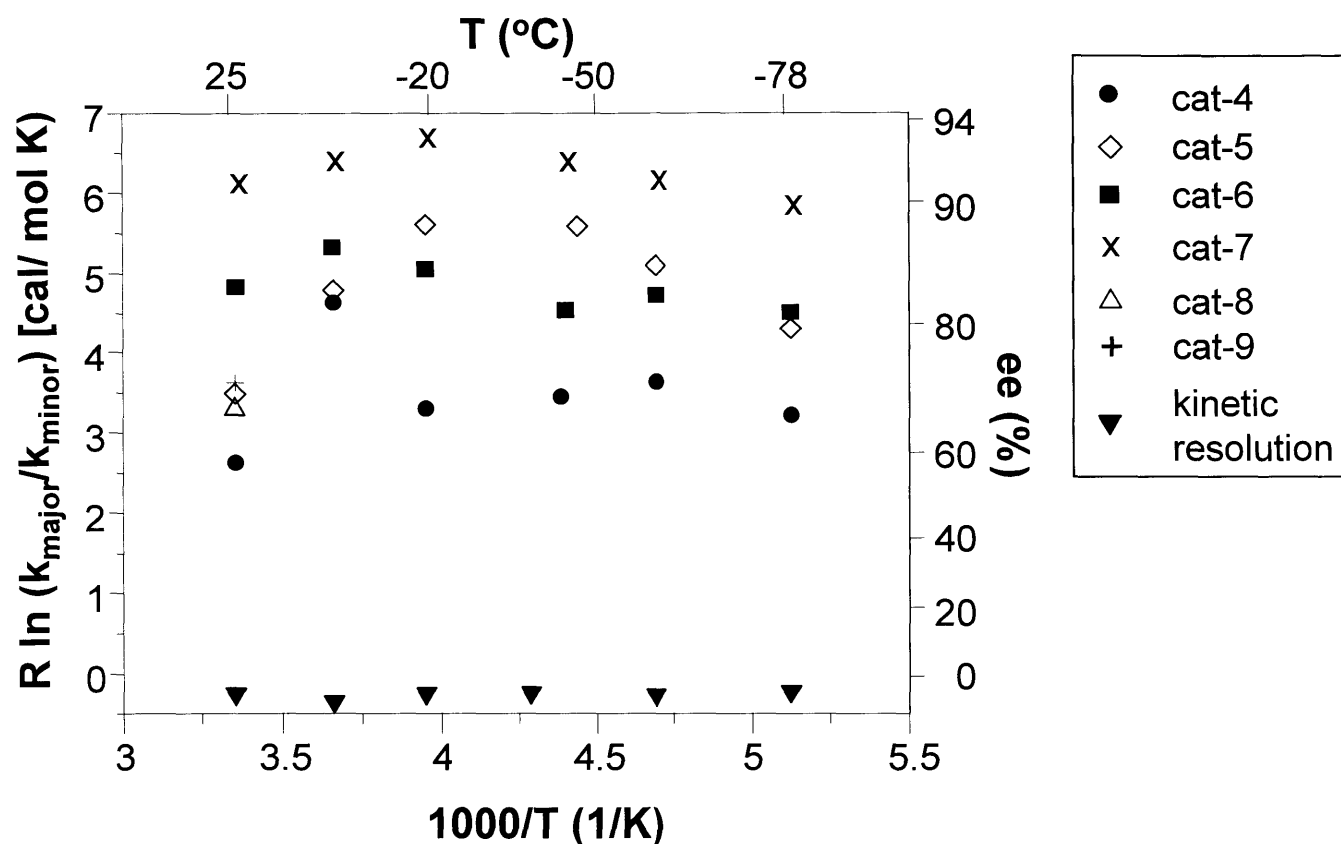
Figure 5.6. Eyring plot for the epoxidation of 6-bromo-2,2,3,4-tetramethyl chromene using various homogeneous Mn(salen) complexes. The reaction was performed at the indicated temperature with 0.125 M olefin and 7.5 mM catalyst in CH_2Cl_2. Prior to the addition of oxidant (mCPBA), NMO was stirred in the reaction solution for 10 min. After 15 min of reaction, the epoxidation reaction was quenched with a 1.35 M solution of methyl sulfide in CH_2Cl_2 and analyzed by GC using a chiral column. Kinetic resolution of racemic epoxide of chromene was conducted using **4** under the identical conditions for epoxidation indicated above

kinetic resolution effects for the olefins used in those studies (styrene and DHN).[7] For styrene, it was argued that the number of reactant molecules that proceed along the isomerization pathway that decreases ee for terminal olefins (section 3.1.1) may change with temperature. The observed decrease in ee at lower temperatures may be a function of an increased number of reactants proceeding along this isomerization pathway rather than the enantioselectivity of the catalyst decreasing. With DHN, the epoxide product is known to undergo a kinetic resolution in the presence of the catalyst such that the minor epoxide is consumed and generates a hydroxylated product.[31] Hence, with DHN, the number of product molecules that undergo kinetic resolution may vary with temperature. The variation of the rate of this competing process may vary differently with temperature than the rate of epoxidation. A decrease in ee at lower temperatures could be a function of the variation of the rate of this competing reaction rather than the catalyst selectivity being altered.

An examination of the potential for isomerization and kinetic resolution processes to cause the deviations from linear (Arrhenius-type) behavior observed for styrene, DHN, and chromene during salen-catalyzed epoxidation was performed. With styrene (Figures 5.4), the possibility of a variation with temperature of the number of reactant molecules that proceed along the isomerization pathway cannot be excluded. However, the cyclic olefins, DHN and chromene, cannot undergo isomerization. For the possibility of a kinetic resolution pathway in which the rate varied with temperature, each of the olefins was also examined. For this investigation, racemic epoxide was placed under the identical conditions for the epoxidation reaction using catalyst (4), and any changes in ee from 0 % for this reaction were monitored. Styrene and chromene showed no kinetic resolution under these conditions, while DHN exhibited a kinetic resolution that varied with temperature. However, the kinetic resolution pathway for DHN cannot account for the magnitude of the decrease in ee observed at the lowest temperatures during the epoxidation of DHN. Namely, at 23 °C, the kinetic resolution pathway is negligible, so the ee measured is exclusively a function of the enantioselectivity of the catalyst. At lower temperatures such as –63 and –78 °C, the impact of the kinetic resolution pathway is comparable to that at 23 °C, but the measured ee's for DHN epoxidation are below those at 23 °C. The enantioselectivity of the catalyst must have decreased. Hence, the kinetic resolution pathway cannot completely justify the non-linear behavior observed.

The potential complication of Eyring plot interpretation due to isomerization and kinetic resolution pathways is a valid consideration. However, these pathways cannot completely justify the observed non-linear behavior. For chromene, neither of these pathways is available to the olefin or epoxide, and hence, neither of these arguments is valid in explaining the deviation of this olefin from linear behavior. For DHN, while kinetic resolution does occur, it cannot explain the magnitude of the trend observed in the epoxidation reactions. For styrene, kinetic resolution is not a factor, and the effect of an isomerization pathway with temperature is only conjecture.

Before discussing the implication of the non-linear relationship between enantioselectivity and temperature, the observed conversions and yields require further comment. The issue being addressed is whether an adequate amount of product epoxide is generated at the lowest temperatures as to maintain the significance of the ee values measured by GC. The conversions and yields for the 15 min reaction period decrease with temperature (Appendix B). For styrene, the conversions and yields ranged from 90- 99 % and 60- 90 %, respectively, for a 15 min reaction time over the temperature range of 23 to –78 °C. For DHN and chromene, the conversions and yields decreased more dramatically such that the conversions and yields were only 20 – 40 % and 5 – 15 %, respectively, at T < 60 °C. The enantioselectivity appeared to be independent of the conversions and yields (see section 5.2.3), and the sensitivity of the GC for analysis easily permits quantitation of the enantioselectivity for epoxide yields within these ranges. For similarly conducted reactions, the reported values for conversion and yield were also within these ranges.[7]

In acquiring the Eyring plot data, a quench protocol, involving a solution of dimethyl sulfide,[30] was also implemented to ensure the validity of the measured ee's. As was mentioned earlier, as temperature decreased, conversion also decreased. The incomplete conversion of the reaction mixture proved problematic in obtaining ee values at low temperatures. As samples were extracted for GC analysis, the sampled aliquot was subject to a change in temperature. During the sampling procedure, the additional epoxides formed from the incompletely converted reactants would be generated at a higher temperature and, hence, at a different ee. With the dimethyl sulfide procedure, a quench solution at the temperature of reaction was mixed with the reaction solution. The oxidant, mCPBA, was inactivated prior to sampling by reaction with the sulfide. When samples were not subjected to the quench protocol, slightly higher ee's were observed. The Eyring plot data of Figures 5.4 – 5.6 were obtained using the quench procedure.

After addressing the validity of the non-linear relationship observed for styrene, DHN, and chromene, the implication of these results needs to be examined. Two effects can be suggested for the observed non-linear relationship between enantioselectivity and temperature. As was discussed earlier in this section, the selectivity can be expressed as the difference in Gibbs free energy ($\Delta\Delta G^{\ddagger}$) between two transition states that lead to formation of a major or minor product from a common reaction intermediate. This parameter, $\Delta\Delta G^{\ddagger}/T$, is a linear function of temperature in which $\Delta\Delta H^{\ddagger}$ is the slope and $\Delta\Delta S^{\ddagger}$ is the y-intercept. To describe the observed non-linear relationship, the simplest view is that of two linear regions in which there is a shift from an enthalpically driven process to an entropically driven process. Therefore, in the transition state where selectivity is determined, entropy and the possible impact of sterics (as expressed by the entropic term) may dominate the selectivity step at lower temperatures. In addition to the shift from an enthalpically driven process to an entropically driven one, a non-linear behavior in an Eyring plot has been suggested to correlate to mechanisms involving a reversibly formed intermediate and an irreversible transformation of this intermediate to form a final product.[24] The relevance of this observation in conjunction with the enthalpic and entropic factors mentioned above provide the focus for the mechanistic interpretation offered in the following section.

5.2.5 Mechanistic Interpretation of Mn(Salen)-Catalyzed Asymmetric Epoxidations

The mechanism of asymmetric epoxidations by Mn(salen) complexes has been the subject of intensive research in recent years. Nevertheless, the reaction mechanism is still not understood. This lack of a unifying mechanism to explain ligand effects and variations in selectivity with temperature have resulted in the suggestions that multiple mechanisms may be at work.[21] In many ways, the lack of a unifying mechanistic model hampers the development of rational design principles for these catalysts. More broadly, in establishing design parameters for such asymmetric reactions, the transfer of chirality during these reactions must be understood before the factors that influence this transfer can be defined and potentially manipulated.

The manner in which selectivity varies with temperature is one way that provides mechanistic insight is gained. Such was the case with examinations of the mechanism for asymmetric dihydroxylation of olefins using osmium tetroxide.[32] The non-linearity of Eyring

plots for this reaction suggested the possibility of two enantioselective steps in the mechanism that were weighted differently according to temperature and that were consistent with a metallaoxetane intermediate. The non-linearity of Eyring plots has also been used to justify stepwise mechanisms where a reversibly formed intermediate undergoes an irreversible step to generate the final product.[24] In this latter work, the example used to illustrate the principle involved a photoexcited ketone as the intermediate. While a metallaoxetane was not used as an example, it does follow the scheme of a reversible first step to generate an intermediate followed by the irreversible formation of product.

For the asymmetric epoxidation of olefins using Mn(salen) complexes, this section revisits the hypothesized mechanisms and examines their ability to account for the observed non-linear Eyring data (section 5.2.4). Figure 5.1 summarized three proposed mechanisms for the epoxidation reaction. Pathways **A** and **B** follow concerted and radical mechanisms, respectively, where the enantioselectivity of the product is determined in the first step (formation of the intermediate). The formation of product from this intermediate for each of these pathways does not provide any added level of selectivity between an enantiomeric pair. For the concerted mechanism (**A**), the formation of intermediate involves facial selectivity where the olefin couples to the Mn^V-oxo complex, and the identity of the final enantiomeric product is established. The subsequent step to form product is simply a dissociation step where no further selectivity occurs.

For the radical mechanism (**B**), the formation of the radical intermediate also establishes the selection of an enantiomer among the possible pair. While a reversible first step is a possibility, the radical in this reaction is considered to be a long-lived species such that rotation about the carbon-carbon bond during isomerization is possible.[23,33] Additionally, the reversibility of radical formation would imply the possibility of isomerization of reactant. This process is not observed for the epoxidation reactions, and the reversibility of this radical is considered negligible. The subsequent step to form product from the radical intermediate may involve rotation about the carbon-carbon bond, but this action may only change the diastereomeric configuration of the formed epoxide (varying ratios of cis-/tran- epoxides). The selection of the final enantiomeric configuration of the product among a possible pair is established in the first step. With the exception of terminal olefins, this second step to form final product does not alter ee. Therefore, as reaction temperature is varied, the change in selectivity for the first step to form intermediate determines the changes in enantioselectivity for the product. The selectivity should show a continuous increase as temperature is decreased.

As an aid in conceptualizing the possible scenarios for generation of enantioselectivity for Mn(salen) catalyzed epoxidation, a reaction coordinate diagram (Figure 5.7a) was created for pathway **A** or **B**. For these cases, the olefin and oxidant are initially present in the local minimum in energy between the energy barriers labeled **2** and **3**. The enantioselectivity of a catalyst is related to the relative difference in free energy for the two possible transition states. The energy barriers labeled **1** and **4** correspond to a second stage of the reaction where the final product is formed from an intermediate. In these cases, the enantioselectivity is established in the initial step.

With the Eyring plots of section 5.2.4 indicating a decrease in ee at low temperatures from their values at higher temperatures for the Mn-catalyzed epoxidation, an explanation for such a decrease in ee needs to be proposed. To decrease ee, one possibility would involve a second irreversible selectivity step in the reaction that acts in contradiction to the first. The second stage of selectivity must reverse the selectivity established in the first stage; the opposite enantiomer must be preferentially formed. With the epoxidation reaction, the formation of intermediate occurs with facial selectivity. This step establishes the enantiomeric configuration of the product. A second stage that preferentially creates the opposite enantiomer does not seem feasible. The second possibility for decreasing the ee during epoxidation involves a reversibility of the intermediate. This second possibility is examined further using the case of a metallaoxetane.

For pathway **C**, the inclusion of a reversibly formed intermediate along the pathway to form the final product allows a non-linear relationship between enantioselectivity and temperature. Figure 5.7b shows a collection of reaction coordinate diagrams to illustrate this point. As in mechanisms **A** and **B**, the energy diagram at highest temperature (T_1) shows the dominance of the initial step in determining enantioselectivity. The reversibility of the first reaction to regenerate reactants is reduced due to the lower barrier height to generate the final product from the intermediate (**1** and **4**). As temperature decreases (T_2), the rate of the second stage of reaction (from intermediate to final product) may decrease to a greater degree than the rate of formation of intermediate. A reduced rate of reaction implies that the energy barrier for that step has increased. As the barrier heights for this second stage of reaction (**1** and **4**) approach those that define the first stage (**2** and **3**), the reverse reaction for the enantioselectively produced intermediates to regenerate reactants becomes more probable. In addition, as this reversibility becomes more probable and temperature further decreases (T_3), the potential to overcome barrier
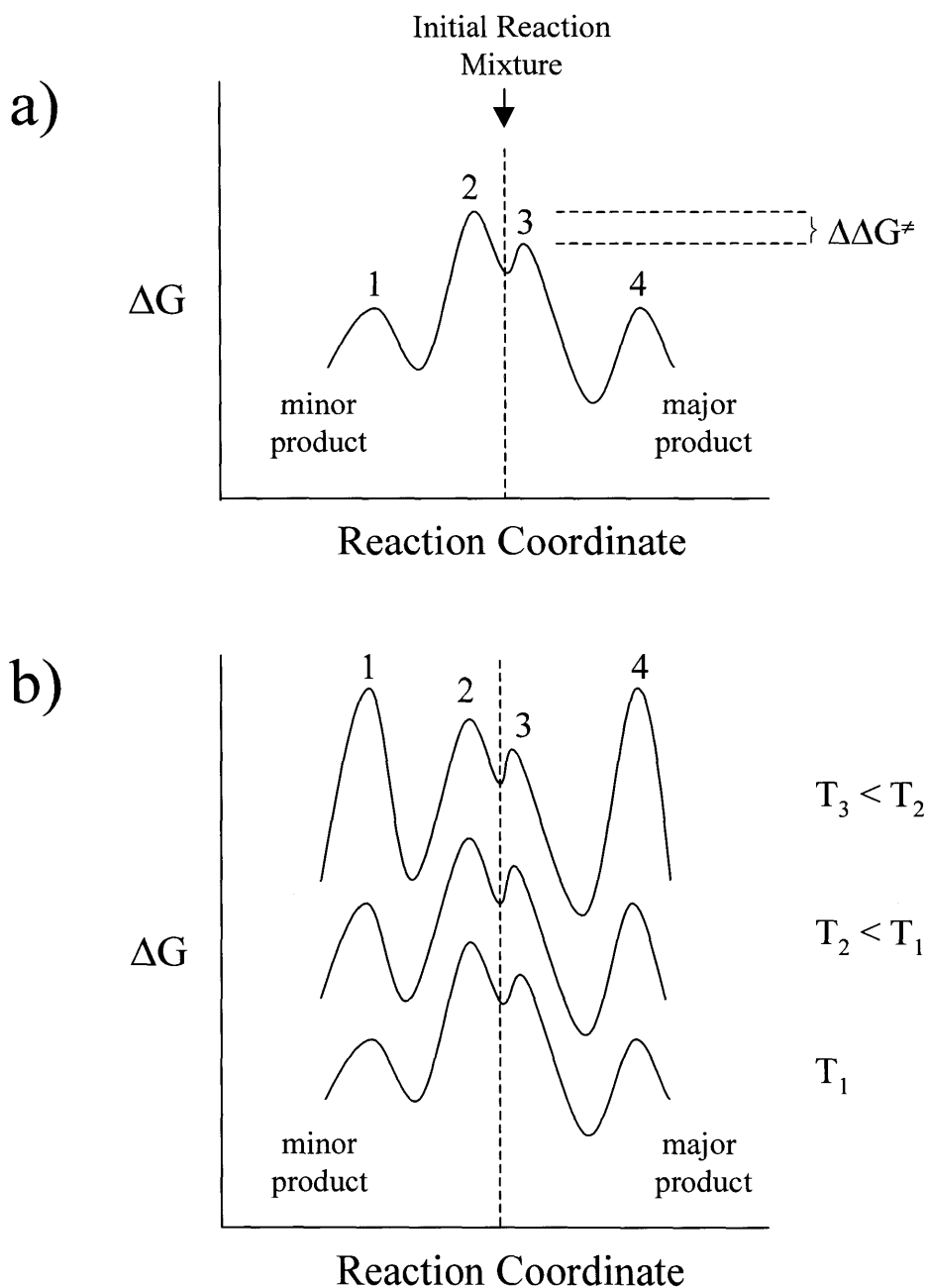
Figure 5.7. Reaction coordinate diagrams for proposed mechanisms for Mn(salen) catalyzed asymmetric epoxidation. The upper diagram applies to the concerted and radical mechanisms where enantioselectivity is strictly governed by the formation of intermediate. The lower diagram applies to the metallaoxetane intermediate where a reversible formation of intermediate is followed by the irreversible formation of product from the intermediate. The latter mechanism allows for the possibility of a non-linear relationship of enantioselectivity with temperature.

heights to form the minor intermediate increases. The net result is an increase in the probability of forming the minor enantiomer and a decrease in ee at these lower temperatures. Therefore, the presence of a reversible step to generate enantioselective intermediates followed by an irreversible step to form the final products provides a pathway to explain the possibility for an inversion in enantioselectivity with temperature. For such a mechanism, a metallaoxetane fits the required criteria as the intermediate.

The implication of the proposed series of reaction diagrams in Figure 5.7 and the existence of a metallaoxetane intermediate is that the reaction is kinetically driven at higher temperatures such that the energetics of the first step in generating the two possible intermediates govern the enantioselectivity of the overall reaction. In this case, the difference in energy barriers to form the major and minor intermediates ($\Delta\Delta H^{\ddagger} = \Delta H^{\ddagger}_3 - \Delta H^{\ddagger}_2$) governs the selectivity. From the Eyring plots for the examined olefins and eq 1, the selectivity in the high temperature reflects the dominance of the enthalpic term over the entropic term.

At lower temperatures, cleavage of the metallaoxetane intermediate to final product becomes a rate-determining step. As the cleavage process is slowed, the reversibilities of other reactions increase. In particular, steric interactions between the catalyst and olefin likely play an increased role. From the Eyring plots and eq 1, this process is reflected by a shift from a dominance of enthalpic effects at higher temperatures to entropic effects at lower temperatures.

The literature contains data exhibiting linear behavior on Eyring plots for asymmetric epoxidation. This case differed from this work in the substitution pattern and ethylenediamine bridge used in the salen complexes.[7] These catalysts were examined over the same temperature range as in this study. However, for different catalyst structures, the difference in energy barriers to form the intermediates are likely affected, as well as the energetics for cleavage of the intermediate to produce the final product. For these cases, the temperature where the reversibility of the first reaction step becomes a significant factor and impacts ee may be below the examined ranges. For such systems (in Figure 5.7b), the peaks associated with the barriers to generate intermediate (**2** and **3**) may be higher than those for fracture of intermediates (**1** and **4**) such that lower temperatures would be required to observe a decrease in ee with temperature. Over the temperature range examined, the performance of these catalysts is enthalpically driven, and the data exhibit a linear Eyring behavior.

At present, the proposed metallaoxetane intermediate remains unproven. A particular issue is whether a Mn^V-oxo complex can attain the hepta-coordinated structure and non-planar

configuration to accommodate a metallaoxetane.[7] The crux of the debate rests on whether the ligand can attain the non-planar configuration that would be required for a metallaoxetane. While the possible existence of a Mn^V-oxo species in salen-catalyzed epoxidations was based on early work reported for the Cr(salen) complex, this Cr work also suggested the possibility of a metallaoxetane intermediate in epoxidation.[19] The isolation of such a 7-coordinate intermediate has not been reported for Mn^V; however, various cases have been reported for Mn^{II}.[34-37] In addition, recent results using empirical force-field models have suggested the possible existence of such a metallaoxetane with a non-planar configuration for the Mn(salen).[17] While this work focused on the possibility of a 6-coordinate structure in the absence of a donor ligand, the authors strongly suggested the possibility that the ligand could attain a non-planar conformation.

Beyond the use of the non-linearity of Eyring plots to justify a metallaoxetane as the intermediate in Mn(salen)-catalyzed asymmetric epoxidations, the non-linear behavior does allow several other observations. In general, the switch from one region of linearity to another corresponds to a change in the dominating nature of the activation parameters for each of the partial selectivity steps.[24] By modeling the Eyring plots for each catalyst (Figure 5.4- 5.6) as two linear regions, two sets of activation parameters, $\Delta\Delta H^{\ddagger}$ and $\Delta\Delta S^{\ddagger}$, for both the high and low temperature regions can be obtained. The differences between these values at the two temperature regions ($\delta\Delta\Delta H^{\ddagger}$ and $\delta\Delta\Delta S^{\ddagger}$, respectively) reflect the respective change in dominance of enthalpy and entropy for the reaction process. A plot of $\delta\Delta\Delta H^{\ddagger}$ vs $\delta\Delta\Delta S^{\ddagger}$ for each catalyst and the three olefins examined in this study show a strong linear correlation (Figure 5.8, r^2= 0.99). Since the values plotted are based on differences between activation parameters rather than ee values, the relationship is independent of the actual ee values measured and, as a result, of the factors which influence the ee (namely, catalyst structure and olefin).

Figure 5.8 also indicates that the relationship passes through the origin. This result corresponds to a negligible $\delta\Delta\Delta G^{\ddagger}$ value and suggests that there is a limited window of change in free energy over which the ee of a reaction can be optimized (see Eyring plots of Figures 5.4- 5.6). As mentioned in section 5.2.2, the ee for an olefin can be optimized a finite amount from the base case values provided by **9** using steric substitutions. Accordingly, an optimization of ee using temperature can only cause finite improvements. A compensating effect appears to occur whereby the dominance of enthalpy at higher temperatures is offset at lower temperatures by entropy. In the Eyring plots, the shifts in the dominance of these thermodynamic parameters offset each other to the extent that an unlimited increase in enantioselectivity with temperature is
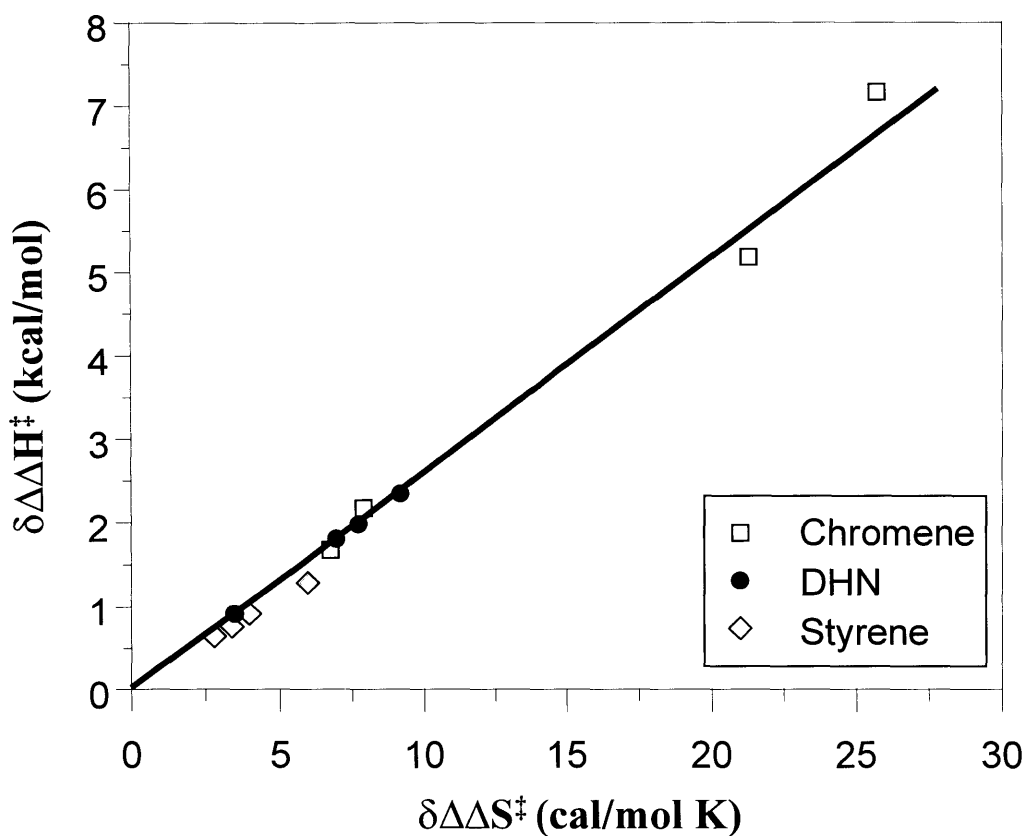
Figure 5.8. Enthalpy/entropy diagram generated from the non-linear Eyring plots using various homogeneous Mn(catalysts) (**4** - **7**) and chromene, DHN, and styrene. The difference values were obtained by assuming two linear regions in the Eyring plot for each catalyst where the thermodynamic parameters are obtained from the best-fit line established for each linear region. The difference for these parameters between the two linear regions provided the data values above. Since the data were obtained from the difference in thermodynamic values, the plot is independent of the actual ee and the factors, such as ligand and olefin, that govern it.

not possible. The enthalpy and entropy terms adjust with temperature such that the overall effect on free energy is within a limited window. In other words, a "poor" system of catalyst and epoxide with low enantioselective ability cannot become a "good" system by simply manipulating temperature. Rather, as was the case with sterics (section 5.2.2), a refinement of enantioselectivity can be attained with temperature within a limited window.

Lastly, the linear correlation in the enthalpy/entropy diagram yields a slope that corresponds to a temperature. This temperature is called the isoinversion temperature (T_i) and is a qualitative measure of the selectivity achievable with a reaction system.[24] As the temperature where the Eyring plots invert approaches T_i, the optimum ee for that system is attained. For systems where the inversion temperature deviates from T_i, the system of catalyst and reactant is considered un-optimized for selectivity, and the deviation between T_i and the inversion temperatures is a qualitative indicator of how poor the system is as a potential candidate for high selectivity. For the Mn(salen) catalyzed epoxidations, Figure 5.8 yields a slope of $T_i = 271$ K. Accordingly, the Eyring plots (Figures 5.4 - 5.6) follow the trend that the proximity of the inversion temperature to T_i corresponds to the more optimized systems (namely, chromene, DHN, then styrene). This work is the first reported instance where such estimation of the effectiveness of the Mn(salen) catalysts can be correlated independent of their ligand-olefin relationship. Rather, the basis of comparison is the unsubstituted salen ligand that is then optimized by either temperature or sterics. The basis of this correlation was provided by the suggested mechanism of a metallaoxetane. Such an estimate could not have been made assuming a radical or concerted mechanism.

5.3   Conclusions

An investigation of substituent and temperature effects for a novel series of homogenous Mn(salen) catalysts was undertaken to develop a fundamental understanding of the impact of these factors on enantioselectivity. A variety of t-Bu substituted, homogeneous Mn(salen) complexes for asymmetric epoxidation were synthesized. The steric architecture of these complexes was varied such that these complexes lacked C_2 symmetry and had less sterics than the full, 4 t-Bu complex traditionally examined in the literature. Examination of these catalysts for the epoxidation of chromene, DHN, and styrene using mCPBA as oxidant indicated that C_2 symmetry is not a requirement for enantioselective behavior and that most of the steric effects of

the substitutions are due to a single *t*-Bu group in the C3 position of the ligand. The inclusion of this single *t*-Bu group is responsible for the largest increase in ee for a single point substitution to the salen structure. Additional steric effects allow some refinement in the ee of product epoxides, and in the case of chromene, the presence of a single *t*-Bu group provided the highest ee value of all the catalysts examined. This result was suggested to be due to the high level of steric interaction between the highly substituted olefin and catalyst.

The activity of the catalysts to DHN and styrene were similar and resulted in complete conversion within a 15 min reaction time at 23 °C. For chromene, the increased steric interaction between the olefin and catalyst resulted in decreased conversion as the catalyst was highly substituted. The enantioselectivity, however, proved to be independent of any changes in activity. For epoxidations of chromene where reaction was incomplete, the addition of oxidant to further convert reactant resulted in increased conversion, but the ee values did not change.

For this set of Mn(salen) catalysts, Eyring plots of the variation in enantioselectivity with temperature indicated a non-linear behavior. These non-linear effects strongly suggest a reversible formation of an intermediate in the reaction and irreversible formation of product from this intermediate. These observations are consistent with the presence of a metallaoxetane intermediate for the Mn(salen) catalyzed asymmetric epoxidation. Other proposed mechanisms for this reaction involving a concerted or radical pathway could not explain the observed non-linear behavior.

Additionally, as opposed to reported views that the lack of correlation of temperature effects and ligand effects on enantioselectivity lends to the indication of several different mechanisms for this reaction,[21] the assumption of a metallaoxetane and the reversibility of the intermediate generation step provides a consistent explanation for all these effects. In extending the implication of a metallaoxetane mechanism, a compensation effect involving enthalpy and entropy was suggested. The entropy term for this effect accounts for the steric interaction between olefin and catalyst. When the variation of enthalpy and entropy were examined, a qualitative prediction of the relative temperature effect on enantioselectivity for each of the olefin/catalyst systems could be established.

5.4   Experimental

5.4.1   Materials and Instrumentation

Solvents and chemicals were obtained from Aldrich and used as received unless specified otherwise. (S,S)-(+)-*N,N'*-Bis(3,5-di-*tert*-butylsalicylidene)-1,2-cyclohexanediamino-manganese(III) chloride was purchased from Aldrich. Infrared spectra were recorded in transmission mode using a Bio Rad FTS 175 spectrometer. ^{1}H NMR spectra were recorded on a Bruker DPX-400 (400 MHz) or a Bruker WM-250 (250 MHz) spectrometer and referenced to residual solvent peaks at 7.24 ppm for chloroform. Deuterated solvents were obtained from Cambridge Isotope Laboratories, Inc.

5.4.2   Synthesis of Aldehydic Compounds and Ligands

3-*Tert*-butyl-2-hydroxybenzaldehyde. The compound was prepared by the procedure of Palucki.[30] Purification by flash chromatography (SiO$_2$, 10 vol% EtOAc/90 vol% hexanes) resulted in the product in 39 % yield and 88 % purity. The principal impurity was 2-*tert*-butyl phenol which is unreactive in the ligand formation step with *trans*-1,2-diaminocyclohexane. ^{1}H NMR (CDCl$_3$, 400 MHz) δ 11.77 (s, 1H, -O*H*), 9.86 (s, 1H, -C*H*O), 7.50 (d, 1H, Ar-*H*), 7.39 (d, 1H, Ar-*H*), 6.93 (t, 1H, Ar-*H*), 1.40 (s, 9H, - C(C*H*$_3$)$_3$).

3-Methyl-2-hydroxybenzaldehyde. This procedure is a modification of that reported for the synthesis of 3-*tert*-butyl-2-hydroxybenzaldehyde.[30] A mixture of o-cresol (14.3 mL, 138.6 mmol), 2,6-lutidine (19.4 mL, 166.6 mmol), and tin(IV) chloride (4.9 mL, 41.9 mmol) in anhydrous toluene (425 mL) was stirred for 10 min under a N$_2$ atmosphere. Paraformaldehyde (16.7 g, 554.8 mmol) was added to the mixture, and the mixture was heated to reflux for 4 h. The solution was then allowed to cool to room temperature. Water (800 mL) and diethyl ether (800 mL) were added, and the mixture was filtered through celite. This solution was washed with water (3 x 500 mL) and then brine (3 x 500 mL).   The organic portion of the solution was dried over Na$_2$SO$_4$ and filtered. The solvent was removed under reduced pressure. Purification by flash chromatography (SiO$_2$, 4 vol% EtOAc/96 vol% hexanes) resulted in the product in 43 % yield and 96 % purity. The principal impurity was o-cresol which is unreactive in the ligand formation step with *trans*-1,2-diaminocyclohexane. ^{1}H NMR (CDCl$_3$, 400 MHz) δ 11.25 (s, 1H, -O*H*), 9.86 (s, 1H, -C*H*O), 7.37 (d, 2H, Ar-*H*), 6.90 (t, 1H, Ar-*H*), 2.25 (s, 3H, -C*H*$_3$).

General synthesis of structurally related symmetric and dissymmetric salen ligands.

***N*-[benzylidene]-*N'*-[3-methyl-2-hydroxybezylidene]-1,2-diamino-cyclohexane (8).** The procedure of Larrow et al. was followed.[38] A mixture of potassium bicarbonate (10.5 g, 1.80 mmol) and (1S,2S)-1,2-diaminocyclohexane D-tartrate (10.0 g, 38 mmol) in water (50 mL) was stirred for 10 min until the diamine compound dissolved. Ethanol (200 mL, Pharmco) was added to the mixture and the mixture heated to 80 °C. A mixture of 2-hydroxybenzaldehyde (4.62 g, 38 mmol) and 3-methyl-2-hydroxybenzaldehyde (7.31 g, 38 mmol) in ethanol (42 mL) was added to the diamine solution (at 80 °C) dropwise over 30 min. The mixture was then heated at reflux for 4 h. Extraction of the solution was then performed with CH_2Cl_2 (3 x 100 mL) and NaOH(aq) (pH ~ 11; 3 x 100 mL). The organic solution was dried over Na_2SO_4 and filtered, and the solvent was removed under reduced pressure. Purification by flash chromatography (SiO_2; 5 vol% EtOAc/95 vol% hexanes) resulted in the title compound in 9 % yield and 91 % purity by ^{1}H NMR. TLC and NMR showed no indication of the other possible ligand structures. ^{1}H NMR (CDCl$_3$, 400 MHz) δ 13.59 (s, 1H, -O*H*), 13.31 (s, 1H, -O*H*), 8.24 (d, 2H, *H*C=N), 7.23 (m, 1H, Ar-*H*), 7.12 (m, 2H, Ar-*H*), 6.97 (m, 1H, Ar-*H*), 6.85 (m, 1H, Ar-*H*), 6.77 (m, 1H, Ar-*H*), 6.69 (m, 1H, Ar-*H*), 3.29 (m, 2H, cyclohexyl-*H*), 2.21 (s, 3H, -C*H*₃), 1.90 (m, 6H, cyclohexyl-*H*), 1.68 (m, 2H, cyclohexyl-*H*), 1.45 (m, 2H, cyclohexyl-*H*). The syntheses of the following compounds were identical in procedure except for their respective use of benzaldehyde, 3-*tert*-butyl-2-hydroxybenzaldehyde, and 3,5-di-*tert*-butylsalicylaldehyde.

***N,N'*-Bis[benzylidene]-1,2-diaminocyclohexane (9).** Purification by flash chromatography (SiO_2; 15 vol% EtOAc/85 vol% hexanes) resulted in product (24 % yield) with a purity of 90 % by ^{1}H NMR. Principal impurities were ethyl acetate and residual salicylaldehyde. ^{1}H NMR (CDCl$_3$, 400 MHz) δ 13.30 (s, 2H, -O*H*), 8.23 (s, 2H, *H*C=N), 7.21 (dd, 2H, Ar-*H*), 7.12 (d, 2H, Ar-*H*), 6.85 (d, 2H, Ar-*H*), 6.77 (dd, 2H, Ar-*H*), 3.29 (m, 2H, cyclohexyl-*H*), 1.84-1.94 (m, 4H, cyclohexyl-*H*), 1.71 (m, 2H, cyclohexyl-*H*), 1.45 (m, 2H, cyclohexyl-*H*).

***N*-[Benzylidene]-*N'*-[3-*tert*-butyl-2-hydroxybenzylidene]-1,2-diaminocyclohexane (7).** Purification by flash chromatography (SiO_2; 8 vol% EtOAc/92 vol% hexanes) resulted in the title compound (25 % yield) with 98 % purity by ^{1}H NMR. No indication was given of the other possible ligand structures. ^{1}H NMR (CDCl$_3$, 400 MHz) δ 13.84 (s, 1H, -O*H*), 13.31 (s, 1H, -O*H*), 8.24 (d, 2H, *H*C=N), 7.21 (m, 1H, Ar-*H*), 7.10 (dd, 1H, Ar-*H*), 6.97 (dd, 1H, Ar-*H*), 6.85 (d, 1H,

Ar-*H*), 6.73 (m, 3H, Ar-*H*), 3.30 (m, 2H, cyclohexyl-*H*), 1.7-1.92 (m, 6H, cyclohexyl-*H*), 1.45 (m, 2H, cyclohexyl-*H*), 1.38 (s, 9H, -C(C*H₃*)₃).

N,N'-Bis[3-*tert*-butyl-2-hydroxybenzylidene]-1,2-diaminocyclohexane (6). The title compound was obtained in 40 % yield with a purity of 93 % by ^{1}H NMR. The principal impurity was residual aldehydic compound. ^{1}H NMR (CDCl₃, 400 MHz) δ 13.87 (s, 2H, -O*H*), 8.26 (s, 2H, *H*C=N), 7.21 (d, 2H, Ar-*H*), 7.12 (d, 2H, Ar-*H*), 6.67 (t, 2H, Ar-*H*), 3.28 (m, 2H, cyclohexyl-*H*), 1.64-1.94 (m, 6H, cyclohexyl-*H*), 1.45 (m, 2H, cyclohexyl-*H*), 1.38 (s, 18H, -C(CH₃)₃).

N-[Benzylidene]-*N'*-[3,5-di-*tert*-butyl-2-hydroxybenzylidene]-1,2-diaminocyclohexane (5). Purification by flash chromatography (SiO₂; 10 vol% EtOAc/90 vol% hexanes) resulted in the title compound (7 % yield) with 95 % purity by ^{1}H NMR. No indication was given of the other possible ligand structures. ^{1}H NMR (CDCl₃, 400 MHz) δ 13.63 (s, 1H, -O*H*), 13.38 (s, 1H, -O*H*), 8.25 (d, 2H, *H*C=N), 7.28 (m, 1H, Ar-*H*), 7.24 (m, 2H, Ar-*H*), 7.10 (m, 1H, Ar-*H*), 6.94 (m, 1H, Ar-*H*), 6.76 (m, 1H, Ar-*H*), 3.30 (m, 2H, cyclohexyl-*H*), 1.68-1.84 (m, 6H, cyclohexyl-*H*), 1.45 (m, 2H, cyclohexyl-*H*), 1.38 (s, 9H, -C(C*H₃*)₃), 1.22 (s, 9H, -C(C*H₃*)₃).

Loading of salen ligands with Mn. These catalysts were prepared using the procedure of Larrow et al.[38]

5.4.3 Representative Reaction for Mn-Catalyzed Epoxidation

Homogeneous ligand (4) catalyzed epoxidation of 1,2-dihydronaphthalene. A solution of 1,2-dihydronaphthalene (49.5 μL, 0.37 mmol), CH₂Cl₂ (3.0 mL), and chlorobenzene as internal standard (7.5 μL, 73.8 μmol) was stirred at room temperature. 4-methylmorpholine-*N*-oxide (543 mg, 4.5 mmol) and ligand 4 (9.8 mg, 15.4 μmol) were added to the mixture and allowed to stir for 10 min at the reaction temperature. mCPBA (258 mg, 1.5 mmol) was equilibrated to the reaction temperature and then added to the reaction flask in 4 equal portions over 2 min. The reaction was quenched 15 min after addition of oxidant using a solution of methyl sulfide (1.35 M in CH₂Cl₂) equilibrated at the reaction temperature. The quench solution was allowed to stir with the reaction solution for 5 min. An aliquot (0.05 mL) of the reaction mixture was removed and characterized by GC using a chiral phase capillary column. The samples were filtered through a pad of alumina before characterization. Typical GC conditions were: 1.3 mL/min at

constant flow, 250 °C inlet temperature, and a temperature program of a 120 °C isotherm for 40 min.

Characterization of catalyzed epoxidation of styrene by GC. Typical GC conditions were: 1.5 mL/min at constant flow, 250 °C inlet temperature, and a temperature program of a 90 °C isotherm for 30 min.

Characterization of catalyzed epoxidation of 6-bromo-2,2,3,4-tetramethyl chromene by GC. Typical GC conditions were: 2.1 mL/min at constant flow, 250 °C inlet temperature, and a temperature program of a 110 °C isotherm for 10 min, 5 °C /min ramp to 150 °C, 150 °C isotherm for 82 min.

5.4.4 Representative Reaction for Kinetic Resolution of Epoxides

Homogeneous ligand (4) resolution of Styrene Oxide. A solution of racemic styrene oxide (43.4 µL, 0.37 mmol), CH_2Cl_2 (3.0 mL), and chlorobenzene as internal standard (7.5 µL, 73.8 µmol) was stirred at room temperature. 4-methylmorpholine-*N*-oxide (543 mg, 4.5 mmol) and ligand **4** (9.8 mg, 15.4 µmol) were added to the mixture and allowed to stir for 10 min at the reaction temperature. mCPBA (258 mg, 1.5 mmol) was equilibrated to the reaction temperature and then added to the reaction flask in 4 equal portions over 2 min. The reaction was quenched 15 min after addition of oxidant using a solution of methyl sulfide (1.35 M in CH_2Cl_2) equilibrated at the reaction temperature. The quench solution was allowed to stir with the reaction solution for 5 min. An aliquot (0.05 mL) of the reaction mixture was removed and characterized by GC using a chiral phase capillary column. The GC conditions mimcked those listed in section 5.4.4. Additionally, the racemic epoxides used for this study were synthesized as indicated in section 3.4.3.

5.5   References

1)   Jacobsen, E. N. *Asymmetric Catalytic Epoxidation of Unfunctionalized Olefins*; Ojima, I. N., Ed.; VCH Publishers: New York, 1993, p 159.

2)   Jacobsen, E. N.; Zhang, W.; Guler, M. L. *J. Am. Chem. Soc.* **1991**, *113*, 6703.

3)   Palucki, M.; Finney, N. S.; Pospisil, P. J.; Guler, M. L.; Ishida, T.; Jacobsen, E. N. *J. Am. Chem. Soc.* **1998**, *120*, 948.

4)   Hughes, D. L.; Smith, G. B.; Liu, J.; Dezeny, G. C.; Senanayake, C. H.; Larsen, R. D.; Verhoeven, T. R.; Reider, P. J. *J. Org. Chem.* **1997**, *62*, 2222.

5)   Linde, C.; Arnold, M.; Norrby, P. O.; Akermark, B. *Angew. Chem., Int. Ed. Engl.* **1997**, *36*, 1723.

6)   Hamada, T.; Fukuda, T.; Imanishi, H.; Katsuki, T. *Tetrahedron* **1996**, *52*, 515.

7)   Finney, N. S.; Pospisil, P. J.; Chang, S.; Palucki, M.; Konsler, R. G.; Hansen, K. B.; Jacobsen, E. N. *Angew. Chem., Int. Ed. Engl.* **1997**, *36*, 1720.

8)   Zhang, W.; Loebach, J. L.; Wilson, S. R.; Jacobsen, E. N. *J. Am. Chem. Soc.* **1990**, *112*, 2801.

9)   Pospisil, P. J.; Carsten, D. H.; Jacobsen, E. N. *Eur. J. Chem.* **1996**, *2*, 974.

10)   Lopez, J.; Liang, S.; Bu, X. R. *Tetrahedron Lett.* **1998**, *39*, 4199.

11)   Kureshy, R. I.; Khan, N. H.; Abdi, S. H. R.; Iyer, P.; Bhatt, A. K. *J. Mol. Catal. A: Chem.* **1997**, *120*, 101.

12)   Du, X. D.; Yu, X. D. *J. Polym. Sci.: Pt A: Polym. Chem.* **1997**, *35*, 3249.

13)   Ito, Y. N.; Katsuki, T. *Tetrahedron Lett.* **1998**, *39*, 4325.

14)   Zhao, S. H.; Ortiz, P. R.; Keys, B. A.; Davenport, K. G. *Tetrahedron Lett.* **1996**, *37*, 2725.

15)   Angelino, M. D.; Laibinis, P. E. *Macromolecules* **1998**, *31*, 7581.

16)   Linker, T. *Angew. Chem., Int. Ed. Engl.* **1997**, *36*, 2060.

17)   Norrby, P. O. *J. Am. Chem. Soc.* **1995**, *117*, 11035.

18)   Srinivasan, K.; Michaud, P.; Kochi, J. K. *J. Am. Chem. Soc.* **1986**, *108*, 2309.

19)   Samsel, E. G.; Srinivasan, K.; Kochi, J. K. *J. Am. Chem. Soc.* **1985**, *107*, 7607.

20)   Feichtinger, D.; Plattner, D. A. *Angew. Chem., Int. Ed. Engl.* **1997**, *36*, 1718.

21)   Fu, H.; Look, G. C.; Zhang, W.; Jacobsen, E. N.; Wong, C. H. *J. Am. Chem. Soc.* **1991**, *56*, 6497.

22)   Sugimoto, H.; Tung, H. C.; Sawyer, D. T. *J. Am. Chem. Soc.* **1988**, *110*, 2465.

23)   Irie, R.; Noda, K.; Ito, Y.; Matsumoto, N.; Katsuki, T. *Tetrahedron Lett.* **1990**, *31*, 7345.

24) Buschmann, H.; Scharf, H. D.; Hoffmann, N.; Esser, P. *Angew. Chem. Int. Ed. Engl.* **1991**, *30*, 477.

25) Lopez, J.; Mintz, E. A.; Hsu, F. L.; Bu, X. R. *Tetrahedron: Asymmetry* **1998**, *9*, 3741.

26) As a note, the synthesis of a salen ligand with three t-butyl groups (R_1= R_2= R_3= t-Bu, R_4= H) was attempted; however, isolation of this ligand from **4** and **6** by column chromatography was unsuccessful.

27) An impurity (< 10 %) consisting of the aldehydic precursors were present in these products; however, these impurities are not a factor in the investigation of the enantioselectivity of the product ligands.

28) Zhang, W.; Jacobsen, E. N. *J. Org. Chem.* **1991**, *56*, 2296.

29) Brandes, B. D.; Jacobsen, E. N. *Tetrahedron Lett.* **1995**, *36*, 5123.

30) Palucki, M. *Studies in Enantioselective Oxygen Atom Transfer Catalyzed by (Salen)Mn(III) Complexes*; PhD Thesis; Harvard University: Cambridge, 1995, p 192.

31) Larrow, J. F.; Jacobsen, E. N. *J. Am. Chem. Soc.* **1994**, *116*, 12129.

32) Gobel, T.; Sharpless, K. B. *Angew. Chem. Int. Ed. Engl.* **1993**, *32*, 1329.

33) Lee, N. H.; Jacobsen, E. N. *Tetrahedron Lett.* **1991**, *32*, 6533.

34) Lah, M. S.; Chun, H. *Inorg. Chem.* **1997**, *36*, 1782.

35) Hulsbergen, F. B.; Driessen, W. L.; Reedijk, J.; Verschoor, G. C. *Inorg. Chem.* **1984**, *23*, 3588.

36) Nishida, Y.; Tanaka, N.; Yamazaki, A.; Tokii, T.; Hashimoto, N.; Ide, K.; Iwasawa, K. *Inorg. Chem.* **1995**, *34*, 3616.

37) Gou, S.; You, X.; Yu, K.; Lu, J. *Inorg. Chem.* **1993**, *32*, 1883.

38) Larrow, J. F.; Jacobsen, E. N. *J. Org. Chem.* **1994**, *59*, 1939.

Chapter 6. Homogeneous Cr(Salen) Ligands: Kinetics and Substituent Effects

6.1   Background: Kinetics of Asymmetric Ring-Opening of Epoxides using Cr(Salen) Complexes

As discussed in Chapter 4, the asymmetric ring-opening (ARO) of epoxides is a reaction of significance to the pharmaceutical industry for its ability to produce difficult-to-synthesize chiral 1-amino-2-ol precursors.[1] Traditionally, the synthesis of chiral amino alcohols is performed by ring-opening an enantiopure epoxide or by reducing an α-amino acid.[2-4] Enantiopure reactants can be used to produce the 1-amino-2-ol compounds, but enantiopure starting materials are often expensive. The alternate method of reduction of amino acids is not an option for this case in that the reduction process produces solely the chiral 2-amino-1-ol compounds. Thus, the development of a catalyzed, ring-opening reaction for racemic epoxides with Cr(salen) complexes provided a highly efficient, synthetic route to chiral 1-azido-2-trimethylsiloxy ethers (precursors to the 1-amino-2-ols).[5] For this salen-catalyzed reaction, trimethylsilylazide (TMSN$_3$) is added to the ring-opened epoxide.

The value of these catalysts for industrial application is a result of their high enantioselectivity in performing the ring-opening of epoxides. However, while the focus in the chemical literature has been their enantioselective performance,[5,6] little work has been reported on the kinetics of this reaction. In particular, the Cr-catalyzed ring-opening reaction requires longer reaction times than its Mn-analogue for asymmetric epoxidation. While the asymmetric epoxidation reaction using the Mn(salen) is complete within minutes, the Cr-catalyzed ring-opening reactions require between 16 and 46 h for complete conversion at room temperature depending on the reactant epoxide.[5] These long reaction times, coupled with the need to operate at reduced temperatures for asymmetric reactions in order to optimize ee, reduce the attractiveness of this process for industrial application. While the Cr(salen)-catalyzed reaction provides an effective route to chiral 1,2-amino alcohols, the lack of a detailed understanding of the kinetics of the process hampers its industrial application.

Kinetic studies have been reported for the reaction between an epoxide, NH$_3$, and Cr(salen) -**1**. The initial rates were monitored by in-situ IR spectroscopy and indicated that the

reaction was second-order in catalyst concentration and zero-order in $TMSN_3$ concentration.[6]

1
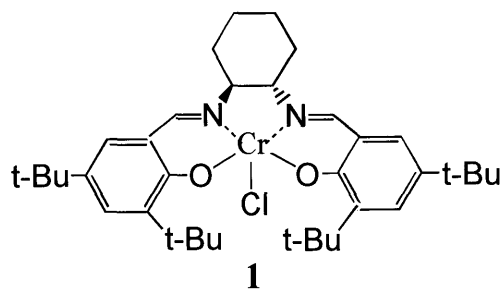
The second-order dependence on the catalyst led to a mechanistic proposal for the asymmetric ring opening reaction that involves the activation of the epoxide and azide by two catalyst molecules (Figure 6.1). In this proposed mechanism, the Cr(salen) complex may act as either an epoxide activating agent or an aide in azide delivery. A critical feature of this proposed mechanism (Figure 6.1) is the formation of a catalyst-substrate complex (**5**) involving both epoxide and $TMSN_3$ complexed to the catalyst.

While some work has been reported on the kinetics of this asymmetric ring-opening reaction, additional parameters that affect the reaction rate need to be elucidated. This chapter provides a characterization of the reaction scheme for the asymmetric ring-opening of a model epoxide (cyclohexene oxide (chex ox)) by a set of structurally-related (S,S)-Cr(salen) catalysts. In particular, the work focuses on the effect of steric variations in the catalyst structure on its activity and enantioselective behavior. The starting point for this study is the Cr(salen)-**1** catalyst that contains four t-butyl groups that symmetrically surround the active metal center.[5,7,8] The majority of work reported in the literature for this reaction has employed this catalyst structure. For this study, three additional catalysts were synthesized that vary in their steric architecture by the number and position of the surrounding t-butyl groups (section 5.2.1).

1:	R_1= t-Bu ;	R_2= t-Bu ;	R_3= t-Bu ;	R_4= t-Bu
2:	R_1= H ;	R_2= t-Bu ;	R_3= t-Bu ;	R_4= H
3:	R_1= t-Bu ;	R_2= t-Bu ;	R_3= H ;	R_4= H
4:	R_1= H ;	R_2= t-Bu ;	R_3= H ;	R_4= H

This study compares the kinetic parameters, as well as the enantioselectivities, of these structurally diverse catalysts to develop a clearer understanding of the activity and enantio-selectivity guidelines at work in this reaction.[9]
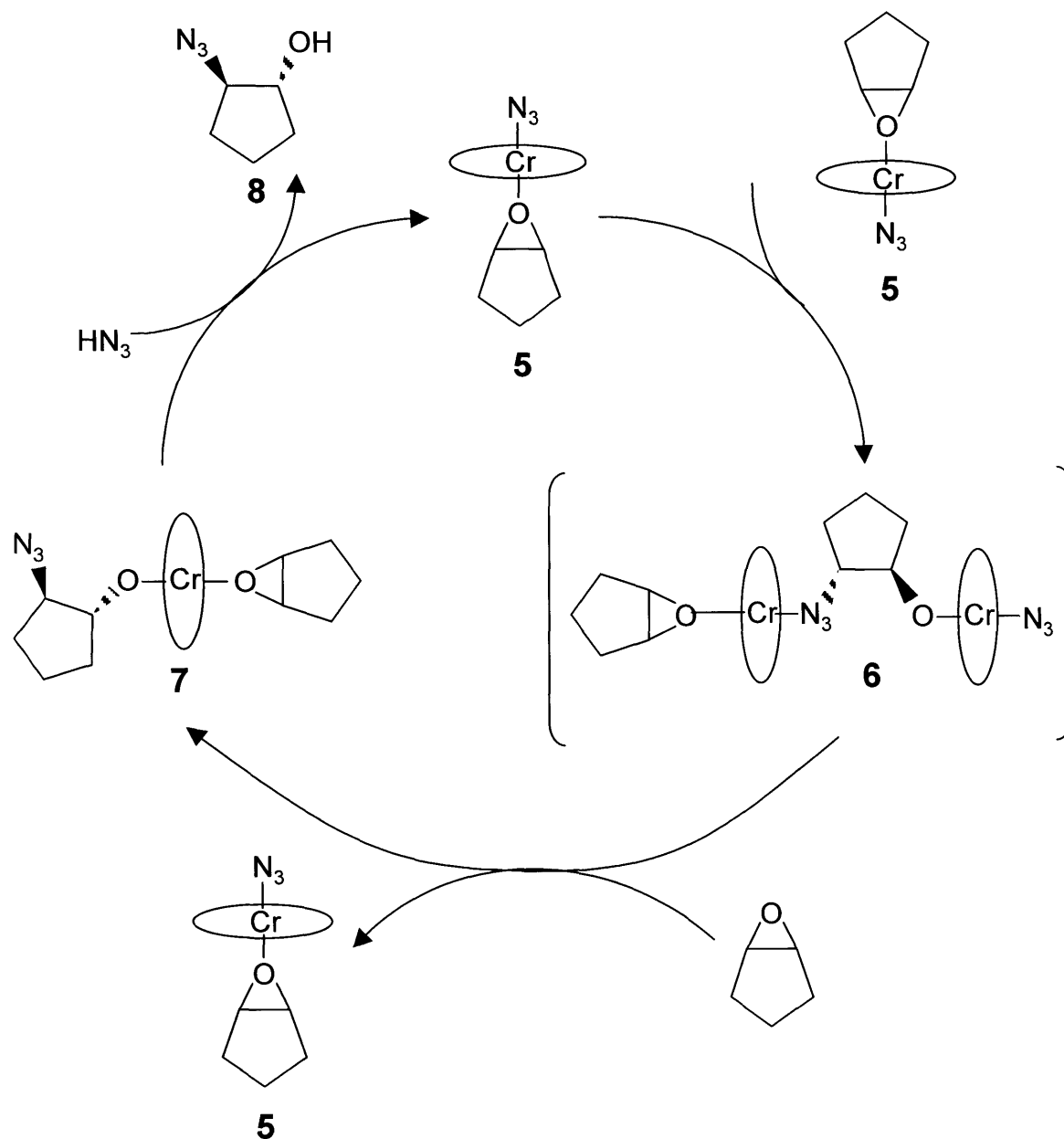
Figure 6.1. Proposed mechanism for the asymmetric ring-opening of epoxides with Cr(salen) catalysts. The second-order dependence of the reaction rate on catalyst concentration is indicative of a cooperative effect between two salen complexes in the addition of azide to the epoxide. *Reference:* Hansen, K.B., et al., *J. Am. Chem. Soc.*, **1996**, 118, 10924.

6.2 Results and Discussion

6.2.1 Reproducibility of Reaction Kinetics

Before examining the kinetics and mechanism of the ring-opening reaction in detail, an initial study was conducted to determine the reproducibility of rate data for this reaction. In short, the initial experiments were difficult to reproduce. For example, when ether, the catalyst, and Chex Ox were stirred together at 0 °C, and $TMSN_3$ (also at 0 °C) was then added, the observed reaction rates varied and depended on the amount of time the catalyst and epoxide had equilibrated before the addition of $TMSN_3$ (Figure 6.2). The rate data indicated that stir times of less than 30 min before the addition of $TMSN_3$ caused variations in the rate of reaction. In contrast, reproducible results were always obtained when the catalyst and epoxide were incubated together for 30 min (or more) before $TMSN_3$ addition. It is likely that in order for the Cr-loaded salen ligand to catalyze the reaction at maximum efficiency, it must first saturate its binding sites with the epoxide.

6.2.2 Asymmetric Ring-Opening Modeled as Series Reaction

Once a reproducible procedure was attained, the reaction rate data were analyzed to generate a kinetic scheme for modeling the asymmetric ring-opening reactions (ARO). In monitoring the reactions by GC, it was noted that at low conversion of reactant the azido-ether product was generated such that the yield of product was less than the converted amount of epoxide. At higher conversion of reactant, the yield value would approach the converted amount of epoxide. This difference between conversion and yield values at early reaction times indicated the possibility of the formation of an intermediate complex. To model this type of reaction, a series reaction was postulated. Such a series reaction that involves one transient intermediate can be generalized as:

$$A \xrightarrow{k_1} B \xrightarrow{k_2} C$$

Figure 6.3 plots the ratio of concentrations for the intermediate and Chex Ox as a function of Chex Ox conversion for the reaction involving Cr(salen)–**3**. The experimental data for this reaction are plotted along with several curves that were generated using the above series reaction
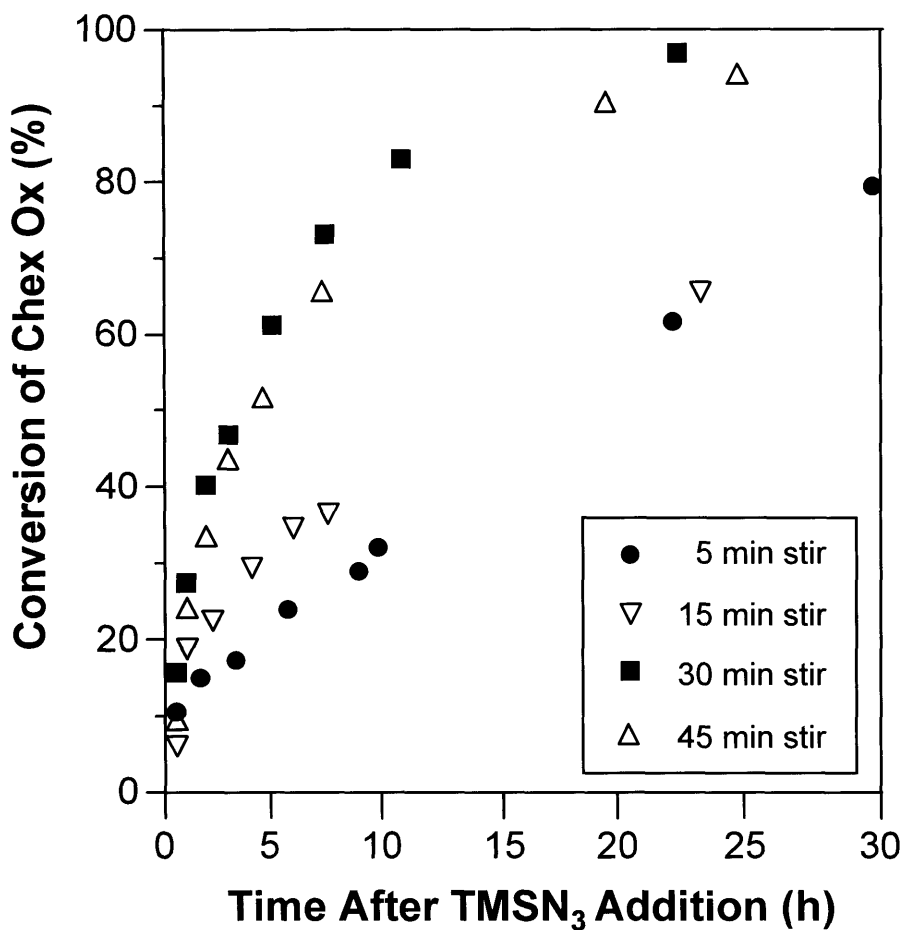
Figure 6.2. The conversion rate for the epoxide depended on the time that the epoxide was permitted to stir with the catalyst before the addition of $TMSN_3$. In these reactions, cyclohexene oxide (2.0 M) was stirred with 0.12 M Cr(salen)-**1** in diethyl ether for different time intervals before $TMSN_3$ was added. Variations in the conversion data were observed for stir times less than 30 min and exhibited minimal reproducibility. With incubation time of 30 min or longer, the conversion profiles for the reactions were the same and were reproducible.
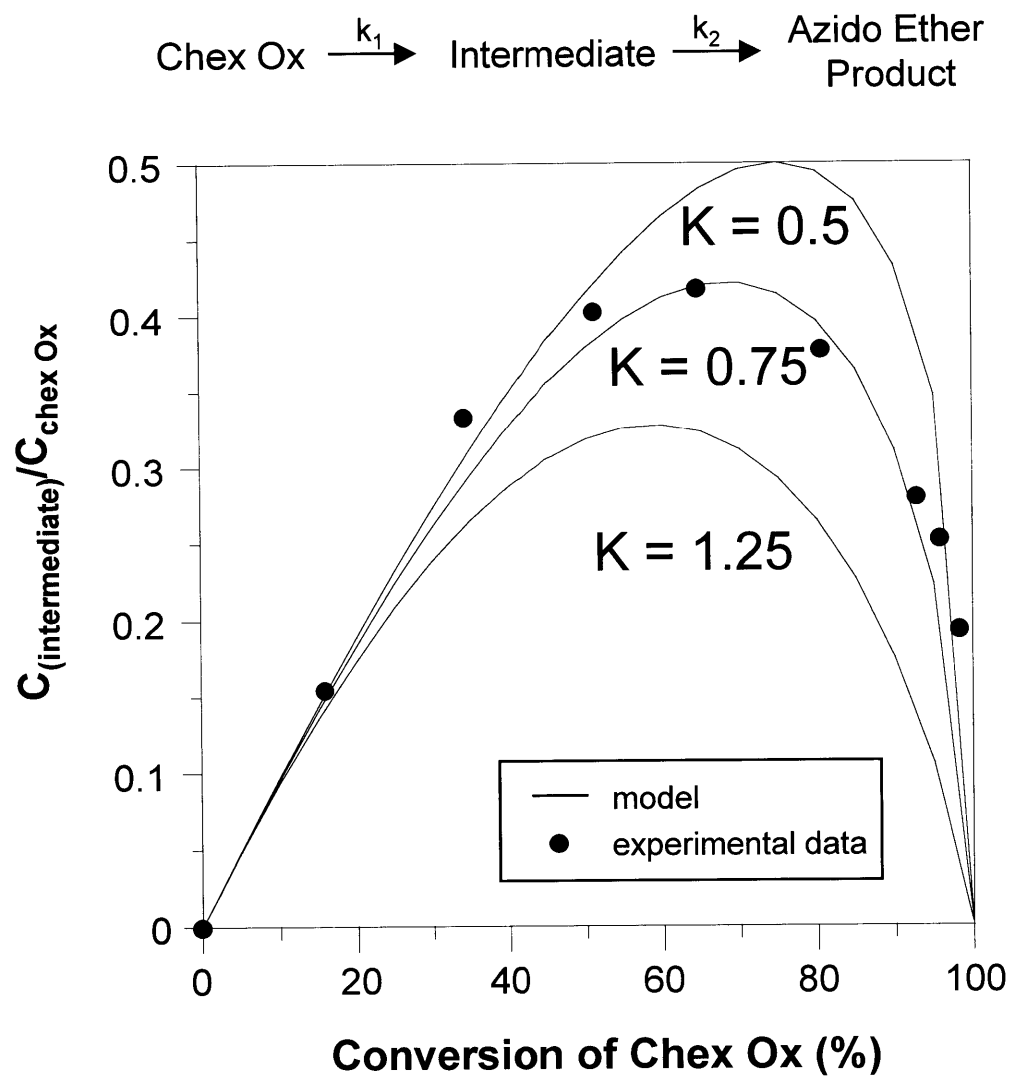
Figure 6.3. Reaction kinetic data for the Cr-catalyzed ring-opening of cyclohexene oxide (Chex Ox) using Cr(salen)-**3**. A model (eq C.3.) was fit to the data assuming a series reaction scheme. The model that best fits the data assumed $K = k_2/k_1 = 0.75$.

model scheme and various values of K (the ratio between the two rate constants, k_2 and k_1). Plots for the other catalysts are provided in Appendix C along with the equations used to generate these curves. All the catalysts investigated were fit by the series reaction model relatively well.

In the above analysis, since the intermediate itself could not be isolated, the difference between the product yield and conversion was use to estimate the amounts of the intermediate by assuming an overall mass balance. This assumption appeared sound since the yields approach 94 % for each Cr(salen) catalyst. The discrepancy of 6 % is due to by-product formation by the chlorine donor atoms on the Cr-catalyst structure (6 mol % relative to epoxide) as they are involved initially in forming ring-opened epoxides with chlorine atoms.

While the series model fit the data, several observations required additional resolution. First, the jump in conversion at the first sampling point is relatively large and consistently observed (Figure 6.4). At a sampling point of 30 sec from the start of the reaction, the conversions ranged from 6 to 15 %. As reaction times were on the order of hours, such high levels of conversion at early times in the reaction were unexpected. The observation of a lag in yield versus conversion at early times indicated that the reactants were likely proceeding through an intermediate. When the reactions were sampled both before and after the addition of catalyst (without TMSN$_3$ present), a corresponding decrease in the epoxide concentration was still observed. This latter result indicates that rather than producing an organic compound as intermediate, the reaction pathway more likely involves a catalyst-substrate complex as intermediate. Additionally, the amount of epoxide converted at these initial times was consistently 1 to 2 times the catalyst concentration relative to epoxide (i.e. 1 to 2 times the 6 mol % catalyst relative to epoxide). These values may reflect the fact that the catalyst presumably can coordinate one or two epoxide molecules, one on each face of the planar catalyst.

Complementary experiments using infrared spectroscopy also indicate the formation of a catalyst-substrate complex. Figure 6.5 presents the IR spectra of samples collected during the first hour of reaction using Cr(salen)-**3**. Before any TMSN$_3$ is added to the reaction vessel, the IR spectrum exhibits no absorptions in the region corresponding to azide stretching modes. After the addition of TMSN$_3$ to the reaction flask, two peaks are observed; at 2058 and 2096 cm^{-1}. The peak at 2058 cm^{-1} is consistent with the reported azide stretching mode for a Cr-azide complex,[7] and the peak at 2096 cm^{-1} is consistent with the product organic azide generated
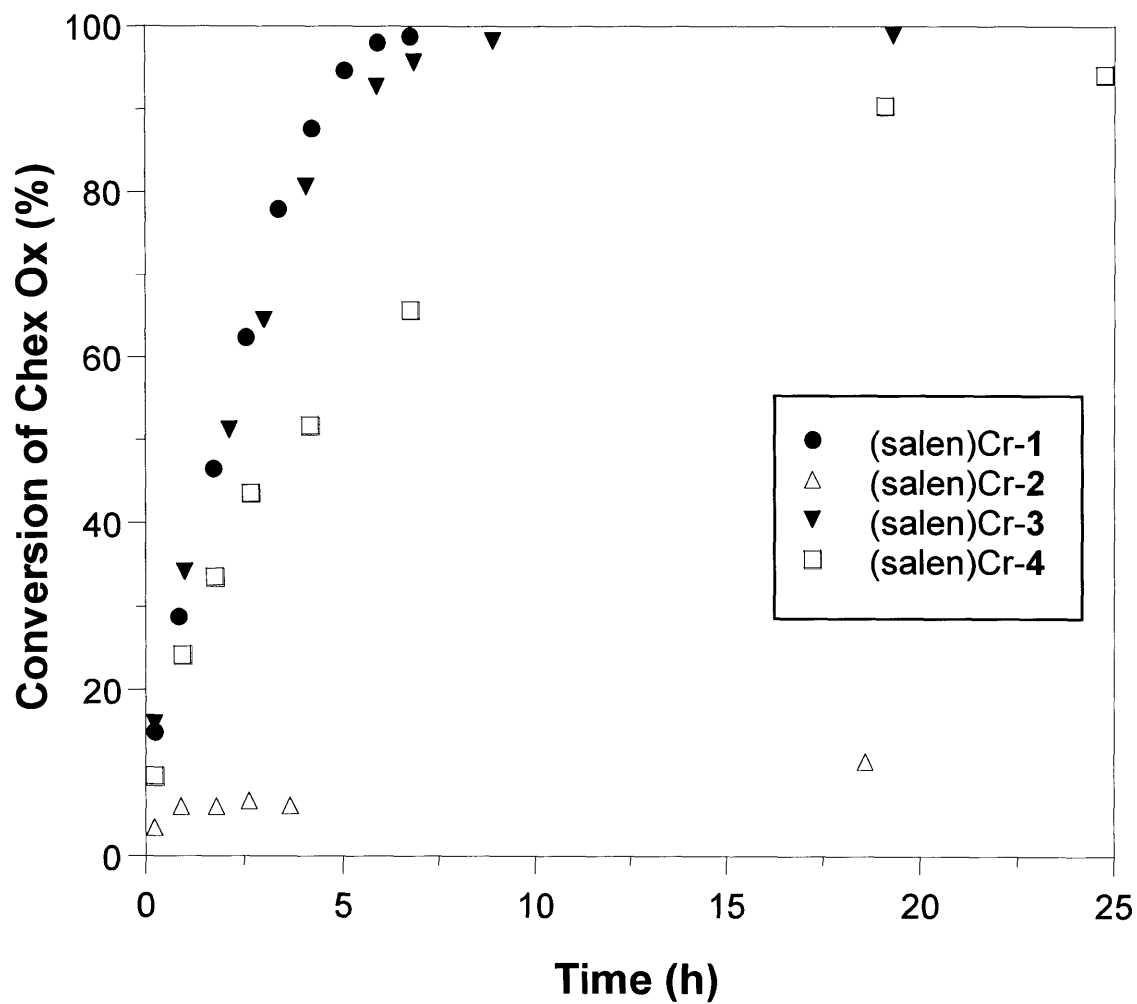
Figure 6.4. The relative rates of reaction for cyclohexene oxide and TMSN₃ using the four Cr(salen) catalysts. The initial points on the plot were taken at 30 s. The conversions at 30 s ranged from 6-15 % while the yields of ring-opened product were negligible.
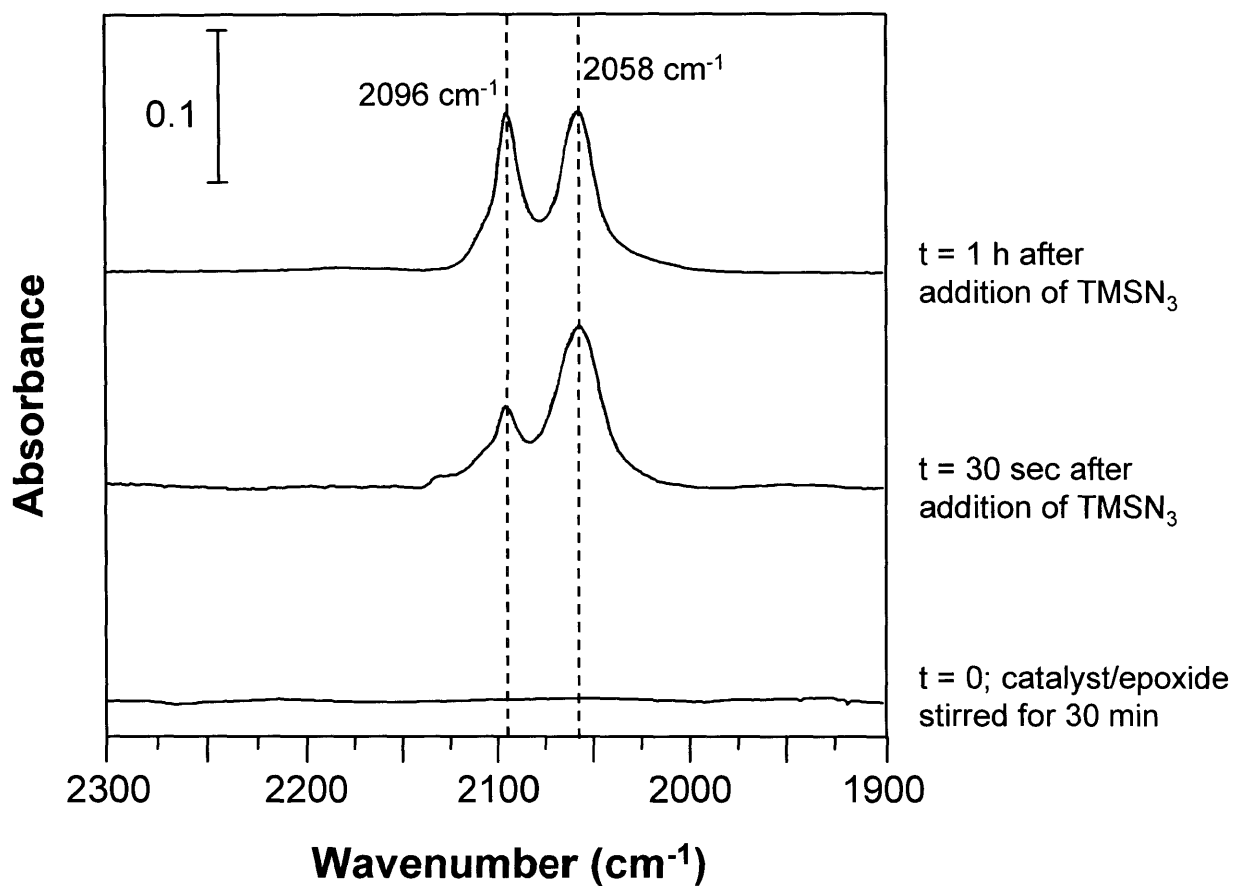
Figure 6.5. Progression of IR spectra for Cr-catalyzed ring-opening of cyclohexene oxide using Cr(salen)-**3**. A reaction solution of 2.0 M epoxide and 0.12 M catalyst were stirred at 0 °C for 30 min. $TMSN_3$ was added at t = 0 and aliquots of solution were examined at t= 30 sec and 1 h. The peaks shown correspond to azido (N_3-) stretching modes with the peak at 2058 cm^{-1} being assigned to a catalytic intermediate and that at 2096 cm^{-1} being assigned to product and intermediate complex.

in the reaction. However, this latter peak may also be due to the epoxide-N_3 intermediate that exists prior to product formation (**7**) (as seen in Figure 6.1). At later times, the peak at 2096 cm^{-1} increased in intensity indicating the formation of product. The IR spectra of samples produced with the other Cr(salen) catalysts showed peaks at the identical locations as those with Cr(salen)-**3**.

As a result of the above evidence regarding the presence of a catalyst-substrate complex (rather than a simple organic species as intermediate) and the necessity for complexation between the catalyst and epoxide (section 6.2.1) for increased rate of reaction, the simple series reaction scheme presented earlier was modified to account for these added complexities. For this analysis, kinetic models based on enzymatic reactions provided a useful system for comparison.

6.2.3   Enzyme Kinetic Model for Cr(Salen)-Catalyzed Ring-Opening of Epoxides

6.2.3.1 Substrate Inhibition

With experimental observations and IR spectra indicating the possibility of a catalyst-substrate complex for the ARO reaction, rate data using the four catalysts were obtained in order to develop a kinetic model. Initial rates of conversion were plotted against initial epoxide concentration for reactions using the four catalysts (Figure 6.6). As further evidence that enzymatic kinetics might be the best model for the epoxide ring-opening reaction, Cr(salen)-**1** exhibited a reduction in rate at high concentrations of epoxide. This behavior is termed substrate inhibition and is a phenomenon observed in enzyme kinetics. The likely cause for this decreased rate of reaction stems from the formation of a tertiary, ineffective intermediate that occupies active catalyst and prevents turnover of the catalyst toward product formation. In such reactions, the formation of product requires two different substrates to bind to the same enzyme or catalyst; in the case of this ring-opening reaction, product is generated when catalyst has both epoxide and -N_3 coordinated to it. The coordination of two epoxide molecules to a catalyst prevents -N_3 (via TMSN$_3$) from coordinating and hence inhibits formation of product. The tertiary, ineffective intermediate forms when the active metal center of a Cr(salen) catalyst binds two epoxides. At
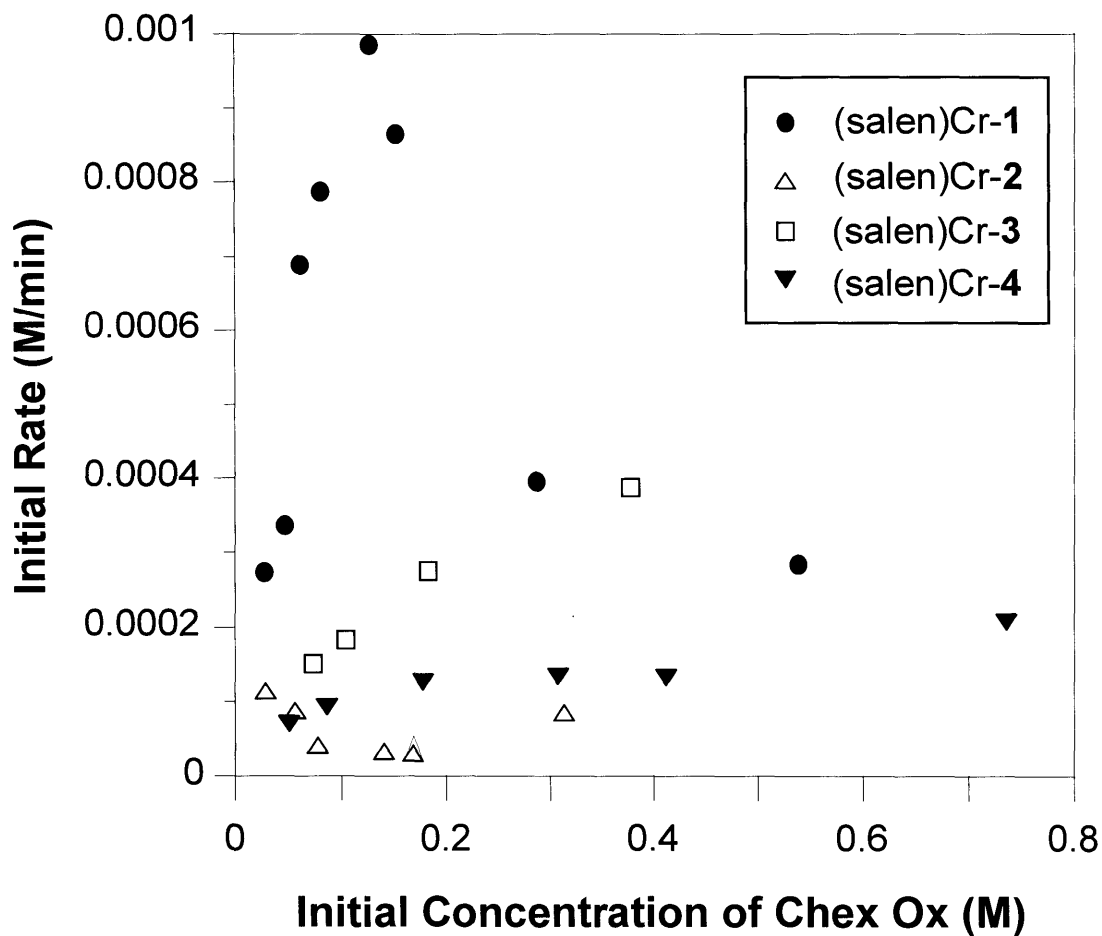
Figure 6.6. The initial rates of conversion of cyclohexene oxide (Chex Ox) are plotted as a function of the initial Chex Ox concentration. The reactions were performed with 0.029 M Cr(salen) catalyst at 0 °C. Substrate inhibition is demonstrated by Cr(salen)-**1** at concentrations > 0.12 M for cyclohexene oxide. Substrate inhibition was not observed for Cr(salen)-**3** and **4** over the epoxide concentrations studied. The rates of reactions involving Cr(salen)-**2** were generally slow and no variation in rate could be observed

higher epoxide concentrations, the likelihood of this occurring increases. This possibility may be represented as

$$E \underset{k_{-1}}{\overset{k_1}{\rightleftharpoons}} ES \overset{k_2}{\longrightarrow} \longrightarrow E + Product$$

$$ES \underset{k_{-3}}{\overset{k_3}{\updownarrow}}$$

$$ES_2$$

Assuming that steady-state conditions apply, equation (1) is derived to model systems with substrate inhibition. This equation is an analogue of that for simplified Michaelis-Menten enzyme catalyzed reactions with an added inhibition term.

$$v = \frac{k_2 C_{co}}{1 + \dfrac{K_m}{C_s} + \dfrac{C_s}{K_{Inh}}} \tag{1}$$

In equation (1), C_s is the substrate concentration (M), C_{Co} is the initial catalyst concentration, and K_M and K_{Inh} are kinetic parameters for the formation of complex ES and for the inhibition complex ES_2, respectively. These kinetic parameters are defined and calculated in the following sections.

Figure 6.6 shows the effect of varying initial epoxide concentration on the rate of conversion. Cr(salen)-**1** was the only catalyst that exhibited substrate inhibition. Cr(salen)-**3** and -**4** did not exhibit as significant substrate inhibition over the range of epoxide concentrations studied as catalyst-**1**, and conclusions could not be drawn for Cr(salen)-**2** due to its negligible conversion rate. The reason for substrate inhibition in the case of Cr(salen)-**1** may have to do with the added substituents associated with this catalyst structure. The sterics may play a part in aiding or stabilizing epoxide coordination to the active metal center. By stabilizing a tertiary complex involving two epoxides, the equilibrium to form the tertiary complex would be favored, and the probability of inhibition enhanced as epoxide concentration increases. An alternate explanation may be that substrate inhibition for the other catalysts may occur at higher

concentrations than the range studied. However, this explanation is less likely in that theoretically, the number of effective collisions between epoxide and catalyst should be higher for the less sterically-hindered ligand structures. Hence, if the number of collisions is increased for these ligand structures, the efficacy of the coordination must be the principle factor as to whether inhibition is observed. The efficacy of the coordination is most likely effected by alterations to the ligand structure.

6.2.3.2 Further Development of Reaction Scheme: Order of Reaction and TMSN₃ Effects

Prior to attempting to fit a kinetic model to the rate data for the various catalysts, several other parameters need to be established within the reaction scheme landscape. One element of this investigation is to ascertain the reaction order with respect to epoxide; the other element involves determining whether coordination of the catalyst with $TMSN_3$ has any effects, as in the case of substrate inhibition with epoxide, that need to be addressed by the reaction scheme.

Before the kinetic scheme could be developed, it was important to ascertain the reaction order with respect to epoxide. The reaction order would provide an insight into how the catalyst and epoxide react to form product. The order of reaction was determined by the method of initial rates (Table 6.1) using excess $TMSN_3$ (2.0 M). The data for Cr(salen)-**2** failed to provide a definitive rate order. The negligible rate of reaction using this catalyst does not make Cr(salen)-**2** amenable to any sort of kinetic analysis. After regression of the rate data (Appendix D) for reactions using the remaining catalyst structures, the rate order was determined to be approximately ½ order. Catalysts-**3** and –**4** were clearly ½ order with respect to epoxide. There was some scatter in the data for catalyst-**1** that did not allow one to distinguish between ½ and 1st order. However, the data at lower concentrations that seem to shift the rate to first order in epoxide were more prone to variation. Therefore, ½ order in epoxide is very likely for catalyst-**1** as well.

From the experimental observations discussed, a reaction scheme was developed to model the ARO of epoxides via a modified version of Michaelis-Menten kinetics. The simple series order reaction scheme of A→B→C was no longer capable of fully describing the reaction system. The possibility that the catalyst can proceed through an intermediate, inhibitory complex before forming the azido-trimethylsiloxy product needs to be given account (Figure 6.7). In

addition, if the catalyst can proceed through an inhibitory complex with epoxide, the possibility of such a complex with TMSN$_3$ must also be investigated.

In such a reaction scheme, the pathway of conversion can take one of two directions: reagent A (epoxide) or reagent B (TMSN$_3$) could complex to the catalyst (E) first (Figure 6.7). The kinetics for the reaction change depending on which intermediate (EA or EB) is formed. Figure 6.8 shows the drastic change in conversion rate depending on which reagent is allowed to first complex with catalyst. For this experiment (Figure 6.8), 5.2 µL of Chex Ox (0.1 M) and 0.0091 g of (salen)Cr-**1** were allowed to complex for 30 min before the addition of 0.153 ml of TMSN$_3$ (2.1 M). The reaction neared complete conversion 2.5 h after the addition of TMSN$_3$. Since there was an excess of TMSN$_3$, the reaction was stirred for an additional 80 min after complete conversion was attained. The purpose of the additional stirring with the remaining TMSN$_3$ in the reaction vessel was to simulate incubation of TMSN$_3$ with Cr(salen)-**1**. After this stir time, additional epoxide was introduced into the system, and the rate of the reaction monitored. The conversion rate for epoxide in this second reaction proceeds more slowly than the initial reaction that was performed with the incubation period done in the reverse order (Figure 6.8).

Reactions using the four catalysts in which TMSN$_3$ was incubated first revealed the same trend that the rate of reaction slows down when TMSN$_3$ is added first. When TMSN$_3$ (0.25 ml, 2 M) was incubated with Cr(salen)-**1** before the addition of Chex Ox (0.1 mol), only 30% conversion was attained after 1.6 hours. On the other hand, when Chex Ox (0.1 mol) was incubated with catalyst before the addition of TMSN$_3$ (0.25 ml, 2 M), nearly complete conversion was attained after 1.6 hours. The difference in rates may be due to the formation of a polymeric network of bridging CrN$_3$ units by Lewis base coordination on Cr.[7] The solubility of this complex network in the reaction mixture is reported to be very poor and may result in the decreased activity. Since the reaction proceeds much faster when the epoxide is incubated with the catalyst first, this reaction pathway was the focus of the kinetic study. The reaction was treated as a compulsory order reaction in that a tertiary complex involving catalyst, TMSN$_3$, and epoxide is required for generation of product, but the sequence of addition of substrates is such that epoxide is required to coordinate first.

Figure 6.7 is the reaction scheme that incorporates many of the observations for the Cr(salen) catalyzed asymmetric ring-opening reaction. The figure makes use of both substrate

EA$_2$

k_{inh} [A] k_{-inh} [A]

k_1 [A]   EA $\xrightarrow{k_2}$ EAB $\xrightarrow{k_3}$ Product + E

k_{-1} [B]

E

k'_1 [B]

k'_{-1} EB $\xrightarrow{k'_2}$ [A]   EAB $\xrightarrow{k'_3}$ Product + E

k'_{-inh} [B] k'_{inh} [B]

EB$_2$

$$K^A_s = \frac{k_{-1}}{k_1} \quad (2)$$
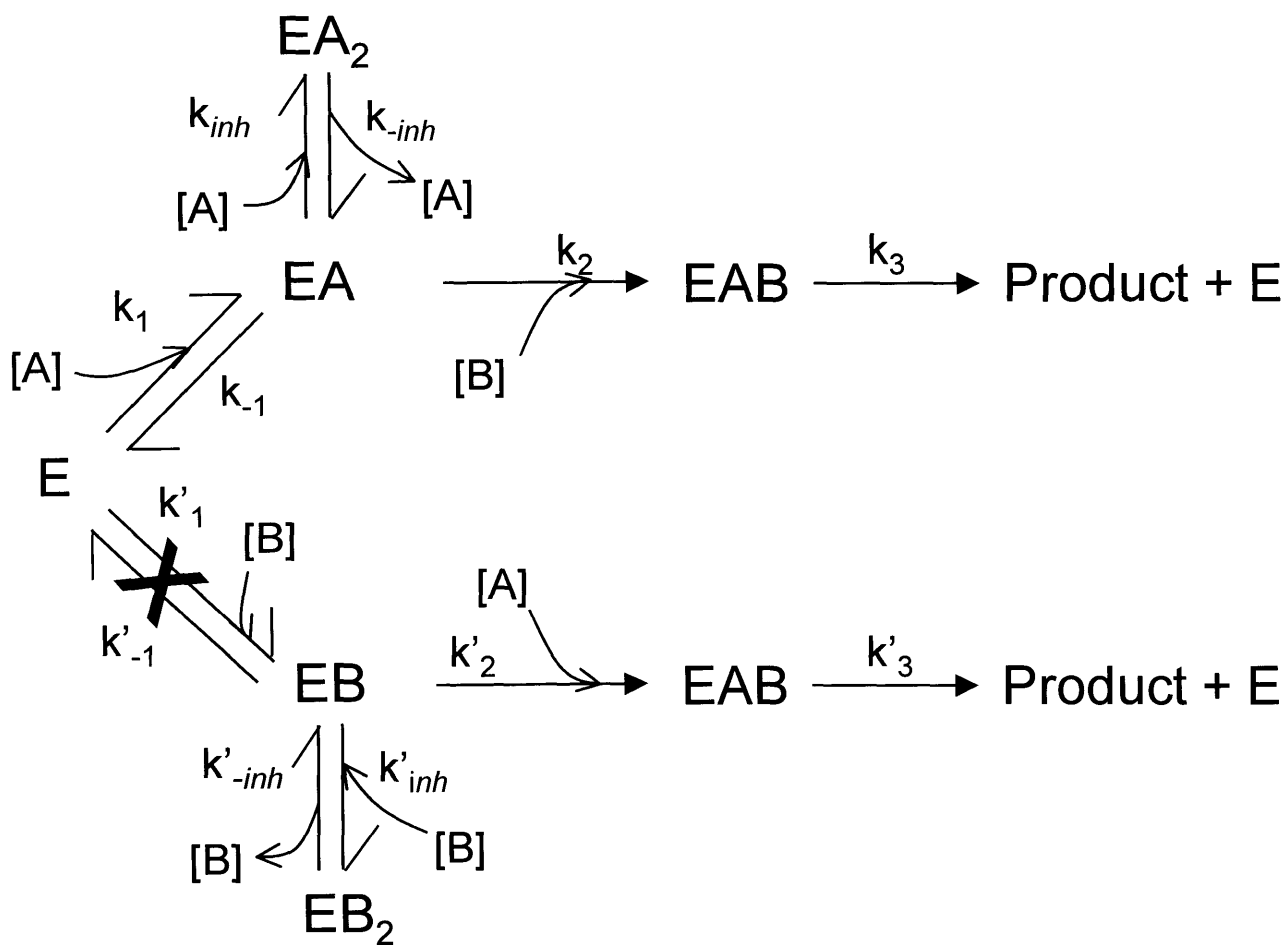
$$K^A_M = \frac{k_{-1} + k_2}{k_1} \quad (3)$$

$$K_{inh} = \frac{k_{-inh}}{k_{inh}} \quad (4)$$

$$K^B_M = \frac{k_3}{k_2} \quad (5)$$

Figure 6.7. Kinetic reaction scheme for the asymmetric ring opening of epoxides including the effects of substrate inhibition. Two substrates, epoxide (A) or TMSN$_3$ (B), can add to the catalyst, but both are required for azido product to form. The schematic depicts how the reaction rates may vary depending on which substrate coordinates first. When TMSN$_3$ was allowed to coordinate first, the reaction proceeded very slowly with minimal variations indicating the possible shutdown of the lower pathway in the schematic. Cr(salen)-1 exhibits substrate inhibition with respect to the epoxide, whereby two epoxides coordinate to the catalysts and inhibit the overall rate. Equations 2-5 list the rate and equilibrium expressions used in this schematic.
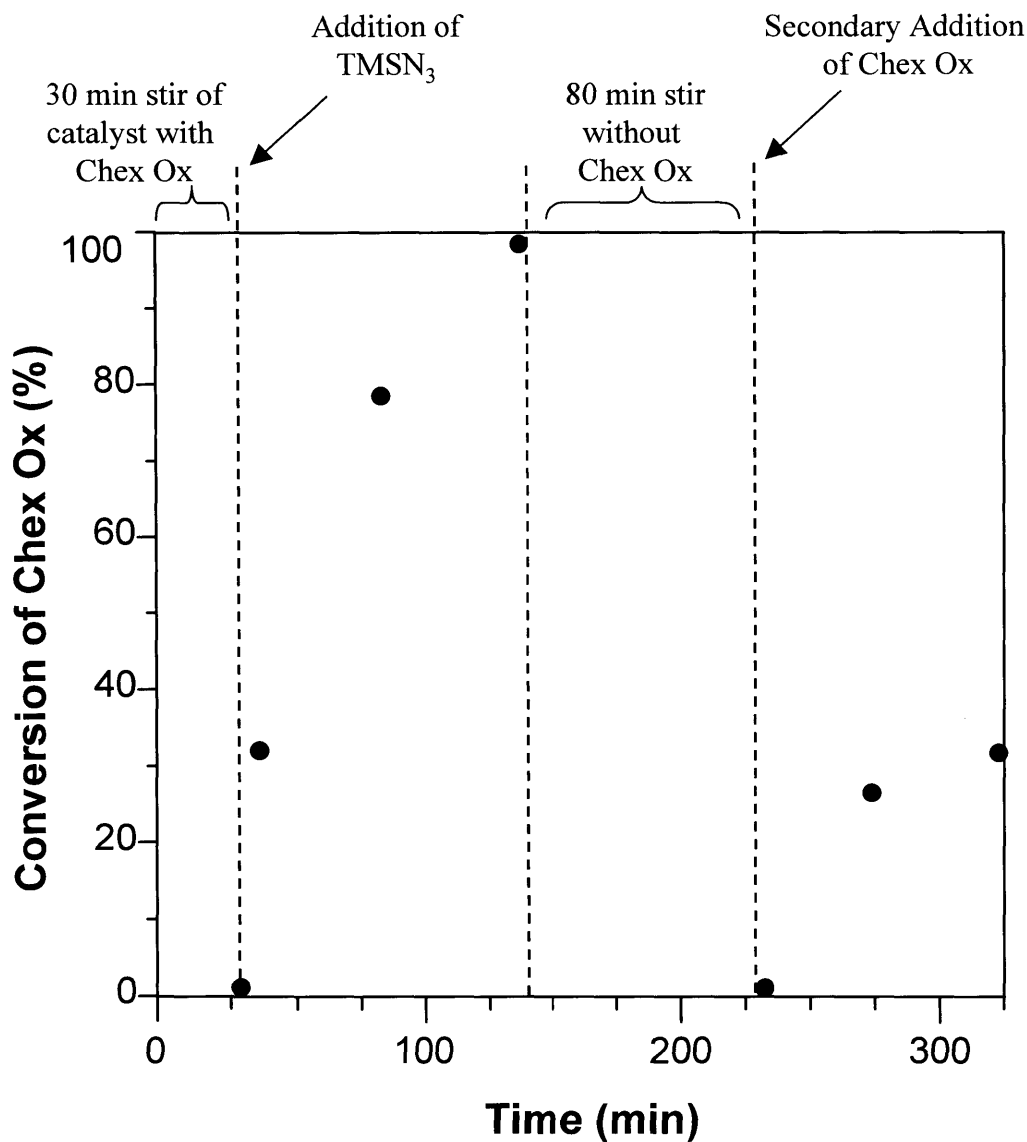
Figure 6.8. Change in reaction rate with the order of addition of substrate into the reaction mixture. Initially, 0.1 M cyclohexene oxide in diethyl ether was allowed to complex with homogeneous Cr(salen)-**3** for 30 min before TMSN$_3$ (2.0 M) was added. Upon complete consumption of the epoxide, the catalyst was stirred for an additional 80 min and an additional equivalent of cyclohexene oxide was added to alter the concentration to 0.1 M again. No additional TMSN$_3$ was provided. The reaction rate for the second batch of cyclohexene oxide was lower than the initial run.

inhibition and compulsory order reactions. Of note in Figure 6.7, the X over the reaction pathway that proceeds with complexation of TMSN$_3$ with catalyst is not meant to indicate that the bottom pathway does not generate product. Rather, while reaction can occur, its rate is much slower than for the top pathway. The bottom pathway involving complexation of TMSN$_3$ does, in fact, contribute to the inhibition effect first noted for epoxide. This effect is discussed in the following section.

6.2.3.3 Discussion of Reaction Parameters

The asymmetric ring opening of epoxides can proceed along two reaction paths. If the epoxide is incubated with the catalyst before the addition of TMSN$_3$, the reaction proceeds must faster. However, inhibition effects that reduce the reaction rate have been observed at high concentrations of both epoxide and TMSN$_3$.

Given the two constraints of compulsory order reactions and substrate inhibition, an enzyme kinetic model was selected to model the system. This model, as described by equation (1) in section 6.2.3.1, is for a system that is inhibited by a single substrate. Since equilibration of the catalyst with epoxide is performed first, it is assumed that the initial rates of reaction should be reflective of the upper pathway of Figure 6.7. However, after catalyst turnover, the free catalyst is exposed to TMSN$_3$ (B) and subsequent turnovers may involve the lower pathway and may include inhibition by TMSN$_3$. Based on the results of equilibration of the catalyst with TMSN$_3$ for which reduced rates were observed as compared to epoxide equilibration, this inhibition is considered to be a significant factor in inhibiting the rate of reaction.

Modeling the asymmetric ring-opening of epoxides as a combination of substrate inhibition and compulsory order reactions using equation (1) facilitates the calculation of the following reaction parameters: K_{ma}, k_2, K_s and K_{Inh}.

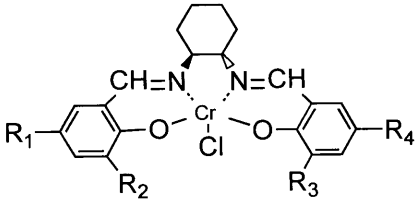$$v = \frac{k_2 C_{co}}{1 + \dfrac{K_m}{C_s} + \dfrac{C_s}{K_{Inh}}} \tag{1}$$

As k_2 was defined in section 6.2.3.1, it is the rate of formation of product. However, this rate constant incorporates much more as it is used here. The reactions performed to calculate these

constants were conducted in excess TMSN$_3$ (B), and hence, these constants incorporate the concentration of B. Additionally, the simplified schematic (section 6.2.3.1) on which this equation is based does not account for the interaction of two complexes needed to form product, the subsequent dissociation rate of product from this larger complex, and the generation of two residual catalyst complexes along with product. The formation of a catalyst complex with a coordinated azide has the possibility of then proceeding along the TMSN$_3$ equilibration pathway (lower path of Figure 6.7).

Table 6.1 presents the values of these constants calculated for Cr(salen)-**1**, -**3**, and –**4** (Appendix E). Because the catalyst is pre-equilibrated with epoxide, it is assumed that the reaction system already exists in an equilibrium involving catalyst (E), catalyst-epoxide complex (EA) and epoxide-catalyst-epoxide complexes (EA$_2$). K$_{ma}$ is the Michaelis-Menten constant for epoxide (A) and accounts for the relative rate of dissociation of EA to either E or product versus the generation of this complex. For the three catalysts examined, this kinetic parameter is essentially equivalent. Hence, the variation of rate that the three catalysts exhibit (Figure 6.4) is not due to this parameter.

Since the relative rates for generation and dissociation of EA do not change, the variation of each of these separate steps was examined for the three catalyst structures. The most dramatic change was noted for the k$_2$ and K$_s$ values using Cr(salen)-**1**. In this case, the rate of reaction of this complex (k$_2$) was several times greater than the respective values for Cr(salen)-**3** and –**4**. In addition, the value for the equilibrium constant for the formation of EA for Cr(salen)-**1** was an order of magnitude greater than the other catalysts. One point that needs to be mentioned is that the error associated with the K$_s$ values are larger than for the other values calculated. The calculation of these values involved the assumption of a complete mass balance such that estimates of the concentration of epoxide complexes and free catalyst could be made. For the reactions conducted at low concentrations of epoxide, variations in concentration were larger and have a greater error associated. In addition, the values for K$_s$ were determined using initial samples of the system with epoxide alone (no catalyst or TMSN$_3$) and an aliquot after 30 sec of reaction. Hence, the observed change in monitored epoxide concentrations may also incorporate some formation of product and not exclusively information about rate of coordination to form complex EA. However, the variation of K$_s$ between catalyst-**1** and that for –**3** and –**4** were consistently different by an order of magnitude.

Table 6.1. Kinetic Parameters for Cr(salen)-Catalyzed Epoxide Ring-Opening Reactions using TMSN$_3$[1]

1: R$_1$= t-Bu ; R$_2$= t-Bu ; R$_3$= t-Bu ; R$_4$= t-Bu
2: R$_1$= H ; R$_2$= t-Bu ; R$_3$= t-Bu ; R$_4$= H
3: R$_1$= t-Bu ; R$_2$= t-Bu ; R$_3$= H ; R$_4$= H
4: R$_1$= H ; R$_2$= t-Bu ; R$_3$= H ; R$_4$= H

Catalyst[2]	Rate Order	K_{ma} (M)	k_2 (min^{-1})	K_s(M)	K_{Inh} (M)
Cr(salen)-1	0.5	0.20- 0.30	0.10- 0.13	0.03- 0.04	0.15[3]
Cr(salen)-3	0.5	0.25- 0.27	0.022- 0.023	0.32- 0.37	∞[4]
Cr(salen)-4	0.5	0.12- 0.20	0.006- 0.007	0.55- 0.65	~2[5]

[1] The kinetic constants are derived for the reaction pathway in Figure 6.7.

[2] The reaction rates for Cr(salen)-2 were slow and roughly constant. A kinetic analysis could not be performed because the changes in rates were negligible.

[3] The value of K_{inh} for Cr(salen)-1 was obtained for excess TMSN$_3$ (2 M). The value does vary with TMSN$_3$ concentration.

[4] For Cr(salen)-3, the inhibition effects were negligible.

[5] The value of K_{inh} for Cr(salen)-4 was obtained for excess TMSN$_3$ (2 M).

As K_s is defined, it is the equilibrium constant for reduction of complex EA to catalyst alone (E). The lower value associated with catalyst-**1** is indicative that the equilibrium favors formation of this active intermediate relative to the other catalysts. One interpretation for this effect is that the catalyst is more active toward coordination of the epoxide. Since the only difference between ligands is the number and position of t-Bu groups. An argument based exclusively on sterics works contrary to the observed result. Rather, the addition of a t-Bu group may slightly alter the electronics of the ligands and induce greater affinity for coordination. This electronic argument is particularly interesting in that it is known that the C5 position of the ligand has been demonstrated to have significance in electronic tuning of the catalyst,[10,11] and the reactions using catalysts having a t-Bu in the C5 position (catalyst-**1** and –**3**) are faster than those without (Figure 6.4).

Finally, regarding the inhibition constants for these catalysts, Cr(salen)-**1** exhibited substrate inhibition at high epoxide concentrations. However, this reaction was conducted in excess TMSN$_3$ which has been demonstrated to impede the rate of reaction if coordination at two sites is achieved (section 6.2.3.2). Single substrate inhibiting systems would obey equation (1), but there is an added element of inhibition that is due to TMSN$_3$. For catalyst-**1**, the activity of the salen complex to coordinate epoxide may also function in an analogous manner to coordinate TMSN$_3$. Then, as was observed when pre-equilibration of catalyst was performed with TMSN$_3$, the reaction rates are slowed. The effect on rate may be due to an added inhibition term due to formation of EB$_2$ (Figure 6.7).

In Figure 6.9, the rate data for a reaction using catalyst-**1** with 2 M TMSN$_3$ is overlaid with the single substrate inhibition model (equation 1) with varied values of K_{inh}. Using the calculated values of K_{ma} and k_2, the data are fit well at low concentration, but the inhibition effect causes a greater decay in rate than can be fit by the single substrate inhibition model. However, if the added element of TMSN$_3$ inhibition is considered, the sharper decline in rate can be explained. Unfortunately, the evaluation of the additional effects of this second substrate are difficult to determine due to the negligible variation in rate if TMSN$_3$ is allowed to pre-equilibrate with the catalyst or the difficulty in monitoring the various complexes (EA, EB, EA$_2$, or EB$_2$). The variation of reaction rates with knowledge of these concentrations would allow the deconstruction of these effects. When the concentration of TMSN$_3$ was reduced to 1 M, the rate data for catalyst-**1** could still be modeled as a single substrate inhibiting system, but with a modified K_{inh} value (K_{inh}= 1.2). The same values of K_{ma} and k_2 were used. The increase in the
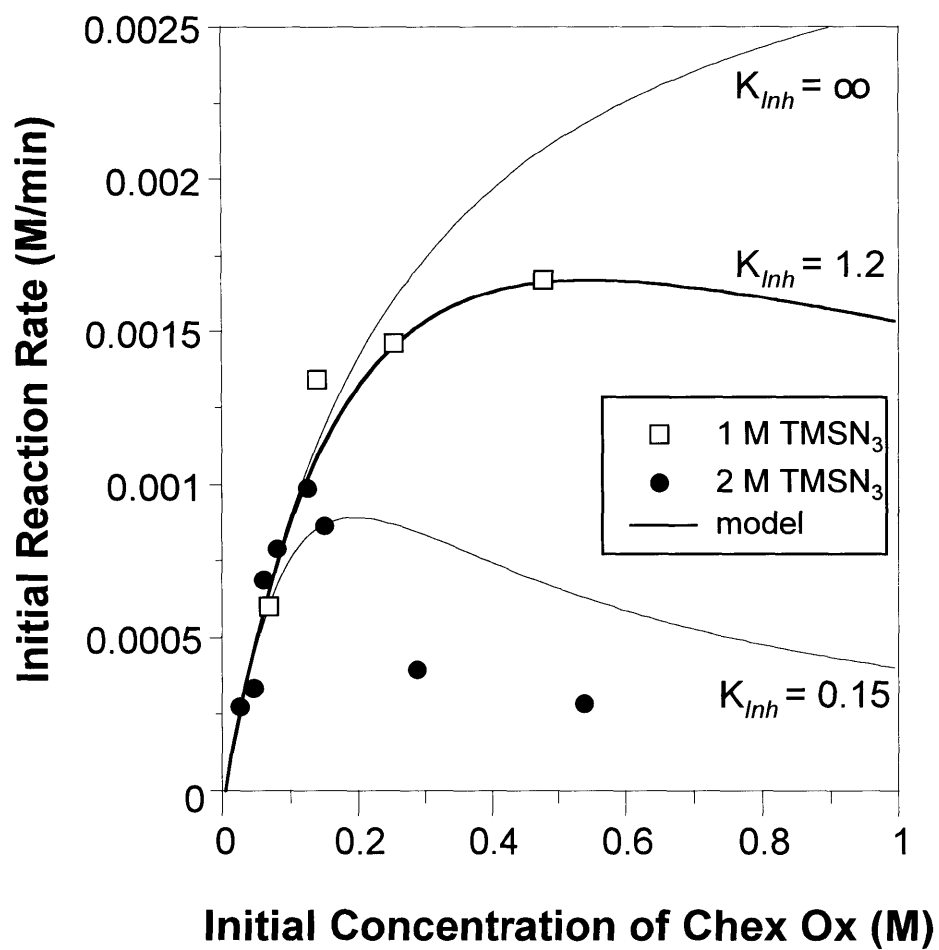
Figure 6.9. Initial rate data for various initial concentrations of cyclohexene oxide using Cr(salen)-**1**. A substrate inhibition model (eq. 1) was fit to the data by varying the inhibition constant (K_{Inh}).

value of K_{inh} from 0.15 to 1.2 could only be explained by the effect of an altered concentration of B on the rate of inhibition. With reduced inhibition by $TMSN_3$, the data is fit well with the single substrate inhibition model.

With regard to catalysts-**3** and –**4** using 2 M $TMSN_3$, the degree of inhibition is reduced from that of catalyst-**1**. Catalyst-**4** does exhibit inhibition, but the rate constant for inhibition is at least an order of magnitude greater than for catalyst-**1** (Figures 6.10-11). With a K_{inh} value of ~2, the equilibrium between the active catalyst complex and the inhibitory complex using **4** is still favoring the reactive intermediate. For catalyst-**3**, the impact of inhibition is negligible; K_{inh} approaches infinity. While there is a large variation in the effect of the inhibition pathway in reducing the rate of reaction using each of the salen catalysts, the most dramatic impact is with the most sterically encumbered catalyst. With a reduction of steric bulk on the salen ligand, the rate of reaction does increase. However, with only three catalysts examined, a more detailed evaluation of the effect on inhibition of these substituents and their position of substitution on the ligand framework is not possible.

With regard to the model presented, the significance of the observation of substrate inhibition for Cr(salen)-**1** is that this is the primary catalytic structure used for the salen-based ARO reactions reported.[5,7] The prolonged reaction times often quoted for these reactions involve systems with high epoxide and high $TMSN_3$ concentrations. Knowledge of the kinetic model readily permits the modification of several reaction parameters to accelerate the rates of reaction to levels acceptable for industrial application.

6.2.4 Enantioselectivity of Cr(salen) Catalysts

While an examination of the factors that govern the rate of the ring-opening reaction has practical significance from an engineering perspective, the value of these catalysts is in the enantioselectivity provided by the ligand. To this effect, the enantioselectivities of these structurally diverse catalysts were examined for the asymmetric ring-opening of cyclohexene oxide, epoxyhexane, and propylene oxide using $TMSN_3$. The latter two compounds are racemic mixtures of epoxides and undergo kinetic resolution as well as asymmetric generation of trimethylsilyl-azido products.

The reactions for which ee are presented (Figures 6.12- 6.14) were conducted using 2 M epoxide, 2.1 M $TMSN_3$, and 0.12 M catalyst in diethyl ether at 0 °C. While high concentrations of substrate have been demonstrated to impede the rate of the reaction, the enantioselectivity is

143

Figure 6.10. Initial rate data for varying initial concentrations of cyclohexene oxide using Cr(salen)-**3**. A substrate inhibition model (eq. 1) was fit to the data by varying the inhibition constant (K_{Inh}).
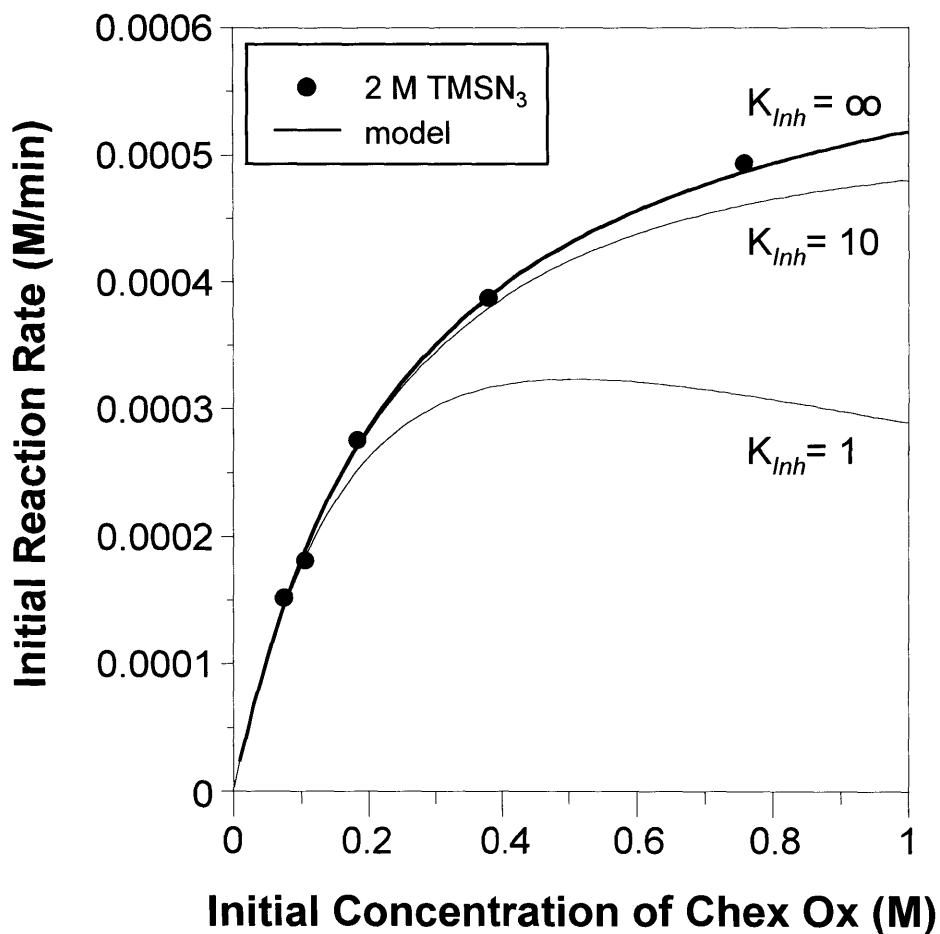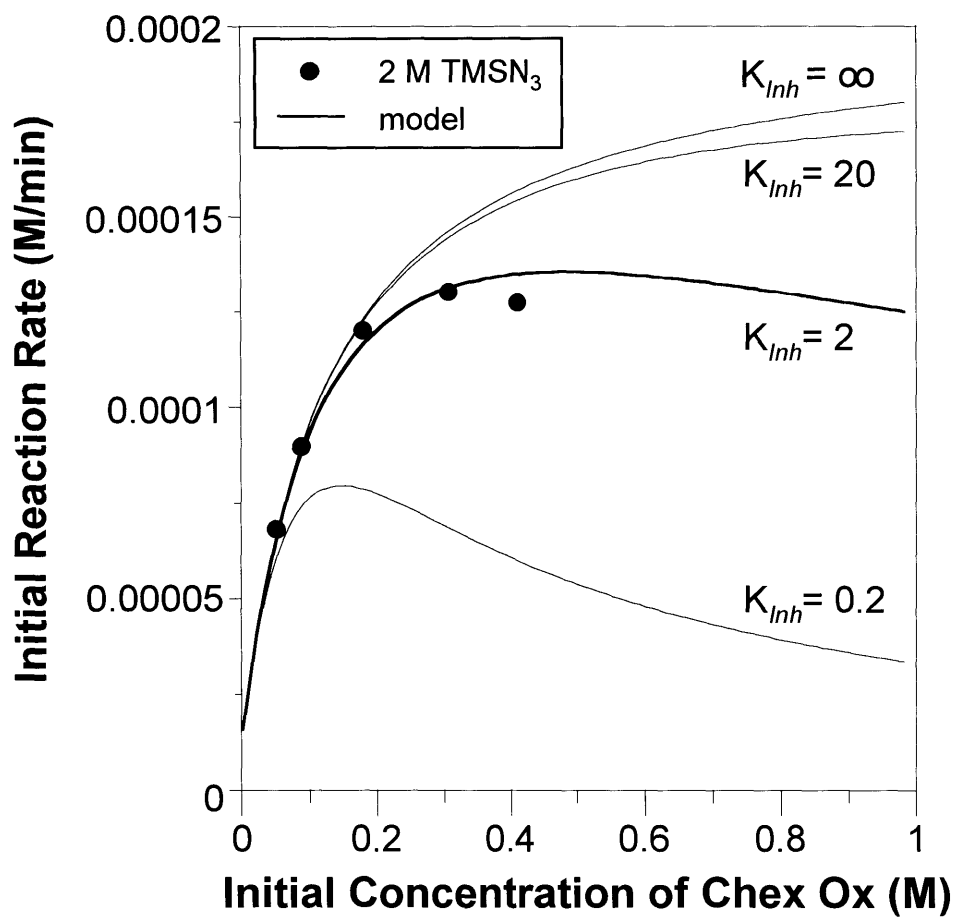
Figure 6.11. Initial rate data for various initial concentrations of cyclohexene oxide using Cr(salen)-**4**. A substrate inhibition model (eq. 1) was fit to the data by varying the assuming various inhibition constants (K_{Inh}).

insensitive to the rate of reaction. For cyclohexene oxide, as concentrations of epoxide and catalyst were reduced, the rate of the reaction decreased, but the ee's were constant and identical. For each of the racemic mixtures of epoxides (epoxyhexane and propylene oxide), ee as a function of yield did not vary as concentrations were altered. For kinetic resolution processes, ee can be expressed as a function of the extent of conversion.[12] Therefore, while the rates changed as concentrations were varied, the variation of product ee with yield did not. In these particular cases, the yield was substituted for conversion because of the presence of the intermediate catalyst complex. Due to the lag between conversion and yield (section 6.2.2), the product ee is not accurately described by conversion, but rather by yield.

With regard to the ee's measured, as opposed to the behavior of the Mn(salen) catalysts where a single t-Bu group provided the biggest increase in enantioselectivity and the addition of t-Bu groups aided in refining the ee, catalysts-2, 3, and 4 were indistinguishable in their enantioselectivity among all three epoxides tested. However, for each system, Cr(salen)-1 was clearly distinguishable as providing the highest enantioselectivity in each case. In the case of cyclohexene oxide (Figure 6.12), an ee of approximately 60 % was observed using (Cr)catalysts– 2, -3, and –4 while a product ee of 90% was observed for catalyst-1.

For both epoxyhexane and propylene oxide, the product ee generally started at 90% using catalysts-2, -3, and –4 and then deteriorated as the kinetic resolution process continued. For both these cases, catalyst-1 generated product with 97-99 % ee initially and then decreased accordingly.

As with the Mn(salen) complexes (Chapter 5), enantioselectivity is generated equally well by catalysts that are either C_2-symmetric or unsymmetric and with varying steric patterns. As for the increased chiral induction observed with catalyst-1, the reported mechanism for this asymmetric reaction involves two salen complexes that sandwich the generated product.[7,13] If such a mechanism is at work, the large steric interaction between two Cr(salen)-1 catalysts is likely to force the $-N_3$ and epoxide to react very specifically and consequently with high enantioselectivity. As the sterics are reduced, there is a decrease in ee. However, since the mechanism involves two ligands, the decrease in sterics only provides an observable change in ee as one shifts from catalyst-1 where the sterics are so high that reactants are converted with enantioselectivity generally greater than 90 %. Additionally, as opposed to the Mn(salen) catalysts for epoxidation where olefin approach to a planer structure dictates enantioselectivity, the use of two ligands provides a higher level of chiral induction by forcing the reactants in a

146

Figure 6.12. Enantioselectivity of Cr(salen) catalysts as a function of yield of the ring-opened product of cyclohexene oxide. The reactions were conducted at 0 °C using 2.0 M epoxide and 0.12 M catalyst in diethyl ether.

Figure 6.13. Enantioselectivity of Cr(salen) catalysts as a function of yield of the ring-opened product of epoxyhexane. The reactions were conducted at 0 °C using 2.0 M epoxide and 0.12 M catalyst in diethyl ether.
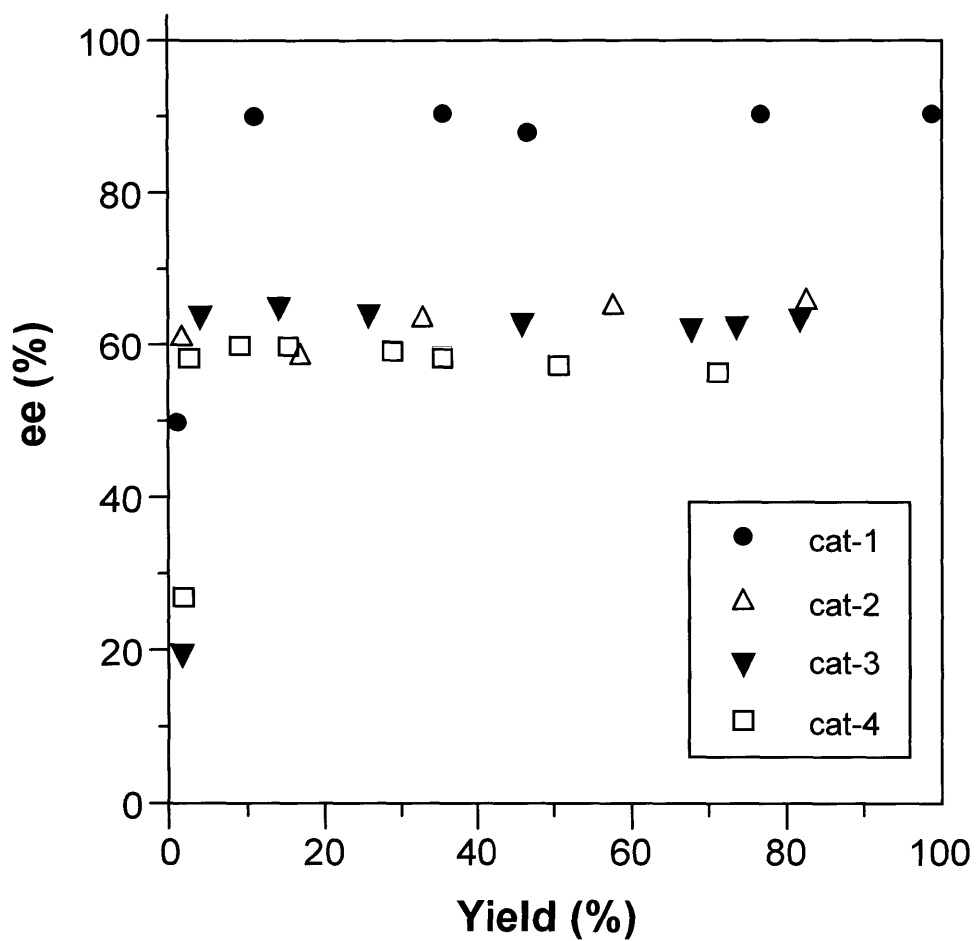
Figure 6.14. Enantioselectivity of Cr(salen) catalysts as a function of yield of the ring-opened product of propylene oxide. The reactions were conducted at 0 °C using 2.0 M epoxide and 0.12 M catalyst in diethyl ether.
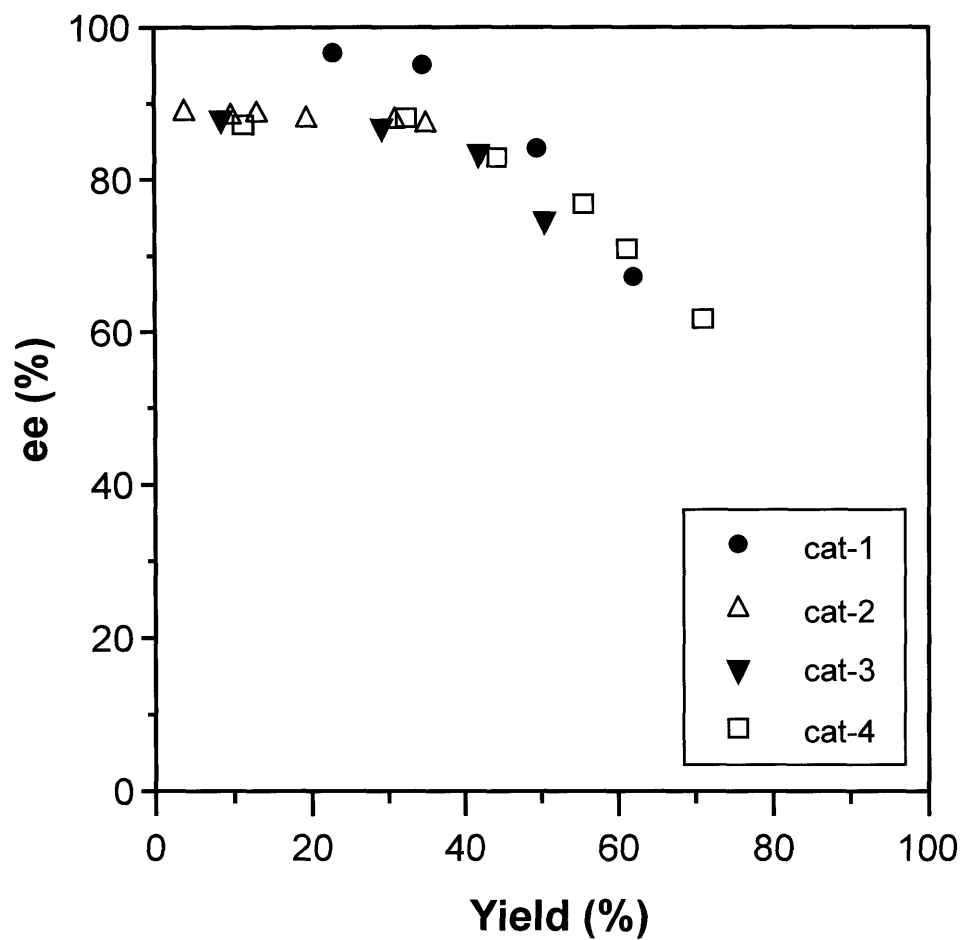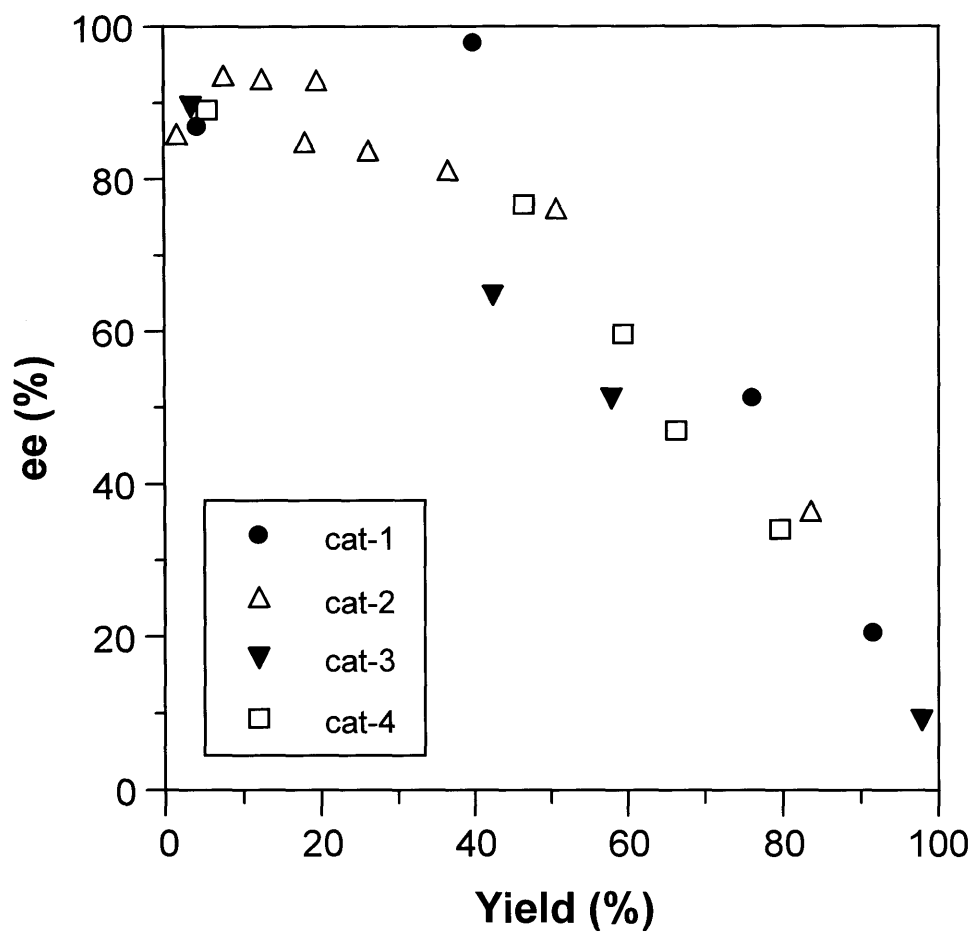
very specific position within the pocket between two ligands. For this reason, high enantioselectivities are generated for alkyl substituted reactants (such as propylene oxide and epoxyhexane) for which the Mn-catalysts for the corresponding case of olefin epoxidation tend to perform poorly.

This reasoning used to explain the high level of chiral induction for the asymmetric ring-opening reaction also allows some interpretation of the enantioselectivities observed with the heterogeneous Cr-ligand (Chapter 4). The reactions using the heterogeneous ligand bound by the polymer on one side and two t-Bu groups on the other indicated that ee could be generated with a Cr(salen) catalyst functioning as a monomeric catalyst. However, the ee's measured were lower than those for the respective homogenous reactions. In the heterogeneous case, ee's of 6, 34, and 36 % were observed for cyclohexene oxide, epoxyhexane, and propylene oxide, respectively (Chapter 4). These values are below those for the homogeneous catalysts (Figures 6.12- 6.14). The reason for this discrepancy was attributed to either the presence of the polymer support or the effects of ligand dissymmetry. While the heterogeneous catalyst does not have the sterics of homogeneous catalyst-1, it was assumed that one of the less substituted, homogeneous catalysts, such as 3, would provide an indication of the effect of ligand dissymmetry on enantioselectivity. However, the less substituted catalysts still provide higher enantioselectivity than the heterogeneous catalyst. Rather, the low enantioselectivity observed using the heterogeneous catalyst may be a result of its immobilization.

By immobilizing the catalyst, these ligands would function much like the Mn(salen) catalyst for epoxidation of olefins. In the case of epoxidation, the ligand generates enantioselective product by manipulation of the approach path of the olefin rather than chiral induction within a highly constrained pocket between two Cr(salen) complexes as suggested by the mechanism for epoxide ring-opening. For the immobilized Cr-ligand, the ee expected would be lower due to this reduced chiral induction. Additionally, the epoxides examined do not have many of the attributes for which the salen catalyst is known to provide high enantioselectivity for a case involving reactant approach as with Mn-catalyzed epoxidation. For example, the lack of an aromatic substituent on the reactant does not allow the added advantage provided by π-π interactions to have an impact on approach paths and ee.[10]

As a note, variation of the heterogeneous ligand was conducted in a similar manner as for the homogeneous Cr-ligands. Namely, ligand structures were synthesized onto a styrene (98 vol%)/ divinylbenzene (2 vol%) support with the terminal benzaldehyde having either a single t-

Bu in the C3 position (**11**) or no t-Bu (**12**). These Cr-loaded ligands were examined for
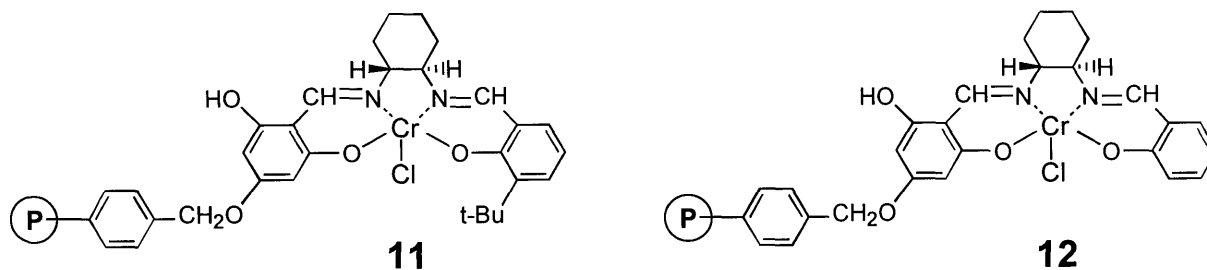
11 **12**

asymmetric ring-opening of cyclohexene oxide, epoxyhexane, and propylene oxide using TMSN₃. The synthetic protocol and reaction procedure are provided in section 4.4. The enantioselectivities for these ligands were below those of the more highly substituted heterogeneous ligand (**13**) of Chapter 4 (Table 6.2). With decreasing substituents, the ee using

Table 6.2. Enantioselectivities (ee %) for Heterogeneous Cr-Catalysts for Asymmetric Ring-Opening Reactions with TMSN₃ at 0 °C

Catalyst	Cyclohexene Oxide	Epoxyhexane	Propylene Oxide
13	6	34	36
11	0	15	13
12	0	10	6

these catalysts decreased. As was discussed, the Cr(salen)-catalyzed reaction using immobilized catalysts most likely derives its enantioselectivity as the Mn(salen) catalysts for epoxidation; selectivity defined by the approach path of the reactant to the metal center. Just as was determined for Mn(salen) catalysts for epoxidation, the sterics of the substituents are a factor in determining these approach paths and ee (Chapter 5.2.2). By forcing the Cr-catalysts to function in an analogous manner, especially for reactants that are sterically unencumbered the enantioselectivities decline.

6.3   Conclusions

The kinetic study into asymmetric ring opening of epoxides with Cr(salen) catalysts revealed that the catalysts function with similarities to enzymes. Given that the catalysts form enzyme-substrate like intermediates, it was possible to model the conversion of epoxides into trimethylsilyl-azido ethers using an enzyme kinetic model. Notably, the Cr(salen)-**1** which is the structure typically reported in the literature exhibited severe levels of substrate inhibition. The fact that the substrate concentration affects reaction rates using Cr(salen) complexes indicates that current attempts to maximize the efficiency of such catalysts for the asymmetric ring opening of epoxides could be done more effectively.

The examination of the effects of symmetry and varied sterics for the salen complexes for ARO reactions resulted in similar conclusions to the case of Mn(salen) complexes for asymmetric epoxidation (Chapter 5). Namely, C_2-symmetry is not a factor in enantioselectivity and variation of the sterics does alter the product ee. However, since the method for chiral induction is different between the ARO and epoxidation reactions, the effects of altering the steric bulk on the homogeneous ligand were also different between these two reactions. For the ARO reaction, the interaction of two salen catalysts to generate product essentially provides a greater level of chiral induction than for the case of epoxidation in which chiral induction is governed by the approach paths of reactants. Hence, for the homogeneous ARO reaction, the sterics of the catalyst are not as essential for the refinement of ee as noted for these same structures in epoxidation. However, for the heterogeneous Cr-ligands where immobilization effectively removed the dimeric interaction between catalysts, the significance of the sterics becomes paramount.

6.4   Experimental Methods

6.4.1 Materials and Instrumentation

Solvents and chemicals were obtained from Aldrich and used as received. Infrared spectra were recorded in transmission mode using a Bio Rad FTS 175 spectrometer. Gas chromatography (GC) data were obtained via a HP6890 series with a cyclodex-β120 column.

6.4.2 Representative Reaction for Cr-Catalyzed Ring-Opening Reaction

An oven dried 5 mL roundbottom flask equipped with a magnetic stir bar was charged with anhydrous ether (0.5 ml, 0.36 g), cyclohexene oxide (chex ox), and 2.5 μL chlorobenzene. 0.0831 g (0.029 mol) of (*S,S*)–**1** catalyst was then added to the solution. The reaction solution quickly became homogeneous and was allowed to stir for several minutes at 0 °C. An initial sample was taken and analyzed by GC. The reaction solution was stirred at 0 °C for an additional 30 min. Azido trimethyl silane (TMSN$_3$, 153 μL, 0.3 mole) which was equilibriated to 0 °C was then added via syringe. The reaction mixture was monitored via GC and IR.

GC conditions: The temperature profile was a 85 °C isotherm for 40 minutes.

6.5   References

1) Shioiri, Y.; Hamada, Y. *Heterocycles* **1988**, *27*, 1035.

2) Blaser, H. *Chem. Rev.* **1992**, *92*, 935.

3) Hanson, R. M. *Chem. Rev.* **1991**, *91*, 437.

4) Klunder, J. M.; Ko, S. Y.; Sharpless, K. B. *J. Org. Chem.* **1986**, *51*, 3710.

5) Martinez, L. E.; Leighton, J. L.; Carsten, D. H.; Jacobsen, E. N. *J. Am. Chem. Soc.* **1995**, *117*, 5897.

6) Larrow, J. F.; Schaus, S. E.; Jacobsen, E. N. *J. Am. Chem. Soc.* **1996**, *118*, 7420.

7) Hansen, K. B.; Leighton, J. L.; Jacobsen, E. N. *J. Am. Chem. Soc.* **1996**, *118*, 10924.

8) Leighton, J. L.; Jacobsen, E. N. *J. Org. Chem.* **1996**, *61*, 389.

9) Background information on the enantioselectivity of the homogeneous Cr(salen) complexes for asymmetric ring-opening of epoxides is provided in Section 4.1. Little work regarding the use of salen complexes and substituent effects for the asymmetric ring-opening reaction has been reported.

10) Jacobsen, E. N. *Asymmetric Catalytic Epoxidation of Unfunctionalized Olefins*; Ojima I., Ed.; VCH Publishers: New York, 1993, p 159.

11) Palucki, M.; Finney, N. S.; Pospisil, P. J.; Guler, M. L.; Ishida, T.; Jacobsen, E. N. *J. Am. Chem. Soc.* **1998**, *120*, 948.

12) Kagan, H. B.; Fiaud, J. C. *Kinetic Resolution*; Interscience: New York, 1987; Vol. 14, p 249.

13) Konsler, R. G.; Karl, J.; Jacobsen, E. N. *J. Am. Chem. Soc.* **1998**, *120*, 10780.

Appendix A

Supplementary IR data for the Synthesis of Immobilized Salen Complexes onto Merrifield Resin.

The principal evidence for construction of the salen ligands onto a chloromethylated polymer resin is the appearance and disappearance of IR absorption peaks for the functional groups involved in the reaction scheme for each stage of moiety attachment. Chapter 2 provided the sequence of IR spectra for the model 4-hydroxybenzaldehyde-based ligand structure (Figure 2.4). The focus was on the appearance and disappearance of imine and carbonyl groups, respectively. In the final stage of synthesis, the *tert*-butyl groups of 3,5-di-tert-butyl-2-hydroxybenzaldehyde were used as independent spectroscopic tags for confirmation of attachment of this terminal moiety. Figure A.1. shows the IR spectra for the resin before and after reaction with the di-*tert*-butyl moiety (Figure A.1a and A.1b, respectively), and the difference spectra (Figure A.1c) obtained by subtraction of the IR spectra for these two resins. The difference spectra clearly indicates the appearance of two peaks which correspond in peak position (2867 and 2964 cm^{-1}) to antisymmetric methyl stretching vibrations for a *t*-butyl substituent.[1]

As was indicated in Chapter 2 for the synthesis of the heterogenized ligands, the synthetic methodology used to generate the 4-hydroxybenzaldehyde-based ligand was repeated using 2,4,6-trihydroxybenzaldehyde (246-HB) and 2-hydroxybenzaldehyde (2-HB) as the initial linker to the polymer resin. The 246-HB based ligand is that which is used with Mn and Cr to test the efficacy of this immobilized ligand for asymmetric catalysis. The 2-HB based ligand was used as a test to verify if the ligand could be completely constructed if the *ortho*-hydroxy group of 246-HB were the position of attachment to the surface. The progression of IR spectra for the synthesis of each ligand is provided in Figure A.2 and A.4, respectively. Figures A.3 and A.5 provide the IR spectra and difference spectra indicating the appearance of the t-butyl spectroscopic tags in the final stage of ligand synthesis for each ligand structure.

Figure A.1. Infrared spectra noting the appearance of tert-butyl groups as independent spectroscopic tags in the final synthetic stage of the synthesis of the anchored salen complex generated with the 4-hydroxybenzaldehyde link (4HB). a) 4HB ligand up to (+/-)-trans-1,2-diaminocyclohexane stage; b) a + 3,5-di-*tert*-butyl-2-hydroxybenzaldehyde; c) difference spectra between a) and b) indicating the appearance of the tert-butyl peaks . The approximate position of these peaks which correspond to methyl antisymmetric stretching modes are 2867 and 2964 cm^{-1}. The spectra have been offset vertically for clarity.

Figure A.2. Infrared spectra for the stagewise synthesis of the anchored salen complex onto Merrifield resin (chloromethylated polymer of 98 vol% styrene and 2 vol% divinylbenzene). a) Merrifield resin; b) a + 2,4,6-trihydroxybenzaldehyde; c) benzyl chloride + 2,4,6-trihydroxybenzaldehyde; d) b + (+/-)-trans-1,2-diaminocyclohexane; e) d + 3,5-di-*tert*-butyl-2-hydroxybenzaldehyde. The approximate position of the aldehydic carbonyl and imine stretching vibrations are 1678 and 1627 cm⁻¹, respectively. The peaks between 1580 and 1610 cm⁻¹ are aromatic stretching modes due to the polystyrene support.
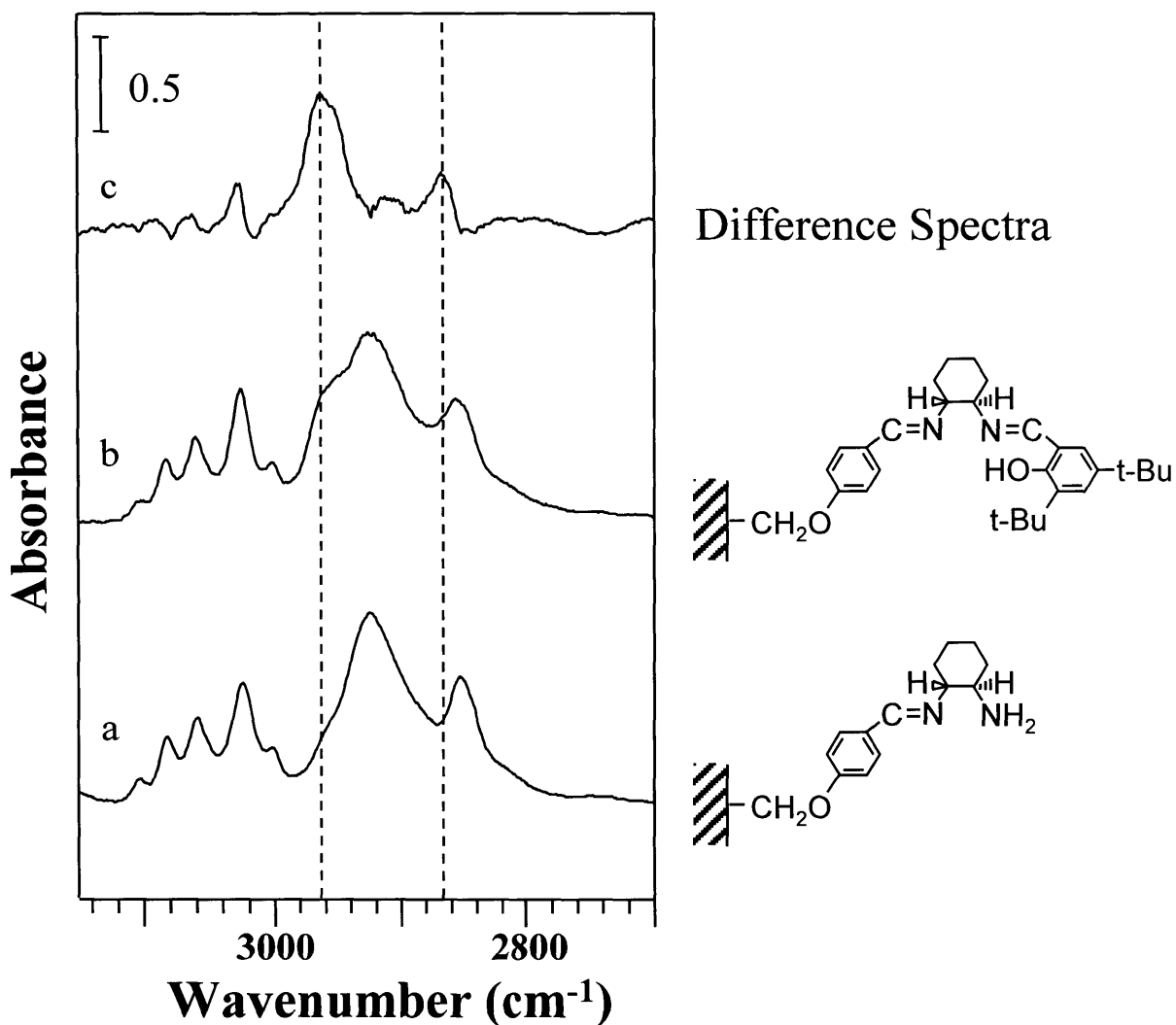
Figure A.3. Infrared spectra noting the appearance of tert-butyl groups as independent spectroscopic tags in the final synthetic stage of the synthesis of the anchored salen complex generated with the 2,4,6-trihydroxybenzaldehyde link (246HB). a) 246HB ligand up to (+/-)-trans-1,2-diaminocyclohexane stage; b) a + 3,5-di-*tert*-butyl-2-hydroxybenzaldehyde; c) difference spectra between a) and b) indicating the appearance of the tert-butyl peaks . The approximate position of these peaks which correspond to methyl antisymmetric stretching modes are 2861 and 2962 cm^{-1}. The spectra have been offset vertically for clarity.
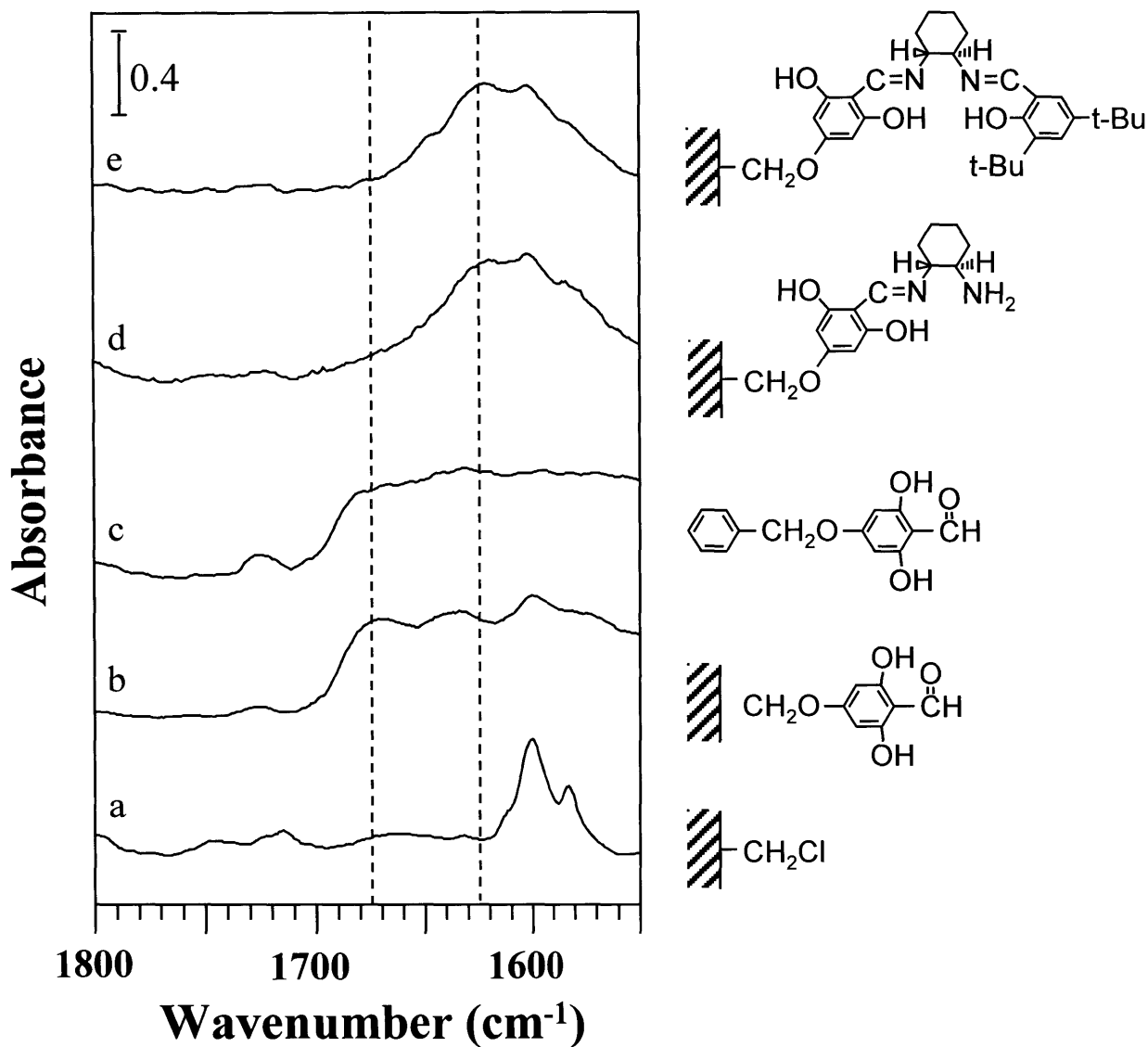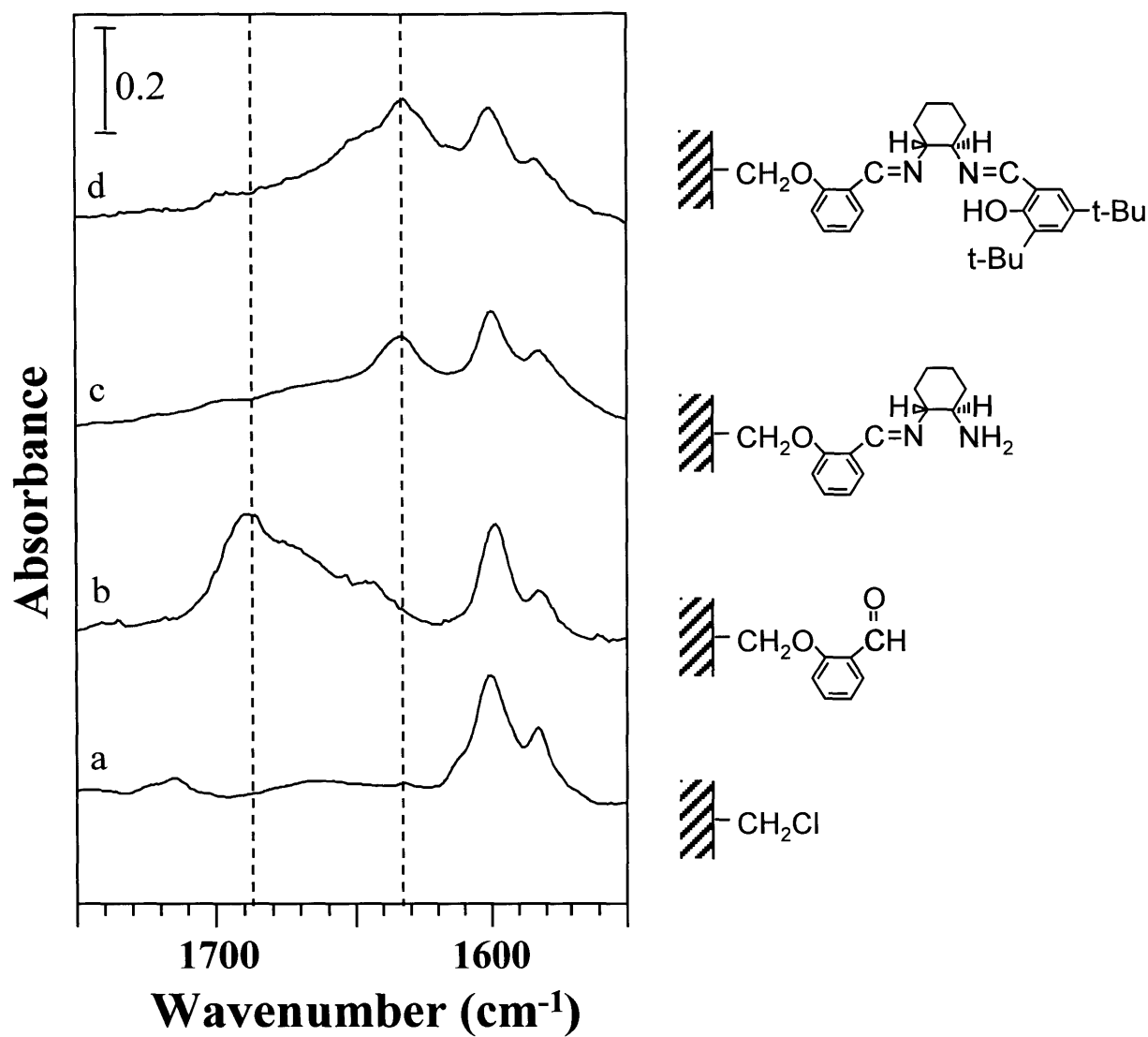
Figure A.4. Infrared spectra for the stagewise synthesis of the anchored salen complex onto Merrifield resin (chloromethylated polymer of 98 vol% styrene and 2 vol% divinylbenzene). a) Merrifield resin; b) a + 2-hydroxybenzaldehyde; c) b + (+/-)-trans-1,2-diaminocyclohexane; d) d + 3,5-di-*tert*-butyl-2-hydroxybenzaldehyde. The approximate position of the aldehydic carbonyl and imine stretching vibrations are 1687 and 1634 cm⁻¹, respectively. The spectra have been offset vertically for clarity. The peaks between 1580 and 1610 cm⁻¹ are aromatic stretching modes due to the polystyrene support.
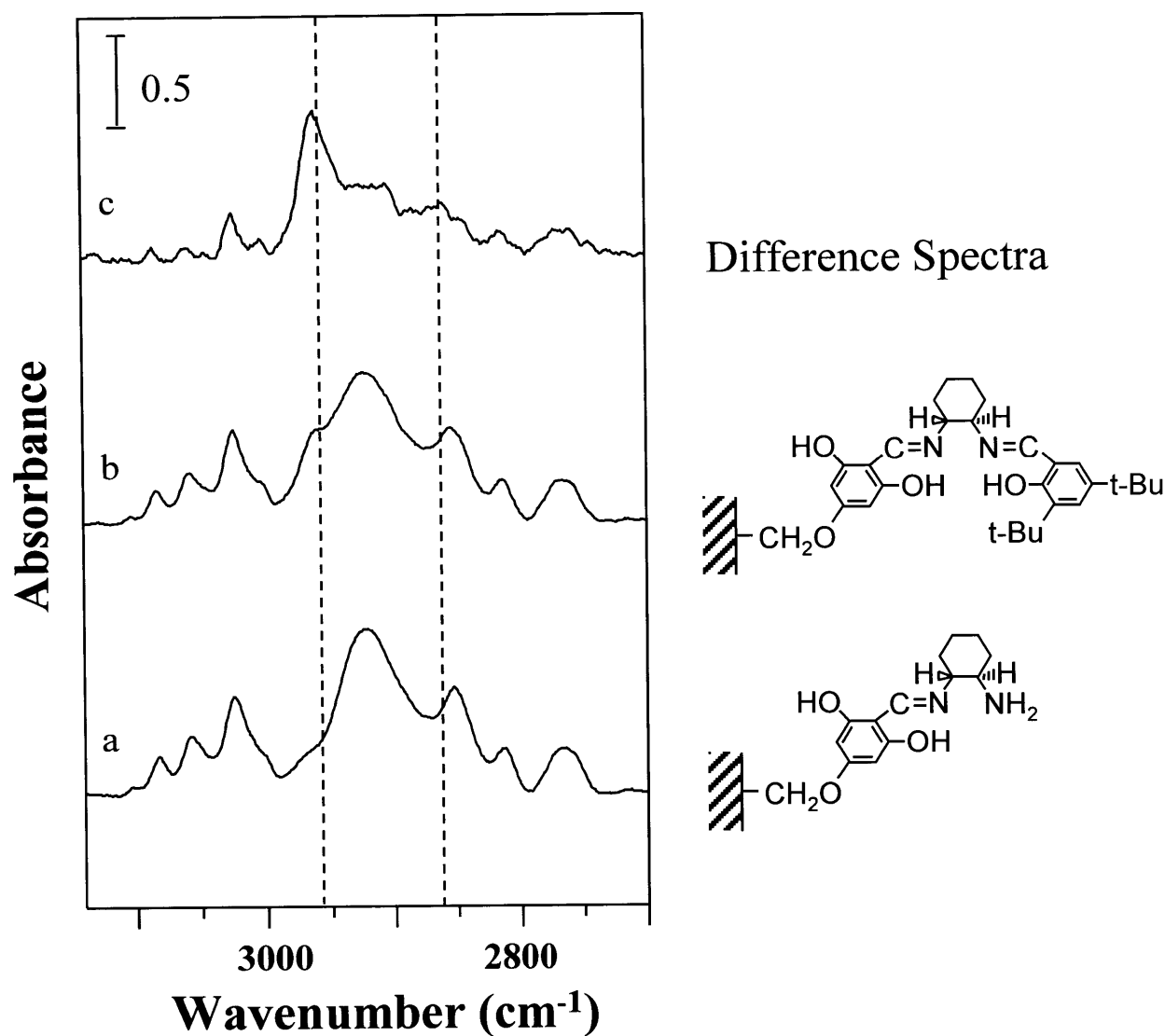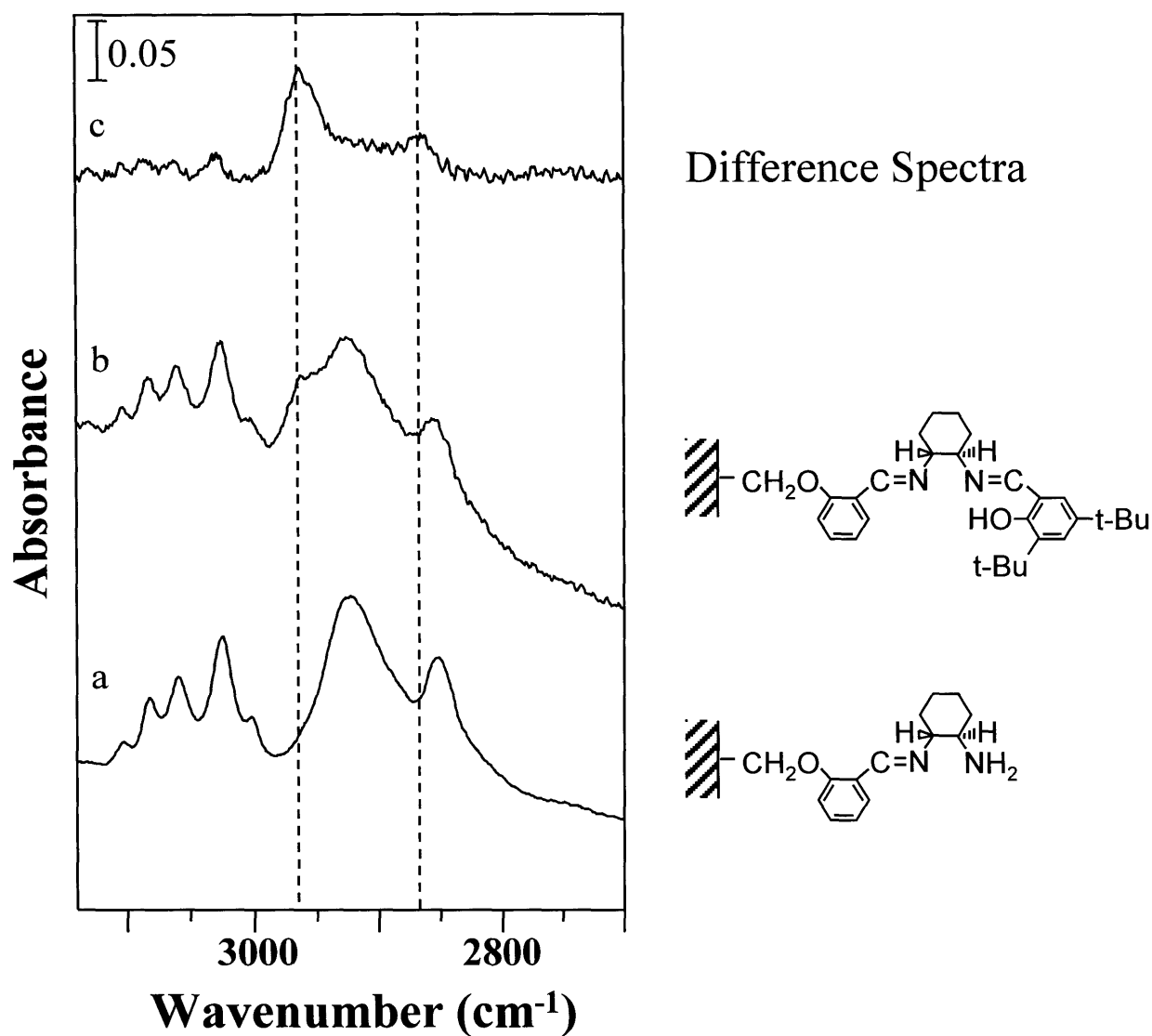
Figure A.5. Infrared spectra noting the appearance of tert-butyl groups as independent spectroscopic tags in the final synthetic stage of the synthesis of the anchored salen complex generated with the 2-hydroxybenzaldehyde link (2HB). a) 2HB ligand up to (+/-)-trans-1,2-diaminocyclohexane stage; b) a + 3,5-di-*tert*-butyl-2-hydroxybenzaldehyde; c) difference spectra between a) and b) indicating the appearance of the tert-butyl peaks . The approximate position of these peaks which correspond to methyl antisymmetric stretching modes are 2868 and 2963 cm^{-1}. The spectra have been offset vertically for clarity.

References

1) Roeges, N. P. G. *A Guide to the Complete Interpretation of Infrared Spectra of Organic Structures*; John Wiley & Sons Ltd.: England, 1994.

Appendix B

Reaction Data for Homogeneous, Mn(salen)-Catalyzed Epoxidations

The asymmetric epoxidation of styrene, DHN, and chromene using homogeneous, Mn(salen) complexes was investigated in Chapter 5. This appendix provides a compilation of the enantioselectivity and reactivity data using the structurally diverse complexes.

The reaction conditions for these epoxidations included mCPBA as oxidant and 4-methylmorpholine-N-oxide as a complexing agent for the oxidant to prevent reaction between oxidant and olefin to generate racemic product. Additionally, a quench procedure involving dimethyl sulfide was used to prevent continued reaction during work-up of the low temperature reactions. The exact experimental details are provided in Section 5.4.

Table B.1. Enantioselectivity and Eyring Data for Homogeneous, Mn(salen)-Catalyzed Asymmetric Epoxidation of Styrene.

Catalyst	Temperature (°C)	Ee (%)	$R\ln(k_{major}/k_{minor})$ (cal /mol K)
4	23	42.3	1.79
4	0	46.6	2.01
4	-20	50.8	2.22
4	-42	53.6	2.39
4	-60	55.4	2.48
4	-78	55.3	2.47
5	23	40.0	1.69
5	0	45.3	1.94
5	-20	48.8	2.12
5	-42	52.7	2.33
5	-60	55.2	2.47
5	-78	49.6	2.16
6	23	47.6	2.06
6	0	51.7	2.28
6	-20	53	2.35
6	-42	57.5	2.60
6	-54	57.6	2.61
6	-61	56.7	2.56
6	-78	54.6	2.43
7	23	44.5	1.91
7	0	48.0	2.08
7	-20	49.9	2.18
7	-42	53.4	2.37
7	-61	54.4	2.42
7	-78	52.3	2.31
8	23	4	0.16
9	23	4.6	0.18
Kinetic Resolution	23	2.6	0.10
Kinetic Resolution	0	1.6	0.06
Kinetic Resolution	-20	2.9	0.11
Kinetic Resolution	-42	1.3	0.05
Kinetic Resolution	-60	1.6	0.06
Kinetic Resolution	-78	0.3	0.01

Table B.2. Enantioselectivity and Eyring Data for Homogeneous, Mn(salen)-Catalyzed Asymmetric Epoxidation of 1,2-Dihydronaphthalene (DHN).

Catalyst	Temperature (°C)	Ee (%)	$R\ln(k_{major}/k_{minor})$ (cal /mol K)
4	23	75.8	3.94
4	2	77.3	4.08
4	-20	81.5	4.54
4	-30	77.8	4.15
4	-40	71.8	3.59
4	-60	69.1	3.38
4	-78	62.0	2.85
5	23	67.3	3.24
5	0	65.2	3.09
5	-20	71.9	3.59
5	-42	48.8	2.12
5	-60	52.1	2.29
5	-78	40.4	1.70
6	23	79.3	4.29
6	0	78.5	4.21
6	-20	81.5	4.54
6	-42	74.5	3.82
6	-60	75.6	3.92
6	-78	74.8	3.84
7	23	66.8	3.21
7	0	68.2	3.31
7	-20	70	3.45
7	-30	65.3	3.10
7	-42	51.1	2.24
7	-61	48.9	2.12
7	-78	40.9	1.73
8	23	27.8	1.13
9	23	20.8	0.84
Kinetic Resolution	23	1.4	0.06
Kinetic Resolution	0	6.3	0.25
Kinetic Resolution	-20	13.0	0.52
Kinetic Resolution	-40	2.0	0.08
Kinetic Resolution	-60	1.3	0.05
Kinetic Resolution	-78	1.2	0.05

Table B.3. Enantioselectivity and Eyring Data for Homogeneous, Mn(salen)-Catalyzed Asymmetric Epoxidation of 6-Bromo-2,2,3,4-Tetramethyl Chromene.

Catalyst	Temperature (°C)	Ee (%)	$R\ln(k_{major}/k_{minor})$ (cal /mol K)
4	23	58.0	2.63
4	2	82.3	4.63
4	-20	68.0	3.29
4	-45	70.0	3.45
4	-60	72.3	3.63
4	-78	67.0	3.22
5	23	70.8	3.51
5	0	83.4	4.77
5	-20	88.7	5.59
5	-48	88.7	5.59
5	-60	85.7	5.10
5	-78	80.5	4.42
6	23	83.8	4.83
6	0	87.2	5.33
6	-20	85.4	5.05
6	-46	81.5	4.54
6	-60	83.0	4.72
6	-78	81.3	4.51
7	23	91.4	6.17
7	0	92.5	6.45
7	-20	93.5	6.74
7	-42	92.5	6.45
7	-61	91.6	6.21
7	-78	90.2	5.89
8	23	71.2	3.62
9	23	67.5	3.34
Kinetic Resolution	23	-7.5[*]	(-) 0.30
Kinetic Resolution	0	-12.1[*]	(-) 0.48
Kinetic Resolution	-20	-7.1[*]	(-) 0.28
Kinetic Resolution	-40	-7.2[*]	(-) 0.29
Kinetic Resolution	-60	-8.0[*]	(-) 0.32
Kinetic Resolution	-78	-6.6[*]	(-) 0.26

[*] Ee values indicate that the catalyst favors consumption of the major enantiomeric epoxide.

Table B.4. Conversion/Yield Data (%) for Homogeneous, Mn(salen)-Catalyzed Asymmetric Epoxidation of Styrene.

Temperature (°C)

Catalyst	23	0	-20	-40	-60	-78
4	97/86	98/70	99/54	99/65	97/61	98/57
5	98/92	99/78	98/71	99/79	95/73	99/69
6	98/86	98/90	99/67	99/89	99/73	99/82
7	97/83	99/89	98/81	99/78	99/72	99/92
8	99/61	NA	NA	NA	NA	NA
9	99/60	NA	NA	NA	NA	NA

Table B.5. Conversion/Yield Data (%) for Homogeneous, Mn(salen)-Catalyzed Asymmetric Epoxidation of 1,2-Dihydronapthalene (DHN).

Temperature (°C)

Catalyst	23	0	-20	-40	-60	-78
4	99/39	99/42	99/27	35/10	27/8	22/4
5	99/33	99/40	99/26	17/5	26/5	11/3
6	99/43	99/71	99/31	34/14	44/10	19/4
7	99/41	99/39	99/31	41/15	33/16	21/6
8	99/39	NA	NA	NA	NA	NA
9	99/38	NA	NA	NA	NA	NA

Table B.6. Conversion/Yield Data (%) for Homogeneous, Mn(salen)-Catalyzed Asymmetric Epoxidation of 6-Bromo-2,2,3,4-Tetramethyl Chromene.

Temperature (°C)

Catalyst	23	0	-20	-40	-60	-78
4	42/32	72/36	44/13	19/5	14/4	14/4
5	60/37	70/56	86/65	23/10	17/10	18/6
6	66/48	84/53	72/45	24/6	21/8	23/4
7	99/41	99/39	99/31	41/15	33/16	21/6
8	99/98	NA	NA	NA	NA	NA
9	99/99	NA	NA	NA	NA	NA

Appendix C

Modeling of Cr(Salen)-Catalyzed Ring-Opening of Cyclohexene Oxide as a Series, Batch Reaction

The general reaction scheme for series order reactions is A→B→C. The performance equations for batch reactions are

$$\frac{C_A}{C_{A_o}} = e^{-k_1 t} \tag{1}$$

$$\frac{C_B}{C_{A_o}} = \frac{k_1}{k_2 - k_1}\left[e^{-k_1 t} - e^{-k_2 t}\right] + \frac{C_{B_o}}{C_{A_o}} e^{-k_2 t} \tag{2}$$

Taking the ratio of concentrations (dividing equation (1) by equation (2)) eliminates the time variable and is useful for finding rate constants. The resulting equation is

$$\frac{C_B}{C_{A_o}} = \frac{1}{K-1}\left[\frac{C_A}{C_{A_o}} - \left(\frac{C_A}{C_{A_o}}\right)^K\right] + \frac{C_{B_o}}{C_{A_o}}\left(\frac{C_A}{C_{A_o}}\right)^K \tag{3}$$

With equation (3), plots of C_B/C_{Ao} versus conversion ($1-C_A/C_{Ao}$) can be generated for various values of K. The experimental data and series-reaction model curves for various values of K are presented as Figures C.1- C.3 for the Cr(salen) catalysts **1**, **2**, and **4**, respectively.
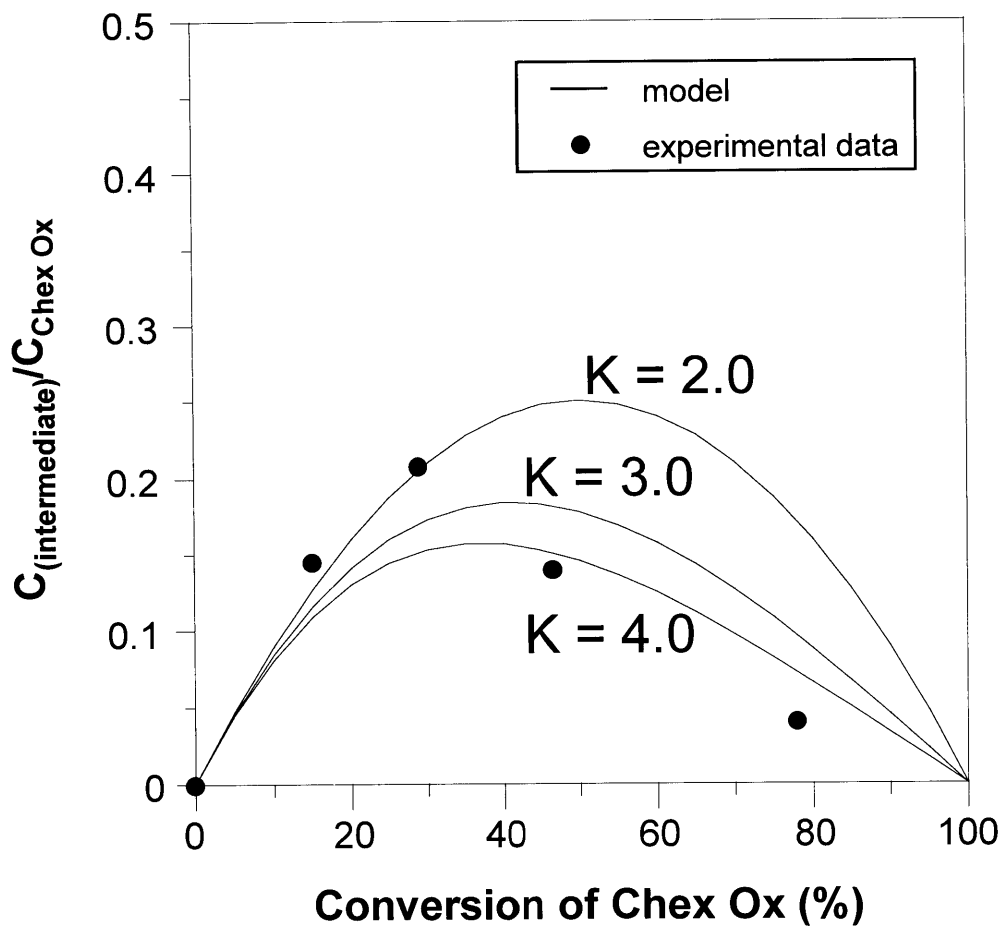
Figure C.1. Reaction kinetic data for the Cr-catalyzed ring-opening of cyclohexene oxide (Chex Ox) using Cr(salen)-**1**. A model was fit to the data assuming a series reaction scheme. The model that best fits the data assumed $K = k_2/k_1 = 3$.

Figure C.2. Reaction kinetic data for the Cr-catalyzed ring-opening of cyclohexene oxide (Chex Ox) using Cr(salen)-**2**. A model was fit to the data assuming a series reaction scheme. The model that best fits the data assumed $K = k_2/k_1 = 8.0$.
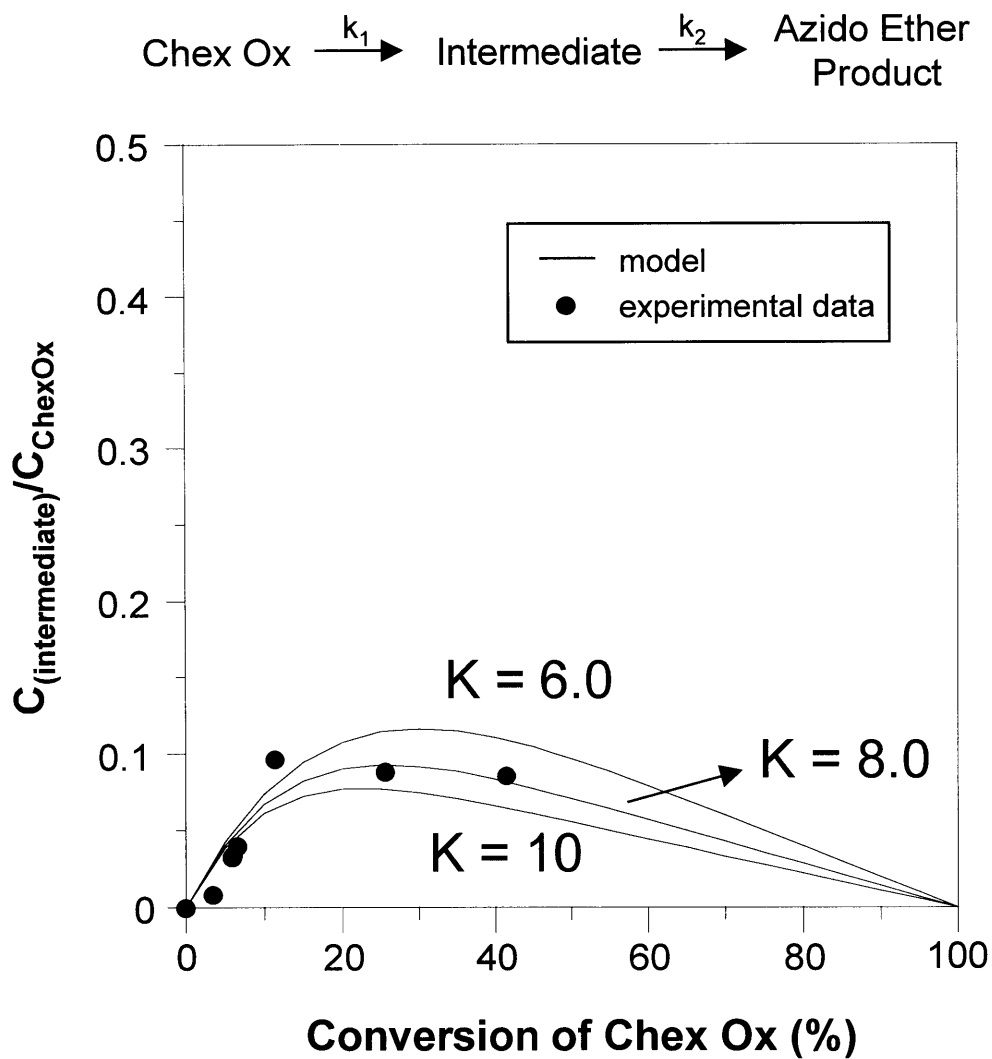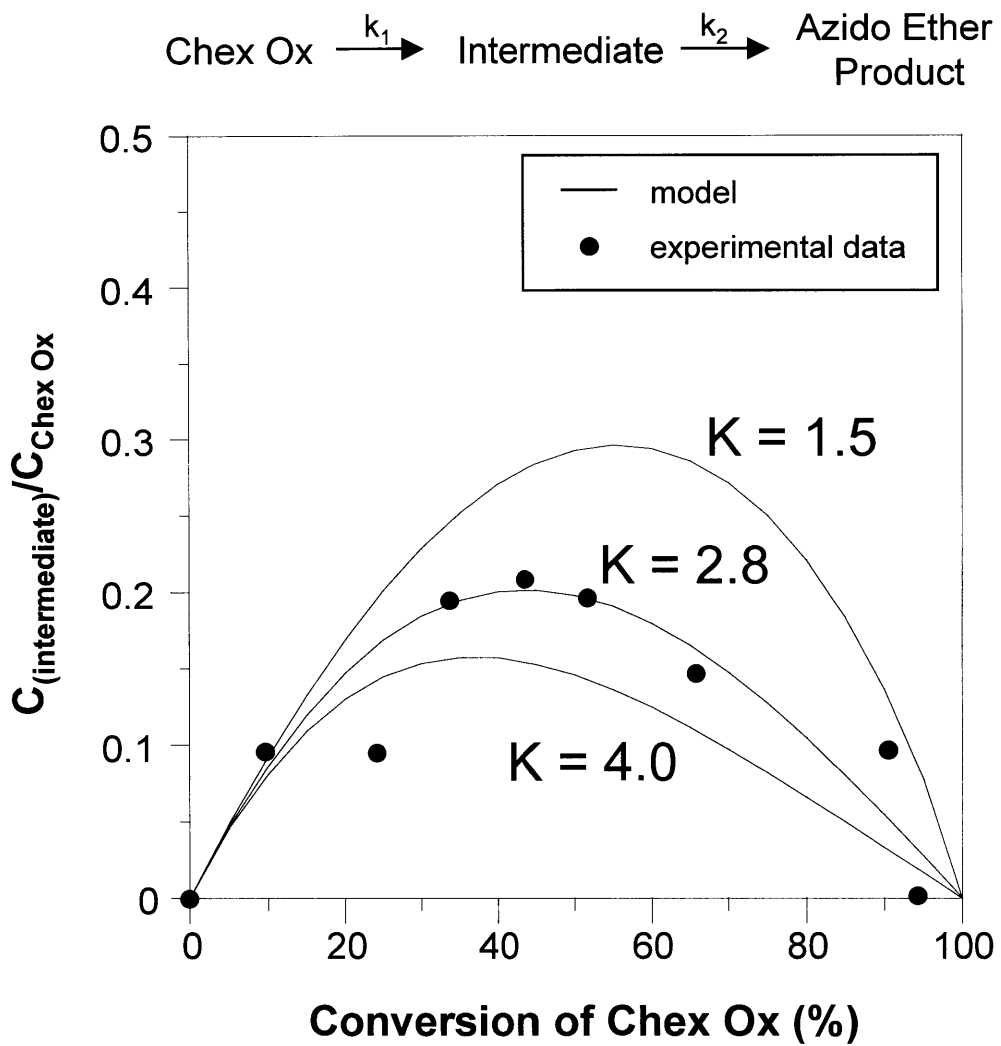
Figure C.3. Reaction kinetic data for the Cr-catalyzed ring-opening of cyclohexene oxide (Chex Ox) using Cr(salen)-**4**. A model was fit to the data assuming a series reaction scheme. The model that best fits the data assumed $K = k_2/k_1 = 2.8$.

Appendix D

Calculation of Reaction Order for the Cr(Salen)-**1** Catalyst

The rate order for the asymmetric ring opening of epoxides was determined with excess TMSN$_3$ and using a catalyst concentration of 0.029 M. The rate equation is

$$\frac{-dC_a}{dt} = k[C_a]^\alpha [C_b]^\beta \qquad (1)$$

Taking the log of both sides of equation (1) and assuming the change in concentration of reagent B (TMSN$_3$) is negligible, the rate equation can be rewritten as follows:

$$\log\left(\frac{-dC_a}{dt}\right) = k' + \alpha \log(C_a) \qquad (2)$$

Plotting equation (2) should reveal the order of the reaction with respect to epoxide as the slope of the line. An example for Cr(salen)-**1** is prsented in Figure D.1. The order of reaction for the other Cr(salen) catalysts was determined in the same manner.

$$\log \left(\frac{-dC_a}{dt} \right) = \log k + \alpha \log \left(C_{a_o} \right)$$

y = 0.9152x - 4.9316
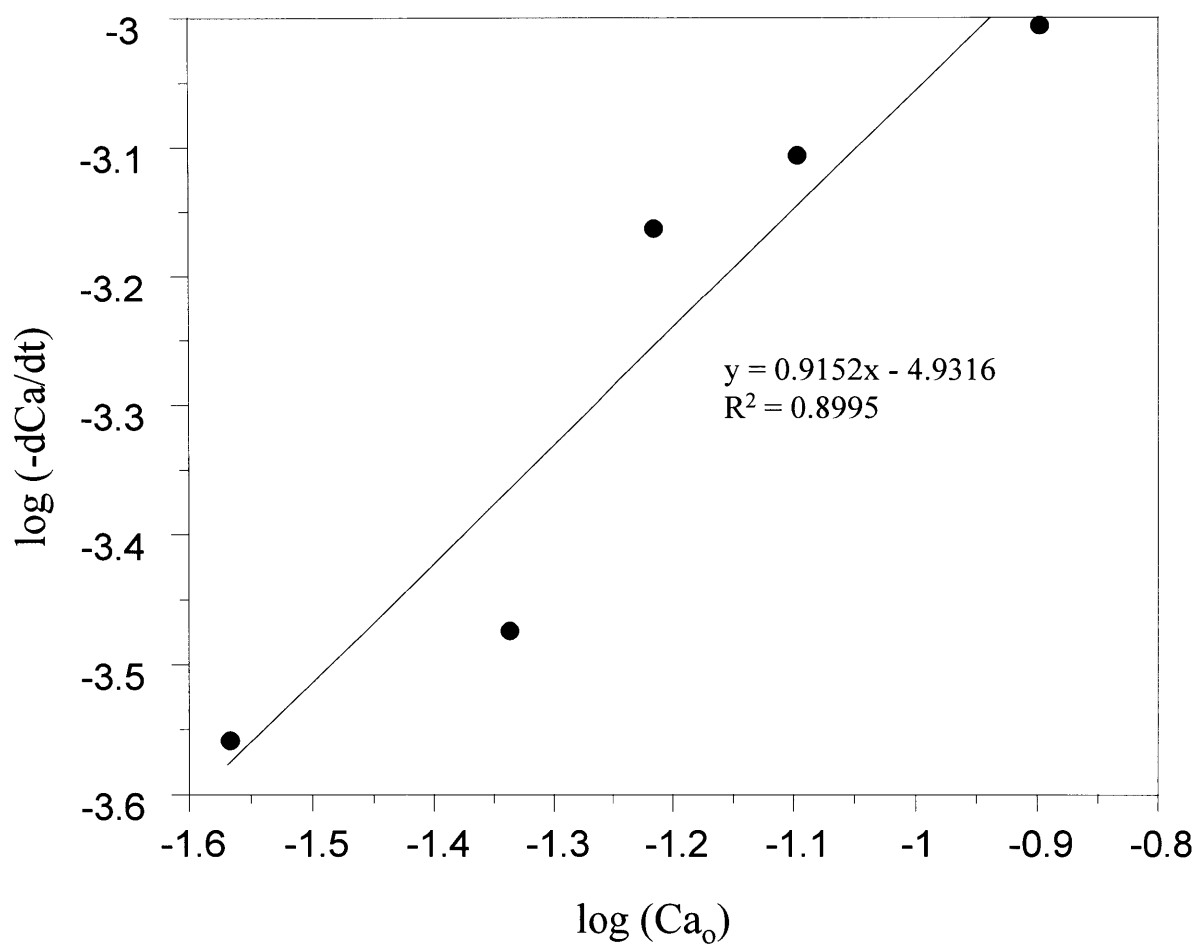$R^2 = 0.8995$

log (-dCa/dt)

log (Ca$_o$)

Figure D.1. Determination of order of reaction with respect to epoxide for Cr(salen)-**1**. The slope of the line represents the order of reaction.

Appendix E

Rate Data for Reactions using Cr(Salen) Catalysts and the Calculation of Kinetic Parameters

The rate data accumulated for the ring-opening reaction of cyclohexene oxide with $TMSN_3$ using the various, homogeneous Cr(salen) catalysts are presented. The following sections outline the methods to calculate the kinetic parameters K_{m-a}, k_2, and K_s for the reactions using Cr(salen)-**1**, -**3**, and –**4** (Chapter 6).

E.1   Rate Data Collected using Cr(Salen) Complexes with Cyclohexene Oxide

For Cr(salen)-**1**:

$[TMSN_3] = 2.1$ M
temperature = 0 °C

C_o of Epoxide (M)	Initial Rate (mM/min)
0.027	0.274
0.046	0.336
0.061	0.689
0.080	0.787
0.126	0.987
0.151	0.865
0.287	0.396
0.539	0.285

For Cr(salen)-**2**:

$[TMSN_3] = 2.1$ M
temperature = 0 °C

C_o of Epoxide (M)	Initial Rate (mM/min)
0.0296	0.124
0.0560	0.0954
0.0774	0.0459
0.140	0.0385
0.168	0.0374
0.312	0.0916

For Cr(salen)-**3**:

$[TMSN_3] = 2.1$ M
temperature = 0 °C

C_o of Epoxide (M)	Initial Rate (mM/min)
0.0729	0.152
0.105	0.182
0.182	0.276
0.379	0.388
0.757	0.494

For Cr(salen)-**4**:

$[TMSN_3] = 2.1$ M
temperature = 0 °C

C_o of Epoxide (M)	Initial Rate (mM/min)
0.0868	0.0900
0.307	0.130
0.0506	0.0679
0.178	0.123
0.411	0.127

E.2   Determination of K_{ma}

The epoxide ring-opening reaction is a two-substrate reaction requiring the presence of an azide donor and epoxide. Denoting epoxide as A and azide as B, experiments run in an excess of B allow the calculation of $K_{m\text{-}a}$ for substrate A from the following relation:

$$v = \frac{V_{max}}{1 + \dfrac{K_{m\text{-}a}}{a}} \tag{1}$$

where V_{max} is the maximum reaction rate (M/min), $K_{m\text{-}a}$ is the Michaelis-Menten constant (M), a is the concentration of substrate (M), and v is the reaction rate (M/min). Equation (1) is identical to the Michaelis-Menten equation for single-substrate reactions, and hence K_m for substrate A can be defined as the concentration of A which at saturating conditions of B will give half maximum velocity. In order to calculate K_m for substrate A, equation (1) was rearranged to yield the following relation.

$$\frac{a}{v} = \frac{K_m^a}{V_{max}} + \frac{1}{V_{max}}a \tag{2}$$

All variables are defined as in equation (1). The slope gives $1/V_{max}$ and the y-intercept gives $K_{m\text{-}a}/V_{max}$. The following figure demonstrates the case for Cr(salen)-**1**.

For Figure E.1, the rate data used was for the lower concentrations of substrate since at higher concentrations, substrate inhibition for the Cr(salen)-**1** is evident. Additionally, the fits for Cr(salen)-**3** and –**4** were improved in that substrate inhibition is not evident, so these sets more easily reduce to the simplified equation (1).

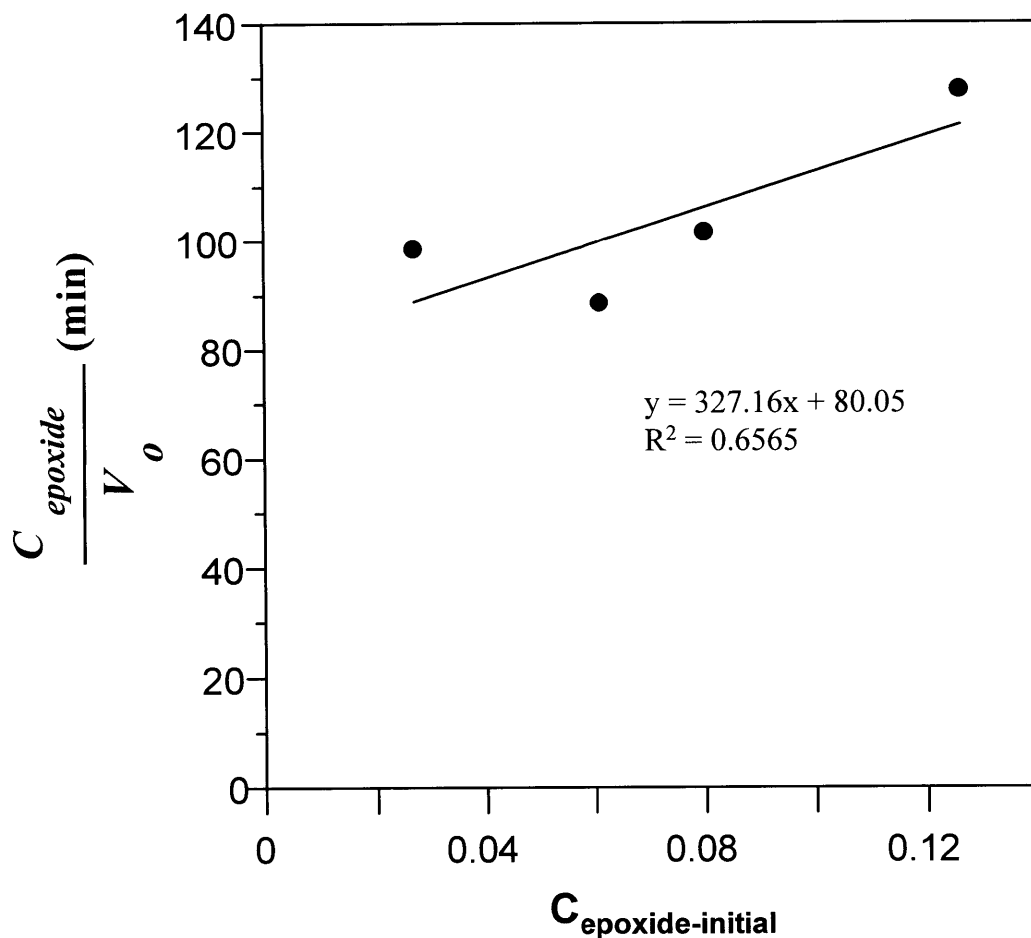$$\frac{C_{epoxide}}{V_o} = \frac{K_m}{V_{max}} + \frac{C_{epoxide}}{V_{max}}$$

Figure E.1. Determination of K_{ma} using Cr(salen)-1 with cyclohexene oxide. K_{ma}, the Michaelis-Menten constant, is the slope divided by the maximum reaction rate. The maximum reaction rate (V_{max}) is the reciprocal of the y-intercept.

E.3   Determination of k_2

At low substrate concentrations, the substrate inhibition model can be reduced to yield an equation that can be plotted to find k_2. The full substrate inhibition equation is

$$v = \frac{k_2 e_o}{1 + \dfrac{K_m^a}{a} + \dfrac{a}{K_{Inh}}} \tag{3}$$

where v is the reaction rate (M/min), e_o is the initial enzyme/catalyst concentration (M), a is the epoxide concentration (M), K_{inh} is the inhibition parameter, K_{ma} is the Michaelis-Menten constant, and k_2 is a rate constant for tertiary complex formation. At low substrate A concentrations, the a/K_{Inh} term is negligible and equation (3) becomes

$$v = \frac{k_2 e_o}{1 + \dfrac{K_m^a}{a}} \tag{4}$$

Plotting v versus $e_o/(1+K_m/a)$ should yield a straight line with a slope of k_2. Figure E.2 is an example of such a plot for Cr(salen)-**1**.

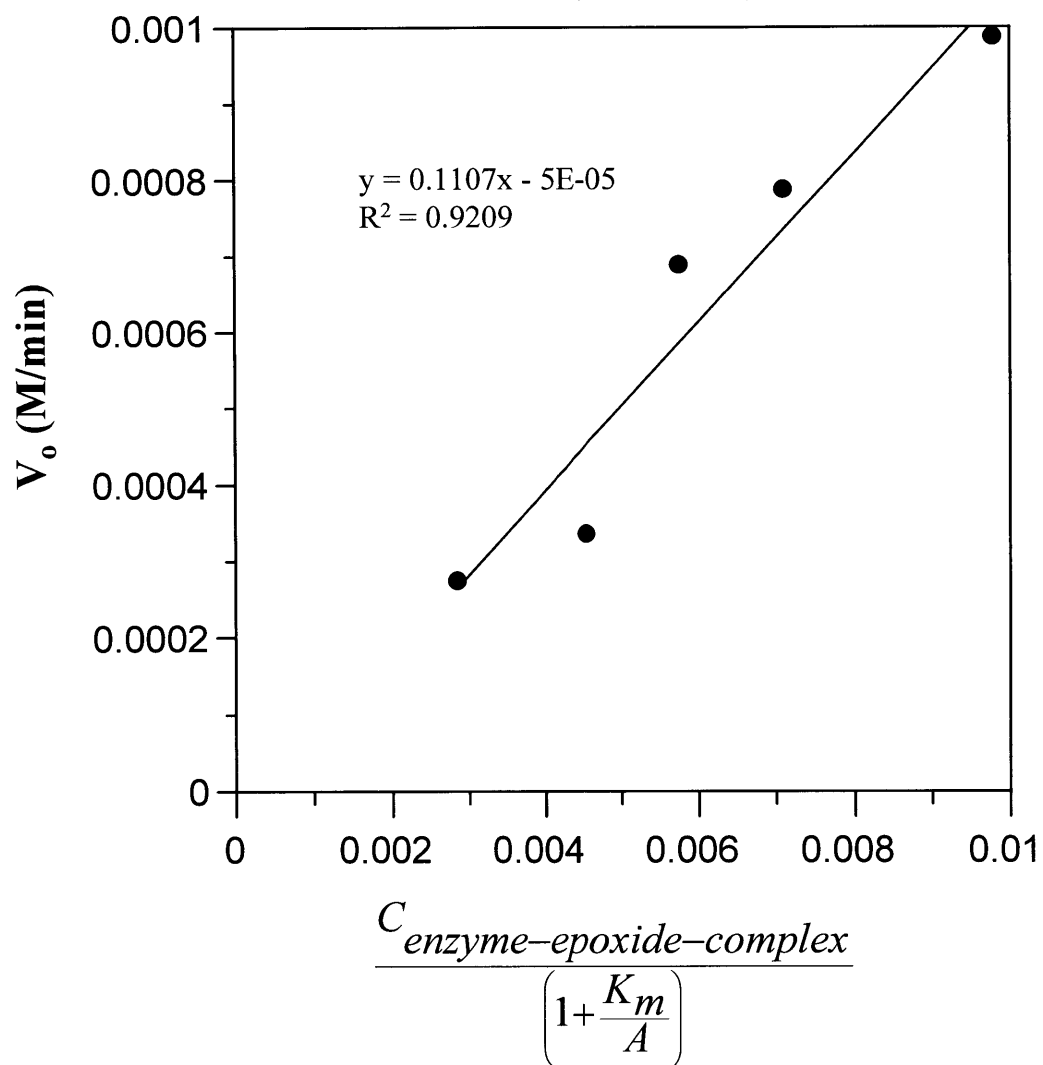$$V_o = k_2 \frac{C_{enzyme-epoxide-complex}}{\left(1 + \dfrac{K_m}{a}\right)}$$

y = 0.1107x - 5E-05
$R^2 = 0.9209$

(plot axes: x-axis $\dfrac{C_{enzyme-epoxide-complex}}{\left(1+\dfrac{K_m}{A}\right)}$ with values 0, 0.002, 0.004, 0.006, 0.008, 0.01; y-axis V_o (M/min) with values 0, 0.0002, 0.0004, 0.0006, 0.0008, 0.001)

Figure E.2. Determination of k_2 using Cr(salen)-**1** for cyclohexene oxide. The slope represents the value of k_2.

E.4 Determination of K_s

The binding of catalyst to substrate is an important step in the overall rate analysis. In many cases, it may be possible to directly study the binding of enzyme to substrate.[Dixon, 1979 #234] For the system

$$E + S \ <--> \ ES$$
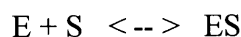
where [E] is the concentration of free enzyme and [S] is the concentration of unbound substrate, a method that allows estimation of the concentration of ES will also make it possible to follow the formation of the bound complex at varying concentrations of S. If we assume that the concentration of enzyme (where enzyme is meant to be equivalent to the Cr(salen) catalyst) is much less than the concentration of [S], the following Michaelis-Menten relation applies.

$$K_S = \frac{([E]-[ES])[S]}{[ES]} \qquad (5)$$

where [ES] is the concentration of the enzyme-substrate complex, and [E] and [S] are the concentration of free enzyme and substrate, respectively. The measurement of [ES] at a series of concentrations of [S] will therefore allow K_s to be calculated by an altered form of equation (5).

$$\frac{1}{[ES]} = \frac{K}{[E]}\frac{1}{[S]} + \frac{1}{[E]} \qquad (6)$$

A number of enzymes contain more than one active site for the binding of substrate. In order to account for this fact, let r represent the number of substrate molecules per molecule of enzyme.

$$r = \frac{[ES]}{[E]} \qquad (7)$$

If the enzyme contains more than one binding site, denoted by n, it is preferable to think in terms of binding sites, n[E] rather than enzyme molecules, [E]. Substituting n[E] for [E] and r[E] for [ES] in equation (6) yields

$$\frac{1}{r} = \frac{K_s}{n}\frac{1}{[S]} + \frac{1}{n} \qquad\qquad (8)$$

Plotting $1/r$ against $1/[S]$ will give a straight line with a slope of K_s/n and a y-intercept of $1/n$.

Due to several factors (section 6.2.3.3), the values generated using this method were taken as only a first approximation of the relative rates of complex formation between the different catalysts.
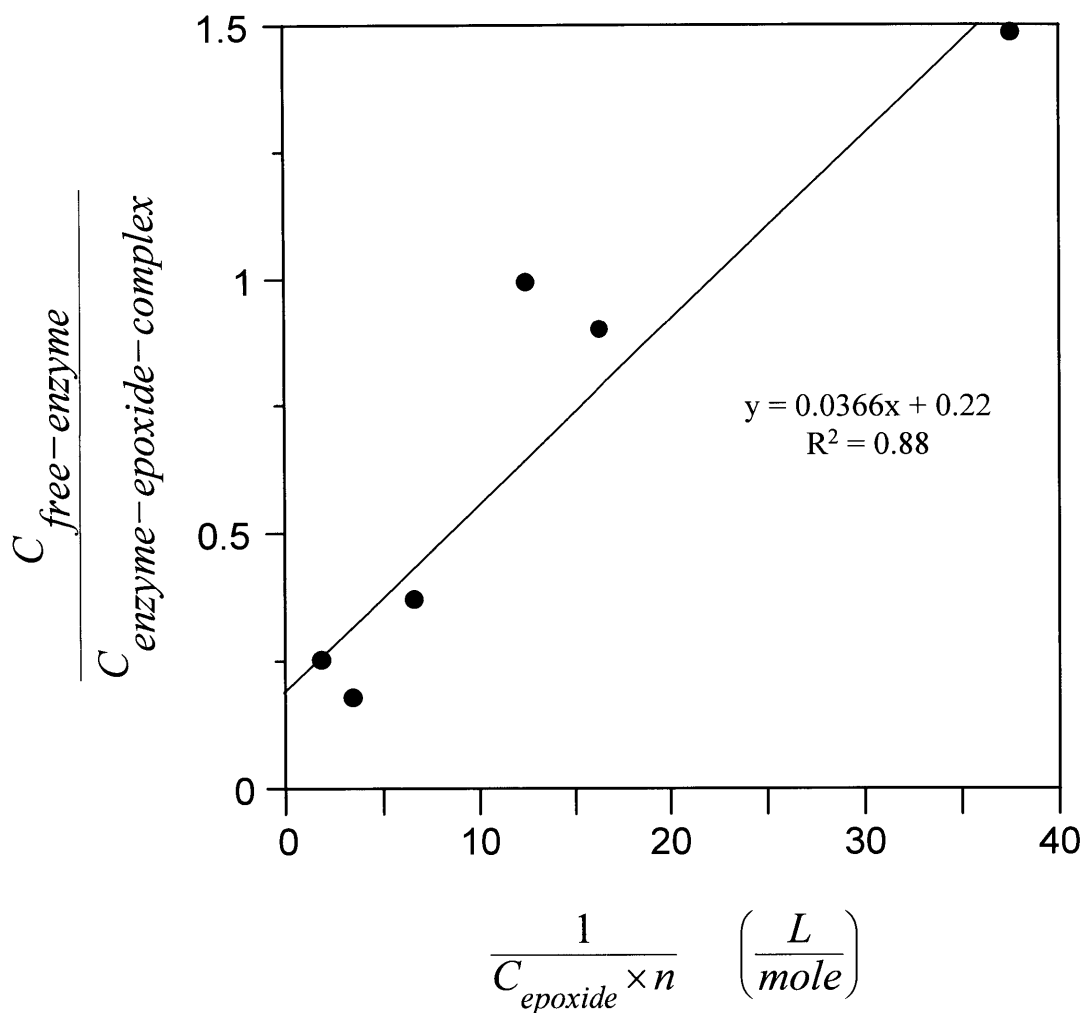
Figure E.3. Determination of K_{s-a}, the equilibrium constant between free enzyme and epoxide. The slope is K_{s-a}/n for Cr(salen)-**1**. The y-intercept is the reciprocal of the number of binding sites (1/n) on each catalyst particle.